# VOLTAGE DEPENDENCE AND ACTIVATION MECHANISMS OF THE NEUROMODULATORY INWARD CURRENT ($I_{MI}$) IN THE STOMATOGASTRIC GANGLION OF *C. BOREALIS*

By

MICHAEL LESLIE GRAY

A dissertation submitted to the

Graduate School-New Brunswick

Rutgers, The State University of New Jersey

In partial fulfillment of the requirements

For the degree of

Doctor of Philosophy

Graduate Program in Behavioral and Neural Sciences

Written under the direction of

Jorge P. Golowasch

And approved by

_____

_____

_____

_____

_____

Newark, New Jersey

October 2015

ABSTRACT OF THE DISSERTATION

# VOLTAGE DEPENDENCE AND ACTIVATION MECHANISMS OF THE NEUROMODULATORY INWARD CURRENT ($I_{MI}$) IN THE STOMATOGASTRIC GANGLION OF *C. BOREALIS*

By Michael Gray

Dissertation Director:
Jorge Golowasch

The Neuromodulatory Inward Current ($I_{MI}$) of the stomatogastric ganglion (STG*)* in *Cancer borealis* is an inward difference current elicited by neuromodulators whose current voltage relation (IV curve) has been shown to be crucial to transitioning the pyloric network of this system from non-oscillating to oscillating states. Here, models of the second messenger signaling of both this current's activation and voltage dependence are constructed and tested. First, we examine how the proctolin receptor activates $I_{MI}$ with the hypothesis that it signals through an intermediate signaling component. This is tested by bath application and pressure injection of agonists and antagonists of second messenger systems and examining their effect on neuromodulator induced $I_{MI}$. Consistent with this hypothesis, it is found that this proctolin-induced $I_{MI}$ is sensitive to modulators of G-protein function. Also consistent with this hypothesis, it is found that proctolin-induced $I_{MI}$ is sensitive to modulators of intracellular calcium concentration and calmodulin activated kinases. In contrast, there

seems to be no effect to acute applications of pharmaceutical activators and inhibitors of cyclic nucleotides, Phospholipase C, and receptor tyrosine kinase signaling. Next, we examine the mechanism of $I_{MI}$ voltage dependence that has been shown to be dependent upon extracellular calcium level and calmodulin signaling which we show is necessary for $I_{MI}$ voltage dependence by finding that application of calmodulin antagonists in normal calcium reduces $I_{MI}$ voltage dependence. However, it is found that calmodulin activators do not rescue $I_{MI}$ voltage dependence in low calcium so we propose that a Calcium Sensitive Receptor (CaSR) maintains $I_{MI}$ voltage dependence by active detection of extracellular calcium. This hypothesis is supported by several lines of evidence. First, $I_{MI}$ slope was increased by the specific calcium sensitive receptor antagonist NPS-2143 suggesting CaSR involvement. Second, $I_{MI}$ slope conductance was increased by exposure to the βγ-subunit inhibitor, gallein, suggesting that voltage dependence can be modulated by the βγ-subunit of trimeric g-proteins. Third, W7 induced linearization of $I_{MI}$ was reduced by pre-incubation of preparations with endocytosis inhibitors, suggesting that downregulation of a receptor is mediating W7 induced changes in $I_{MI}$ voltage dependence. Together, these results support the hypothesis that $I_{MI}$ voltage dependence is mediated at least in part by a CaSR-like G-protein coupled receptor (GPCR).

# Table of Contents:

# Table of Figures:

## Chapter 1: Figures:

# Chapter 1: Introduction

## 1.1 Introduction and Importance

Neuromodulators enhance the flexibility of neural networks by many means such as modulating intrinsic properties (i.e., preexisting conductances) (Benson and Levitan, 1983; Kiehn and Harris-Warrick, 1992; Harris-Warrick et al., 1995a; Harris-Warrick et al., 1995b) , modulation of synaptic properties (Johnson and Harris-Warrick, 1990; Johnson et al., 1993a, b; Zhao et al., 2011), reconfiguration of participating neurons within the network (Hooper and Moulins, 1990; Fenelon et al., 1998; Swensen and Marder, 2000, 2001), and modulation of plasticity itself (Zhou et al., 2007; Zhang et al., 2009; Pawlak et al., 2010). Recently, it has been shown that many neuromodulators mediate their effects by modulating currents whose IV curves contain regions of negative slope that are relatively linear in that region (Xu et al., 2009; Zhao et al., 2010) and can thus be thought of as effectively modulating leak currents. A model system to understand how neuromodulators control ionic currents, and possibly leak currents and therefore network activity, is the relatively simple pyloric network of the stomatogastric ganglion (STG) of *Cancer borealis*. In this system, the modulator-activated inward current ($I_{MI}$) has been shown to be downstream of the neuromodulator receptors that activate this rhythm (Golowasch and Marder, 1992b; Swensen and Marder, 2000, 2001). We use this system to test two hypotheses. First, we hypothesize that the proctolin

receptor that activates $I_{MI}$, does so by activating a pathway that involves a G-protein and a second messenger pathways that includes calmodulin, which then activates $I_{MI}$. As it has previously been shown that convergence of neuromodulators onto this current is important for enabling diverse network outputs, identifying an intermediate for proctolin-induced $I_{MI}$ would further the study of neuromodulation in the STG and the activation of diverse patterns of activity in general. Second, we hypothesize that $I_{MI}$ voltage dependence is due to extracellar calcium activation of a calcium sensitive receptor (CaSR). Previous studies have shown that the negative slope portion of $I_{MI}$'s IV curve allows it to effectively act as if it were a linear negative leak current in physiological voltage ranges (Zhao et al., 2010; Bose et al., 2014a). Therefore, it is important to understand the mechanism of $I_{MI}$ voltage dependence in order to understand oscillatory transitions. As negative conductance does not exist in biological cells, it is $I_{MI}$'s voltage dependence that enables it to produce this pattern of negative slope conductance. As $I_{MI}$ appears to be sensitive to intracellular calcium signaling (Swensen and Marder, 2000), it is also necessary to understand the second messenger mechanisms involved in $I_{MI}$ voltage dependence in order to properly understand neuromodulation in general.

*Leak conductance as the effector of neuromodulation.*

Neuromodulators can alter neuronal networks by targeting leak currents directly via downregulation (Kehoe, 1990; Bayliss et al., 1992; Talley et al., 2000; Xu et al., 2009) or upregulation (Brickley et al., 2007). More indirectly, neuromodulators can alter leak

functionally, by activation of regenerative currents (Izhikevich, 2007; Zhao et al., 2010). These currents, have negative regions of slope conductance in their IV curves and have historically been called negative slope conductances (Zhao et al., 2010; Bose et al., 2014a), or currents that counterintuitively increase what is called 'apparent resistance' (Engberg et al., 1978; Dingledine, 1983; Crunelli and Mayer, 1984; Mayer and Westbrook, 1984, 1985a; Haj-Dahmane and Andrade, 1996)[1]. This is because within certain voltages, measuring their resistance will lead to an apparent resistance increase, despite the demonstrated opening of currents (Engberg et al., 1978; Dingledine, 1983; Crunelli and Mayer, 1984; Mayer and Westbrook, 1984, 1985a; Haj-Dahmane and Andrade, 1996). An example of a leak current being directly downregulated by neuromodulators is shown in rat hypoglossal neurons where acidification, 5-HT, norepinephrine, substance P, Thryrotropin Releasing Hormone (TRH) and mGluR1 class agonists all reduce leak currents mediated via TASK-1 channels (Talley et al., 2000; Xu et al., 2009). Similarly, the importance of leak channels in neuronal rhythmic activity is shown by artificial deletion of TASK-3 channels in mice. Task-3 channels, thought to mediate leak conductance, can eliminate cortical EEG type II theta activity when deleted (Pang et al., 2009). Counterintuitively, Brickley et al., (2007) show that deletion of these same channels can actually reduce firing rate once action potential threshold has been reached as shown by increased accommodation. The authors show that this can be functionally rescued by artificial injection of the same current. The authors argue that

[1] Consider Figure 1.4B. Within a certain voltage-range, the slope of red is less than the slope of black, within this range apparent input resistance will look as if it had increased.

the reason for decreased excitability during high frequency firing is due to changing input conductance on the upstroke of the action potential and not due to the observed hyperpolarized resting membrane potential (RMP) of wild type relative to TASK-3 KOs (Brickley et al., 2007). A more indirect argument can be made for the importance of leak in controlling oscillatory activity in the Pre-Bötzinger complex. Del Negro et al., (2002) showed that when predicting which cells are oscillatory, the persistent sodium current, the traditional pacemaking current of this system, is, by itself, a relatively poor predictor. Instead, the authors of the paper show that the ratio of the persistent sodium current to leak current is a better predictor of whether a given cell will exhibit oscillatory activity (Del Negro et al., 2002). In contrast to a direct mechanism where neuromodulators actively reduce leak, Zhao et al., (2010) suggest that neuromodulators that activate currents with negative slope regions of their IV curves, such as $I_{MI}$, can be thought of as if they were effectively reducing the leak of a cell and therefore increasing excitability (Izhikevich, 2007; Zhao et al., 2010). The authors support this by decomposing $I_{MI}$ into positive and negative linear components. Using a dynamic clamp procedure, they injected these components of $I_{MI}$ into a cell that is part of the pacemaker of this system, the PD cell. They showed that while the negative component was necessary and sufficient to generate oscillatory activity, the positive component was not. This suggests that the functional importance of this current is given by the role of its negative slope portion and not simply due to its depolarized reversal potential (Zhao et al., 2010). Supporting this hypothesis further is the observation that many

regenerative currents such as voltage activated sodium and calcium currents share this characteristic negative conductance (Armstrong and Cota, 1991; Hille, 2001; Izhikevich, 2007), while still other poorly understood neuromodulator-activated currents also have negative leak portions of their IV curve (Benson et al., 1988; Freschi and Livengood, 1989b; Kehoe, 1990; Trimmer, 1994, 1995; Zhao et al., 2010).

## 1.2 $I_{MI}$ and the Stomatogastric Nervous System (STNS):

*Importance of conditional oscillators and the stomatogastric nervous system (STNS)*

Conditional oscillators are networks that require neuromodulation to transition from a non-oscillating to an oscillating state. These networks are a specific class of central pattern generators (CPGs), which are neural networks that produce oscillatory outputs without need of oscillatory inputs. Historically, neuronal activities now known to be mediated by CPGs, were wrongly explained as complex series of reflex arcs requiring sensory inputs. This was resolved when Wilson et al., (1961) showed in the locust wing, that ablation of timed input did not destroy oscillatory output (WILSON, 1961; Marder and Calabrese, 1996; Edwards, 2006) thereby proving that neurons could produce rhythmic outputs without patterned inputs. CPGs have important consequences for spatial encoding (Dragoi and Buzsaki, 2006), sleep wake transitions (Steriade et al., 1993), control of breathing (Butera et al., 1999; Del Negro et al., 2002; Doi and Ramirez, 2008) and especially locomotion (Forssberg et al., 1980; Harris-Warrick and Cohen, 1985; Marder and Calabrese, 1996; Edwards, 2006). This makes understanding the mechanism that switches a conditional oscillator from non-oscillatory to oscillatory states important. A relatively simple system that has been employed for the study of conditional oscillators with great success is the pyloric network of the crustacean STG.

*The pyloric rhythm of the stomatogastric ganglion.*

The STG is part of the stomatogastric nervous system (STNS) and consists of 25-26 neurons (Kilman and Marder, 1996) and two CPGs, a gastric network that controls movements of the gastric mill chamber and the teeth found there, and the pyloric network that controls the pylorus, a structure thought to act as a filtering apparatus. This is an ideal system for studying conditional oscillators due to its robustness, relative simplicity, easy control of endogenous neuromodulation, and identifiable cell types. The STG is innervated by three anterior ganglia that send endogenous neuromodulatory inputs to the STG neuropil through the stomatogastric nerve (*stn*). Here we focus on the pyloric network, as the connectivity of this system is well known, and the mechanism of action of a given neuromodulator can be systematically studied in different cell types. To remove endogenous neuromodulation the *stn* nerve is cut (decentralized), which results in the system falling silent. Figure 1.1A shows a preparation with its *stn* cut. As illustrated in Figure 1.1B, exogenous neuromodulators can then be applied (in this case pilocarpine), one at a time or in combination to study their effects on the network, and subsequently washed out (Figure 1.1C). Importantly, the application of different neuromodulators produces distinct patterns of activity, demonstrating the flexibility of this system (Swensen and Marder, 2001). This system also enables repeatable identification of cell type as will be described in chapter 2 (Figure 1.3). Both activation and the distinct patterns of activity produced by this system have been shown to be due to a mechanism common to a number of neuromodulators, the activation of the modulator activated inward current ($I_{MI}$).

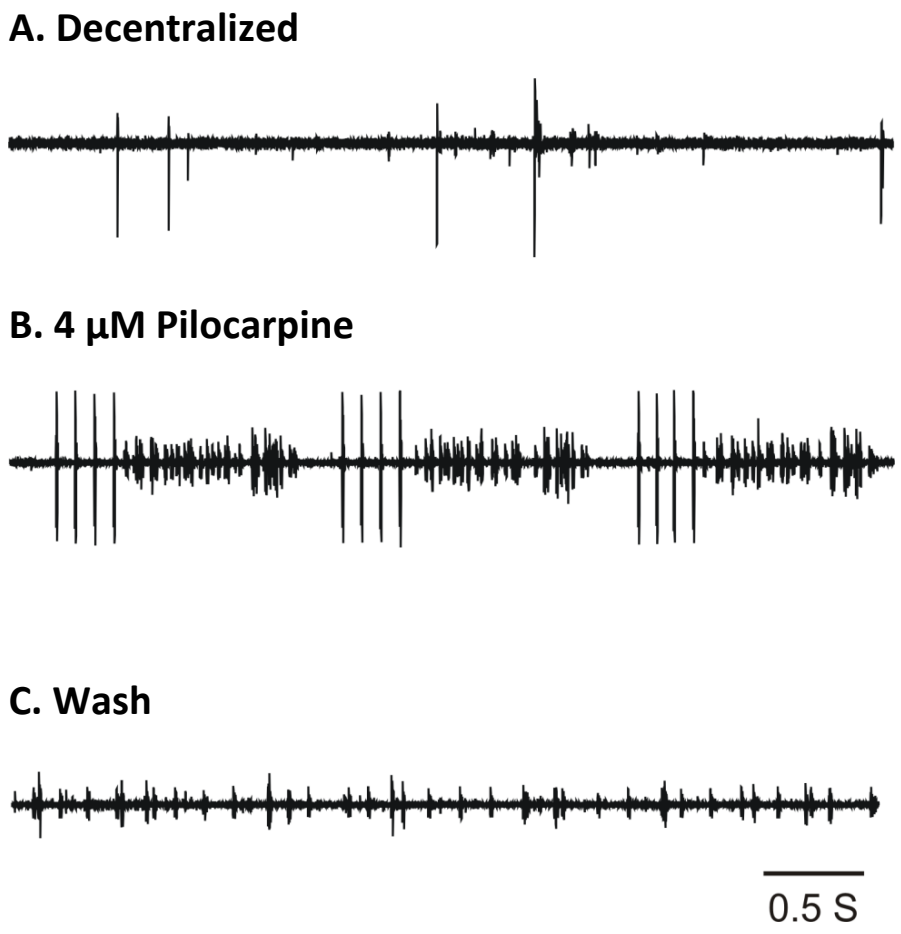


**Figure 1.1: The Stomatogastric Ganglion: a Model System for Study of Neuromodulation of Conditional Oscillators.** Effect of muscarinic agonist pilocarpine on decentralized preparation. (A) With endogenous neuromodulation removed recordings from *lvn* nerve are arrhythmic. (B) 4 µM pilocarpine induced a triphasic rhythm. (C) Upon washout, *lvn* falls silent.

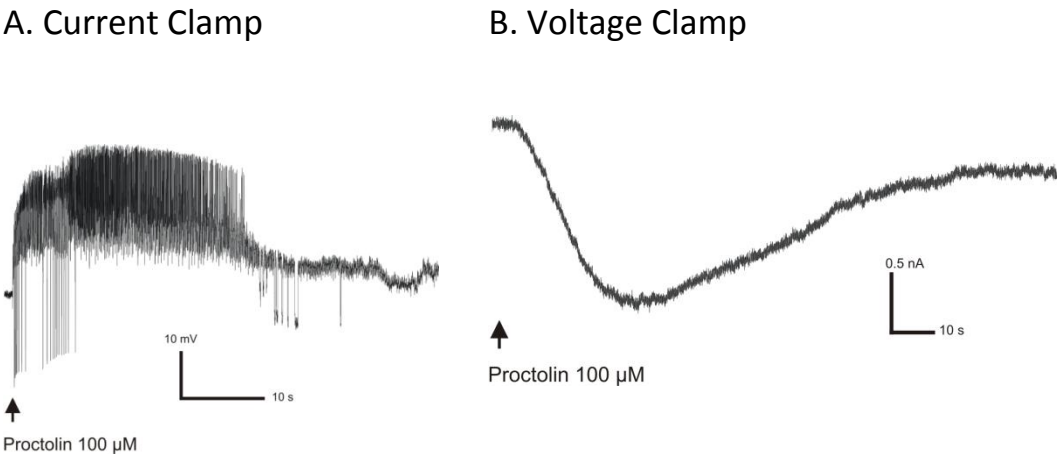


**Figure 1.2. Measurement of the Modulatory Inward Current ($I_{MI}$) in Current Clamp and Voltage Clamp**. (A) Current Clamp response of LP cell to 500 ms puff application of 100 µM proctolin (*arrow*) in 0.1 µM TTX, 10 µM PTX and 10 mM TEA. (B) Voltage clamp response of LP cell to 500 ms puff application of 100 µM proctolin (*arrow*) in 0.1 µM TTX held at -50 mV.

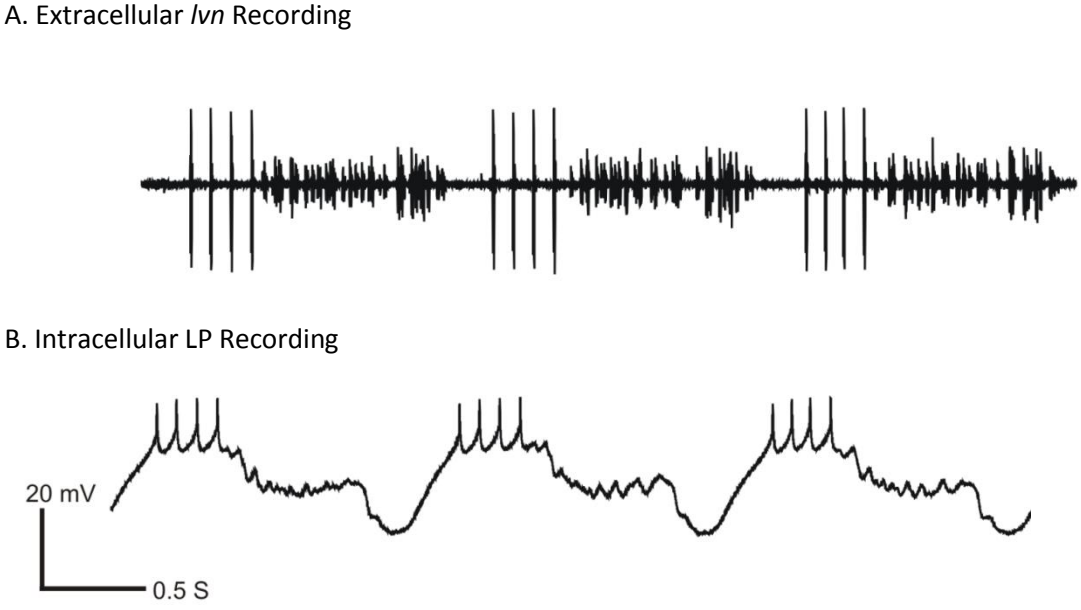


**Figure 1.3. Simultaneous Extracellular Nerve Recording and Intracellular Recordings Enable Unambiguous Identification of Cell Type in the STG.** (A) Extracellular recording from *lvn* nerve. (B) Intracellular recording from LP cell.

*The Modulator Activated Inward Current ($I_{MI}$): a common mechanism for oscillatory induction and pattern flexibility.*

As mentioned previously, neuromodulators that activate the pyloric rhythm of the STG are capable of not only of activating the rhythm, but also of producing distinct outputs that are characteristic of specific neuromodulators. As shown in Figure 1.2A for proctolin and in Swensen and Marder (2000), when these neuromodulators are applied (in this case proctolin), they all produce the same characteristic depolarizing response in an identified neuron, such as the LP cell (Swensen and Marder, 2000). The underlying source of this depolarization was shown to be $I_{MI}$. This current, first identified by Golowasch and Marder (1992), was shown to be an inward current with a region of negative slope conductance in its IV curve. This current, was measured in voltage clamp, by either step or ramp protocols as a difference current, that is, by executing the protocols in the presence or absence of the neuromodulator proctolin and calculating the current difference which is referred to as $I_{MI}$ (Figure 1.4B). Through ion replacement experiments, these authors showed evidence that the current was dependent on sodium while changes in chloride or potassium concentrations did not affect $I_{MI}$. Additionally, the authors showed that many divalent ions such as cobalt, barium and calcium were capable of blocking this current. Figure 1.4D shows this peculiar effect of calcium on $I_{MI}$. In normal calcium (**Black),** the current demonstrates characteristic voltage dependence, with an apparent reversal potential greater than zero mV, and

negative slope at negative voltages. When extracellular calcium is reduced (**Red**), this voltage dependence is lost. Golowasch and Marder (1992) noted the similarity of $I_{MI}$ to an NMDA-activated current (Nowak et al., 1984), and hypothesized that, instead of extracellular magnesium blockade, perhaps $I_{MI}$ was blocked by extracellular calcium, electrostatically drawn to the mouth of the channels, to explain the voltage dependence of the current. When extracellular calcium is lowered, calcium ions become less available to block the channel, thus reducing voltage dependence (Golowasch and Marder, 1992b) (Figure 1.4D). This is similar to what happens to the NMDA receptor in low magnesium conditions (Mayer et al., 1984; Nowak et al., 1984; Mayer and Westbrook, 1987; Purves, 1997). Consistent with this hypothesis is the finding that as calcium blocks the current at -40 mV, so too do other divalent ions (Golowasch and Marder, 1992b). This may represent a rescue of voltage dependence. It will be important to identify whether this block by cations other than calcium is linear or nonlinear because a restoration of voltage dependence rather than uniform block would support the NMDA-like hypothesis, similar to the finding that certain ions such as $Mn^{++}$, $Co^{++}$, and $Ni^{++}$ are capable of producing voltage dependent block of the NMDA receptor similar to $Mg^{++}$ (Nowak et al., 1984; Mayer and Westbrook, 1987; Ascher et al., 1988). Interestingly, magnesium was the only divalent tested that did not block $I_{MI}$ (Golowasch and Marder, 1992b). Later, Swensen and Marder (2000) contradicted this hypothesis. They showed that $I_{MI}$ might depend on calmodulin signaling, as the current was changed in the presence of the calmodulin inhibitor W7 (Swensen and Marder, 2000). Although it

had been shown by Hooper and Marder (1984) that both the peptides proctolin and FMRFamide were capable of restoring rhythm in quiescent preparations, as well as controlling the pyloric frequency in intact preparations (Hooper and Marder, 1984), the mechanism by which these peptides restored oscillatory activity was not understood. This was resolved by a series of papers that extended the study of $I_{MI}$ to different cell types and neuromodulators, and demonstrated its importance in generating oscillatory activity (Swensen, 2000; Swensen and Marder, 2000, 2001; Zhao et al., 2010).

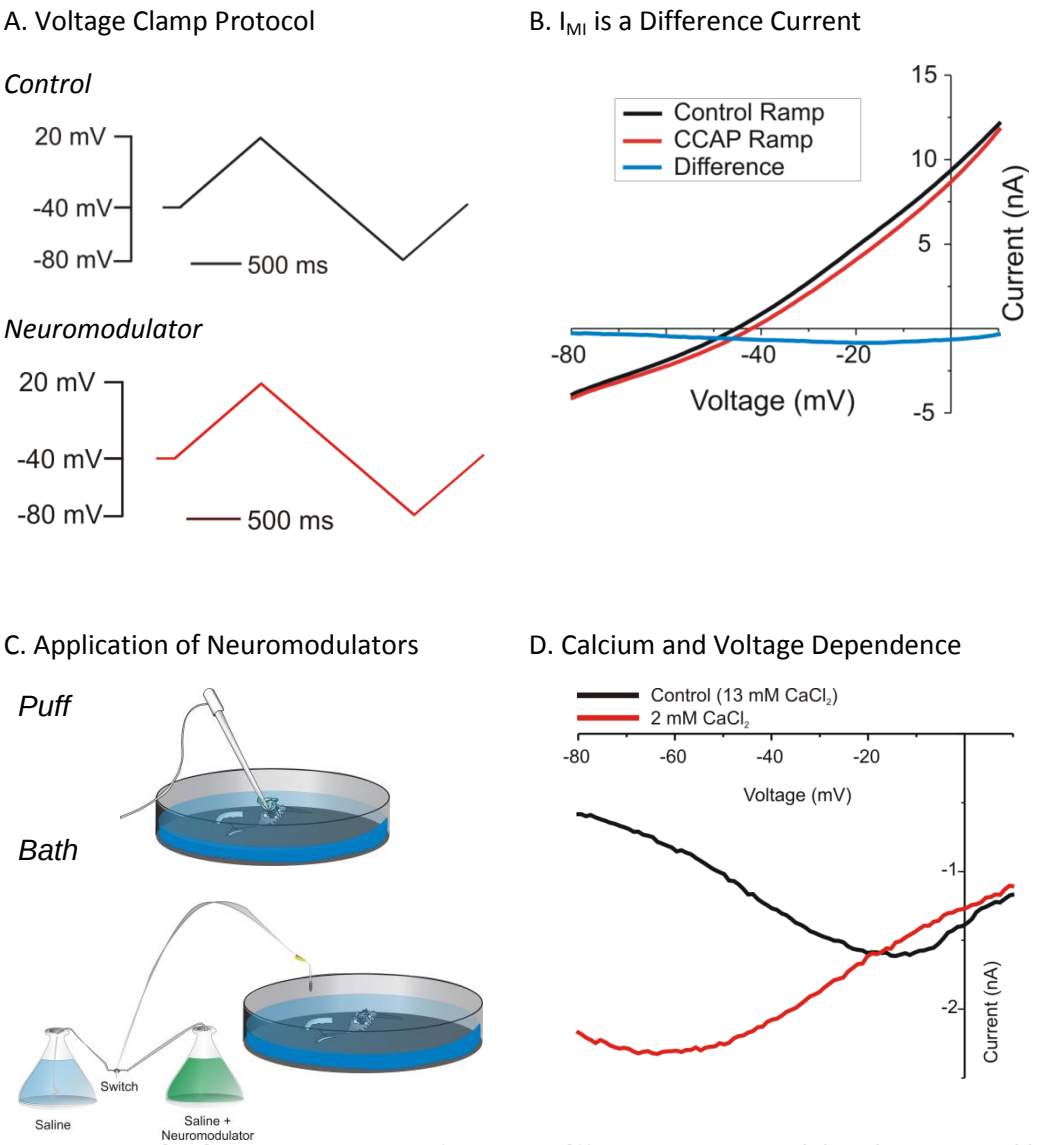


**Figure 1.4. Methods: Measurement of $I_{MI}$ as a Difference Current:** (A) $I_{MI}$ is measured in voltage clamp with a holding potential of -40mV. Voltage ramp protocol used for measurement of $I_{MI}$: the voltage is ramped from -40mv to +20 mV, down to -80mV and back to -40 mv. All ramps were done at -75mV/s. The center ramp was used for all experiments unless otherwise stated. This **black** ramp is the control ramp. A neuromodulator is then applied (CCAP) and the ramps are repeated after the neuromodulator has been applied (**Red**). (B) The **black** control ramp is subtracted from the **red** neuromodulator ramp and the resulting **blue** difference current is defined as $I_{MI}$. (C) Neuromodulators were either applied to the neuropil through pressure injection (*bottom*), or through bath application of 5-10ml of neuromodulator at the specified concentration (*top*). Due to the poor reproducibility and run down observed for pressure injection, all second messenger drug experiments used bath application of neuromodulator (D) $I_{MI}$ current voltage (IV) curve. Note that in normal calcium (**Black**) $I_{MI}$ has a negative slope from -80 mv to +20 mV. When extracellular $CaCl_2$ is

reduced to 2 mM, this slope becomes positive.

Aside from showing that these neuromodulators produced a current that shared the same calcium sensitive voltage dependence, Swensen and Marder (2000) revealed that different neuromodulators converged to activate the same current ($I_{MI}$) within an identified cell (Swensen and Marder, 2000). The authors did this by measuring the response to pressure application of proctolin in voltage clamp. They then bath applied CabTRP, another neuromodulator that activates $I_{MI}$, and then applied proctolin again. The authors noted that the proctolin response was much smaller in the presence of CabTRP suggesting that these neuromodulators converge to the same current, thereby occluding one another. In their methods section, these authors report that they tested various modulators of second messenger mechanisms including phospholipase C signaling[2], arachidonic acid signaling, and calcium chelators but do not report any positive or negative findings for these drugs. They did, however, find that preincubation of the calmodulin inhibitor W7 augmented $I_{MI}$ in response to proctolin. Interestingly, the enhancement was greater when the voltage was clamped at -80 mV rather than -40 mV, but while the authors noted a change in voltage dependence, they did not pursue this with follow up IV curves (Swensen and Marder, 2000). Here, we hypothesize that this effect is not enhancement of $I_{MI}$, but instead is a consequence of the reduction of $I_{MI}$

[2] The author says that for 2 preparations the PLC inhibitor U73122 had no repeatable effects on $I_{MI}$ (Swensen 2015, personal communication).

voltage dependence similar to that seen in low calcium. In a subsequent study, Swensen and Marder (2001) showed that all cells of the pyloric network are capable of producing $I_{MI}$, but that different cells respond to a specific subset of neuromodulators (they dubbed this 'divergence'). For example, while proctolin stimulated the LP, PD, anterior burster (AB), pyloric constrictor (PY), and inferior cardiac (IC), the neuromodulator crustacean cardioactive peptide (CCAP) only stimulated the AB, IC and LP neuron. The authors hypothesized that different neuromodulators produce distinct patterns of activity, because even though all cells produce $I_{MI}$, differential receptor expression on different cell types could allow cells to participate differently in the presence of different neuromodulators. The authors supported this hypothesis by using a dynamic clamp procedure to show that if artificial $I_{MI}$ current is injected into the PY and PD neurons (two cells that are not activated by CCAP), a CCAP-activated rhythm could be transformed into a typical proctolin-activated rhythm. The logic behind this is that as the major difference between CCAP and proctolin is that proctolin stimulates both PD and PY while CCAP does not, while both activate AB, IC and LP. By injecting the artificial current into PY and PD and quantifying the properties of the pyloric rhythm generated, the authors showed that this CCAP-induced rhythm was indistinguishable from a proctolin-induced rhythm. This result demonstrated that not only is $I_{MI}$ important for enabling oscillations, but cell-specific expression of different neuromodulator receptors that activate $I_{MI}$ confers the ability of different neuromodulators to produce different patterns of activity (Swensen and Marder, 2001).

As mentioned earlier, Zhao et al., (2010) proposed that leak is an important target of neuromodulation, and some neuromodulator-activated currents can be thought of as acting as negative leak conductances and can, therefore, be understood as reducing 'effective leak' to increase cell excitability. The authors support this claim by showing that normal oscillatory activity in the pyloric network can be restored by injection of a current with negative linear conductance with dynamic clamp into the pacemaker neurons (AB or PD), but not the follower neuron (LP). The authors also show that when preparations are decentralized (and consequently lose their rhythm), their leak increases. However, in a phenomenon known as 'recovery', where preparations decentralized for long periods spontaneously recover rhythmic activity, the leak drops to near control levels corresponding with currents with IV curves containing negative conductance regions. This suggests that the recovery may at least be in part due to downregulation of leak. In the case of neuromodulation, the authors argue that this is due to $I_{MI}$ effectively acting in the pacemaker to decrease leak. Further, the authors demonstrate that when only the negative slope portion of $I_{MI}$ is injected into the pacemaker, oscillatory activity is restored. In contrast to this, when only the positive conductance portion of $I_{MI}$ is injected, oscillatory activity is not restored. This suggests that generation of oscillatory activity is due to $I_{MI}$'s negative leak portion, and not just its ability to depolarize the neuron due to its depolarized reversal potential. Together, these results support the claim that the functionally relevant portion of $I_{MI}$ is its negative conductance region (Zhao et al., 2010). This makes understanding how $I_{MI}$ voltage

dependence is controlled, an important issue to understand activation of oscillatory mechanisms in general. Yet the cellular mechanism responsible for the negative slope region (or more generally the voltage dependence of $I_{MI}$) is not known, and this is one of the central topics of this thesis.

## 1.3 Receptors and Downstream Second Messenger Pathways of Proctolin and CCAP in Crustaceans and Invertebrates

As the first goal of this study is to identify how neuromodulator receptors activate $I_{MI}$, what is known of the neuromodulator receptors that activate $I_{MI}$, and mechanisms of signal transduction in other invertebrate systems will be reviewed. This is to provide background on why certain signaling mechanisms were tested first, as an exhaustive pharmacological study is usually not possible when dissecting mechanisms of this sort. Here, we examine the case that $I_{MI}$ induced by muscarinic agonists, CCAP and proctolin are mediated by G-protein coupled receptors (GPCRs). The reason for this is that despite the enormous diversity of GPCRs, they still represent only a subclass of receptors. It is wrong to assume that $I_{MI}$ is automatically mediated by these receptors without proper proof or precedent. For example, crustacean hyperglycemic hormone (CHH) has been shown to be mediated by a membrane-bound guanyl cyclase in the y-organ of crustaceans (Zarubin et al., 2009; Mykles et al., 2010b) and some FMRFamide receptors have been shown to be ionotropic in *Drosophila melanogaster* (Darboux et al., 1998). Therefore, the literature will be reviewed on what type of receptor is most likely downstream of the neuromodulators that activate $I_{MI}$. Further, we will examine what signal transduction pathways are classically downstream of a given neuromodulator. In the interest of brevity, we will focus on what is known about proctolin, as it is one of the best-studied invertebrate neuromodulators, and point out similarities and differences

between FMRFamide, muscarinic and CCAP neuromodulator receptors as needed. First, however we turn to the only peptide receptor that has any genetic basis to the claim that it is a GPCR in the STG specifically, the CCAP receptor.

*A CCAP receptor has been identified in the STG that correlates with a cell's ability to produce CCAP-induced $I_{MI}$.*

Garcia, Daur, Temporal, Schulz and Bucher (2015) recently sequenced a putative CCAP G-protein coupled receptor in the nervous tissues of *Cancer borealis*, CbCCAPr (accession number KM349850), and demonstrated that this mRNA had a higher copy number in cells that physiologically respond to CCAP with $I_{MI}$ (AB, LP, IC), than cells that do not (PY, PD) by using quantitative PCR with primers derived from the honey bee *Apis mellifera,* the flour beetle *Tribolium castaneum,* and the fruit fly *Drosophila melanogaster* (Garcia et al., 2015). This correlation of mRNA in cells responding to CCAP with mRNA copy number suggests that CCAP-induced $I_{MI}$ may be mediated by a GPCR in the STG.

*Pilocarpine induced $I_{MI}$ is suggestive of a muscarinic receptor, which in turn is indicative of a GPCR.*

As the nonspecific muscarinic agonist pilocarpine activates $I_{MI}$ directly in *C. borealis* (Swensen and Marder, 2000), it is very likely that pilocarpine induces $I_{MI}$ through a muscarinic receptor, which are GPCRs (Pfaffinger et al., 1985; Pfaffinger et al., 1988; Trimmer, 1995; Hille, 2001; Gomperts et al., 2002). Whether pilocarpine is acting

specifically and at what type of receptor, however, is another issue. Supporting the idea that pilocarpine acts as a muscarinic agonist and not nonspecifically, is the finding that oxotremorine, pilocarpine and muscarine have all been shown to activate the pyloric rhythm, a hallmark of $I_{MI}$, from quiescent preparations in *Jasus lallandi* (Bal et al., 1994). Likewise, Marder and Paupardin-Trisch (1978) found that methacholine, a muscarinic agonist, activates an inward $I_{MI}$-like current in this system whose amplitude decreased at hyperpolarized voltages (Marder and Paupardin-Tritsch, 1978). Also supporting pilocarpine activation of a GPCR, is the finding that two currents similar to $I_{MI}$ were identified in the cardiac ganglion of the lobster, *H. americanus,* in response to proctolin (Freschi, 1989) and the muscarinic agonist methacholine (Freschi and Livengood, 1989a). These currents both showed a striking resemblance to $I_{MI}$ in that both were mainly permeable to sodium, are inward and showed strong voltage dependence (reducing inward current with hyperpolarization), and reversal potentials of +18 mV and +24 mV for proctolin and methacholine, respectively (Freschi, 1989; Freschi and Livengood, 1989a). Although the author did not examine the effect of calcium on voltage dependence, or whether these currents occlude one another, it is difficult not to compare this to $I_{MI}$. In a later paper, Freschi (1991) characterized the methacholine current finding showing that it was produced by both pilocarpine and oxotremorine (Freschi, 1991). The author characterized this current by applying different muscarinic antagonists and compared the antagonist profile to that of other systems. The author found that this current was inhibited in order of potency of antagonists by: atropine >

pirenzepine> 4-diphenylacetoxy-N-methylpiperidine (4-DAMP)> methocryptine> hexahydodifenol≫AF-DX-116, gallamine. Although the sensitivity to pirenzepine was suggestive of a muscarinic receptor similar to M1 of mammals, the authors cautioned that 'pirenzepine-sensitive' would be a better label than 'M1-like' due to the failure of the current to be elicited by MCN-343 (an M1 specific antagonist). Although not shown for crustaceans, recent literature has demonstrated insect muscarinic GPCRs with similar signaling of m1/m3 class GPCRs of vertebrate species through PLC dependent pathways (Lecorronc and Hue, 1993; Trimmer, 1994, 1995; Qazi and Trimmer, 1999b). Interestingly, both pirenzepine and 4-DAMP sensitive cation currents elicited by muscarine in neurons of the thoracic ganglia in the locust *Locusta migratoria* (Benson, 1992; Trimmer, 1995), and also oxotremorine elicited currents in the ventral nerve cord of the tobacco hornworm *Manduca sexta* (Trimmer, 1994, 1995) and have been shown to have a similar pattern of voltage dependence (reduced inward current with hyperpolarization) to $I_{MI}$. Importantly, this literature suggests that pilocarpine-induced $I_{MI}$ is elicited by a GPCR rather than nonspecific action, and that this current appears to be mediated by M1/M3 like receptors in the cardiac ganglion of the lobster.

A less direct reason to believe that many neuromodulator receptors that activate $I_{MI}$ are GPCRs is that many of the receptors for proctolin (Mazzocco-Manneval et al., 1998; Puiroux et al., 1998; Egerod et al., 2003; Johnson et al., 2003), CCAP (Park et al., 2002; Cazzamali et al., 2003; Li et al., 2011; Lee et al., 2013) and FMRFamide (van Tol-Steye et al., 1997; Meeusen et al., 2002; Johnson et al., 2003) have been found to be

GPCRs (or at least dependent on GTP-hydrolysis) in other invertebrate preparations. Among these GPCRs, a PubMed literature search found only one example, FMRFamide-activated current, that was found not to be a GPCR (interestingly this was ionotropic) (Darboux et al., 1998). Although not conclusive, this literature suggests that GPCRs would be likely to be involved in the activation of $I_{MI}$ through CCAP, pilocarpine and proctolin until proven otherwise.

*What signaling pathways are downstream of proctolin, CCAP and muscarinic receptors in invertebrate systems?*

Assuming the receptors for proctolin, FMRFamide, CCAP and pilocarpine elicit $I_{MI}$ through GPCRs, what can the literature inform us about signal transduction pathways downstream of these receptors? Interestingly, there seems to be a recurring theme of convergence of these neuromodulators to cyclic nucleotides, PLC metabolites and calcium signaling. However, while the literature of proctolin signaling is quite rich for both skeletal and visceral invertebrate muscle, there seems to be a limited amount available for neuronal signaling.

*Proctolin signaling has been shown to be associated with cyclic nucleotides.*

In both crustaceans and insects, the pentapeptide proctolin has been show to produce reductions in both cAMP (Hiripi et al., 1979; Orchard et al., 1989; Banner et al., 1990; Bishop et al., 1991b; Mykles et al., 2010b; Mykles et al., 2010a) and less frequently in cGMP (Philipp et al., 2006). Interestingly, although cAMP reductions are

commonly associated with proctolin, the few examples of proctolin increasing cAMP levels are somewhat ambiguous (Hiripi et al., 1979; Bishop et al., 1991a; Erxleben et al., 1995). For example, in muscle of the crayfish *Procambarus clarkii*, Bishop, Krouse and Wine (1991) found that when inside out excised patches of crayfish skeletal muscle were exposed to proctolin 5 minutes prior to seal formation, the open probability of calcium channels was increased. In an attempt to identify a mechanism, the authors compared the probability of finding large calcium conductances in their control solution vs the same with bath application of the cAMP analogue CPT-cAMPs. The authors found significantly more large calcium channels in CPT-cAMP (58%) exposed patches than control patches (17%; $p < 0.01$). This result, though suggestive that the open probability induced by proctolin was mimicked by CPT-cAMP, was far from conclusive in showing that proctolin increases open probability in these channels via a cAMP dependent mechanism. First, there were no complementary experiments (e.g. does application of IBMX enhance detection as well?) to confirm this result. Second, the authors consistently reported the proportion of channels found, mean open time and mean close time for all other experiments but only report the proportion of large calcium channels found in the CPT-cAMP experiment. Interestingly, the authors report that the modulation of probability by proctolin was not present in winter months but can be restored by application of octopamine, an agent that does not affect the current by itself (Bishop et al., 1991a). This is an interesting result in that in both the oviducts of Locust *Locusta migratoria* and the foregut of the grasshopper *Schistocerca americana*,

where proctolin signaling is via cAMP reduction, proctolin often plays an antagonistic role to octopamine, a neuromodulator that signals through cAMP increase (Orchard and Lange, 1987; Banner et al., 1990; Nykamp and Lange, 2000). Another example of this ambiguity -- whether proctolin increases or decreases cyclic nucleotide levels-- is given by Hiripi and Miller (1979) who show that in homogenized brains of the *Locusta migratoria*, cAMP production was modulated by developmental stage. While proctolin produced no significant change in cAMP activity in larvae, it was shown to decrease cAMP in molting, and increase cAMP in adults. cGMP activity, however, was shown to be slightly decreased in both adults and larvae. Unfortunately, this paper was lacking in statistical analyses (Hiripi et al., 1979). A more complicated example of proctolin signaling by cyclic nucleotide reduction is given by Philipp et al., (2006), who show in muscle of the crustacean *Idotea emarginata*, that proctolin potentiation of muscle contracture is accompanied by a concomitant decrease in cGMP. Interestingly, this potentiation was independent of phosphodiesterase (PDE) as it remained in the presence of the PDE inhibitor 3-isobutyl-1-methylxanthin (IBMX). In addition, the potentiation could be mimicked by application of the PKC activator phorbol-12-myristate. Further, the proctolin-induced potentiation could be blocked by the PKC blocker bisindolylmaleimide-1 (BIM-1). The authors therefore argued that cGMP reduction was downstream of a PKC dependent mechanism and not due to direct coupling to a phosphodiesterase (Philipp et al., 2006). This literature suggests that while cyclic nucleotides are often downstream of proctolin signaling in invertebrates, proctolin

signaling by reduction of nucleotide levels appears more common than enhancement of cyclic nucleotide synthesis.

*PLC signaling downstream of proctolin receptor activation in invertebrate muscle*.

Along with the implication that PLC signaling is involved in proctolin signaling as shown by sensitivity to PKC inhibitors (Philipp et al., 2006), there are many other demonstrations of PLC pathways being downstream of proctolin signaling in invertebrate systems. Surprisingly, almost all of these examples are in skeletal or smooth muscle. By contrast, proctolin signaling in neurons is less well understood. Proctolin has been shown to increase the hydrolysis of phosphoinositides and has been directly assayed in oviducts (Lange, 1988), and hindleg muscle (Baines et al., 1996) of *Locusta migratoria,* and foregut of the roach *Blaberus craniifer* (Mazzocco-Manneval et al., 1998). In heart muscle of the horseshoe crab *Limulus polyphemus,* proctolin potentiates tension both in response to electrical stimulation and baseline tension. This effect was mimicked by application of the PKC activator phorbol 12, 13-dibutyrate (Groome and Watson, 1989). An interesting example of proctolin being dependent on PLC hydrolysis is shown in the stridulation behavior of the male grasshopper *Chorthippus biguttulus*. In this preparation, stridulation behavior can be induced by direct injection of muscarine, or proctolin into the protocerebrum. This can then be reversibly blocked with PLC inhibitors U73122 and Neomycin as well as the inositol-phosphatase inhibitor lithium [which indirectly inhibits PLC signaling by reducing the phospholipid pool (Berridge, 1989)] (Heinrich et al., 2001; Vezenkov and Danalev,

2009). Although these experiments show the necessity of phospholipase C in stridulation, it is unclear whether they are acting directly downstream of their receptors, or at secondary and tertiary neurons downstream of these primary neurons. Collectively, this literature suggests that examination of PLC signaling is a worthwhile candidate pathway for proctolin-induced $I_{MI}$.

*Proctolin downstream effectors are often dependent on extracellular and intracellular calcium.*

Many studies have linked proctolin directly or indirectly to modulation of calcium channels in both crustaceans (Nwoga and Bittar, 1985; Bishop et al., 1991a; Rathmayer et al., 2002) and insects (Baines and Downer, 1992; Wegener and Nassel, 2000). It is not clear, however, whether these actions represent direct activation of calcium channels, or a PLC dependent pathway, as some of these studies have shown PKC involvement (Groome and Watson, 1989), while others were unaffected by the inositol phosphatase inhibitor lithium (Wegener and Nassel, 2000). Yet others have shown the necessity for calcium influx despite being independent of PKC (Baines and Downer, 1992). An example of proctolin showing dependency on both external and internal calcium is shown in muscle of the barnacle *Balanus nubilus*. In this preparation, the authors injected radioactively labeled sodium into muscle fibers in the presence of oubain (a sodium/potassium ATPase inhibitor), and noted that application of proctolin increased the rate of sodium efflux. While changing external sodium concentration did not affect this efflux, lowering external calcium concentration completely abolished the response.

Similarly, the L-type calcium channel blockers verapamil and WB-4101, and the nonspecific calcium channel blocker $Cd^{++}$, completely abolished sodium efflux in response to proctolin. The authors also noted the response was reduced by intracellular injection of EGTA suggesting a role for intracellular calcium. In contrast, phosphodiesterase inhibitors, modulators of cAMP activity, and calmodulin inhibitors had no effect on the proctolin response. The authors suggested that proctolin mediates its response through modification of calcium channels (Nwoga and Bittar, 1985). These studies suggest that proctolin is not just dependent on intracellular calcium, but external calcium is also associated directly with proctolin signaling, or at least as a common effector.

*In invertebrates, CCAP, FMRFamide, and muscarinic signaling show similar second messengers systems to proctolin.*

One interesting finding is that a number of these currents activated by these neuromodulators have a sodium dependent conductance that decreases with hyperpolarization (Benson, 1992; Trimmer, 1994, 1995). There is also evidence for muscarinic signaling in insects through decreases in cAMP (Trimmer, 1995), and (unlike proctolin) increases in cGMP (Qazi and Trimmer, 1999a). In contrast to proctolin and muscarinic signaling, literature for CCAP signaling is scarce, although CCAP staining neurons are usually the target of ecdysis studies in insects and are associated with increases in cGMP, it is thought that this is due to eclosion hormone and not CCAP itself (Morton and Simpson, 2002). The only known requirement for CCAP to this author's

knowledge, is that stimulation of smooth muscle is dependent on extracellular calcium in the oviducts of *Locusta migratoria* and targets L-type calcium channels (Donini and Lange, 2002). Similar to proctolin and muscarinic 'M1/M3'-like receptors, FMRFamide has been shown to signal through PLC signaling in the heart of the snail *Lymnae stagnalis* (Willoughby et al., 1999). FMRFamide-like peptides have also been shown to signal through PLC in *C. elegans* (Kubiak et al., 2008), and surprisingly even vertebrates (Han et al., 2002). This literature suggests that neuromodulator receptors that activate $I_M$ –like currents seem to activate via nucleotides or PLC signaling in invertebrates. This finding led to a focus on these pathways as possible mechanisms of $I_{MI}$ activation.

## 1.4 Voltage Dependence Mechanisms of Currents Similar to $I_{MI}$ in Other Systems

*Voltage dependence of $I_{MI}$-like currents in other systems.*

$I_{MI}$ is unique in that it is a TTX and $Cd^{++}$ insensitive current whose voltage dependence is abolished by lowering external calcium. We will therefore review what is known about voltage dependence of sodium currents in other systems, especially those whose voltage dependence can be modified by external and internal calcium. A literature review suggests two primary mechanisms by which external calcium alters voltage dependence, and a third, less understood time-dependent desensitization. The first type, is direct blockade by ions or organic molecules, and is best exemplified by the previously mentioned NMDA current (Nowak et al., 1984; Mayer and Westbrook, 1985b; Kumamoto, 1996) and the NMDA hypothesis proposed by Golowasch and Marder (1992). There are also many other examples where calcium or divalent ions directly modulate sodium currents by charge screening or directly blocking them (Steinbach et al., 1944; Frankenhaeuser and Hodgkin, 1957; Yamamoto et al., 1984; Leibowitz et al., 1986; Nilius, 1988; Armstrong and Cota, 1991). The second primary mechanism by which calcium can control voltage dependence of cation conductances is by intracellular calcium carried from the outside of the cell via calcium permeability of the current itself or by activation of associated calcium currents. An example of this is the voltage dependence of the cyclic nucleotide gated channel activated by mGluR6

receptors in the retina of dogfish, mediated by both intracellular calcium and CamKII (Shiells and Falk, 1992; Shiells, 1999; Shiells and Falk, 1999, 2000, 2001, 2002), and by calcium in the salamander (Nawy, 2000). Other examples are given by voltage shifts in calcium channel inactivation by $Ca^{++}$ flux directly (Deleon et al., 1995) and indirectly via calmodulin (Peterson et al., 1999). A third, and less well understood example that appears independent of external calcium, is the agonist concentration dependent desensitization of $I_{CAT}$ (Cation current) of mammalian smooth muscle. This current is initially voltage independent, but increases its voltage dependence with increasing agonist application times or concentrations (Chen et al., 1993; Zholos and Bolton, 1995).

*The NMDA current is blocked in a voltage dependent manner by other divalent Ions.*

In addition to the voltage dependent block by magnesium mentioned earlier, the NMDA current can be blocked by many ions. An example is given by Mayer and Westbrook (1987) who found that in $Mg^{++}$ free saline, $Cd^{++}$ [3], $Mn^{++}$, $Co^{++}$, $Ni^{++}$ all produced significant block of the NMDA response, but only $Mn^{++}$, $Co^{++}$, $Ni^{++}$, produced this block in a voltage dependent manner similar to $Mg^{++}$ (Mayer et al., 1984). In support of the result for cobalt, Ascher et al., (1988) found in outside out patch clamp recordings, that cobalt but not cadmium produced channel flickering similar to magnesium without changing single conductance (Ascher et al., 1988). These results are relevant as they indicate that divalent ions can be used as a molecular probe to support

[3] Note that this concentration was 20 mM $CdCl_2$, 20 times the concentration previously reported to not affect NMDA currents by the same author and others.

the NMDA hypothesis proposed by Golowasch and Marder (1992). Interestingly, as external magnesium has been shown to provide outward rectification for NMDA receptors, Kupper et al., (1998) have shown that in the absence of external magnesium, intracellular magnesium produces inward rectification of NMDA receptors. This inward rectification can be abolished by mutations of certain asparagine residues that are believed to bind magnesium ions intracellularly (Kupper et al., 1998). Internal magnesium as well as many other positively charged organic molecules have been shown to mediate inward rectification internally (Ficker et al., 1994; Panama and Lopatin, 2006; Zhang et al., 2006; Vemana et al., 2008) . This literature provides a mechanism by which divalent ions can mediate both inward and outward rectification, internally and externally respectively. Further, these studies support the use of these ions as tools to establish a pharmacological profile for currents whose voltage dependence is mediated by extracellular block.

*Sodium currents in high calcium exhibit more voltage dependence than the same currents low calcium.*

The modulation of voltage dependence of sodium currents by external calcium has been known for close to 60 years now. For example, Frankenhauser and Hodgkin (1957) demonstrated that lowering calcium from high to low concentrations both hyperpolarizes the sodium current activation curve (less depolarization to activate the same conductance) and slows down deactivation without affecting maximal conductance. According to Armstrong and Cota (1991) this can at least be partially

explained by charge screening (gate shifting), where the positively charged calcium ions stabilize sodium channels in the closed conformation and direct block of calcium of sodium channels by calcium. (Armstrong and Cota, 1991; Hille, 2001). These results with others (Steinbach et al., 1944; Yamamoto et al., 1984; Leibowitz et al., 1986; Nilius, 1988), suggest that whether by direct blockade or gate shifting, calcium is an important modulator of the voltage dependence of sodium currents.

*Intracellular calcium and calmodulin provide feedback inhibition to inactivate L-type calcium channels.*

Many calcium channels, especially but not exclusively L-type calcium channels, exhibit time and calcium dependent feedback inactivation (Brehm and Eckert, 1978; Tillotson, 1979). A hyperpolarizing shift in calcium current inactivation can be shown by replacement of external calcium with permeable divalents such as $Sr^{++}$ and $Ba^{++}$ and examining the steady state currents. While the currents produced in normal calcium strongly inactivate with time, currents in these other divalents do not inactivate and maintain relatively constant amplitude. (Brehm and Eckert, 1978; Budde et al., 2002). Recent work has shown that there are calcium sensors that mediate calcium inactivation that detect calcium both directly and indirectly. Some L-type channels detect calcium directly as they have been shown to have an EF-hand domain in their structure (Deleon et al., 1995). Indirectly, calcium activates calmodulin that then inactivates the channel by binding to the calmodulin binding IQ domain that some L-type calcium channels possess (Peterson et al., 1999). In both cases, replacement of calcium with other

divalents that do not activate calmodulin lead to a hyperpolarizing shift of L-type channel inactivation. This makes it appear that these currents lose voltage dependence at depolarized voltage ranges when extracellular calcium is substituted for other divalents (Brehm and Eckert, 1978; Peterson et al., 1999).

*cGMP-gated currents of 'on'-bipolar cells have a CamKII dependent mechanism of desensitization that results in a change in voltage dependence.*

In the absence of light, 'on' bipolar cells of the dogfish retina hyperpolarize due to activation of mGluR6 by an increased level of glutamate produced by rod cells. This in turn activates a pertussis and cholera toxin sensitive G-protein[4] that activates a phosphodiesterase that reduces cGMP and closes a cGMP-gated cation current (Shiells and Falk, 1992). Shiells and Falk (1999) found that in the presence of calcium, these cells rapidly adapted to an extended light step, something that was abolished with intracellular BAPTA or the non-selective kinase inhibitor H-7 (Shiells and Falk, 1999). It was later found in both dogfish (Shiells and Falk, 2001) and the salamander retina (Nawy, 2000), that these responses were voltage-independent in low calcium conditions, and voltage dependent in normal calcium conditions with a negative slope conductance region in their IV-curves (reduced current with hyperpolarization). Shiells and Falk (2001) found that by including the CamKII inhibitor autocamtide-2 in the patch pipette, this voltage dependence could be abolished even in the presence of calcium.

[4] This is actually very unique for transducin as ADP-ribosylation is usually an indicator of $G_I/G_O$ for pertussis while the same by cholera is an indicator for $G_S$. Transducin is one of the few α-subunits with both a cholera and pertussis ADP-ribosylation site See Shiells and Falk (1992) or Gilman (1987) for review.

The authors concluded that this desensitization mechanism was a phosphorylation by CamKII of the cGMP-dependent cation channel that switched the channel from a linear to non-linear state (Shiells and Falk, 2001). These findings suggest that changes in voltage dependence can be due to intracellular second messenger modulations of ionic currents.

*$I_{CAT}$ of mammalian smooth muscle is instantaneously linear but voltage dependent at steady state.*

Another sodium permeable, voltage-dependent, current that superficially resembles $I_{MI}$ is the non-selective, cation, current ($I_{CAT}$) of smooth muscle in the rabbit and guinea pig ileum (Benham et al., 1985; Zholos and Bolton, 1995). This current, mediated via M2 type receptors (Bolton and Zholos, 1997; Komori et al., 1998), has the interesting property that it is instantaneously linear, but after prolonged application of muscarinic agonists, it displays increasing voltage dependence (Zholos and Bolton, 1995). Zholos and Bolton (1995) showed that, although this current is inhibited by both calcium and magnesium, and its voltage dependence is increased by magnesium, this voltage dependence is not exclusively mediated by divalent ions because it is still present in their absence. The authors showed that extended applications of the muscarinic and nicotinic agonist carbachol resulted in depolarizing shifts of this current's activation curve. (Zholos and Bolton, 1995). Similarly, Zholos and Bolton (1996) showed that voltage dependent desensitization was not sensitive to holding potential and that $I_{CAT}$ induced by the G-protein activator GTP-γS had a slower desensitization rate than

carbachol elicited $I_{CAT}$. The authors found that while large amounts of the G-protein inhibitor GDP-βS abolished $I_{CAT}$, small amounts increased carbachol induced $I_{CAT}$ voltage dependence (it depolarized the activation curve). The authors suggested that changes in $I_{CAT}$ amplitude and voltage dependence were due to G-proteins rather than other mechanisms such as ion blockade (Zholos and Bolton, 1996). These papers suggest that G-protein interactions and agonist concentrations can affect the voltage dependence of ionic currents.

*Currents with negative slope conductance: distinguishing reduced potassium currents from activation of anomalously rectifying cation currents can only be done through ion substitution.*

Sodium currents like $I_{MI}$ (Zhao et al., 2010), NMDA (Engberg et al., 1978; Dingledine, 1983; Crunelli and Mayer, 1984; Mayer and Westbrook, 1984, 1985a), and other currents with regions of negative slope conductance (Haj-Dahmane and Andrade, 1996) can be misinterpreted as reducing outward conductances due to an increase in their apparent resistance (Engberg et al., 1978; Dingledine, 1983; Crunelli and Mayer, 1984; Mayer and Westbrook, 1984, 1985a; Haj-Dahmane and Andrade, 1996). Examples of neuromodulator activated cation currents with negative-slope conductances were given previously, here we will provide an example of proctolin acting by closing outward conductances, where proper ion substitution experiments were done. An example is proctolin's capacity to close leak currents in the muscle fibers in the crustacean *Idotea baltica* (Erxleben et al., 1995). In this paper, the authors found that proctolin

potentiated muscle contraction by closing voltage-independent potassium channels (leak) which increased the resistance of these cells. These authors found that these effects were dependent on PKA, as they were mimicked by the cAMP analogue db-cAMP, and prevented by the PKA inhibitor Rp-cAMPS (Erxleben et al., 1995). This, and other examples (Nowak and Macdonald, 1983; Walther et al., 1998; Talley et al., 2000; Xu et al., 2009), suggest downregulation of outward conductances is an important target of neuromodulation that can result in negative-slope conductance difference currents.

## 1.5 The Calcium Sensitive Receptor (CaSR) and the sodium Leak Current (NaLCN)

The inhibition of NaLCN by CaSR (Lu et al., 2010) was a guiding model for this thesis. The original hypothesis that we had proposed was that neuromodulator-induced $I_{MI}$ was mediated by NaLCN, whose voltage dependence was controlled by the calcium sensing receptor. Although NaLCN has been shown to be voltage independent in other systems (Lu et al., 2007), we thought that the inhibition of NaLCN by CaSR observed in other systems could be thought of as inducing voltage dependence in this system. Therefore, a background on NaLCN and CaSR is reviewed.

*The Sodium leak current (NaLCN) is inhibited by the calcium sensitive receptor (CaSR)*.

An interesting mechanism by which sodium currents are regulated in vertebrate systems is illustrated by the sodium leak current (NaLCN) and its modulation by the calcium sensitive receptor (CaSR). NaLCN is a non-selective cation (sodium, potassium and calcium permeable), voltage-independent leak channel structurally related to voltage gated sodium and calcium channels in vertebrates (Lu et al., 2007). Lu et al., (2010) found that this channel is negatively regulated by the GPCR CaSR. These authors found that in wild type pyramidal cells of mouse hippocampus, reduction of calcium level leads to activation of a sodium dependent leak current. In NaLCN KO cells however, calcium had no effect on this current. Furthermore, the authors found that the response to lowering calcium could be rescued by injection of NaLCN cDNA, suggesting

that this gene was responsible for a sodium dependent leak current. The authors showed that this response was dependent on G-proteins by injecting the G-protein activator GTP-γS, which abolished the low calcium-induced sodium-dependent response. Similarly, when injecting GDP-βS, the cells were leaky in all conditions, displaying a high amount of sodium-dependent current regardless of calcium condition. The authors concluded that the sodium-dependent leak current induced by lowering calcium or blocking G-proteins with GDP-βS, was due to a lack of CaSR repression of NaLCN. The authors also showed this response could be reconstituted in HEK293 cells by expression of NaLCN, UNC80 and CaSR (Lu et al., 2010). This study suggests that NaLCN is repressed by a calcium sensitive receptor, and when switching to low calcium, the lack of repression increases the sodium-leak current. Many other studies have shown NaLCN to be downstream of neuromodulators such as substance-P (Lu et al., 2007; Lu et al., 2009; Lu et al., 2010; Kim et al., 2012) and neurotensin (Lu et al., 2009) in the hippocampus, ventral tegmental area, and coupled to M3 receptors in pancreatic β cells (Swayne et al., 2009). There have also been demonstrations that NaLCN-like currents that are regulated by extracellular calcium play an important role in parafollicular cells of the thyroid in sheep (McGehee et al., 1997). This literature suggests that NaLCN is both an important effector of changes in calcium concentration, and common effector of neuromodulators and hormones in both neurons, pancreas and the parathyroid gland.

*NaLCN is a non-selective cation channel that is activated by Substance P through a GPCR that is independent of G-protein activation.*

NaLCN is a non-selective, voltage-independent, TTX-resistant, $Gd^{+3}$ sensitive current that is activated by lowered calcium levels in the hippocampus (Lu et al., 2010). It is activated independently of G-proteins by substance P and neurotensin in hippocampus and VTA (Lu et al., 2010), and also independently of G-proteins by M3 receptors in β-cells of the pancreas (Swayne et al., 2009; Swayne et al., 2010; Kong and Tobin, 2011). In contrast to its G-protein dependence when responding to changes in extracellular calcium (Lu et al., 2010), it was shown by Lu et al., (2009) in the mouse hippocampus and VTA that the NaLCN response is mediated by a GPCR that is independent of G-protein activation. The authors showed that in mice with NaLCN KO, the substance P response is completely absent, and this can be restored by transfection with NaLCN cDNA. This suggests that the substance P response is mediated by NaLCN. Lu et al., (2009) then showed that the substance P response was mediated by a GPCR as it was blocked by the specific NK1R (the substance P receptor, which is a GPCR) blocker RPWK-SP (peptide sequence). The authors then found that while the G-protein modulators GTP, GTP-γS , GDP-βS, produced no change in the SP response, application of the tyrosine kinase blocker Genistein, or the specific Src family kinase(SFK)-inhibitor PP1 abolished the substance P response. Similarly, the authors showed intracellular perfusion of an SFK-activator induced a NaLCN-like response, and occluded response to substance P. Finally, the authors showed this system could be reconstituted in HEK-293

cells by transfecting them with NaLCN, NK1R, and UNC-80 (Lu et al., 2009). This paper suggests that substance P activates NaLCN through a GPCR that is independent of G-protein activation, and instead is dependent on SFK signaling. This has also been found for activation of NaLCN by M3 receptors in β-cells of the pancreas, where G-protein modulators are ineffective at modulating the response to acetylcholine but the same response is abolished by PP1 (Swayne et al., 2009; Swayne et al., 2010; Kong and Tobin, 2011). This report was quite interesting and strange in the idea that GPCRs can transduce signals through G-protein-independent pathways via SFKs, while calcium, in contrast, which is normally thought of as an intracellular messenger and not as an extracellular messenger, at least outside of tissues directly concerned with calcium metabolism (bone, liver, thyroid, and parathyroid) activates NaLCN through a G-protein dependent mechanism.

*CaSR is a GPCR that requires binding of activated calmodulin for continued expression on the cell surface.*

The CaSR is a calcium and amino acid binding receptor belonging to family C GPCRs with a binding site for activated calmodulin on its carboxy terminus that binds in the presence but not the absence of calcium (Huang et al., 2010; Huang et al., 2011; Chakravarti et al., 2012). A crucial assumption of this thesis is that activated calmodulin binding to CaSR stabilizes cell surface expression. This assumption is based on a very thorough study of calmodulin binding to CaSR by Huang et al., (2010) who predicted and then tested the presence of this intracellular calmodulin-binding domain. Consistent

with their prediction, through a coimmunoprecipitation assay[5] and other methods, they found that CaSR could be brought down in the presence of calcium, but not in the presence of low calcium buffered with EGTA. This confirmed the predicted calmodulin binding domain on CaSR was indeed a calmodulin binding domain that bound calmodulin in a calcium dependent way.

In a different vein of the same paper, Huang et al., (2010) showed that the predicted calmodulin binding site affected cell surface expression of CaSR through mutational analysis of the site. The authors expressed CaSR with various mutations in the calmodulin binding site in HEK293 cells and showed that raising extracellular calcium induced intracellular calcium oscillations in these cells. When the authors mutated CaSR and these mutations lay within the predicted calmodulin-binding domain, oscillations ceased, while mutations outside this site had no effect on oscillations. Fascinatingly, they demonstrated that the calmodulin inhibitor W7 itself was sufficient to stop oscillations in cells with wild type CaSR. This suggests that calmodulin is involved in CaSR signaling or activity.

Huang et al (2010) went on to show that cells with mutations in the calmodulin binding domain of CaSR were endocytosed and proposed a model for the function of this calmodulin binding site in stabilizing cell surface expression. This was done by doing a biotin protection assay, where CaSR was labelled with disulfide cleavable biotin; they found that mutations to the predicted calmodulin binding sites resulted in more

[5] IP= antiflag (incorporated into CaSR). IB= anti-calmodulin.

protected CaSR. This suggested that the lack of calmodulin binding (caused by mutation of the calmodulin binding domain) led to internalization of the receptor, where the biotin-cleaving enzyme could not access the biotin. The authors found no significant change in cAMP levels and proposed a model for PKC mediated endocytosis.

Huang et al., (2010) proposed a model for calmodulin stabilization of CaSR that is a central assumption of the current thesis. They proposed that bound calmodulin protected the T888 site from phosphorylation by PKC in a calcium dependent manner. In low calcium, the site would be unprotected by calmodulin and the receptor would be endocytosed, in high calcium however, the receptor would be covered by activated calmodulin. This would protect the site from phosphorylation by PKC and therefore CaSR cell surface expression would be stabilized. (Huang et al., 2010). These results are suggestive that not only does CaSR bind calmodulin in a calcium-dependent manner, but also that activated calmodulin is required for the continued surface expression of CaSR.

**1.6 Thesis Statement:**

The goal of this dissertation is to examine the second messenger mechanisms of $I_{MI}$ activation by the neuromodulators proctolin and CCAP and the mechanism of $I_{MI}$ voltage dependence. Understanding the second messenger systems activated by neuromodulators may provide a simple, coherent mechanism, for the phenomenon of neuromodulator convergence described by Swensen and Marder (2001). Further, previous research has shown that the process of recovery of pyloric activity after decentralization can be blocked by application of transcriptional inhibitors (Thoby-Brisson and Simmers, 2000). As this process is initiated by the withdrawal of the same neuromodulators under study (Thoby-Brisson and Simmers, 1998, 2000; Luther et al., 2003; Khorkova and Golowasch, 2007), and it has been shown that this process is independent of activity (Thoby-Brisson and Simmers, 1998), it can be therefore presumed that these neuromodulators are having an active suppressive effect on a transcription dependent process necessary for the regulation of several ionic currents and ultimately the recovery of pyloric activity. This makes understanding the second messenger mechanisms by which neuromodulator receptors activate $I_{MI}$ important. Second, understanding the second messenger mechanisms of $I_{MI}$ voltage dependence is crucial for understanding transitions between oscillatory states. This is due to the finding of Zhao et al., (2010) that the importance of $I_{MI}$ lies in the effects of its region of negative conductance, and not its role as a depolarizing leak conductance. $I_{MI}$ voltage

dependence appears to be sensitive to calmodulin signaling, but the full pathway is not known. It is therefore important to understand this mechanism in order to understand oscillatory transitions in this system. Finally, as this system has a proven record of providing insight into modulation of conditional oscillators, study of these second messenger mechanisms should advance understanding of neuromodulation not only within the STG community, but also for the study of neuromodulation in other conditional oscillators.

*Hypothesis One: Neuromodulator receptors that activate $I_{MI}$ do so through a GPCR activated signaling pathway.*

Insofar as Swensen and Marder (2000) showed that different neuromodulators converge to the same current, (Golowasch and Marder, 1992b; Swensen, 2000; Swensen and Marder, 2000), it would make sense that different neuromodulator receptors activate $I_{MI}$ through a common intermediate. Therefore, it is hypothesized that neuromodulator receptors activate an intermediate signaling pathway that activates $I_{MI}$ rather than activating $I_{MI}$ directly. The reasoning behind this hypothesis is merely parsimony. At least six neuromodulators have been shown to activate the same current (Swensen and Marder, 2000, 2001). Therefore, this hypothesis is most reasonable to start with because it is the simplest. An alternative to this hypothesis would be that neuromodulator receptors discretely signal to $I_{MI}$ through distinct pathways. To examine the first hypothesis, it will be determined whether $I_{MI}$ signaling is G-protein dependent and what, if any, specific downstream signaling pathways are

involved. Due to the limited scope of this thesis, only proctolin (mainly) and CCAP (secondarily) will be examined with the assumption that once an intermediate is identified, only then can the hypothesis of convergence be examined.

*Hypothesis Two: Calcium-sensitive voltage-dependence of $I_{MI}$ is due to active sensing of extracellular calcium by a G-protein coupled receptor whose ligand is calcium.*

The finding by Swensen and Marder (2000) that shows that $I_{MI}$ voltage dependence can be influenced by the calmodulin antagonist W7 in the presence of normal calcium suggests that intracellular calcium signaling, rather than blockade of $I_{MI}$ by external calcium, mediates $I_{MI}$ voltage dependence. In this thesis, it will be shown that although calmodulin is necessary for $I_{MI}$ voltage dependence, it is not sufficient. Instead, it is proposed that LP cells actively sense extracellular calcium by a calcium sensitive receptor. This, in turn, sends a 'voltage dependence' signal to the current, which switches $I_{MI}$ from a voltage-independent to a voltage-dependent state.

# Chapter 2: Methods

## 2.1 Introduction:

This chapter will discuss the general methods used to pharmacologically dissect and measure the second messenger mechanisms of $I_{MI}$ activation and its voltage dependence. The chapter will also address the problem of stability of $I_{MI}$ amplitude and slope, which is necessary in order to determine the effects of these slow acting pharmaceutical agents. An outline description is provided for how the current was measured, what blockers were used for its measurement and the effect of voltage protocols on its measurement. The cell types and neuromodulators used for its measurement are specified. This is followed with a discussion of the differences in the desensitization rate between normal and low calcium. A central theme of this thesis is the separation of $I_{MI}$ voltage dependence and activation. It is unknown a priori whether a particular activator or inhibitor will affect $I_{MI}$ activation or voltage dependence or both. A systematic methodology for separating and quantifying the two is developed.

## 2.2 General methods

*Preparation.*

Crabs of the species *Cancer borealis* were purchased from local fisheries and housed in saltwater aquaria at 8-12°C. Crabs were anesthetized on ice at least 30 minutes prior to dissection. The stomatogastric nervous system (STNS) was dissected out and pinned on Sylgard dishes as previously described (Maynard and Dando, 1974; Selverston et al., 1976). The isolated STNS was continuously perfused with chilled saline (12-14°C) composed of (in mM): 440 NaCl, 11 KCl, 13 $CaCl_2$, 26 $MgCl_2$, 5 maleic acid, 11 Trizma base and adjusted to a pH of 7.4-7.5. For low calcium solutions, $MgCl_2$ was added in equimolar amounts to compensate for reduced calcium. In all experiments, the STG was exposed by desheathing and pinning down the surrounding connective tissue to expose the neuropil. Unless otherwise noted, all data reported here were obtained from LP neurons. Concentrations of calcium at or below 2 mM were found to depolarize LP cells and increase their input conductance (See figure 2.9, 2.10 and below). To attenuate this effect, low calcium saline was supplemented with 0.5% bovine serum albumin in all low calcium experiments.

*Electrophysiology.*

Extracellular recordings were made by making Vaseline wells around *lvn* or *dvn* nerves and recorded through stainless steel wires using an AM systems 1700 differential AC amplifier (Carlsberg, WA). Ground electrodes were either AgCl pellets (Molecular

Devices, Sunnydale, CA) or chlorided silver wires. All intracellular recordings, unless otherwise stated, were obtained with an Axoclamp 2B amplifier (Molecular Devices, Sunnydale, CA) and digitized with either a Digidata 1322A or 1440 (Molecular Devices, Sunnydale, CA) and recorded onto a windows PC using the pClamp 9 or 10.4 software suite (Molecular Devices, Sunnydale, CA). Currents were recorded in two-electrode voltage clamp (TEVC) and were passively filtered using an RC filter at 4 KHz cut off frequency. A circuit diagram of this filter is available at stg.rutgers.edu. Electrodes were pulled on a Sutter P-97 puller (Navato, CA) with resistances of 15-25 MΩ for the voltage electrode (ME1) and 10-20MΩ for the current electrode (ME2). All recording solutions were 20 mM KCl + 0.6M $K_2SO_4$. The same was used for current injection solutions except for pressure injection experiments. These used 500 mM KCl with or without 20 mM TEA. Pertussis toxin injection experiments and their controls used solutions buffered with 10 mM HEPES to a pH of 7.2. dsRNA injection experiments used dsRNA dissolved in 30 mM KCl.

*Cell Identification*.

LP cells were identified by hyperpolarizing LP to silence the LP phase of extracellular *lvn* recordings (Figure 1.3). If *lvn* recordings were not available, LP cells were hyperpolarized and the disappearance of LP inhibition from simultaneous intracellular recordings of PD neurons were used to confirm LP identity.

*Neuromodulators.*

Proctolin was purchased from American Peptide or BaChem. CCAP was initially purchased from American Peptide, but in winter 2013-spring 2014 this peptide did not produce comparable $I_{MI}$ to that reported in the literature (Swensen and Marder, 2000) and to that in our own previous experiments with different samples from the same company , so all CCAP data from 2013-2014 was omitted and all later CCAP came from BaChem. All other neuromodulators were obtained from Sigma.

*Signal Transduction Modulators/ Chemicals:*

N-(6-Aminohexyl)-5-chloro-1-naphthalenesulfonamide hydrochloride (W7), tetraethyl ammonium (TEA), caffeine, picrotoxin, forskolin, $LaCl_3$, $GdCl_3$, $BaCl_2$, $CoCl_2$, $MnCl_2$, pilocarpine, dopamine, 8-Bromoadenosine-3',5'-cyclic monophosphate sodium salt (8-Br-cAMP), 8-Bromoguanosine cyclic 3',5'-monophosphate sodium salt (8-Br-cGMP), guanosine 5'-[β-thio]diphosphate trilithium salt (GDP-βS), genistein, 1,2-Bis(2-Aminophenoxy)ethane-N,N,N',N'-tetraacetic acid (BAPTA-TAA), Dynasore, N-[2-(p-Bromocinnamylamino)ethyl]-5-isoquinolinesulfonamide dihydrochloride (H89), 1-(5-Iodonaphthalene-1-sulfonyl)-1H-hexahydro-1,4-diazepine hydrochloride (ML-7), Guanosine 5'-[γ-thio]triphosphate tetralithium salt (GTP-γS), Okadaic Acid, Gallein, Thapsigargin, Fluphenazine, and Neomycin came from Sigma-Aldrich. W7, 1,2-Bis(2-aminophenoxy)ethane-N,N,N',N'-tetraacetic acid tetrakis(acetoxymethyl ester) (BAPTA-AM), calcium ionophore A21387, Cyclosporine A, edelfosine (Et-18-$OCH_3$) and tetrodotoxin (TTX) came from Tocris Bioscience. Calmidazolium, dantrolene, ryanodine, pertussis toxin A protomer and staurosporine came from Enzo Life Sciences. CALP1

(Sequence: VAITVLVK) and proctolin came from American Peptide. CCAP and proctolin came from BaChem. TTX came from Calbiotech. Bovine Serum Albumin (BSA) came from Fisher Scientific. N-[2-[[[3-(4-Chlorophenyl)-2-propenyl]methylamino]methyl]phenyl]-N-(2-hydroxyethyl)-4-methoxybenzenesulphonamide (KN-93) came from EMD Bioscience. Dasatinib came from Selleck Chemical. NaLCN and mRNAs were a kind gift from Dr. David Schulz. All chemicals were aliquoted in either $dH_2O$ or DMSO and frozen until use.

*Statistics and Data Analysis.*

All calculations for $I_{MI}$, difference currents and leak subtractions were done in the pClamp 9 or 10.4 (Molecular Devices) family of software. All data were electronically filtered using a 8-pole Bessel filter with a cut-off frequency of 320 Hz. Data were reduced so that the currents measured in a ramp were divided into 1 mV bins of approximately 13.3 ms. This data was stored in Microsoft excel for databasing and graph making. All statistics were done in SigmaPlot 11 except for those analyses that required analysis of covariance. These were done in IBM SPSS Statistics 22. Some data were found to be non-normal and/ or not homoscedastic. For two group comparisons, Mann-Whitney Rank-Sum tests were run. In multiple group comparisons, the dependent variable was ranked, and statistics were run on this rank score. All data after this transformation passed either a SigmaPlot 11 equal variance test (f-test) or Levene's test (SPSS). If data passed normality testing (Shapiro-Wilk; $p > 0.05$) after a transformation, statistical testing was carried out on the ranked dependent variable. If data failed normality testing after transformation, all statistical testing was carried out on the

original data. With the exception of the forskolin difference current (figure 3.8), no data failed equal variance testing after rank transformation. All graphs making comparisons between conditions show averages ± standard error of the mean (SEM).

We set experiment-wise significance level (alpha) for our pilot experiments at $p = 0.10$ to reduce type II error at the expense of increasing type I error. Originally it was anticipated that slope conductance centered at -55 mV and amplitude at -15 mV would be relatively independent of one another. Upon analyzing these variables, however, it was found that they had a strong linear dependence (data not shown; e.g. a violation of the assumption of independence). Therefore, for experiments in which both slope and amplitude were measured, a multiple comparisons procedure was done to account for the lack of independence of these variables. Specifically, we used the Bonferroni inequality (Ott and Longnecker, 2001), a conservative test, to account for multiple comparisons ($m = 2$) of these two related variables, such that we considered only a $p \leq 0.05$ to be significant to maintain experiment-wise $\alpha$ of $p < 0.10$.

*Measurement of Ionic Currents*

The high threshold potassium current ($I_{HTK}$) was measured in TEVC by stepping from a holding potential of -40 mV, down to -60 mV and then up to +30 mV in 10 mV increments for 800 ms with 3 seconds in between sweeps. This current was leak subtracted using the input resistance ($R_{IN}$) calculated at -50 mV in voltage clamp from the same protocol. The peak current typically occurred after 3-9 ms after a voltage step,

and the average of this was used for IV curve construction and statistical analysis and was reported as transient $I_{HTK}$. The portion of this same current from 750- 800 ms after a step was defined and reported as $I_{HTK}$ steady state. $I_A$ was defined as the non-leak subtracted $I_{HTK}$ subtracted from the same protocol except with a holding potential of -80 mV. This is because it has been shown that at a holding potential of -40 mV $I_A$ is completely inactivated (Golowasch and Marder, 1992a) and therefore residual current should be $I_A$. $I_A$ inactivation was measured by steps to pre-pulses from -100 mV to -30 mV, in 10 mv increments to a test-pulse of +20 mV. The current measured at the test pulse was plotted as a function of pre-pulse voltage for curve fitting and analysis. Calculation of maximal conductance values ($I_{MAX}$), step widths ($V_C$) and half activations ($V_{1/2}$) were made by fitting data to a first order Boltzmann charge-shift function present in Clampfit 9 or 10 (Molecular Devices, Sunny Dale California). This was made based on the assumption of first order activation[6], and equations found in Bucholtz et., al (1992). $I_A$ inactivation was normalized to peak values before fitting, as this fitting function was prone to failure if individual seed values were not provided to the program one at a time prior to fitting.

[6] It is noted that this may not be appropriate for some cases, especially transient $I_{HTK}$, as shown by Golowasch and Marder (1992), this current is made up of at least two components. The first is calcium sensitive, while the second is similar to the delayed rectifier. It was decided that since this was not the main objective of this study, this assumption was adopted for convenient comparisons across conditions.

## 2.3 Measurement of $I_{MI}$

*Solutions.*

Unless otherwise stated, all recordings of $I_{MI}$ were made in the following standard "$I_{MI}$ recording saline" that contained normal Cancer saline plus 0.1 µM tetrodotoxin (TTX) to block sodium currents, 20 mM tetraethylammonium (TEA) to block potassium currents, 10 µM picrotoxin (PTX) to block synaptic currents, 5 mM CsCl to block the H-current, and 200 µM $CdCl_2$ to block calcium currents. In some cells, spontaneous oscillations were observed under these conditions, when this happened, TTX and PTX concentrations were transiently raised to 1 µM and 30 µM respectively until oscillations stopped or were attenuated. Then, normal solution was resumed for at least 20 minutes prior to measurement of $I_{MI}$.

*Neuromodulator and Drug applications:*

Neuromodulators were either pressure injected (puff) (Figure 1.4C top) or bath (Figure 1.4C bottom*)* applied. Due to the poor reproducibility of puff applications, only bath applications were examined statistically. Both Proctolin and CCAP were bath applied at 1 µM for a volume of 5-10 ml at a perfusion rate of 3-4.5 ml/s. External pressure injection of neuromodulators and intracellular pressure injection of drugs both used a Picospritzer II (Holzheim, Germany). Puff applications were calibrated by eye with 1% fast green and neuromodulator responsiveness on the *lvn* nerve. However, this was later abandoned as fast green did not appreciably increase the visibility of cells during

intracellular pressure injections and increased the variability for required injection pressure compared to solutions without fast green.

*$I_{MI}$ Voltage Clamp Protocol.*

A holding potential of -40 mV was used (Golowasch and Marder, 1992a) to prevent $I_A$ contamination. Figure 1.4 illustrates the procedure used to obtain $I_{MI}$. The voltage was ramped from a holding potential of -40 mV, up to 20 mV, down to -80 mV, and back to -40 mV at 75mV/s. The descending ramp was used to build IV curves and determine $I_{MI}$ properties. This is because it has been shown in our lab that measurement of $I_{MI}$ on descending ramps is less sensitive to ramp speed than ascending ramps (D. Fox Personal communication, 2015). These ramps were applied every 35-45s until the current recorded stabilized, that is, no change in leak was observed. At this point, the average of the last 3-5 ramps was defined as the control ramp. Figure 1.4B shows this control ramp (**black**). Neuromodulator was then applied by volume for 5-10ml. The average of 3-5 ramps at the peak of the response to neuromodulator was defined as the neuromodulator ramp (**red**). The control ramp (**black**) was subtracted from the neuromodulator ramp (**red**), and this difference current (**blue**) is defined as $I_{MI}$. Generally, any neuromodulator application where the wash ramp did not reduce to at least ½ of its maximum value was discarded. This was not done, however, in experiments where controls could not be measured in the same preparation (pressure injection experiments). Because the base value of $I_{MI}$ was unknown in these experimental conditions. Therefore, the failure rate in controls must be factored into

this analysis so as not to bias data in favor of control experiments (see chapter 3 for further explanation). The raw data for this procedure is illustrated in figure 2.1. where the voltage in both control (**Black**) and neuromodulator (**Red**) is “ramped”. Note the difference in $I_{MI}$ current (**Blue**) relative to the actual ramp position.

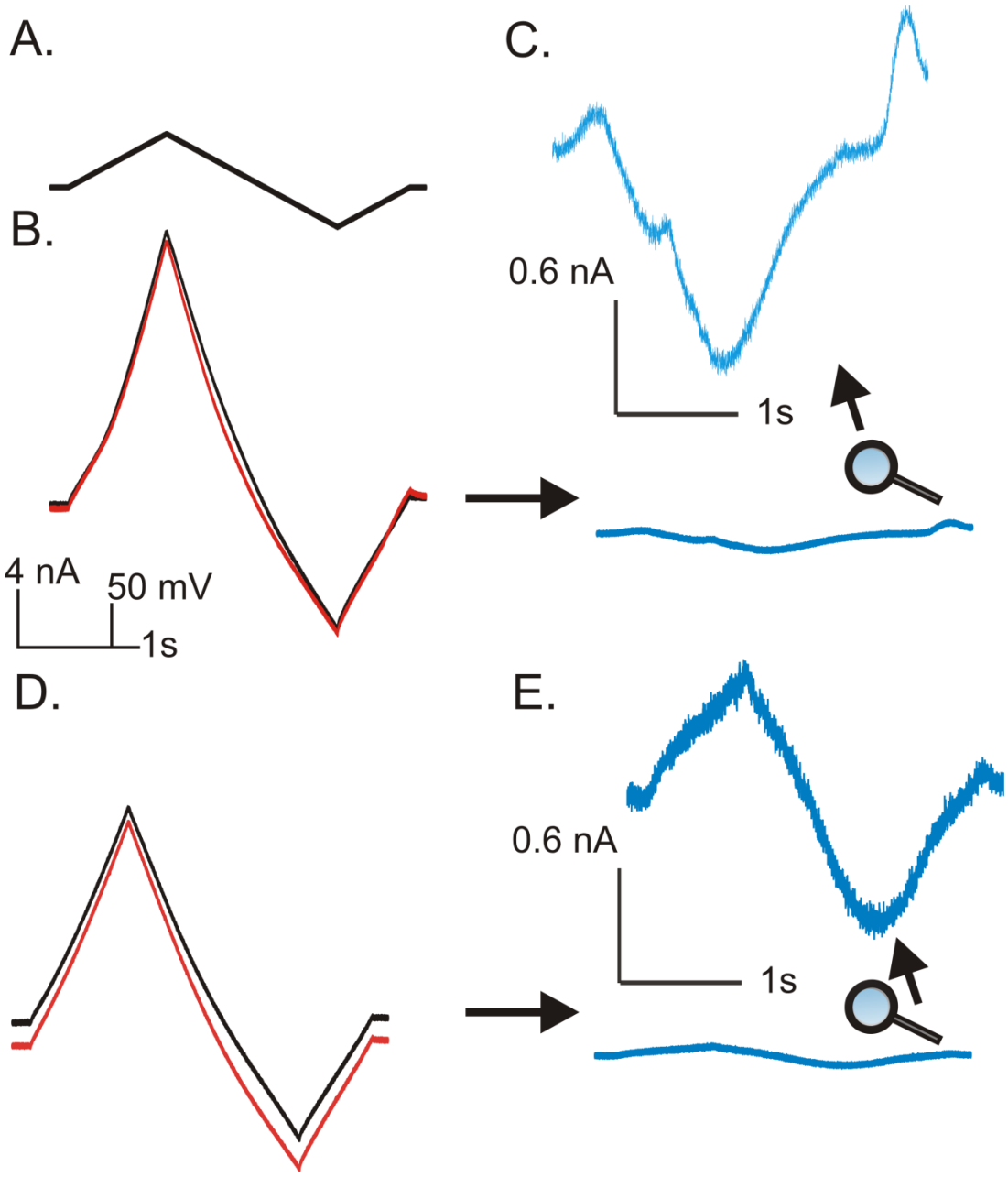


**Figure 2.1. Raw traces of Proctolin-induced $I_{MI}$.** Proctolin (1 µM) induced $I_{MI}$ IV relations in the same LP cell in the normal calcium and low calcium. Saline contained 0.1 µM TTX, 10 µM PTX, 200 µM CdCl2, 5 mM CsCl and 20 mM TEA, (A) Ramp Protocol. (B) Ramp Current (**Black**) and ramp current after application of proctolin (**Red**). (C) $I_{MI}$ Difference current (**Blue**) (D-E) same as in B & C except in the presence of 2 mM $CaCl_2$.

## 2.4 Properties of $I_{MI}$ that Affect its Measurement.

As mentioned previously, $I_{MI}$ is a relatively slow, sodium permeable current that loses its voltage dependence when extracellular calcium is reduced (Golowasch and Marder, 1992b). Figure 1.2A shows the response of an LP neuron to a pressure application of proctolin applied directly to the ganglion. Despite the presence of TTX, TEA, and PTX, the cell shows fast oscillations. A similar experiment is shown in Figure 1.2B where proctolin is pressure applied in a voltage clamped LP neuron. Note the slow time course of these experiments despite the 500 ms application time. This slow time course enables averaging of ramps for better signal to noise ratios but unfortunately requires long washout times. It was found additionally that there was a higher variability when proctolin was pressure applied versus bath applied. Thus, all following data shown for this thesis used bath application of neuromodulators.

*Proctolin induced $I_{MI}$ is similar when measured using step and ramp protocols.*

In order to examine the effect of second messenger modulators on $I_{MI}$ voltage dependence it is desirable to measure at as many voltage points as possible, as is the case during a voltage ramp. As $I_{MI}$ was first measured with step protocols, but shown to be similar when measured with ramp protocols (Golowasch and Marder, 1992b), we wished to verify that this was true for our protocol. Figure 2.2 shows a step protocol (A), and the resulting proctolin induced $I_{MI}$ (B). Figure 2.2C shows the standard ramp protocol and its resulting proctolin induced $I_{MI}$ (D) under the same conditions. Although

not identical, these samples show that using ramp or step protocols produces similar results.

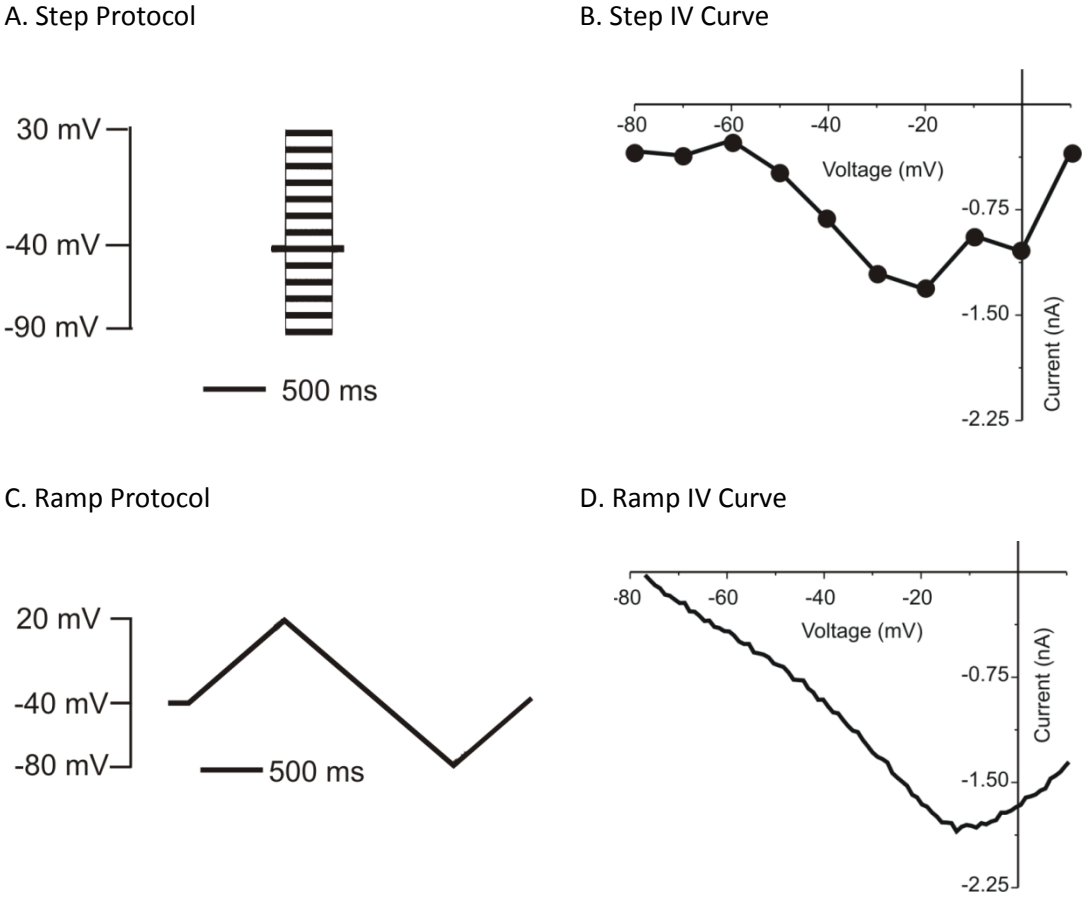


**Figure 2.2: Steps vs Ramps.** Proctolin (1 μM) induced $I_{MI}$ IV relations from 2 different LP cells in the presence of 0.1 μM TTX, 10 μM PTX, 200 μM $CdCl_2$, 5 mM CsCl and 20 mM TEA, (-40 mV resting voltage). (A) Step protocol from -80mV to +20 mV in 10 mV steps. (B) $I_{MI}$ IV curve obtained from using step protocol. (C) Standard voltage ramp protocol. (D) IV curve obtained from using standard ramp protocol. Note that these samples are very similar. (IVs truncated above +10 mv due to high variability)

## 2.5 Quantification of $I_{MI}$

As the purpose of this thesis is to examine the effect of a second messenger modulator on $I_{MI}$ activation and $I_{MI}$ voltage dependence, it was necessary to create an independent quantification for each of these properties.

*$I_{MI}$ activation.*

To quantify $I_{MI}$ activation the current amplitude was measured at -15 mV and all statistical analyses were done on this point. The intended goal of this choice was to develop a quantifiable measure that had high reliability, but was minimally affected by changes in voltage dependence. This is more rigorously defined below. Figure 2.3 shows that $I_{MI}$ peaks around -15 mV (**Green arrow**). Note that using voltages more negative than -15 mV, would be more unreliable in separating $I_{MI}$ activation from voltage dependence due to the differences between normal and low calcium conditions.

*$I_{MI}$ voltage dependence*.

In order to quantify $I_{MI}$ voltage dependence, the slope of its current to voltage relationship was quantified from -75 mV to -20 mV (Figure 2.3 **Red**). In order to determine whether this was a reliable measure of $I_{MI}$ voltage dependence or not, we compared the coefficient of variation (CV) of this slope conductance at different voltages and voltage ranges (Bin size). The logic of this was that if any combination of bin size and voltage were better than others we should see a minimum of standard

deviation and maximum of the absolute value of mean amplitude. Therefore, we should see a minimum in CV for different voltages and bin sizes if there were optimal measurement values. In contrast to $I_{MI}$ amplitude, the quantification of $I_{MI}$ voltage dependence was relatively robust and independent of bin size and voltage midpoint used. As illustrated in figure 2.4 voltage range (bin size) did not affect $I_{MI}$ slope's coefficient of variation adversely. There was a slight increase in coefficient of variation with increasing voltages, suggesting that negative voltages should be used to measure slope. It was found that the reason for the lack of change in CV with different bin sizes was that even though $I_{MI}$ peak slope occurred around -50 mV, and smaller bins (10 mV) around this voltage increased its peak, this gain was offset by larger variability. So, a -75 mV to -20 mV slope was chosen as an optimal balance between mean amplitude and low variance. Since a regression line might add more statistical power than just estimation of slope based on two points, we analyzed our data on proctolin-induced $I_{MI}$ using a least squares regression analysis vs estimation with -75 to -20 mV slope for different application numbers with the hypothesis that, if least squares fit was more sensitive to changes in slope than the normal method, then we should have a greater F-statistic. In contrast to our expectation of greater statistical power for the effect of application number on $I_{MI}$ slope, a least squares regression gave a smaller F statistic than the 2 point calculation of slope ($F(5, 166) = 8.157$ vs $F(5, 166) = 8.287$), but the greatest difference between estimates was less than 2 % (between applications one and six). This

data suggests that no appreciable statistical power can be obtained from least squares fitting, and slope conductance was therefore estimated from -20 mV and -75 mV.

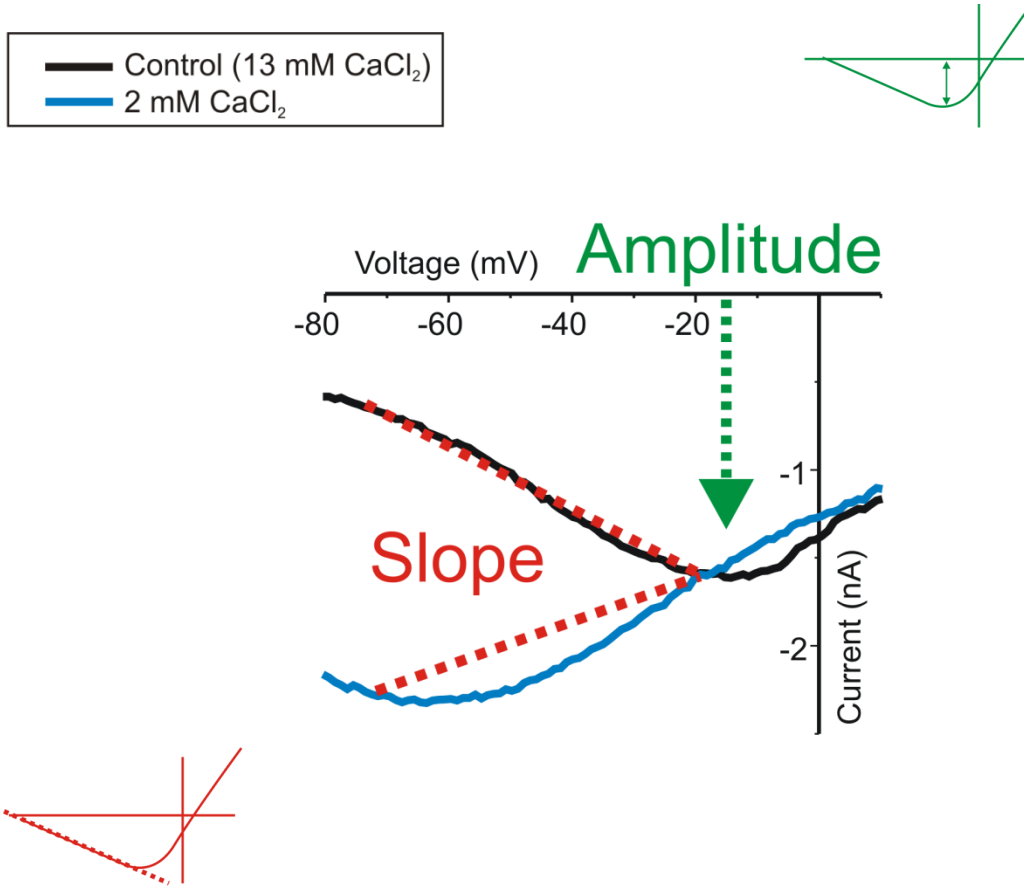


**Figure 2.3: Quantification of $I_{MI}$: Separating $I_{MI}$ Voltage Dependence from Activation.** Quantification of $I_{MI}$ activation and voltage dependence. IV relation of $I_{MI}$. Changes in slope between -75 mv to -20mv (**Red**) are taken as a measure of $I_{MI}$ voltage dependence. Amplitude at -15 mV (**Green**) is taken as a measure of $I_{MI}$ activation. Note that $I_M$I is close to maximal at this voltage and there is minimal difference between normal calcium (**Black**) and low calcium (**Blue**).

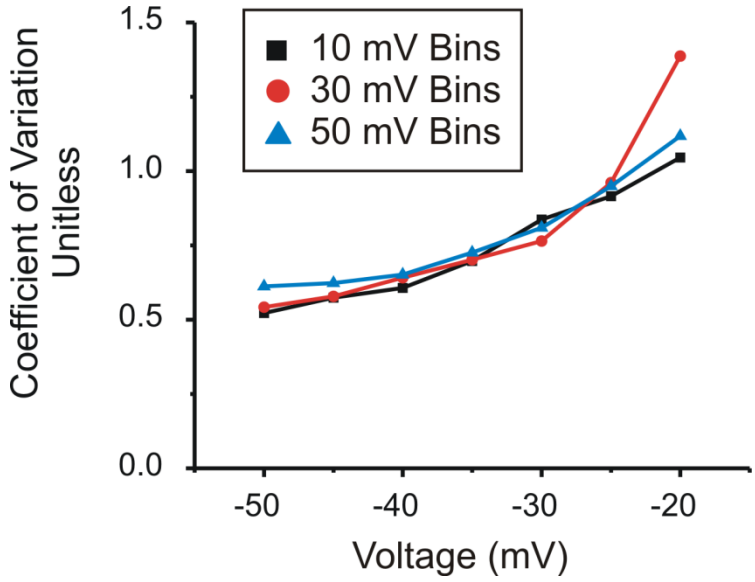


**Figure 2.4 $I_{MI}$ Coefficient of Variation for Slope is Unaffected by Bin Size but Increases as a Function of Voltage.** Proctolin-induced $I_{MI}$ coefficient of variation of slope (standard deviation divided by mean) from -75 mV to -20 mV was quantified and plotted as a function of voltage. Note that while bin size does not differ dramatically, CV increases as a function of voltage.

*The effect of reducing external calcium supports the quantifications proposed for proctolin induced $I_{MI}$.*

As it has already been shown that reducing external calcium reduces $I_{MI}$ voltage dependence (Golowasch and Marder, 1992b; Swensen and Marder, 2000, 2001), this condition can be used to set a standard to measure voltage dependence and, independently, activation. If a voltage below $I_{MI}$'s reversal potential exists where $I_{MI}$ does not significantly differ in amplitude between calcium conditions, then this voltage can be taken as a value below which $I_{MI}$ voltage dependence is relatively independent of $I_{MI}$ amplitude. Figure 2.5A-D shows that for proctolin induced $I_{MI}$; -15 mV is a voltage where

$I_{MI}$ amplitude is relatively unaffected by external calcium levels. However, the -75 mV to -20 mV slope is clearly affected by lowering calcium. Interestingly, it seemed that this is not the case for CCAP. Figures 2.5E-H show that there is significant enhancement of $I_{MI}$ amplitude in low calcium when measured at -15 mV. Surprisingly, there was no significant effect on $I_{MI}$ slope. This suggests that these two modulators may have different calcium dependencies but it is difficult to determine this with confidence as CCAP induced $I_{MI}$ has not been measured in a wide range of calcium concentrations. These experiments suggest that for proctolin induced $I_{MI}$, voltages of -15 mV and above are largely independent of $I_{MI}$ voltage dependence. The same criteria were used for CCAP for consistency, and the later finding that application of the calmodulin inhibitor W7 also increased $I_{MI}$ slope when using this criterion (see Chapter 4).

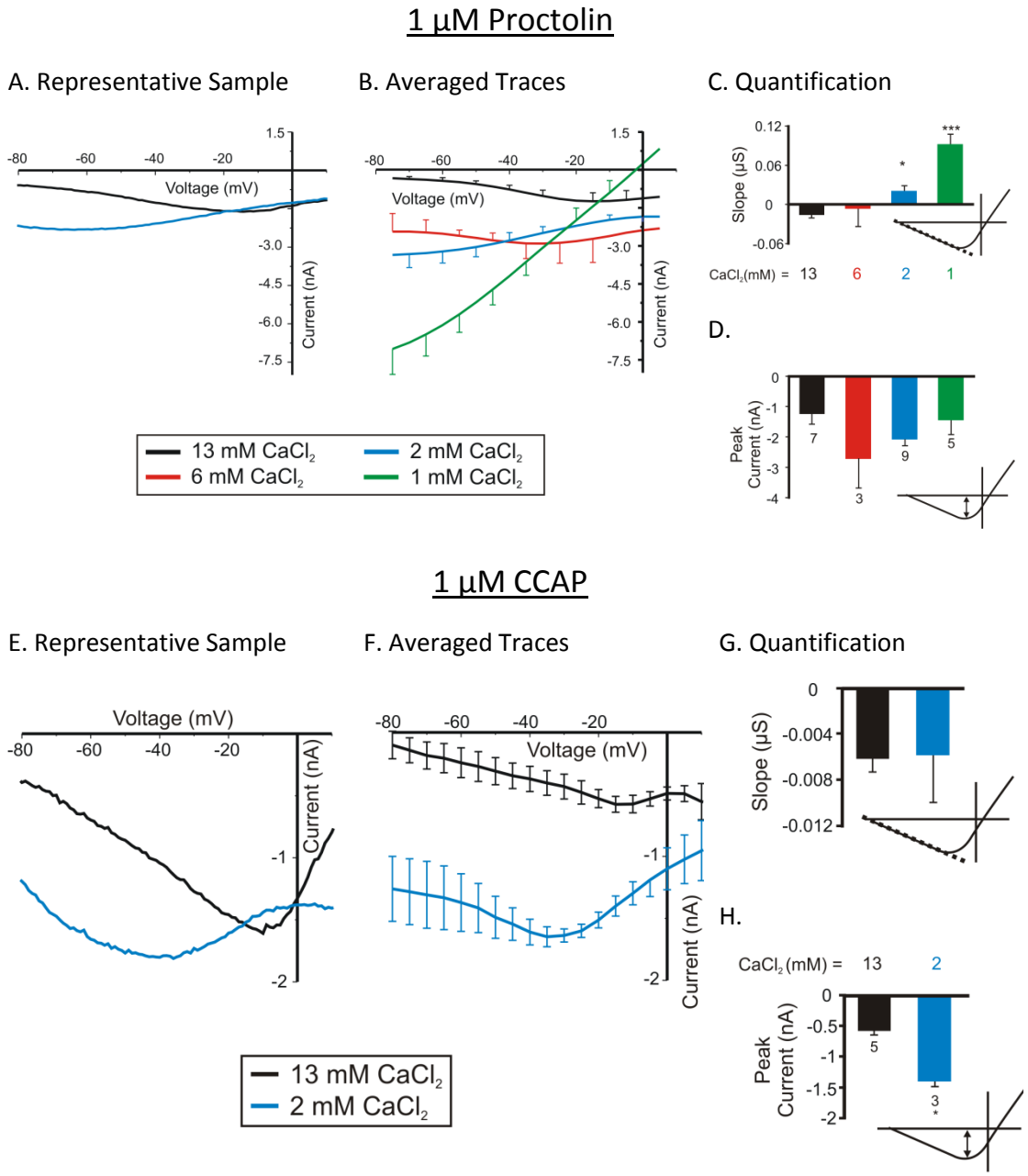


**Figure 2.5: $I_{MI}$ Loses Voltage Dependence as Extracellular Calcium is Reduced.** IV curves and quantification for effect of extracellular calcium on $I_{MI}$ induced by either 1 µM proctolin (*top*) or 1 µM CCAP (*bottom*). Saline contains 20 mM TEA, 200 µM $CdCl_2$, 5 mM CsCl, 0.1 µM TTX, 10 µM PTX. (A) Representative LP cell showing proctolin-induced $I_{MI}$ IV curves at different calcium concentrations. (B) Averaged IV curves for 2$^{nd}$ application of proctolin from different LP cells. Note the reduction in voltage dependence with decreasing calcium concentration. (C) Quantification of $I_{MI}$ slope showed that lowering calcium concentration significantly increased $I_{MI}$

slope. (One-Way ANOVA [F (3, 20) = 18.303, p = 5.96 x $10^{-6}$]). (D) Quantification of $I_{MI}$ amplitude showed that lowering calcium did not significantly alter $I_{MI}$ amplitude. (One-Way ANOVA [F (3, 20) = 2.373, p = 0.101]). (E) Representative IV curves for CCAP (1 µM) induced $I_{MI}$ in 13 mM $CaCl_2$ (**Black**) and 2 mM $CaCl_2$ (**Blue**). (F) Averaged IV curves from fourth CCAP application.(G) In contrast to the expected increase of slope conductance, decreasing calcium concentration to 2 mM had no effect on $I_{MI}$ slope conductance ( t-test, [ t (6) = -1.38, p = 0.895),. (H) Lowering calcium increased CCAP induced $I_{MI}$ amplitude (current is more negative) (t-test, [t (6) = -3.783, p = 0.008]). Post hoc Tukey tests vs control, * p < 0.05, ** p < 0.01, *** p < 0.001. (error bars SEM).

*$I_{MI}$ reversal potential and coefficient of variation sets higher limits for $I_{MI}$ amplitude quantification.*

Although CCAP-induced $I_{MI}$ amplitude was shown to increase when calcium was lowered to 2 mM, we sought to determine boundaries at how high a voltage $I_{MI}$ amplitude should be measured. The first boundary is shown by the coefficient of variation (CV) of $I_{MI}$ amplitude as a function of voltage for both proctolin and CCAP. Both of these neuromodulators showed an $I_{MI}$ current amplitude whose CV steadily increased as a function of voltage when higher than 0 mV (Figure 2.6A). One might expect that near its reversal potential, the coefficient of variation of current amplitude would increase dramatically due to its mean approaching zero. Consistent with the increase in CV at these voltages, is the finding that reversal potential of proctolin induced $I_{MI}$ when it could be measures was 10.8 mV ± 9.8 mV n = 43 (figure 2.6). This large variability in reversal potentials also supports not measuring $I_{MI}$ at voltages above zero mV due to the reduced driving force, and, therefore, reduced signal to noise ratio. We observed that the CV of $I_{MI}$ amplitude increased by more than 25% of its minimum level at voltages above 0 mV. Together with the previous arguments to select a voltage measure of $I_{MI}$ activation, this led us to choose -15 mV for this measurement. In conclusion, it appears

that for proctolin induced $I_{MI}$ amplitude at -15 mV and voltage dependence for slope between -75mV and -20mV are adequate independent parameters for quantification. As a practical matter, and for comparisons, CCAP was measured with the same criteria, but it is noted that separation of $I_{MI}$ voltage dependence and activation was less clear.

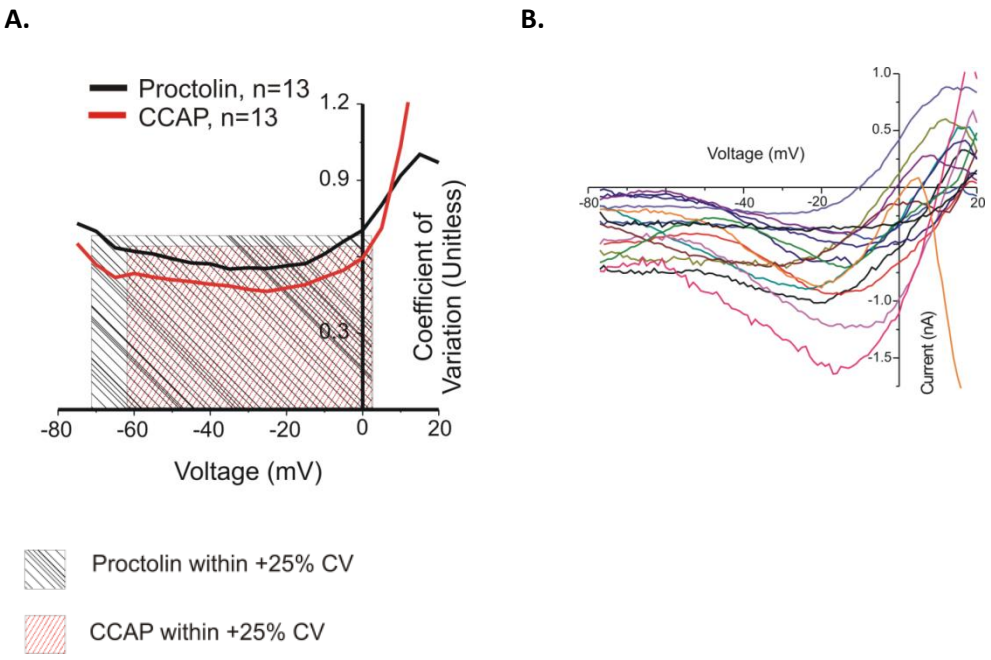


**Figure 2.6. Boundaries for $I_{MI}$ Amplitude Measurement: Coefficient of Variation and $I_{MI}$ Reversal Potential.** Saline contained 0.1 µM TTX, 10 µM PTX, 200 µM $CdCl_2$, 5 mM CsCl and 20 mM TEA. (A) Coefficient of variation for Proctolin (**Black*)*** and CCAP (**Red**) Cross hatched regions represent voltages where CV is within 25% of its minimum. Note that at positive voltages both proctolin and CCAP induced $I_{MI}$ increase in CV. (B) Sample of proctolin-induced $I_{MI}$'s that reversed. ($E_{rev}$ =+10.77 mV ± 9.8 mV ;SD).

## 2.6 $I_{MI}$ Stability

*$I_{MI}$ is not stable over many applications.*

The goal of this study was the pharmacological dissection of the second messenger mechanisms of $I_{MI}$ voltage dependence and activation. With the exception of Forskolin and 8-Br-cAMP, there was a scarcity of evidence as to the efficacy of many second messenger modulators not only in *Cancer borealis* species, but also in higher osmolarity marine saline in general. It was, therefore, necessary not only to test many different drugs targeting the same second messenger mechanism (as is often the case with many pharmacological studies), but also to describe the sensitivity of the system to these drugs by constructing dose response curves for many of these drugs. It became necessary that either different concentrations be tested in different animals (a time intensive process), or that many measurements of $I_{MI}$ be taken in the same preparation. The latter is the preferable option so the problem of response stability was examined.

*$I_{MI}$ stability in normal calcium*

Figure 2.7A-B shows the effect of application number on proctolin-induced $I_{MI}$ in the presence of normal calcium for six consecutive applications. A two way ANOVA for voltage and application number showed that both factors were significant as main effects without significant interactions. [Main effect application number; $F(5, 306) = 14.367$, $p < 10^{-8}$. Main effect voltage; $F(16, 306) = 10.723$, $p < 10^{-8}$. Interaction; $F(80, 306) = 0.476$, $p = 1.0$.] A post-hoc Tukey test showed that only applications 1 and 6

showed significant differences from all other applications. All subsequent amplitude and slope testing, therefore, excluded applications 1 and 6. Similarly, a one-way ANOVA on slope and amplitude (Figure 2.7C-D) shows that when quantifying amplitude at -15 mV, application number affects amplitude [Application number; $F(5, 22) = 4.293$, $p = 0.007$)].However, a Tukey test-shows that all of these differences are due to applications 6 and 1. (6 vs 1; p = 0.021.2 vs 1; p = 0.03.4 vs 1; p = 0.032.) Similarly, a one-way ANOVA showed that there was a significant effect of application number was observed on $I_{MI}$ slope [$F(5, 22) = 4.133$, $p = 0.008$]. Again, this was due to applications 1 and 6. (1 vs 6; p = 0.031. 4 vs 1; p = 0.026. 3 vs 1; p = 0.045.). Similar results are shown for CCAP in Figures 2.8 E-H, where one-way ANOVAs showed that both $I_{MI}$ slope [Application number; $F(5, 13) = 4.517$, $p = 0.013$] and amplitude, [Application number; $F(5, 13) = 2.733$, $p = 0.067$] were insensitive to application number when applications 1 and 6 are omitted (Tukey tests for slope; 6 vs 1; p = 0.023, 2 vs 1; p = 0.035. 4 vs 1; p = 0.036.). Based on these results we use application 2 as a control, and applications 3-5 test points for both proctolin and CCAP.

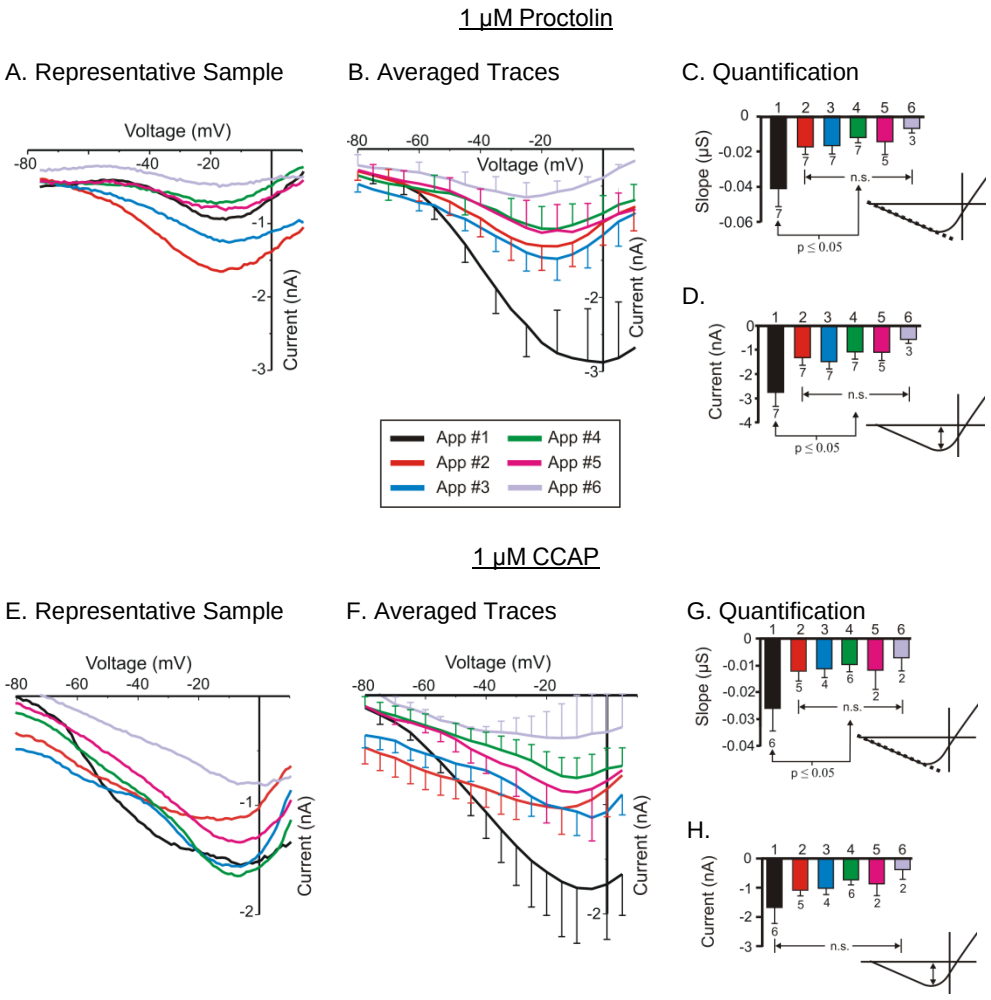


**Figure 2.7. $I_{MI}$ Slope and Amplitude are Stable for Proctolin and CCAP Applications 2-5.** IV curves and quantification to determine stability of $I_{MI}$ induced by either 1 μM proctolin (*top*) or 1 μM CCAP (*bottom*). Saline contains 20 mM TEA, 200 μM $CdCl_2$, 5 mM CsCl, 0.1 μM TTX, 10 μM PTX. (A) Representative IV curves showing a slow desensitization of proctolin-induced $I_{MI}$ response. (B) Averaged IV curves of proctolin-induced $I_{MI}$ at different applications. (C) Quantification of application number effect on $I_{MI}$ slope. A repeated measures one-way ANOVA showed that application number had a significant effect on $I_{MI}$ slope (1 way ANOVA [F (5, 22) = 4.133, p = 0.008]). A Tukey test showed that application one was significantly different from all others, while no differences were observed between applications 2-6. (D) Quantification of effect of application number on $I_{MI}$ amplitude. A one way ANOVA showed that application number affected proctolin-induced $I_{MI}$ amplitude at -15 mV [Application number; F (5, 22) = 4.293, p = 0.007)].A Tukey test showed these differences were attributable to application one. (E) Representative IV curves for CCAP induced $I_{MI}$. (F) Averaged IV curves of CCAP induced $I_{MI}$. (G) A one-way Repeated measures ANOVA showed that application numbers

significantly altered $I_{MI}$ slope [Application number; F (5, 13) = 4.517, p = 0.013]. A Tukey test showed that only application one was significantly different from all others. (H) A one-way ANOVA showed that application numbers (2-5) did not significantly affect $I_{MI}$ amplitude at -15 mV [Application number; F (5, 13) = 2.733, p = 0.067]. Error bars are SEM.

*$I_{MI}$ stability in low calcium*

In contrast to what was found for normal calcium, lowering calcium affected desensitization rate. Similar to results found for normal calcium, it was found that proctolin induced $I_{MI}$ slope was stable in low calcium. Figure 2.8 shows an experiment where the effect of repeated applications of proctolin in either normal (Figure 2.8A-B) or low calcium (Figure 2.8C-D) were examined in two sets of three preparations. . While lowering calcium was effective at increasing $I_{MI}$ slope across these sets, a two way repeated measures ANOVA showed that slope was unaffected by application number [Application number; F (4, 16) = 0.711, p=0.596. Calcium; F (1, 4) = 23.3, p = 0.008. Interaction; F (4, 16) = 1.439, p = 0.267]. In contrast to the stability of $I_{MI}$ slope found for both conditions, $I_{MI}$ amplitude was stable for normal calcium applications 2-5, but not in low calcium. A two-way repeated measures ANOVA and a Tukey test showed that only applications 2 & 3 were stable in low calcium. [Application number; F (4, 16) = 0.711, p=0.596. Calcium; F (1, 4) = 23.3, p = 0.008. Interaction; F (4, 16) = 1.439, p = 0.267]. This data suggests that proctolin induced $I_{MI}$ desensitization is much faster in low calcium than high calcium, a counter intuitive result considering calcium has been shown to be a common mechanism in the induction of desensitization [7](Partington et al., 1980;

[7] Application one was done in normal calcium to ensure a good baseline current for low calcium group.

Rosenmund et al., 1995; Oancea and Meyer, 1996; Shiells, 1999; Nawy, 2000; Hille, 2001; Mandadi et al., 2004). Due to this accelerated desensitization rate, here low calcium conditions were always compared to separate controls that were not exposed to the drug under study. This way, an analysis of covariance for application number as a covariate could be done on top of experiment and this desensitization rate could be accounted for.

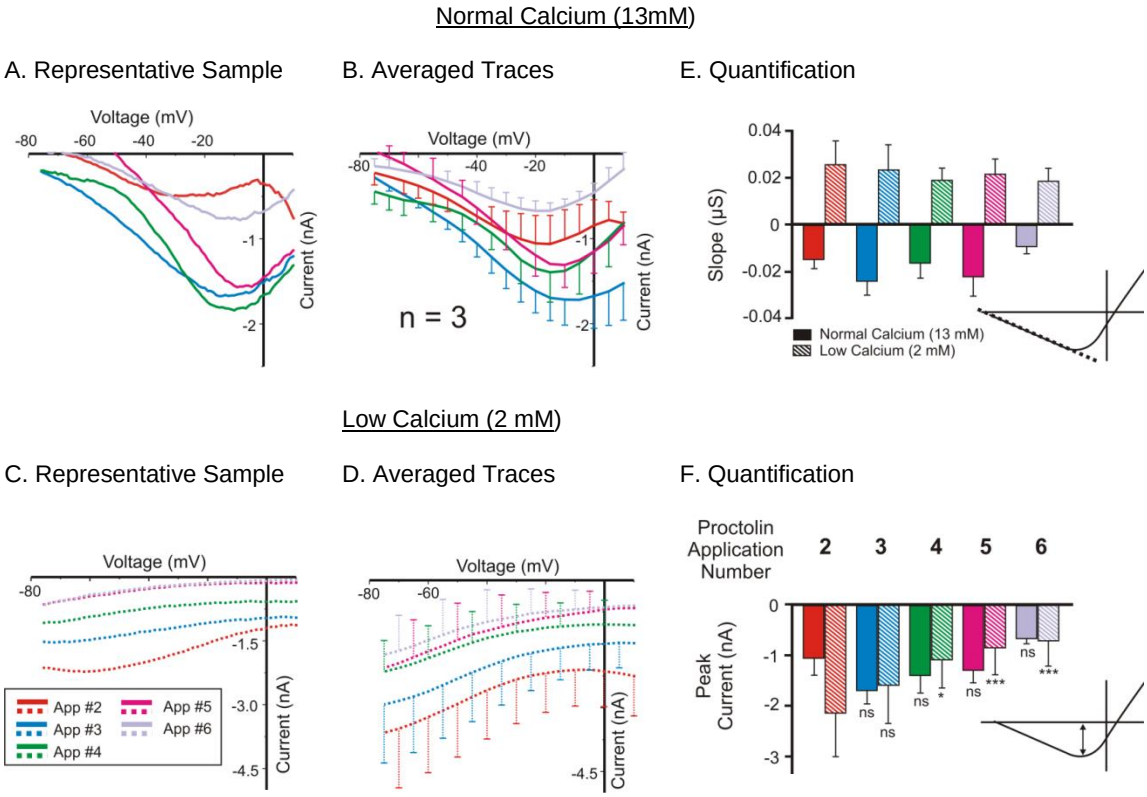


**Figure 2.8. In Low Calcium $I_M$ Amplitude Decreases with Application Number While $I_M$ Slope Remains Stable.** Effect of application number on proctolin (1 µM) induced $I_{MI}$ in control (13 mM) and low (2 mM) $CaCl_2$. Saline contains 20 mM TEA, 200 µM $CdCl_2$, 5 mM CsCl, 0.1µM TTX, 10 µM PTX. (A) Representative IV curves for repeated applications of proctolin in normal calcium. (B) Averaged IV curves for repeated applications in normal calcium. (C) Representative IV curves for repeated applications of proctolin in low calcium. (D) Averaged IV curves for repeated applications of proctolin in low calcium. (E) Quantification of effect of low calcium and repeated proctolin applications on $I_{MI}$ slope. A 2–way repeated measures ANOVA showed that application number did not significantly alter $I_{MI}$ slope, while exposure to low calcium significantly increased $I_{MI}$ slope. (2-way RM ANOVA, application number, calcium. [Main effect Application number; $F(4, 16) = 0.711$, $p=0.596$. Main effect Calcium; $F(1, 4) = 23.3$, $p = 0.008$. Interaction; $F(4, 16) = 1.439$, $p = 0.267$]). (F) $I_{MI}$ amplitude significantly decreased with application number in low calcium but not in normal calcium. (2-way RM ANOVA (application number, calcium). [Main effect application number; $F(4,16) = 6.118$, $p = 0.003$. Main effect calcium; $F(1, 4) = 0.00586$, $p = 0.943$. Interaction; $F(4, 16) = 3.589$, $p = 0.028$.] A post hoc Tukey test showed that while in normal calcium, only application 6 differed from application 2. In contrast, when in low calcium, applications 4, 5 & 6 were all significantly different from application 2. * $p<0.05$, *** $p < 0.005$.

*A note on occlusion vs inhibition.*

As will be noted more thoroughly in the next chapter, many of the studies done on $I_{MI}$ activation are based on the finding of Swensen and Marder (2000) that since $I_{MI}$ is a difference current, both inhibition and activation of a second messenger responsible for activation of $I_{MI}$, should theoretically lead to the same result when activated with proctolin or CCAP: $I_{MI}$ amplitude reduction (Swensen and Marder, 2000). This is because the partial activation of $I_{MI}$ in the control, which is then subtracted from the neuromodulator induced current, leads to a smaller observed $I_{MI}$. Due to this ambiguity, reduced $I_{MI}$ will have to be interpreted in the context of other factors to discriminate whether inhibition, or activation and thus occlusion is occurring by surveying a drug's effect on resting potential changes or its ability to increase or decrease the burst frequency of the ongoing rhythm. This will be discussed in depth in the next chapter.

## 2.7 Problems with Measurement in Low Calcium are Mitigated by Use of Bovine Serum Albumin (BSA).

*Lowering extracellular calcium reduces input resistance ($R_{IN}$) and depolarizes $V_{Rest}$.*

To examine proctolin induced $I_{MI}$ voltage dependence, many of our experiments called for lowering calcium concentrations. Despite equimolar substitution with $MgCl_2$, switching from normal calcium to low calcium (2 mM) made cells depolarized and leaky. This is illustrated in figure 2.9. When incubating cells with certain membrane permeable drugs that we suspected were not permeating the membrane, we included BSA in hopes that this would help with increasing the permeation and/or preventing precipitation of higher molecular weight drugs. Although it did not help us in this regard, as illustrated in figure 2.10, we found that it prevented the change in depolarization, although it did not significantly change input resistance. This data suggested that supplementation with BSA seemed to help with stability of cells in low calcium for extended periods, and was the reasoning behind our supplementation of low calcium media with 0.5% BSA.

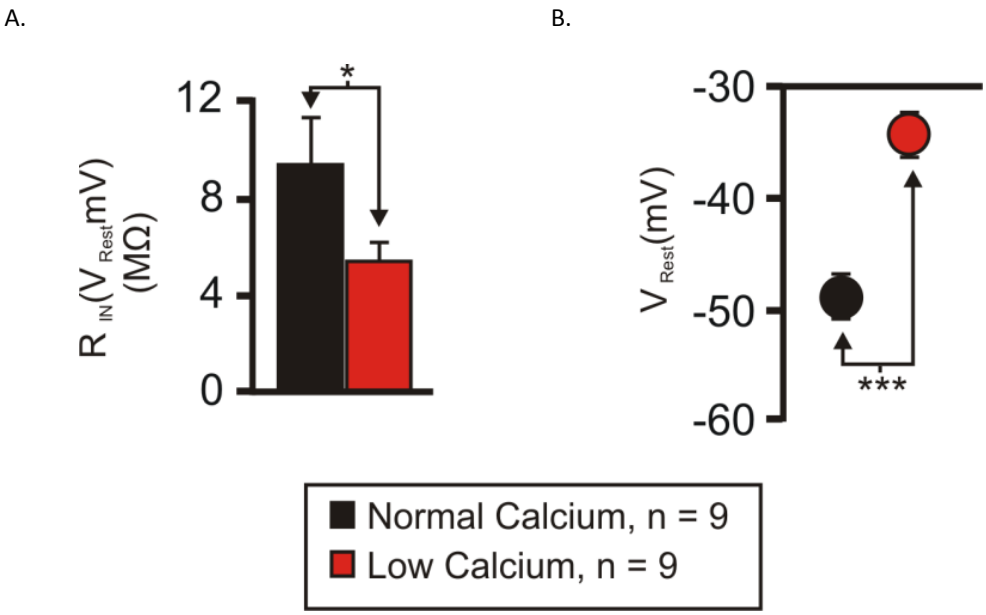


**Figure 2.9. Low Calcium Induces Depolarization and Reduces Input Resistance.** Saline contained 20 mM TEA, 200 µM $CdCl_2$, 5 mM CsCl, 0.1µM TTX, 10 µM PTX, in either normal calcium (**Black,** 13 mM) or low calcium (**Red**, 2 mM). (A) A paired t-test showed that 30 minutes after start of low calcium input resistance measured from $V_{Rest}$ was significantly reduced [ t (8) = 3.468, p = 0.008.] (B) A paired t-test showed that depolarization induced by lowering calcium was significant [t(8) = -15.158, p = 3.6 x $10^{-7}$.] Error bars are SEM.

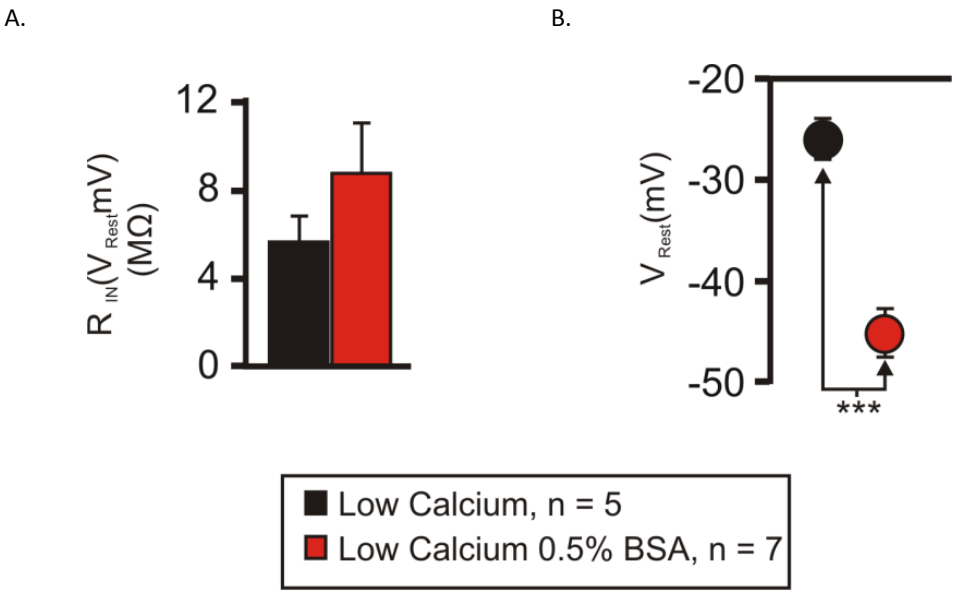


**Figure 2.10. 0.5% Bovine Serum Albumin (BSA) Mitigates Low Calcium Induced Depolarization but not $R_{IN}$ Drop.** 2 hours in incubation of 2 mM low calcium saline that contained 20 mM TEA, 200 µM $CdCl_2$, 5 mM CsCl, 0.1µM TTX, 10 µM PTX, in either no BSA (**Black**) or supplemented with 0.5% BSA (**Red**). (A) A Mann-Whitney rank sum U-test showed that BSA had no effect on $R_{IN}$ measured from $V_{Rest}$.[ $Median_{Control}$ = 5.5 MΩ, $Median_{BSA}$ = 6 MΩ. U = 12, p = 0.413.] (B) A t-test showed that cells without BSA were significantly more depolarized than cells with BSA [t (10) = 5.783, p =1.77 x $10^{-4}$.] Data shown are means ± SEM. ***; p< 0.001.

*BSA does not affect $I_{HTK}$, $I_A$, $V_{Rest}$ or $R_{IN}$ in normal calcium saline with TTX.*

Although we knew that BSA prevented low calcium induced depolarization, it was important to determine that this added factor would not change other properties of the cell. Figure 2.11 shows that for $I_{HTK}$ and $I_A$ at +20 mV, $I_{HTK}$ and $I_A$ $V_{1/2}$ activation, $R_{IN}$ at -50 mV, and $V_{Rest}$, concentrations of BSA up to 2 % had no significant effect on these measurement [statistics in figure 2.11]. This suggests that BSA can be used to stabilize

the membrane and prevent depolarization without affecting the measurement of these currents.

*BSA does not affect proctolin induced $I_{MI}$ or amplitude.*

Most importantly, BSA does not affect measured proctolin induced $I_{MI}$ amplitude or voltage dependence. As illustrated in figure 2.12, concentrations of BSA up to 2% did not affect proctolin induced $I_{MI}$ slope [BSA; $F(5, 33) = 1.562$, $p = 0.198$. Application number; $F(1, 33) = 3.854$, $p = 0.058$.], or amplitude [BSA; $F(5, 33) = 0.498$, $p = 0.776$. Application number; $F(1, 33) = 8.432$, $p = 0.007$.]. Together, these results suggest that BSA can be used to prevent the problematic depolarization when lowering extracellular calcium without affecting measurement of $I_{MI}$ or the other ionic currents. Further, the finding that BSA did not hyperpolarize the membrane in normal calcium saline with TTX (Figure 2.12), suggests that BSA only prevents low calcium induced depolarization, and is therefore a good preventative measure of this phenomenon.

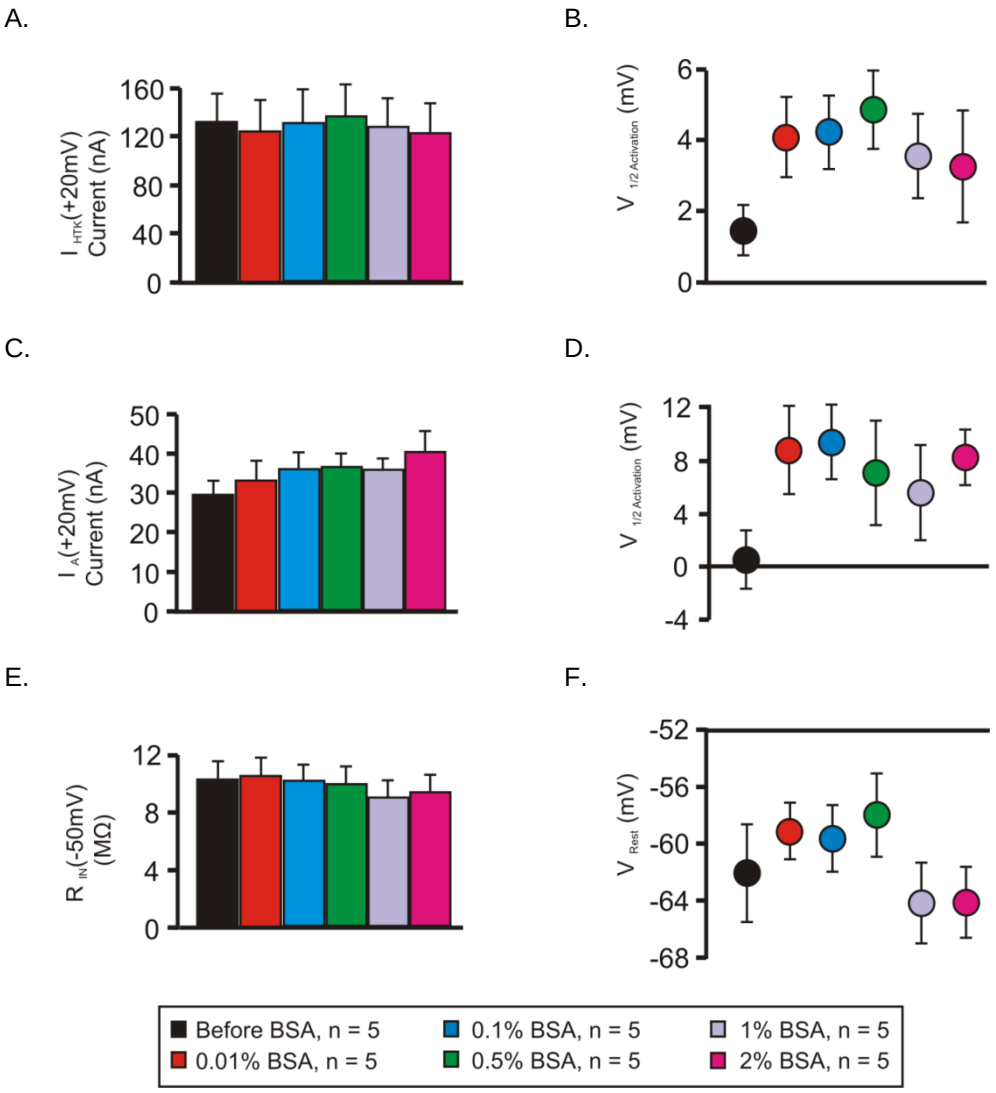


**Figure 2.11. BSA Concentrations Up to 2% do Not Affect $I_{HTK}$, $I_A$, $R_{IN}$ (-50 mV), or $V_{Rest}$ in Normal Calcium and TTX.** Normal calcium saline contained 0.1 µM TTX in various concentrations of BSA. (A) A one-way repeated measures ANOVA showed that BSA did not affect $I_{HTK}$ at +20 mV [BSA; F (5, 20) = 1.446, p = 0.251.] (B) A one-way repeated measures ANOVA showed that BSA did not affect $I_{HTK}$ $V_{1/2}$ Activation [BSA; F (5, 20) = 1.072, p = 0.451] (C) A one-way repeated measures ANOVA showed that BSA did not affect $I_A$ at +20 mV [BSA; F (5, 20) = 2.219, p = 0.093.] (D) one-way repeated measures ANOVA showed that BSA did not affect $I_A$ $V_{1/2}$ Activation [BSA; F (5, 20) = 1.096, p = 0.391] (E) A one-way repeated measures ANOVA showed that BSA did not affect $R_{IN}$ at -50 mV [BSA; F (5, 20) = 1.457, p = 0.248.] (F) one-way repeated measures ANOVA showed that BSA did not affect $V_{Rest}$ [BSA; F (5, 20) = 0.971, p = 0.451] Error bars are SEM.

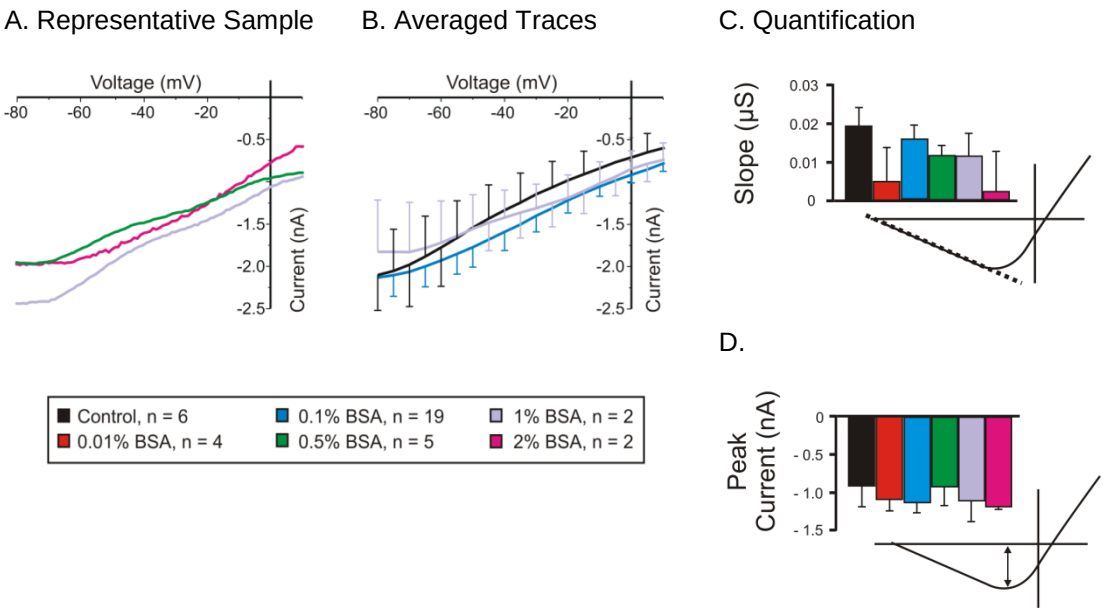


**Figure 2.12. BSA Does Not Inhibit Proctolin-induced $I_{MI}$ in Low Calcium.** 2 mM low calcium saline that contained 20 mM TEA, 200 µM $CdCl_2$, 5 mM CsCl, 0.1µM TTX, 10 µM PTX, in different concentrations of BSA.(A) Representative IV trace of BSA experiment. (B) Averaged IV curves of BSA and non-BSA experiments in low calcium. (C) A one-way ANOVA with covariate application number showed that BSA did not affect proctolin-induced $I_{MI}$ slope [BSA; F (5, 33) = 1.562, p = 0.198.Application number; F (1, 33) = 3.854, p = 0.058.] (D)A one-way ANOVA with covariate application number showed that BSA did not affect proctolin-induced $I_{MI}$ amplitude at -15 mV [BSA; F (5, 33) = 0.498, p = 0.776. Application number; F (1, 33) = 8.432, p = 0.007.] Error bars are SEM.

## 2.8 Discussion

In this chapter, general methods and a procedure for quantifying $I_{MI}$ activation and voltage dependence were discussed. The reasoning behind supplementation with BSA, and application stability were examined. The quantifications for measuring proctolin induced $I_{MI}$ amplitude at -15 mV were supported by several factors, the most important of which is that when exposed to lower calcium concentrations, amplitude at this voltage did not significantly change. This suggests that when measuring proctolin induced $I_{MI}$ at this voltage, measurements are not greatly affected by its voltage dependence. Other factors supporting this quantification are that peak $I_{MI}$ occurs around this voltage, this voltage is not too close to $I_{MI}$ reversal potential, and at higher voltages the coefficient of variability for $I_{MI}$ amplitude increases rapidly. Although the case for CCAP did not support this quantification as robustly, it was decided that $I_{MI}$ amplitude at -15 mV would also be used for CCAP quantification. In support of this we point out that the reversal potential and coefficient of variation observed for CCAP and proctolin induced $I_{MI}$ were similar. It is primarily for consistency that this quantification is acceptable for CCAP induced $I_{MI}$. Despite this, there is the caveat that voltage dependence is not as strongly separated for CCAP induced $I_{MI}$ as it is for proctolin induced $I_{MI}$ when measured at this voltage. The second quantification was estimating $I_{MI}$ voltage dependence as $I_{MI}$ slope from -75 mV to -20 mV. This quantification was found to be robust for proctolin, but not as robust with CCAP. The same criterion was adopted for CCAP based on the finding in chapter 4 that the calmodulin inhibitor W7 produced

significant changes in CCAP voltage dependence when quantified in this way. In this chapter, the stability of $I_{MI}$ was examined. It was found that in normal calcium, applications 1 and 6 were significantly different from all other applications, while applications 2-5 were not significantly different from one another. Therefore, exclusion of applications 1 and 6 leaves to four useful data points per experiment, allowing repeated measures of $I_{MI}$. It was also noted that the same was not true for low calcium, and therefore application number would have to be controlled for by comparing these experiments to independent controls of the same application number. It was also briefly noted, that drugs that reduce $I_{MI}$ amplitude must be disambiguated for whether they are producing inhibition or occlusion. Together, these methodologies established a systematic means for quantifying the effects of second messenger modulators for both $I_{MI}$ activation and voltage dependence. As will be seen in later chapters, these methods were invaluable as certain drugs that were thought to have an effect on activation, turned out to have an effect on voltage dependence instead (e.g., gallein; chapter 4).

# Chapter 3: $I_{MI}$ Activation

## 3.1 Introduction

In this chapter, the mechanisms of $I_{MI}$ activation by neuromodulators are discussed. The consequences of application of various second messenger modulators and their effect on $I_{MI}$ amplitude are assessed. Before the findings found for each signaling pathway are discussed, methodology specific to the agonists and antagonists and a brief rationale of why certain second messengers were examined are discussed.

First, we test the hypothesis that proctolin-induced $I_{MI}$ is mediated by a G-protein coupled receptor by pressure injection of G-protein inhibitor GDP-βS. This application is followed by an attempt to narrow which G-protein by application of the more specific G-protein inhibitor pertussis toxin. Further, we see if the G-protein agonist GTP-γS is capable of occluding proctolin induced $I_{MI}$.

Second, we explore classical signal transduction pathways including cyclic nucleotides and phospholipase C by application of activators and inhibitors of these pathways. Further, we determine whether proctolin-induced $I_{MI}$ depends on downstream effectors of these pathways such as phosphatases or kinases by using phosphatase and kinase inhibitors both general and specific. Before these specific

hypotheses are examined, we briefly discuss the expectations of these experiments that are contingent upon the model used.

## 3.2: G-protein Coupled Receptors are Necessary for Proctolin-induced $I_{MI}$.

*Pressure injection of G-protein modulators methodology.*

As reviewed in Chapter 1, we suspected that proctolin, pilocarpine and CCAP induced $I_{MI}$ was mediated through GPCRs. To test this, we pressure injected modulators of G-protein function. Recording electrodes (ME1) used a standard 20 mM KCl + 0.6 M $K_2SO_4$ recording solution. We pressure injected and injected current through the same electrodes, in particular the current-passing electrode (ME2), but never pressure injected during voltage clamp as it was observed that this could alter holding currents and make the voltage clamp very unstable. Pressure injection electrodes were filled with 20 mM TEA +500 mM KCl with or without *G-protein* modulators. It was found that clogging was more frequent with the higher resistance electrodes used for recording electrodesTherefore, pressure injection electrodes were made with much lower resistance (8-15 MΩ). 20 mM TEA was included to monitor the efficacy of the pressure injection experiments by monitoring the known inhibition of the high threshold potassium current ($I_{HTK}$) by TEA {ref}. All experiments began in 0.1 µM TTX. In order to assess whether pressure injection was working, $I_{HTK}$ was continuously measured during the pressure injection procedure once every hour. Figure 3.1 shows how pressure injection efficacy was assessed during experiments. First, $I_{HTK}$ was measured (A). Second, pressure was applied (B). $I_{HTK}$ was then remeasured (C). If there was no significant

reduction in $I_{HTK}$ injection pressure was slightly increased and the process was repeated. This was repeated until $I_{HTK}$ was half its original value. It typically took at least 30 minutes to the first measurement where transient $I_{HTK}$ began to reduce and most experiments required many cycles of pressure injection, $I_{HTK}$ measurement and repeating. When this 50 % reduction in $I_{HTK}$ criterion was reached, then bath application with saline containing 20 mM TEA, 200 µM $CdCl_2$, 5 mM CsCl, 0.1 µM TTX, 10 µM PTX was started and proctolin-induced $I_{MI}$ was measured as described in Chapter 2. The first and second applications were done in normal calcium, while the third application was done in 2 mM low calcium.

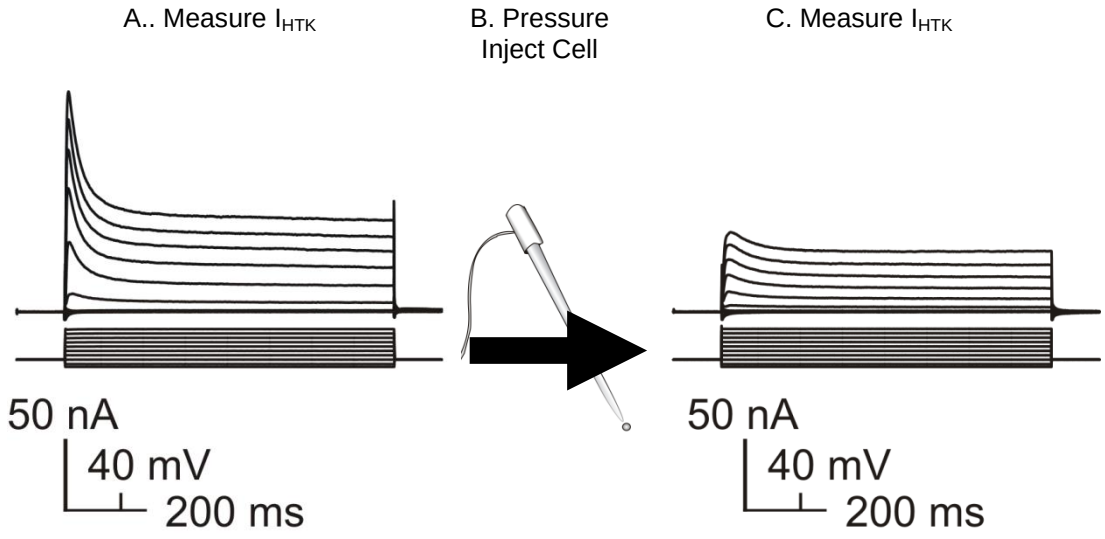


**Figure 3.1. Two Methods for Evaluating the Efficacy of Pressure Injection of LP Cells.** (A) Schematic of how efficacy of pressure injections was monitored using 20 mM TEA and 500 mM KCl electrodes. A. $I_{HTK}$ was measured. B. Pressure injection was applied. C. $I_{HTK}$ was measured again. If $I_{HTK}$ was not inhibited to 50% or less of original, pressure injection was repeated until criterion was met.

*The G-protein inhibitor GDP-βS reduces proctolin-induced $I_{MI}$.*

To determine whether proctolin-induced $I_{MI}$ was dependent on the activation of G-proteins, and presumably, G-protein coupled receptors (GPCRs), we pressure injected 10 mM of the G-protein inhibitor GDP-βS. This inhibitor, is a non-membrane permeable GDP analogue that has an insignificant phosphorylation rate compared to GDP, and competes with GTP binding to G-proteins (Eckstein et al., 1979), thus locking G-proteins in the inactive $G_{\alpha\beta\gamma}$• GDP-βS state (Tam et al., 2011). This inhibits G-protein coupled receptors (Lemos and Levitan, 1984; Kitazawa et al., 1989; Tam et al., 2011). Note that it is common for many papers (Sigma as well) to identify GDP-βS as a 'non'-hydrolysable' GDP analogue, although it is, it is the non-phosphorylatable nature of GDP-βS that is the mechanism of its inhibition (Eckstein et al., 1979).

Pressure injection of the G-protein blocker GDP-βS reduced proctolin-induced $I_{MI}$. Figure 3.2A shows averaged IV curves of control pressure injections (**Black**) and 10 mM GDP-βS pressure injections (**Red**) in normal calcium. Note that pressure injection of 10 mM GDP-βS completely abolishes proctolin-induced $I_{MI}$ in normal calcium. This shows that proctolin-induced $I_{MI}$ is dependent on G-proteins in normal calcium. Figure 3.2B shows averaged IV curves for the same cells in low calcium. Again, proctolin-induced $I_{MI}$ is reduced but this reduction does not appear to be as great. Figure 3.2C shows the quantification of the effect of calcium and GDP-βS on proctolin-induced $I_{MI}$ amplitude at -15 mV. A 2-way ANOVA showed that both calcium and GDP-S were capable of significantly altering $I_{MI}$ amplitude in opposite directions [Calcium; $F(1, 30) = 5.993$, $p = 0.02$. GDP-βS; $F(1, 30) = 15.034$, $p = 5.34 \times 10^{-4}$. Interaction; $F(1, 30) = 0.376$, $p =$

0.544.]. A Tukey test showed that within normal calcium, GDP-βS reduced the mean amplitude of $I_{MI}$ by 96 ± 19% (SEM; $n_{Control}$ = 10, $n_{GDP\text{-}\beta S}$ = 6; p = 0.003). In contrast, in low calcium, GDP-βS only reduced the mean amplitude of $I_{MI}$ by 50 ± 14% (SEM; $n_{Control}$ = 10, $n_{GDP\text{-}\beta S}$ = 6; p = 0.035). These results are consistent with the hypothesis that $I_{MI}$ is mediated by a G-protein coupled receptor. Similar results were obtained injecting cells with electrodes containing only 500 mM KCl and no TEA as vehicle or the same with GDP-βS (Figure 3.2D-F). Interestingly, in the absence of TEA, the inhibition of proctolin-induced $I_{MI}$ by GDP-βS did not seem to be modulated by external calcium condition. These results suggest that proctolin-induced $I_{MI}$ is dependent on G-proteins.

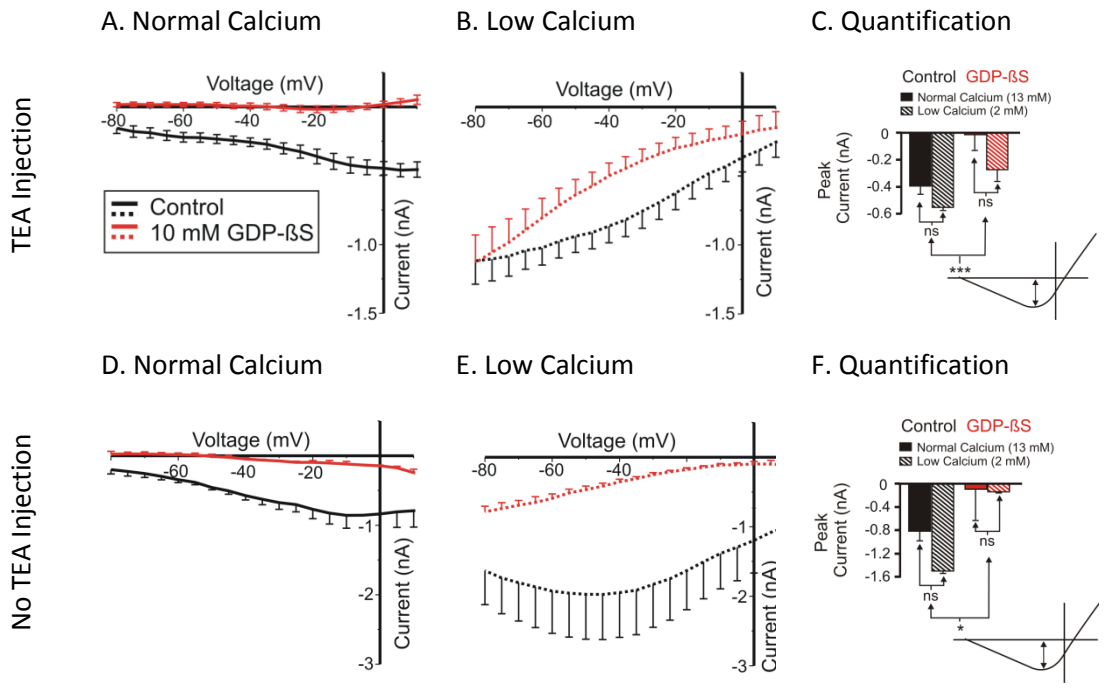


**Figure 3.2: Proctolin-induced $I_{MI}$ Requires G-proteins as shown by Pressure Injection of the G-Protein Inhibitor GDP-βS.** GDP-βS (**Red**) or control solutions (**Black**) were pressure injected in normal (**Solid**) or Low (*Stripes*) calcium. All recording electrodes used 20 mM KCl and 0.6 M $K_2SO_4$. At the time of $I_{MI}$ measurement saline contained 0.1 µM TTX, 10 µM PTX, 200 µM $CdCl_2$, 5 mM CsCl and 20 mM TEA. *Top, 20 mM TEA recording solution.* (A) Averaged IV curves of proctolin-induced $I_{MI}$ in normal calcium in control (**Black),** or with 10 mM GDP-βS (**Red**). (B) Averaged IV curves for GDP-βS (**Red**) vs control (**Black**) in 2 mM low calcium. (C) $I_{MI}$ amplitude at -15 mV in normal (**Solid**) or low calcium (*Striped*), and control (**Black**) vs 10 mM GDP-βS (**Red**). A 2 way ANOVA showed that 10 mM GDP-βS was capable of reducing $I_{MI}$ amplitude. [Calcium ; $F(1, 30) = 5.993$, $p = 0.02$. GDP-βS; $F(1, 30) = 15.034$, $p = 5.34 \times 10^{-4}$. Interaction; $F(1, 30) = 0.376$, $p = 0.544$.] *Bottom, no TEA:* (D) Averaged IV curves of proctolin-induced $I_{MI}$ in normal calcium in control (**Black),** or with 10 mM GDP-βS (**Red**). (E) Averaged IV curves of proctolin-induced $I_{MI}$ in control (**Black)** or 10 mM GDP-βS (**Red**) in 2 mM low calcium. (F) A 2 way ANOVA showed that GDP-βs significantly altered $I_{MI}$ amplitude at -15 mV [2-way ANOVA; Calcium; $F(1, 6) = 1.102$, $p = 0.334$. GDP-βS; $F(1, 6) = 6.263$, $p = 0.046$ Interaction; $F(1, 6) = 0.929$, $p = 0.372$.] Tukey comparisons, * $p < 0.05$, *** $p < 0.001$. Error bars are SEM

*GTP-γS occludes $I_{MI}$ response to Proctolin.*

If $I_{MI}$ activation is mediated by GPCR activation, we hypothesized that application of the G-protein activator GTP-γS would reduce (occlude) proctolin-induced $I_{MI}$ amplitude. GTP-γS is a non-hydrolysable GTP analogue that binds Gαβγ stably and permanently by displacing GDP similar to GTP locking the α subunit in its active state (Yamanaka et al., 1986; Harrison and Traynor, 2003). As shown in Figure 3.3, pressure injection of GTP-γS reduced proctolin-induced $I_{MI}$ amplitude, in both normal calcium (3.3A), and 2 mM low calcium (3.3B). A 2-way ANOVA showed that GTP-γS, but not calcium, was capable of altering $I_{MI}$ amplitude [Calcium; $F(1, 22) = 2.136$, $p = 0.158$. GTP-γS; $F(1, 22) = 13.562$, $p = 0.001$. Interaction; $F(1, 22) = 0.0817$, $p = 0.778$.]. A Tukey post-hoc test showed that considering all conditions, GTP-γS lowered proctolin-induced mean $I_{MI}$ amplitude by 69 ± 18% (SEM; $n_{Control} = 9$, $n_{GTP\text{-}\gamma S} = 5$; $p = 0.001$) . Within normal calcium, GTP-γS lowered mean $I_{MI}$ amplitude by 59 ± 33 (SEM; $n_{Control} = 9$ $n_{GTP\text{-}\gamma S} = 5$; $p = 0.02$). In low calcium, GTP-γS lowered mean $I_{MI}$ amplitude by 74 ± 17% (SEM; $n_{Control} = 8$, $n_{GTP\text{-}\gamma S} = 4$; $p = 0.014$). These results are consistent with our prediction that GTP-γS would occlude proctolin-induced $I_{MI}$.

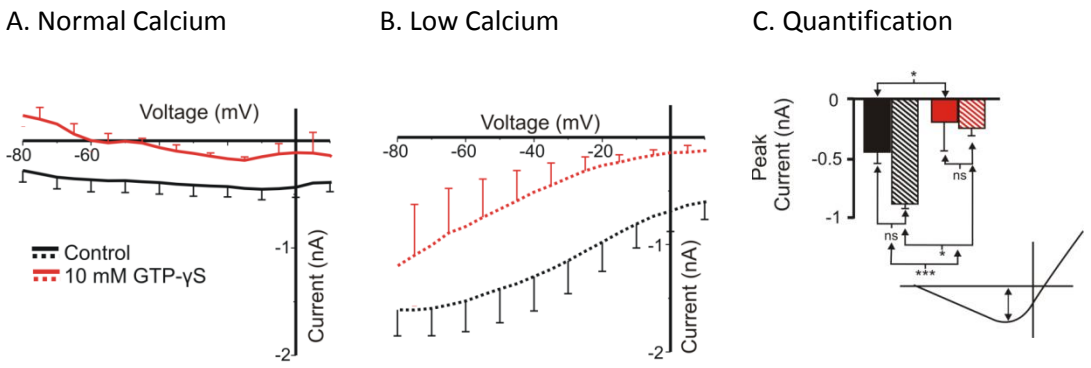


**Figure 3.3. The G-protein Activator GTP-γS Occludes Proctolin-induced $I_{MI}$.** GTP-γS was pressure injected in 500 mM KCl and 20 mM TEA solution. Control pressure injection solutions were 500 mM KCl and 20 mM TEA. All recording electrodes used 20 mM KCl and 0.6 M $K_2SO_4$. Saline contained 0.1 µM TTX, 10 µM PTX, 200 µM $CdCl_2$, 5 mM CsCl and 20 mM TEA. (A) Averaged IV curves of proctolin-induced $I_{MI}$ in normal calcium (13 mM) after pressure injection with either 20 mM TEA and 500 mM KCl (**Black)** or 20 mM TEA, 500 mM KCl and 10 mM GTP-γS (**Red**). (B) Averaged IV curves of proctolin-induced $I_{MI}$ in low calcium (2 mM) with either control (**Black**) or 10 mM GTP-γS injection (**Red**). (C) Quantification of the effect of GTP-γS on $I_{MI}$ amplitude at -15 mV. A 2-way ANOVA showed that GTP-γS but not calcium was capable of occluding $I_{MI}$ amplitude [Calcium; $F(1, 22) = 2.136$, $p = 0.158$. GTP-γS; $F(1, 22) = 13.562$, $p = 0.001$. Interaction; $F(1, 22) = 0.0817$, $p = 0.778$.] (Tukey post hoc test; *, $p < 0.05$, ***, $p<0.001$.)

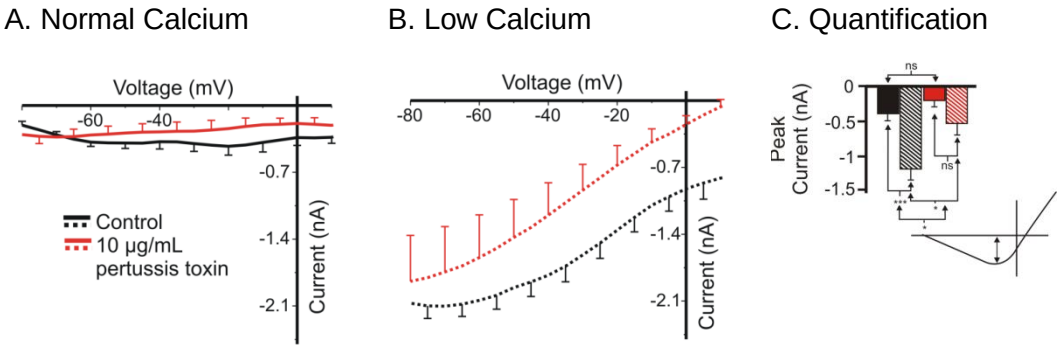


**Figure 3.4. The Specific G-protein Inhibitor Pertussis Toxin Inhibits Proctolin-induced $I_{MI}$ in Low Calcium.** Control pressure injection solutions of 500 mM KCl and 20 mM TEA (**Black**) or the same with 10 µg/mL Pertussis toxin (**Red**) were pressure injected in either normal (**Solid**; 13 mM) or Low (*Striped*; 2 mM) calcium. All recording electrodes used 20 mM KCl and 0.6 M $K_2SO_4$. Saline contained 0.1 µM TTX, 10 µM PTX, 200 µM $CdCl_2$, 5 mM CsCl and 20 mM TEA. (A) Averaged IV curves of proctolin-induced $I_{MI}$ in normal calcium after pressure injection of control solution (**Black**) or 10 µg/mL pertussis toxin solution (**Red**).(B) $I_{MI}$ IV curves in low calcium (2 mM), for control (**Black**), or pertussis (**Red**). ( (D) A 2 way-ANOVA showed that both calcium and pertussis were capable of altering $I_{MI}$ amplitude at -15 mV. [Calcium; $F(1, 22) = 20.630$, $p = 1.61 \times 10^{-4}$. Pertussis; $F(1, 22) = 11.735$, $p = 0.002$. Interaction; $F(1, 22) = 3.541$, $p = 0.073$.] Post Hoc Tukey *, $p < 0.05$, ***, $p < 0.001$. Error bars SEM.

*The specific G-protein inhibitor pertussis toxin (PTX) inhibits proctolin-induced $I_{MI}$ amplitude in low calcium but not in normal calcium.*

As the GDP-βS and GTP-γS results implied that G-protein signaling was necessary for proctolin-induced $I_{MI}$ activation, we attempted to narrow the pool of potential G-proteins further. In order to determine what specific G-protein was activating $I_{MI}$, we used the specific G-protein blocker PTX. This toxin functionally decouples trimeric G-proteins from their receptors by ADP-rybosylation of the α-subunit. This renders $G_I$, $G_T$, $G_O$, but not $G_S$ subunits, unable to couple to the GPCR (Gierschik, 1992; Krueger and Barbieri, 1995; Lodish, 2008; Katada, 2012). Figure 3.4 shows that pressure injection of

10 µg/mL PTX (**Red**) reduced proctolin-induced $I_{MI}$ IV curves versus control (**Black**). As shown in figure 3.4C, a 2-way ANOVA showed that while calcium was capable of increasing $I_{MI}$ amplitude, PTX significantly decreased $I_{MI}$ amplitude [Calcium; $F(1, 22) = 20.630$, $p = 1.61 \times 10^{-4}$. PTX; $F(1, 22) = 11.735$, $p = 0.002$. Interaction; $F(1, 22) = 3.541$, $p = 0.073$.]. A post hoc Tukey test showed that within all conditions, PTX significantly reduced mean proctolin-induced $I_{MI}$ amplitude by 53 ± 11% (SEM; $n_{Control} = 7$. $n_{Pertussis} = 6$; $p = 0.003$). This is consistent with our hypothesis that proctolin-induced $I_{MI}$ is mediated by a PTX sensitive G-protein. Interestingly, however, within normal calcium, PTX did not effectively reduce mean $I_{MI}$ amplitude ($p = 0.268$). In contrast, $I_{MI}$ mean amplitude was reduced by PTX in low calcium by 55 ± 11% (SEM; $n_{Control} = 7$ $n_{Pertussis} = 6$; $p = 0.002$). There are two problems with this result. First, our assumption that low calcium did not affect $I_{MI}$ amplitude was wrong. Second, it appears that proctolin induced $I_{MI}$ is pertussis-sensitive in low calcium conditions, while pertussis-insensitive in normal calcium conditions. Our initial assumption was that this was due to low statistical resolution, but when doing a t-test on just the normal calcium data, pertussis did not affect $I_{MI}$ amplitude at -15 mV [$t(12) = 1.485$, $p = 0.163$][8]. In order to determine why our assumption that $I_{MI}$ voltage dependence was not separable from activation in these experiments, we examined any differences between these experiments and our other pressure injection experiments.

[8] Note that this p value would have to be lower than 0.0025 to maintain experiment-wise $p < 0.05$.

*Buffering of Pressure Injection Electrodes may Affect Responsiveness to Extracellular Calcium.*

To address the concern of whether our initial assumption that proctolin-induced $I_{MI}$ amplitude could be separated from voltage dependence for pressure injection experiments; we reexamined all control data for pressure injection experiments. It is noted that this is strictly speaking not statistically valid (Payne and Dyer, 1975; Wagenmakers et al., 2012)[9], and a good example of why a priori hypothesis making is ideal but is not always possible (Zwiernik et al., 2008)[10], and is only provided as an exploratory analysis to understand why our assumptions did not hold true. As the only difference between our previous pressure injection experiments and pertussis experiments in control conditions was the inclusion of 10 mM HEPES and adjustment to a pH of 7.2, we wanted to see if this made a significant difference to our control experiments. As shown in figure 3.5B, lowering calcium made a significant difference in proctolin-induced $I_{MI}$ amplitude [Calcium; $F(1, 40) = 15.070$, $p = 3.79 \times 10^{-4}$. Buffer; $F(1, 40) = 3.042$, $p = 0.089$. Interaction; $F(1, 40) = 3.389$, $p = 0.073$.]. A post-hoc Tukey test showed that calcium did not significantly increase $I_{MI}$ amplitude in the absence of buffer ($p = 0.058$), but did significantly augment it when buffer was included ($p = 0.002$). This suggests that our separation of voltage dependence and amplitude is valid in the absence of buffer but not in the presence of buffer. As Pertussis-toxin experiments were

[9] These papers note that without an a priori hypothesis, statistics are not very meaningful but necessary for exploratory research, but it is essential to label it as such.

[10] This paper attempts to balance the problems addressed in 9, balanced with the real world finding that in physiology, it is naïve to assume that all hypotheses can be made a priori.

carried out with buffer its effects cannot be interpreted as purely on amplitude due to the confounding effects we found of buffer.

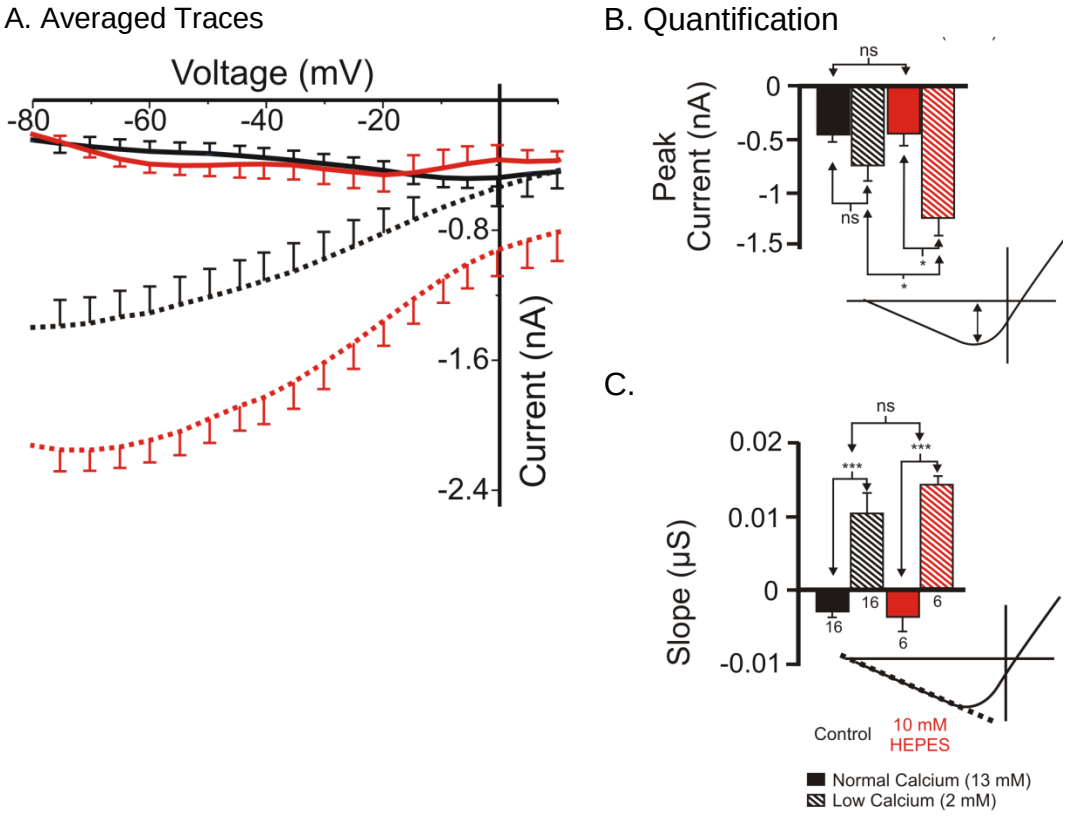


**Figure 3.5. Effect of 10 mM HEPES on Extracellular Calcium Modulation of $I_{MI}$ Amplitude.** Control pressure injection solutions of 500 mM KCl and 20 mM TEA (Black) or the same with 10 mM HEPES with pH adjusted to 7.2 (Red) in either normal (Solid; 13 mM) or Low (Striped; 2 mM) extracellular calcium. All recording electrodes used 20 mM KCl and 0.6 M $K_2SO_4$. During $I_{MI}$ recording, saline contained 0.1 µM TTX, 10 µM PTX, 200 µM $CdCl_2$, 5 mM CsCl and 20 mM TEA. (A) Averaged IV curves for pressure injection experiments. (B) A 2-Way ANOVA showed that calcium significantly affected proctolin-induced $I_{MI}$ amplitude at -15 mV slope [Calcium; $F(1, 40) = 15.070$, $p = 3.79 \times 10^{-4}$. Buffer; $F(1, 40) = 3.042$, $p = 0.089$. Interaction; $F(1, 40) = 3.389$, $p = 0.073$.] A Tukey test showed that in the absence of buffer, this modulation was not significant ( $p = 0.058$) while in the presence of Buffer, calcium significantly increased amplitude ($p = 0.002$). (C) A 2-way ANOVA showed that calcium but not buffer significantly increased proctolin-induced $I_{MI}$ slope [Calcium; $F(1, 40) = 36.083$, $p = 4.6 \times 10^{-7}$. Buffer; $F(1, 40) = 0.408$, $p = 0.527$. Interaction; $F(1, 40) = 0.378$, $p = 0.378$.] Post Hoc Tukey *, $p < 0.05$, ***, $p < 0.001$. Error bars SEM.

The findings shown by Pertussis-toxin, GDP-βS and GTP-γS suggest that proctolin-induced $I_{MI}$ activation is dependent on G-proteins but these pertussis results add an interesting wrinkle in our model, as we had not predicted that calcium should modulate G-protein sensitivity. While there are examples of calmodulin modulation of regulators of G-protein signaling (RGS) proteins, which in turn modulate G-protein rate of GTP hydrolysis (Blazer et al., 2010), and also examples where calmodulin is in direct competition with βγ-subunit in the mGluR7 receptor (El Far et al., 2001a), it does not seem intuitive that this should modulate PTX binding to its target, as once a protein is ADP-rybosylated, this should be a permanent modification. That is, if the alpha subunit is inactivated, then hydrolysis should have no effect on activity because there is none. These results confirm that proctolin-induced $I_{MI}$ activation is dependent on GPCRs, at least in low calcium, as pertussis inhibition is a hallmark of trimeric G-proteins (Katada, 2012). These results suggest that proctolin-induced $I_{MI}$ in low calcium signals through the pertussis toxin sensitive G-proteins $G_I$, $G_O$, or $G_T$ and that this seems to be modulated by calcium.

*Conclusion: Proctolin-induced $I_{MI}$ requires a pertussis sensitive G-protein in low but not normal calcium.*

As shown by the effects of G-protein inhibitors and the finding that the G-protein activator, GTP-γS, produced the expected occlusion of proctolin-induced $I_{MI}$, *it* has been

shown that proctolin-induced $I_{MI}$ is dependent on GPCRs. Although the findings of GDP-βS and GTP-γS do not exclude the possibility of involvement of monomeric G-proteins, the pertussis toxin results lead to the conclusion that proctolin binds to a GPCR whose G-protein dependence may be modulated by extracellular calcium since pertussis toxin is known to only bind heterotrimeric G-proteins (Katada, 2012).

## 3.3 Role of Cyclic Nucleotides in Proctolin-induced $I_{MI}$ Activation.

*The Case for Cyclic Nucleotides.*

Initially we hypothesized that $I_{MI}$ activation and a common intermediary upon which other neuromodulators converged as shown by Swensen and Marder (2000) is a cyclic nucleotide. As discussed in Chapter 1, the literature is ambiguous as to whether cyclic nucleotide signaling is commonly downstream of proctolin and CCAP receptors. In examples where the pyloric rhythm is restored by cyclic nucleotide agonists such as that shown by Spruston and Nusbaum (1991), it is unclear whether this was due to activation of $I_{MI}$ or other mechanisms such as augmentation of $I_H$ or reduction in outward currents (Spruston and Nusbaum, 1991). In lobster, Flamm et al., (1987) found that neuromodulators that activated $I_{MI}$, proctolin, pilocarpine and FMRFamide, were incapable of raising STG-wide levels of cAMP. In contrast, the cAMP agonist forskolin and the neuromodulator octopamine were capable of raising cAMP to detectable levels. As this same study also reported that dopamine did not alter cAMP levels, and dopamine has since been shown to modulate cAMP in a receptor-subtype and cell-type specific manner in opposing directions (Zhang et al., 2010), it is uncertain whether negative results using this method are truly meaningful. Another experiment using a cAMP imaging in specific cell types in lobster replicated the lack of proctolin and pilocarpine producing significant changes in cAMP (Hempel et al., 1996). Together these results suggest that proctolin, pilocarpine and FMRFamide do not activate $I_{MI}$ via cAMP in lobster unless they do so in such small, localized amounts or opposing directions

depending on receptor subtype—such that they are beyond the level of detection in these experiments. As reviewed in Chapter 1, in other invertebrate systems, some evidence has been shown to support proctolin-mediated cAMP increase (Hiripi et al., 1979; Erxleben et al., 1995; Mazzocco-Manneval et al., 1998). There is also evidence for a PKC mediated decrease in cGMP in crustacean muscle (Philipp et al., 2006). With this in mind, we investigated the effect of cyclic nucleotides on proctolin-induced $I_{MI}$ in *Cancer borealis*.

*Statistical Criterion and definition of an '$I_{MI}$-like' difference current.*

As described in Chapter 2, we wanted to see if pharmaceutical agents were capable of producing an $I_{MI}$-like difference current. To analyze this data statistically, we defined an $I_{MI}$-like difference current by two criteria. First, such a difference current would have to be significantly from zero in the presence of the drug and eventually wash out (at least partially) in the absence of the drug. Second, this current would have to demonstrate significant voltage dependence with negative slope. To quantify these criteria statistically, a difference current would be analyzed by a three-way ANOVA with factors of agonist, time and voltage. To meet the first criterion, there should be a significant interaction of time with agonist showing that this difference current is due to agonist and not ramps alone. To meet the second criterion, we require voltage to be significant as a main effect and display negative slope. We first examined this method for cAMP signaling.

*The specific cAMP agonist 8-Br-cAMP is not sufficient to produce an '$I_{MI}$'-like current.*

To test the hypothesis that cAMP was downstream of the neuromodulators that activate $I_{MI}$, we applied the cAMP agonist 8-Br-cAMP. We predicted 500 µM 8-Br-cAMP should produce an $I_{MI}$-like difference current. We used 500 µM as it was somewhat higher than concentrations used in our system by previous authors (Ballo et al., 2010b; Zhang et al., 2010). Figure 3.6 shows the difference current produced by voltage ramps alone or application of 500 µM of 8-Br-cAMP, at either 5 (ommited in Figure 3.6A for clarity) or 10 minute intervals. A three-way ANOVA showed that neither ramps alone nor 500 µM 8-Br-cAMP were significantly different from zero [8-Br-cGMP; $F(1, 3) = 0.461$, $p = 0.546$. Time; $F(1, 3) = 0.852$, $p = 0.424$. Interaction; $F(1, 3) = 0.234$, $p = 0.661$]. Even longer applications showed no effect of 8-Br-cAMP producing an $I_{MI}$-like difference current in LP cells (Not shown). There were many examples of increased leakiness (the exact opposite of an '$I_{MI}$'-like difference current) but nothing resembling $I_{MI}$ (not shown).

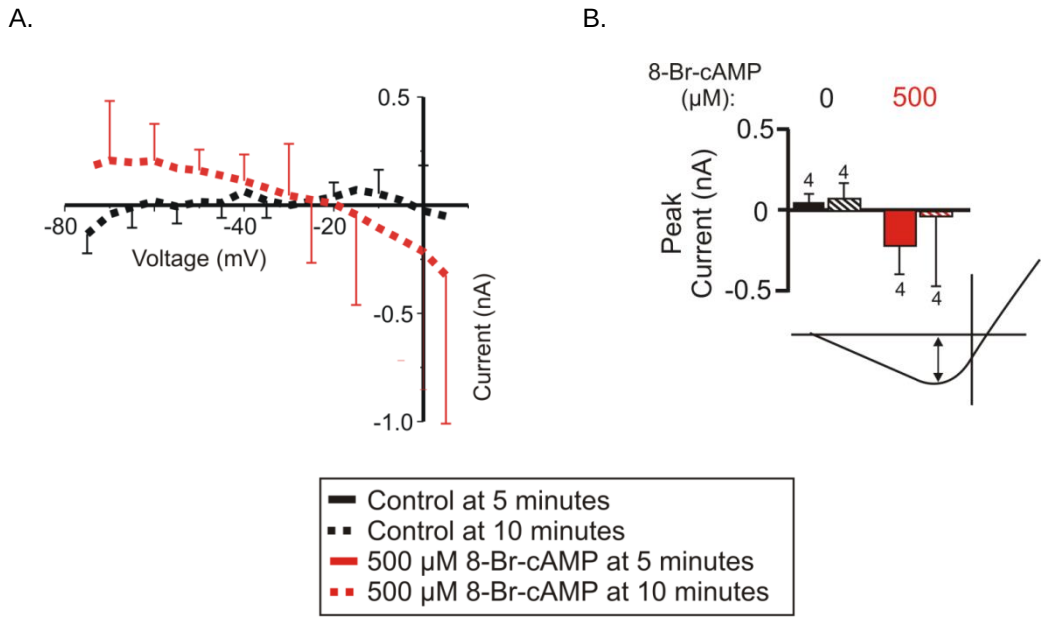


**Figure 3.6: The cAMP agonist 8-Br-cAMP 10 minute Difference Current is not Significantly Different from Voltage Ramps Alone.** Difference current from ramps alone (**Black**) vs 500 μM 8-Br-cAMP (**Red**) at either 5 minutes (**Solid**) or 10 minutes (*Striped.)* Saline contained 0.1 μM TTX, 10 μM PTX, 200 μM $CdCl_2$, 5 mM CsCl and 20 mM TEA. (A)Averaged IV curves for 10 minute difference currents for ramps alone or 500 μM 8-Br-cAMP. 5 minute ramps were omitted for clarity. A 3 way ANOVA for 8-Br-cAMP, time and voltage showed that 500 μM 8-Br-cAMP difference current was not significantly different from ramps alone. [8-Br-cAMP; F (1, 204) = 0.227, p = 0.634. Time; F (1, 204) = 1.199, p = 0.275. Voltage; F (1, 204) = 0.683, p = 0.809. Full factorial model; no significant interactions found.] (B) Amplitude for 500 μM 8-Br-cAMP difference current at -15 mV. Error bars are SEM.

*The cAMP agonist 8-Br-cAMP does not alter proctolin-induced $I_{MI}$.*

As mentioned previously, we predicted that any second messenger agonist that activates $I_{MI}$ should reduce (occlude) the response to known neuromodulators. We therefore measured proctolin-induced $I_{MI}$ in the presence of the membrane permeable cAMP agonist 8-Br-cAMP. Only applications 2 ,3 and 4 were included in this analysis to

reduce variability. Figure 3.7A shows a representative sample of proctolin-induced $I_{MI}$ in the presence and absence of 500 µM 8-Br-cAMP. Typically, we saw no difference between measured proctolin-induced $I_{MI}$ before (**Black** solid) and after exposure to 500 µM 8-Br-cAMP (**Red**). We did notice however that there seemed to be a reduction of proctolin-induced $I_{MI}$ after washout (*Red dotted*). We therefore included the wash in the statistical analysis to determine if there may be a delayed effect of 500 µM 8-Br-cAMP on activation or acceleration of desensitization, since a rich literature suggests protein kinase A (PKA) mediated desensitization of β-2-adrenergic receptor (Pitcher et al., 1992; Gomperts et al., 2002; Tran et al., 2004; Alberts, 2008; Lodish, 2008). Even including the washout, a two-way ANOVA showed no significant interaction or main effects between 8-Br-cAMP and application number [8-Br-cAMP; $F(1, 10) = 0.476$, $p = 0.506$. App#; $F(1, 10) = 4.344$, $p=0.064$. Interaction; $F(1, 10) = 1.729$, $p = 0.218$. ]. These data suggest that 8-Br-cAMP does not mediate $I_{MI}$ signalling. The observed washout effect is not statistically significant. However, as these studies were designed to examine whether cAMP is directly involved in $I_{MI}$ signalling, it would still be interesting to see whether longer term incubations could significantly enhance proctolin-induced $I_{MI}$ desensitization rate. Further, applications for up to 1 hour after exposure show no signs of accelerated desensitization.

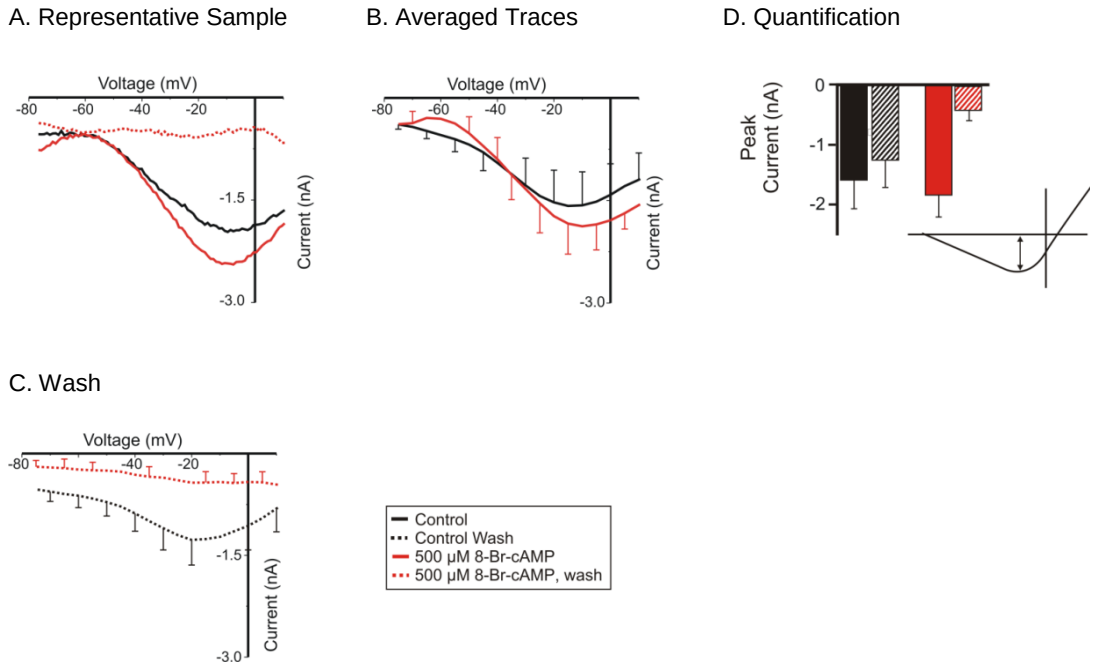


**Figure 3.7: 20 Minute Exposure to 8-Br-cAMP does not Occlude or Inhibit $I_{MI}$ but May Accelerate Desensitization.** Proctolin-induced $I_{MI}$, in control (**Black**; n = 4), or in 500 µM 8-Br-cAMP (**Red**); n = 4). Exposure during (**Solid**) or after wash (*Stripes).* Saline contained 0.1 µM TTX, 10 µM PTX, 200 µM $CdCl_2$, 5 mM CsCl and 20 mM TEA. (A) Representative IV curves of proctolin-induced $I_{MI}$. (B) Averaged IV curves of proctolin-induced $I_{MI}$. (C) One hour wash from 500 µM 8-Br-cAMP or control conditions. (D) A 2 way ANOVA showed neither 8-Br-cAMP nor application number were capable of reducing proctolin-induced $I_{MI}$ amplitude at -15 mV. [8-Br-cAMP; $F(1, 10) = 0.476$, $p = 0.506$. Application number; $F(1, 10) = 4.344$, $p=0.064$. Interaction; $F(1, 10) = 1.729$, $p = 0.218$.] Error bars are SEM.

*The adenyl cyclase agonist forskolin produces a significant difference current that is not an $I_{MI}$-like difference current.*

To further test the hypothesis that cAMP is mediating $I_{MI}$, we used the adenyl cyclase agonist forskolin. As illustrated in Figure 3.8, application of 10 µM forskolin induced a significant difference current. A 3-way ANOVA showed that the forskolin induced current was significantly different from ramps alone, and had several significant interactions [Forskolin; $F(1, 204) = 48.041$, $p < 10^{-8}$. Time; $F(1, 204) = 55.333$, $p < 10^{-8}$. Voltage; $F(16, 204) = 1.622$, $p = 0.065$. Interaction (forskolin v voltage); $F(16, 204) = 1.988$, $p = 0.015$. Interaction (forskolin v time); $F(1, 204) = 15.828$, $p = 9.635 \times 10^{-5}$.]. Despite the two significant second order interactions (forskolin with time, forskolin with voltage) this difference current was not considered $I_{MI}$-like for two reasons. First, a post hoc Tukey test showed that forskolin was only significantly different from zero at voltages from -50 to -80 mV.This region is precisely where proctolin-induced $I_{MI}$ is already waning. Second, this difference current displayed positive and not negative slope conductance suggesting it was not $I_{MI}$. These data, along with the previously mentioned findings from 8-Br-cAMP, suggests that cAMP agonists are not sufficient to activate an $I_{MI}$ like difference current.

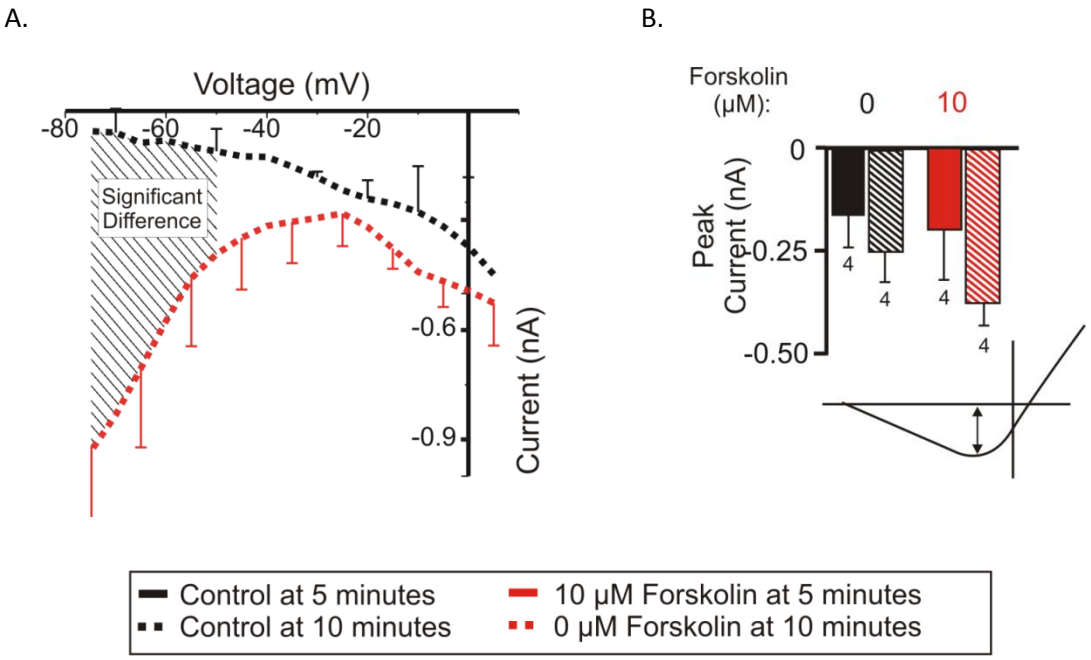


**Figure 3.8: The Adenylyl Cyclase Agonist Forskolin Produces a Voltage Dependent Difference Current that is Not $I_{MI}$.** 10 Minute difference current for voltage ramps alone (**Black**) and ramps after 10 minutes of 10 μM Forskolin application (**Red)**.At 5 minutes (**Solid**) or 10 minutes (*Striped)* Saline contained 0.1 μM TTX, 10 μM PTX, 200 μM $CdCl_2$, 5 mM CsCl and 20 mM TEA. (A) Averaged IV curve for 10 minute difference current. A 3-way ANOVA showed that this difference current was significantly different from ramps alone. [Forskolin; $F(1, 204) = 48.041$, $p < 10^{-8}$. Time; $F(1, 204) = 55.333$, $p < 10^{-8}$. Voltage; $F(16, 204) = 1.622$, $p = 0.065$. Interaction (forskolin v voltage); $F(16, 204) = 1.988$, $p = 0.015$. Interaction (forskolin v time); $F(1, 204) = 15.828$, $p = 9.635 \times 10^{-5}$.] A post-hoc Tukey test, however, showed that this difference was only significant from -50 mv to -80 mV (Shaded region). (B) Forskolin difference current vs voltage ramps alone at -15 mV. Error bars are SEM.

*The adenyl cyclase agonist forskolin does not affect proctolin-induced $I_{MI}$ slope or amplitude.*

To determine whether cAMP was mediating activation of $I_{MI}$, we measured proctolin-induced $I_{MI}$ in the presence and absence of 10 µM of the adenyl cyclase agonist forskolin. We hypothesized that if the proctolin receptor activates $I_{MI}$ through a cAMP intermediate we should observe a reduced response to proctolin-induced $I_{MI}$ amplitude (Occlusion). As illustrated in Figure 3.9, a 2-way ANOVA showed that forskolin did not significantly reduce proctolin-induced $I_{MI}$ during or after forskolin application [Forskolin; $F(1, 12) = 3.278$, $p = 0.095$. Condition (During vs Wash); $F(1, 12) = 0.102$, $p = 0.755$. Interaction; $F(1, 12) = 0.0454$, $p = 0.835$.]. This data agrees with our results for 8-Br-cAMP, and suggests that proctolin-induced $I_{MI}$ does not depend on cAMP signalling.

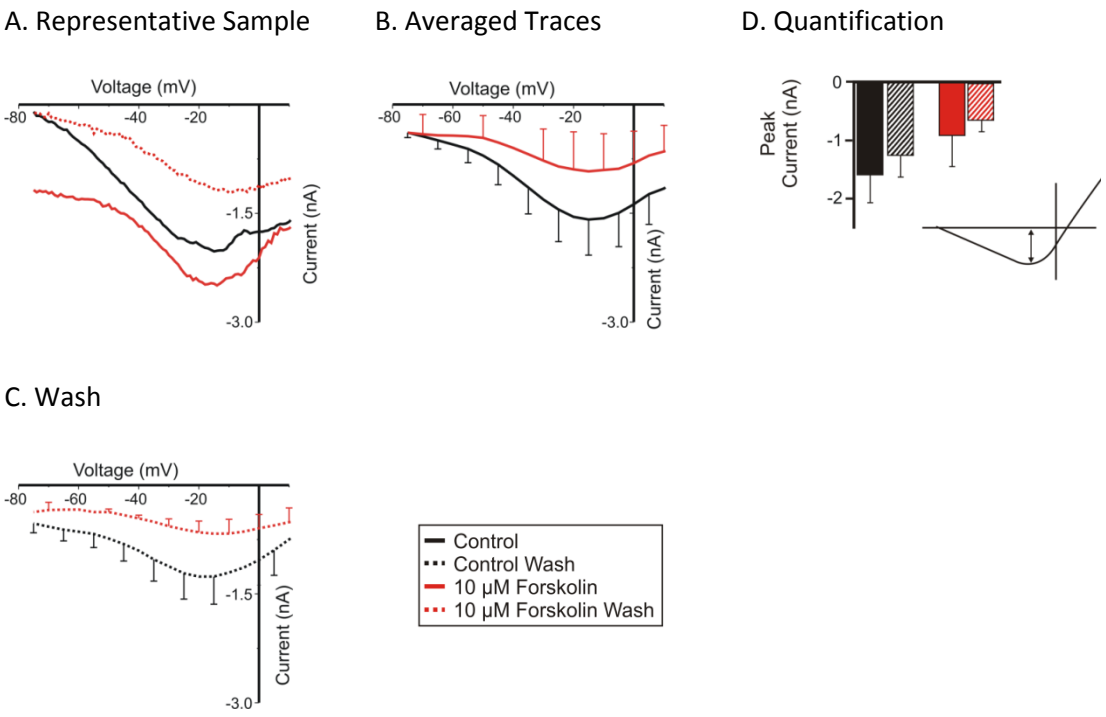


**Figure 3.9: The Adenylyl Cyclase Agonist Forskolin does not Significantly Occlude or Inhibit $I_{MI}$.** Proctolin-induced $I_{MI}$ in control (**Black**) or in 10 μM forskolin (**Red**), before (**Solid**) and after washout (*Striped)*. Saline contained 0.1 μM TTX, 10 μM PTX, 200 μM $CdCl_2$, 5 mM CsCl and 20 mM TEA (A) Representative sample of proctolin-induced $I_{MI}$ IV curves (B) Averaged IV curves of proctolin-induced $I_{MI}$. (C) Averaged IV curves of proctolin-induced $I_{MI}$. after 1-hour washout of 10 μM forskolin or control saline (D). A 2-way ANOVA showed that 10 μM forskolin had no significant effect on $I_{MI}$ amplitude at -15 mV either during its application or upon its washout. [Forskolin; F (1, 12) = 3.278, p = 0.095. Condition (During vs Wash); F (1, 12) = 0.102, p = 0.755. Interaction; F (1, 12) = 0.0454, p = 0.835.] Error bars are SEM.

*Application of the cGMP agonist 8-Br-cGMP produces a significant difference current that is, unlike $I_{MI}$, independent of voltage.*

In order to test the hypothesis that the proctolin receptor activates $I_{MI}$ through a cGMP intermediate, we used the membrane permeable cGMP agonist 8-Br-cGMP. As

illustrated in Figure 3.10, a 3-way ANOVA showed that 8-Br-cGMP produced a significant difference current that was independent of voltage [8-Br-cGMP; $F(2, 238) = 14.110$, $p = 1.62 \times 10^{-6}$. Time; $F(1, 238) = 8.276$, $p = 0.004$. Voltage; $F(16, 238) = 0.373$, $p = 0.987$ Interaction (8-Br-cGMP, time); $F(2, 238) = 11.878$, $p = 1.21 \times 10^{-5}$.]. This current showed no dependence on voltage and therefore did not meet our criterion of voltage dependence. Further, when analyzed at -15 mV, a Tukey post-hoc test showed that 8-Br-cGMP was not significantly different from ramps alone (500 µM vs 0, $p = 0.946$; 1000 µM vs 0, $p = 0.983$). This suggests that although this current is significant, the lack of significant voltage dependence, or any significant interactions with voltage suggests that 8-Br-cGMP was not sufficient to produce an $I_{MI}$-like difference current.

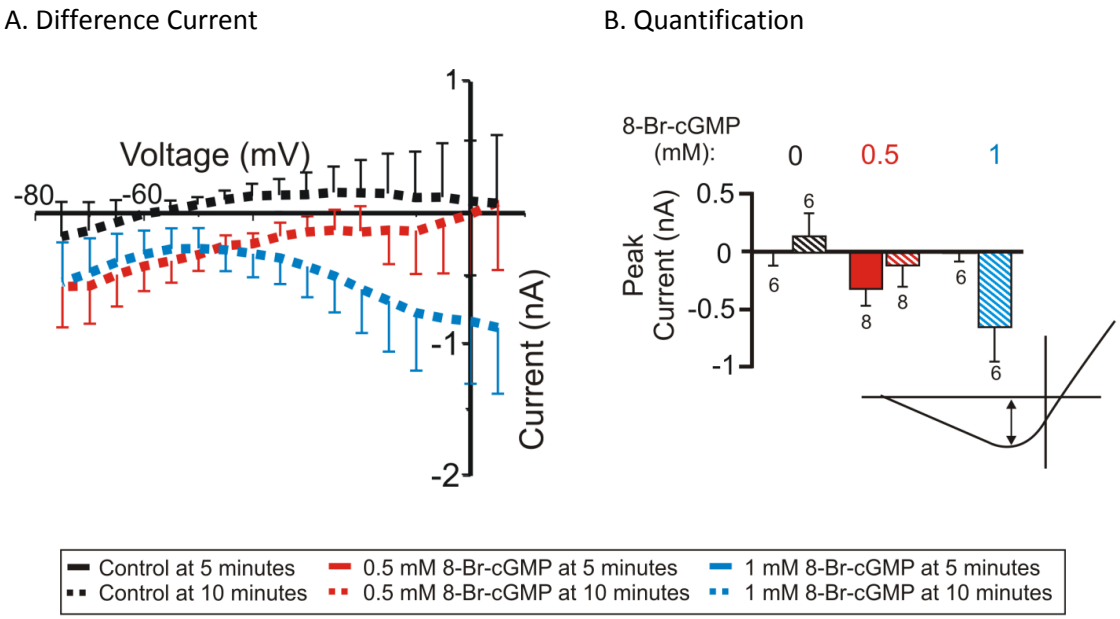


**Figure 3.10: The cGMP Agonist 8-Br-cGMP Produced a Voltage-Independent Difference Current.** Voltage was ramped continuously in 0.1 μM TTX, 10 μM PTX, 200 μM $CdCl_2$, 5 mM CsCl, and 20 mM TEA and measured at 5 and 10-minute intervals. Then 0 mM (**Black**), 0.5 mM (**Red**), and 1 mM (**Blue**) concentrations of the agonist 8-Br-cGMP were applied. The resulting IV curves for these difference currents were plotted at 5 (**Solid)** and 10-minute intervals (*Striped)*. (A) Averaged IV curve for difference current produced by ramping the voltage for 10 minutes in different concentrations of 8-Br-cGMP (5 minute difference currents were omitted for clarity). To determine if these currents were significantly different from 0, voltage dependent and different from ramps alone, a 3-way ANOVA was done for factors 8-Br-cGMP, voltage, and time. This analysis showed that 8-Br-cGMP interacted significantly with time and peaked at 10 minutes. This current was independent of voltage. [8-Br-cGMP; $F(2, 238) = 14.110$, $p = 1.62 \times 10^{-6}$. Time; $F(1, 238) = 8.276$, $p = 0.004$. Voltage; $F(16, 238) = 0.373$, $p = 0.987$ Interaction (8-Br-cGMP, time); $F(2, 238) = 11.878$, $p = 1.21 \times 10^{-5}$.] A Tukey post-hoc test showed that there was a significant difference between 5 and 10 minute difference currents in both 500 μM 8-Br-cGMP ($p = 0.002$) and 1000 μM 8-Br-cGMP ($p = 0.004$), but not in the absence of 8-Br-cGMP ( $p = 0.415$). (B) Amplitude of the 8-Br-cGMP difference current at -15 mV.

*Application of the cGMP agonist 8-Br-cGMP does not affect proctolin-induced $I_{MI}$ amplitude or slope.*

To test the hypothesis that the proctolin receptor activates $I_{MI}$ through cGMP, we measured proctolin-induced $I_{MI}$ in the presence and absence of the membrane permeable, specific cGMP agonist 8-Br-cGMP. As shown in Figure 3.11, application of 8-Br-cGMP had no effect on $I_{MI}$ amplitude. A 1-way ANOVA showed that 8-Br-cGMP had no significant effect on $I_{MI}$ amplitude [F (2, 9) = 0.350, p = 0.714]. This data suggests that proctolin-induced $I_{MI}$ does not signal through cGMP.

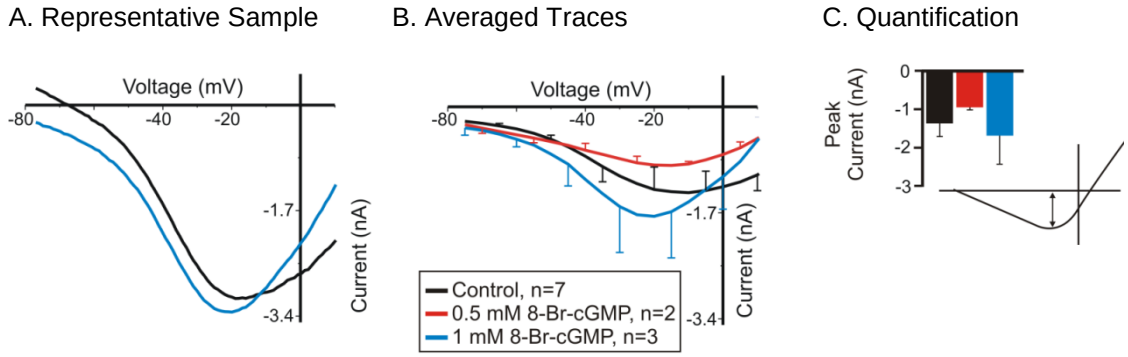


**Figure 3.11: The cGMP Agonist 8-Br-cGMP Does Not Alter $I_{MI}$ Slope or Amplitude.** Proctolin-induced $I_{MI}$ in control (**Black**), 0.5 mM (**Red**), or 1 mM (**Blue**) of 8-Br-cGMP. Saline contained 0.1 µM TTX, 10 µM PTX, 200 µM $CdCl_2$, 5 mM CsCl, and 20 mM TEA (A) Representative IV curves of proctolin-induced $I_{MI}$ before and during application of 1 mM 8-Br-cGMP. (B) Averaged IV curves of proctolin-induced $I_{MI}$ in different concentrations of 8-Br-cGMP. (C) Quantification of effect of 8-Br-cGMP on $I_{MI}$ amplitude at -15 mV. A 1-way ANOVA showed that 8-Br-cGMP had no significant effect on $I_{MI}$ amplitude. [F (2, 9) = 0.350, p = 0.714.]

*The Protein Kinase A inhibitor H89 does not produce a significant difference current.*

Although we did not expect $I_{MI}$ activation to occur by inhibition of PKA, we did expect that PKA may be involved in $I_{MI}$ desensitization due to our earlier observations that long term incubation in 8-Br-cAMP appeared to reduce $I_{MI}$ amplitude. We measured

the difference current produced by voltage ramps alone vs voltage ramps in the presence of H89 as illustrated in Figure 3.12. A 3-way ANOVA showed that H89 did not produce a significant difference current that was different from ramps alone [H89; $F(1, 357) = 3.230$, $p = 0.073$. Time; $F(2, 357) = 2.648$, $p = 0.072$. Voltage; $F(16, 357) = 3.250$, $p = 2.77 \times 10^{-5}$. No significant interactions.]. Although it is tempting to see the shape of averaged H89, as resembling an $I_{MI}$ like current, this current was not significantly different from ramps alone. This data suggests that PKA inhibition is not sufficient for $I_{MI}$ activation. This data also suggests that H89 does not produce any modulation of leak different from ramps alone.

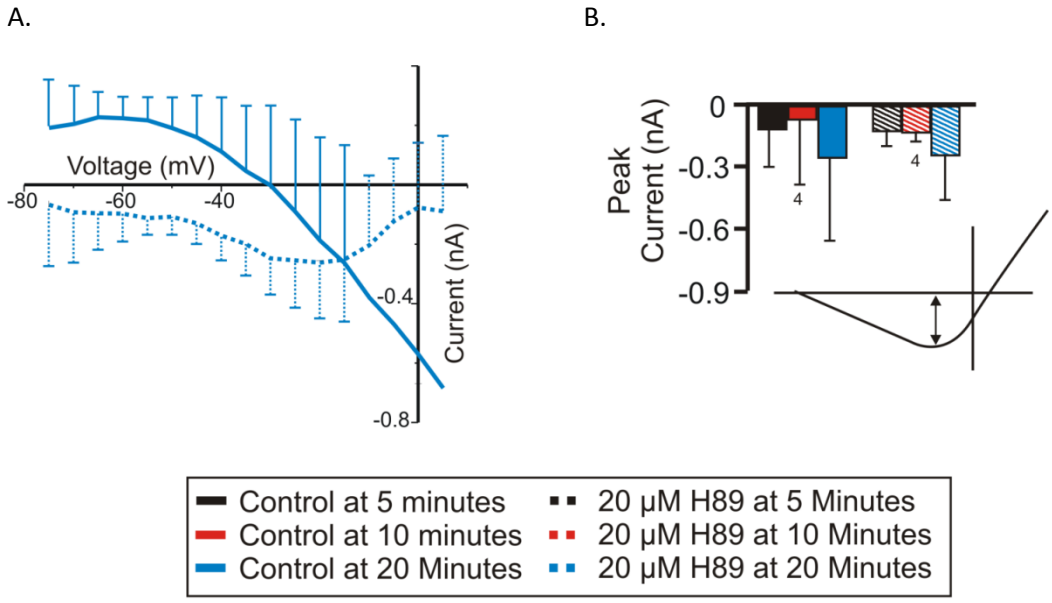


**Figure 3.12: The Protein Kinase A (PKA) Inhibitor H89 does Not Produce a Significant Difference Current.** Saline contained 0.1 μM TTX, 10 μM PTX, 200 μM $CdCl_2$, 5 mM CsCl, and 20 mM TEA Voltage ramps were applied in the presence (*Striped*) and absence (**Solid**) of the PKA inhibitor H89. Difference currents were plotted at 5 (**Black**), 10 (**Red**), and 20 (**Blue**) minute intervals.(A) Difference current IV curves produced after 20 minutes of ramping in presence and absence of H89 (5 and 10 minutes omitted for clarity). A 3-way ANOVA showed that the H89 difference current was not significantly different from 0. [H89; $F(1, 357) = 3.230$, $p = 0.073$. Time; $F(2, 357) = 2.648$, $p = 0.072$. Voltage; $F(16, 357) = 3.250$, $p = 2.77 \times 10^{-5}$. No significant interactions.] B) Difference current amplitudes at -15 mV.

*The PKA inhibitor H89 does not alter proctolin-induced $I_{MI}$ amplitude but may modulate its voltage dependence.*

We tested the response of proctolin-induced $I_{MI}$ in the presence and absence of the PKA inhibitor H89. H89 has more promiscuous activity than once thought; it has been shown to block S6K1, MSK1, ROCK-II, PKB-α, and MAPKAP-K1b at similar IC50s to PKA (Lochner and Moolman, 2006), and an effect of H89 may reveal a signalling

pathway independent of PKA. The main reason that H89 was originally studied was the prediction that H89 may augment proctolin-induced $I_{MI}$ following the hypothesis that PKA was mediating proctolin-induced $I_{MI}$ desensitization. As illustrated in Figure 3.13, application of H89 was unable to modulate $I_{MI}$ amplitude either during application or after its wash out [H89; $F(1, 17) = 1.934$, $p = 1.82$. Time; $F(1, 17) = 0.197$, $p = 0.663$. Interaction; $F(1, 17) = 0.460$, $p = 0.507$]. Although as will be described later in chapter 4 there were significant effects of H89 on voltage dependence. As shown in the appendix and its ability to modulate voltage dependence (discussed in Chapter 4) suggested that H89 was active. This, along with its inability to affect $I_{MI}$ amplitude, suggests that PKA is not involved in $I_{MI}$ activation. Unfortunately, not enough long term multiple application[11] data was collected to see whether H89 could reduce the proctolin-induced $I_{MI}$ desensitization rate. However, H89 did not produce the expected enhancement of proctolin-induced $I_{MI}$. These results suggest that PKA (or other H89 sensitve kinase) may play a role in $I_{MI}$ voltage dependence, but PKA activation is not required for proctolin-induced $I_{MI}$ activation.

[11] As discussed in chapter 2, this would require at least 6 applications to be significant. (Application one is reserved to measure the 'health' of the response).

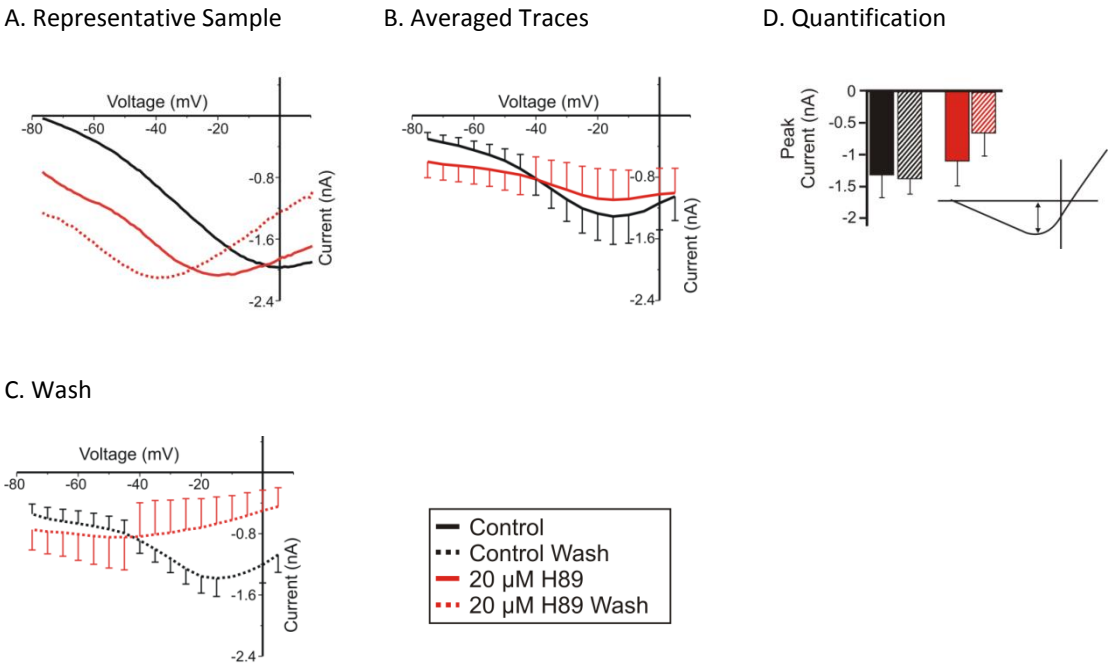


**Figure 3.13. The PKA Inhibitor H89 Does not Affect Proctolin-induced $I_{MI}$ Amplitude or Desensitization but May Modulate Its Voltage Dependence.** Measurement of proctolin-induced $I_{MI}$ in control (**Black**) or 20 μM H89 (**Red**), measured during (**Solid**) and after washout (*Striped*). Saline contained 0.1 μM TTX, 10 μM PTX, 200 μM $CdCl_2$, 5 mM CsCl and 20 mM TEA (A) Representative IV trace of cell exposed to H89. (B) Averaged IV traces during exposure to control saline or the same with 20 μM H89. (C) 30-60 minute washout from control saline or 20 μM H89. (D) A 2-way ANOVA showed that neither H89 nor time were capable of significantly altering proctolin-induced $I_{MI}$ at -15 mV. [H89; $F(1, 17) = 1.934$, $p = 1.82$. Time; $F(1, 17) = 0.197$, $p = 0.663$. Interaction; $F(1, 17) = 0.460$, $p = 0.507$].Error bars are SEM. Tukey Post hoc test; *, $p < 0.05$.

*Caffeine did not affect $I_{MI}$ in washout experiments.*

In order of increasing concentrations, caffeine is a an adenosine receptor antagonist (Fisone et al., 2004), competitive inhihibitor of phosphodiesterase (Kehoe,

1990; Fisone et al., 2004), and mobilizer of intracellular calcium release (Fisone et al., 2004){Levi, 2003 #94633}. At the end of some experiments, we washed out for at least 2 hours and tested whether application of this phosphodiesterase inhibitor would affect $I_{MI}$ amplitude. Figure 3.14 demonstrates that caffeine was unable to significantly alter proctolin-induced $I_{MI}$ amplitude [Caffeine; F (1, 8) = 0.248, p = 0.632. Application Number; F (1, 8) = 11.496, p = 0.009.]. at 5 mM. The same was observed for 1mM and 10mM but these results could not be statistically analyzed due to differing conditions. Although these results had low n, together with the previous results, they argue against $I_{MI}$ being mediated by cyclic nucleotides.

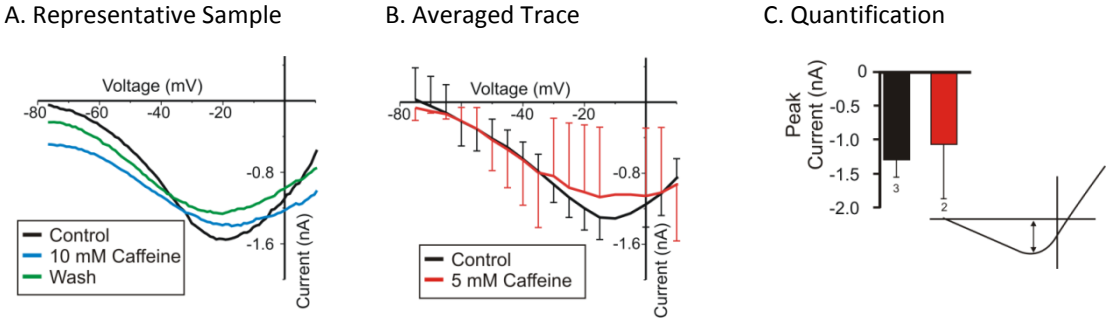


**Figure 3.14. The Phosphodiesterase Inhibitor Caffeine Does not Affect $I_{MI}$ Slope or Amplitude.** Measurement of proctolin-induced $I_{MI}$ in Control (**Black**), 5 mM (**Red**) or 10 mM (Blue) caffeine. Saline contained 0.1 µM TTX, 10 µM PTX, 200 µM $CdCl_2$, 5 mM CsCl and 20 mM TEA. Note: these experiments were run after 2-hour washout from other experiments. (A) Representative IV curve of proctolin-induced $I_{MI}$.(B) Averaged IV curves of proctolin-induced $I_{MI}$ in the absence (app #5) and presence of caffeine (Averaged app #5.5). (C) A one way ANOVA for caffeine with analysis of covariance for application number showed that caffeine had no significant effect on $I_{MI}$ amplitude at -15 mV.[Caffeine; F (1, 8) = 0.248, p = 0.632. Application Number; F (1, 8) = 11.496, p = 0.009.] Error bars are SEM.

*Summary of Cyclic Nucleotides.*

Our results suggest that $I_{MI}$ is not dependent on cyclic nucleotide signalling. Thanks to the positive controls presented, we are confident that $I_{MI}$ activation is not dependent on cGMP signalling. We make the case based on forskolin making a significant difference current, and a literature precedent for the use of 8-Br-cAMP in this system that $I_{MI}$ signalling is unlikely to rely directly on cAMP despite the lack of direct positive controls. Interestingly, however, there appears to be a role for H89 sensitive kinases, presumably PKA, not in $I_{MI}$ activation, but in modulating $I_{MI}$ voltage dependence as discussed in Chapter 4. This was counter to our expectations in that we expected PKA to be involved with desensitization and activation but not voltage dependence. The fact that we did find a positive result for both $I_{MI}$ and $I_A$ with H89 application suggests that this agent was working but does not affect $I_{MI}$ activation. Although the n for caffeine was low, in the context of the prevcious results, the lack of augmentation of the current argues against cyclic nucleotide signalling, while the lack of inhibition argues against inhibition of nucleotide signalling (a mechanism for transducin signalling (Shiells and Falk, 1992) and proctolin-induced signalling in crustaceans (Philipp et al., 2006)) as the primary mechanism of $I_{MI}$ signalling. Together these results make it unlikely that neuromodulator receptors activate $I_{MI}$ by cyclic nucleotides.

## 3.4: Phospholipase C Signaling

*The PLC inhibitor edelfosine (Et-18-$OCH_3$) does not produce an $I_{MI}$–like difference current.*

Due to the large amount of literature suggesting that PLC-associated mechanisms operating downstream of proctolin, muscarinic and FMRFamide receptors in other systems, (as discussed in Chapter 1), we wanted to carefully test the hypothesis that $I_{MI}$ activation is mediated by PLC signalling. Swensen and Marder (2000) and Swensen (Personal comunication 2015) reported that U73122 had been tested unsuccessfully for its effect on $I_{MI}$ (n = 2). We wanted to test a different PLC inhibitor. We used edelfosine (Et-18-$OCH_3$), which has been tested with some success in invertebrates {Powis, 1992 #86840;Clark, 2004 #92830}. We used this to test the hypothesis that a reduction in PLC signalling was responsible for $I_{MI}$ activation. If this hypothesis was correct, then voltage ramps alone in $I_{MI}$ recording saline in should produce an $I_{MI}$-like difference current when subtracted from ramps in edelfosine. As shown in Figure 3.15, a 3-way ANOVA showed that edelfosine was not sufficient to produce an $I_{MI}$-like difference current vs voltage ramps alone [Edelfosine; $F(2, 476) = 7.330$, $p = 7.32 \times 10^{-4}$. Time; $F(2, 476) = 0.293$, $p = 0.746$. Voltage; $F(16, 476) = 1.384$, $p = 0.145$. Eldefosine x Time; $F(4, 476) = 2.359$, $p = 0.053$. Eldefosine x voltage; $F(32, 476) = 1.451$, $p = 0.055$.]. Notice also that in Figure 3.15B, that if edelfosine produced a current

at -15 mV, this current is outward relative to voltage ramps alone. This is opposite the direction expected if this were an $I_{MI}$-like difference current. This suggests that $I_{MI}$ signalling is not due to reductions in PLC signalling. Due to the absence of results with this difference current method, we stopped doing difference currents unless we discovered some reason to suspect that the second-messenger modulator would either activate $I_{MI}$ directly or have unexpected effects on the leak current.

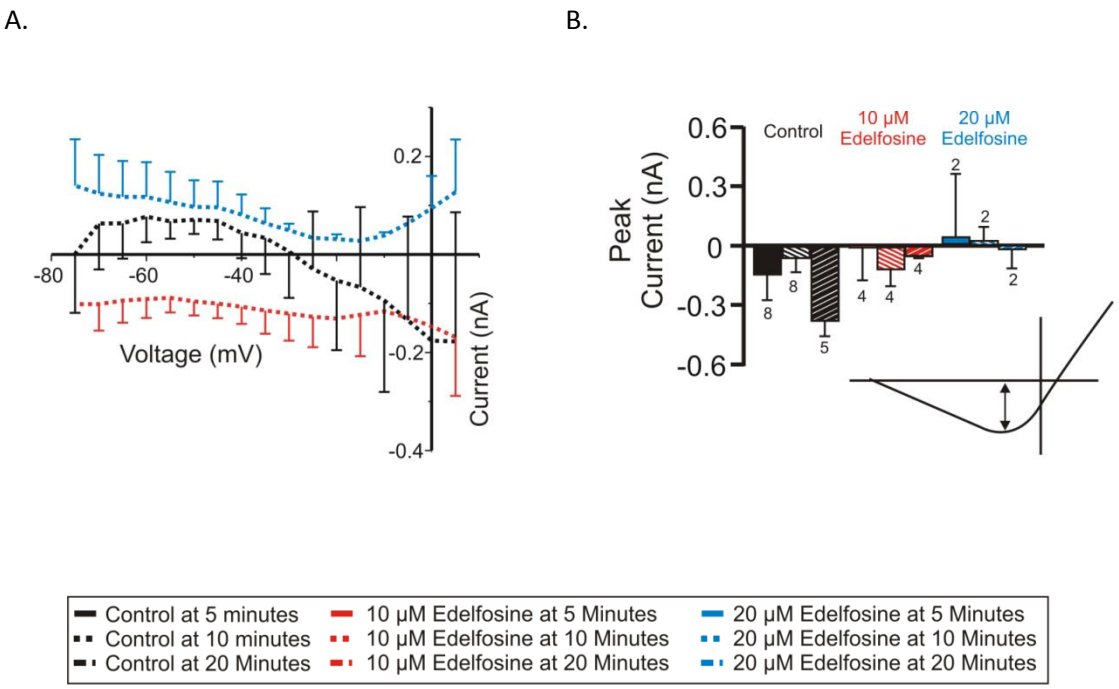


**Figure 3.15. The Phospholipase (PLC) Inhibitor Edelfosine Does not Produce a Difference Current Greater than Voltage Ramps Alone.** Saline contained 0.1 μM TTX, 10 μM PTX, 200 μM $CdCl_2$, 5 mM CsCl, and 20 mM TEA. Voltage ramps were applied in different concentrations of the PLC inhibitor Edelfosine at 0 μM (**Black**), 10 μM (**Red**), and 20 μM (**Blue**). Difference currents were assessed at 5 minutes (**Solid**), 10 minutes (*Striped*), and 20 minutes (*Dashed*). (A) Difference currents at 10 minutes (5 and 20 minutes omitted for clarity). A 3-way ANOVA showed that Edelfosine produced a *smaller* difference current than ramps alone. [Edelfosine; $F(2, 476) = 7.330$, $p = 7.32 \times 10^{-4}$. Time; $F(2, 476) = 0.293$, $p = 0.746$. Voltage; $F(16, 476) = 1.384$, $p = 0.145$. Eldefosine x Time; $F(4, 476) = 2.359$, $p = 0.053$. Eldefosine x voltage; $F(32, 476) = 1.451$, $p = 0.055$.] Tukey post-hoc tests showed no significant differences at -15 mV. (B) Difference current amplitudes at -15 mV.

*The PLC inhibitor Edelfosine does not affect proctolin-induced $I_{MI}$ slope or amplitude.*

To test our hypothesis that proctolin-induced $I_{MI}$ was dependent on PLC signalling, we measured proctolin-induced $I_{MI}$ in the presence of different concentrations of edelfosine. As illustrated in Figure 3.16, a one-way ANOVA showed that edelfosine was not capable of altering proctolin-induced $I_{MI}$ amplitude [Edelfosine; $F(2, 9) = 1.112$, $p = 0.370$]. These results argue against the hypothesis that proctolin receptors activate $I_{MI}$ through a PLC-dependent pathway.

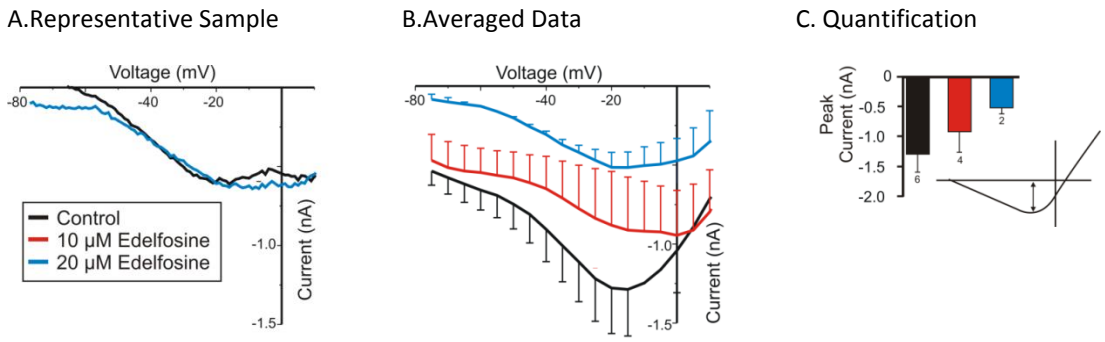


**Figure 3.16: The PLC Inhibitor Edelfosine does not Inhibit Proctolin-induced $I_{MI}$ Amplitude or Slope.** Saline contained 0.1 µM TTX, 10 µM PTX, 200 µM $CdCl_2$, 5 mM CsCl, and 20 mM TEA. Effect of PLC Inhibitor Edelfosine on proctolin-induced $I_{MI}$ in Control (Black), 10 µM (Red), and 20 µM (Blue) Eldefosine. (A) Representative IV curves of Edelfosine on proctolin-induced $I_{MI}$. (B) Averaged IV curves of Edelfosine on proctolin-induced $I_{MI}$.(C)A one-way ANOVA showed that edelfosine was unable to significantly reduce proctolin-induced $I_{MI}$ amplitude at -15 mV [Edelfosine; $F(2, 9) = 1.112$, $p = 0.370$].

*The PLC inhibitor neomycin does not affect proctolin-induced $I_{MI}$ slope or amplitude.*

To further test the hypothesis that proctolin activated $I_{MI}$ is mediated by PLC signalling, we applied the PLC inhibitor neomycin, that has been shown to succesfully inhibit PLC signalling in other invertebrate species (Willoughby et al., 1999; Rivers et al., 2002; Wenzel et al., 2002; Vezenkov and Danalev, 2009; Brown et al., 2010). This inhibitor has also been shown to significantly reduce PLC activity at concentrations as low as 10 µM directly in the cerebral cortex of guinea pigs (Schacht, 1976), and indirectly in the STG as shown by the inhibition of the L-quisylate (mGluR agonist) response in MG neurons (Levi and Selverston, 2006). This experiment was done in the presence of 2 mM low calcium, as it was thought at the time that low calcium would enhance the $I_{MI}$ response, and for other reasons explained in Chapter 4. Since this experiment was done in low calcium where desensitization was significant (Figure 2.9), it was compared to controls done without neomycin by using the covariate of application number. As Illustrated in Figure 3.17, a one way ANOVA for neomycin with covariance for application number showed that neomycin was unable to alter $I_{MI}$ amplitude at -15 mV [Neomycin; $F(3, 18) = 1.867$, $p = 0.171$. Application number; $F(1, 18) = 4.449$, $p = 0.049$.][12]. These results, along with those from Et-18-$OCH_3$, suggest that proctolin-induced $I_{MI}$ is not dependent on PLC. Note that neomycin at 1000 µM represents an extremely high concentration of this inhibitor and it still did not produced

[12] In order to reduce the chance of type II error, at the expense of increasing type I error, this data was also examined at application 3, with a one way ANOVA where again, no statistical significance was found. In fact, any trend seemed to show that increasing neomycin concentrations increased proctolin induced $I_{MI}$ ($\mu_{control} = -0.816$, $n = 2$; $\mu_{100\mu M} = -1.445$, $n = 3$, $\mu_{333\mu M} = -1.100$, $n = 2$ ($p = 0.171$)).

significant inhibition. The neomycin results also argue against PLD activation in $I_{MI}$ signalling, as it has been shown that neomycin, at higher concentrations than that required for PLC inhibition (Kidney, PLC IC50 = 30 µM; Brain, PLD IC50 = 65 µM in kidney), inhibits PLD activity (Liscovitch et al., 1991). Therefore, activation of $I_{MI}$ by PLD is also unlikely.

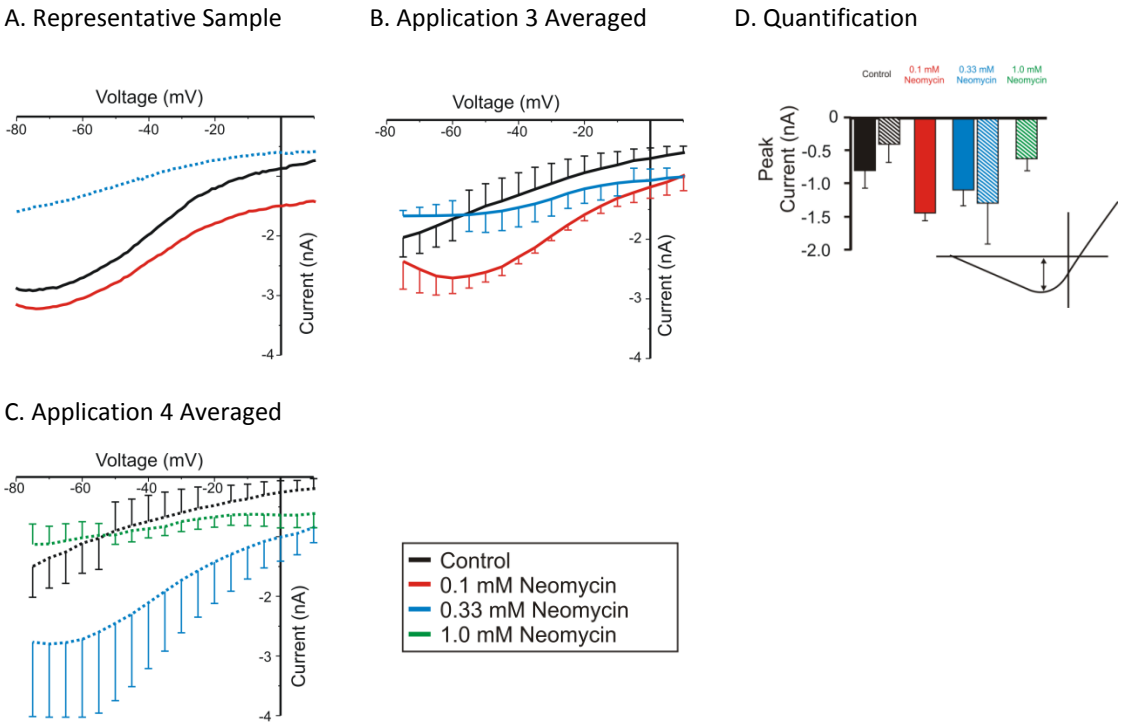


**Figure 3.17: The PLC Inhibitor Neomycin does not Affect $I_{MI}$ Amplitude or Slope in Low Calcium.** Low calcium saline (2 mM) contained 0.1 µM TTX, 10 µM PTX, 200 µM $CdCl_2$, 5 mM CsCl, and 20 mM TEA. Proctolin-induced $I_{MI}$ in control (**Black**), 0.1 mM (**Red**), 0.33 mM (**Blue**), and 1.0 mM (**Green**) of the PLC antagonist/ CaSR agonist neomycin. Measurement at either application 3 (**Solid**), or application 4 (*Striped*). (A) Representative IV curves for proctolin-induced $I_{MI}$ at different concentrations of neomycin. (B) Averaged IV curves for application 3 for proctolin-induced $I_{MI}$ for different concentrations of neomycin. (C) Averaged IV curves for application 4 for proctolin-induced $I_{MI}$ for different concentrations of neomycin.(D) A one way ANOVA with analysis of covariance for application number showed that application number, but not neomycin was capable of reducing $I_{MI}$ amplitude at -15 mV. [Neomycin; F (3, 18) = 1.867, p =

0.171. Application number; F (1, 18) = 4.449, p = 0.049.]

*The protein kinase C (PKC) and general kinase inhibitor staurosporine does not alter proctolin-induced $I_{MI}$ amplitude but may change $I_{MI}$ voltage dependence.*

In order to determine if proctolin-induced $I_{MI}$ is dependent on PKC, and kinase activity generally, we used the non-specific kinase inhibitor staurosporine. At nanomolar concentrations staurosporine is a potent inhibitor of protein kinase C (IC50 = 5 nM), Phosphorylase kinase (IC50 = 3 nM), S6 Kinase (IC50 = 5 nM), v-Src (IC50 = 6 nM), and c-FGR (IC50 = 2 nM) (Tamaoki et al., 1986; Meggio et al., 1995), at higher concentrations staurosporine acts as a more general kinase inhibitor (Toullec et al., 1991); inhibiting PKA (IC50 = 15 nM), PKG (IC50 = 18 nM), MLCK (IC50 = 21 nM), CamKII (IC50 = 9 nM), and others (Meggio et al., 1995). Furthermore, this inhibitor has been shown to work in invertebrate preparations (Johansson and Soderhall, 1993; Friedrich et al., 1998; Van Soest et al., 2000; Ransdell et al., 2012). This experiment was done in 2 mM low calcium to facilitate its measurement, as at the time it was done, it was not established that low calcium increased proctolin-induced $I_{MI}$ desensitization rate (Figure 2.9). As illustrated in Figure 3.18, staurosporine, at any concentration, was incapable of altering proctolin-induced $I_{MI}$ amplitude. A one-way ANOVA for staurosporine with the covariate application number, showed that staurosporine did not significantly alter $I_{MI}$ amplitude [Staurosporine; F (2, 19) = 2.853, p = 0.083. Application Number; F (1, 19) = 3.947, p = 0.062.]. Although this was close to statistical significance, these results suggest that PKC,

and kinases more generally may play a role in proctolin-induced $I_{MI}$ voltage dependence, but are unneccesary for proctolin-induced $I_{MI}$ activation.

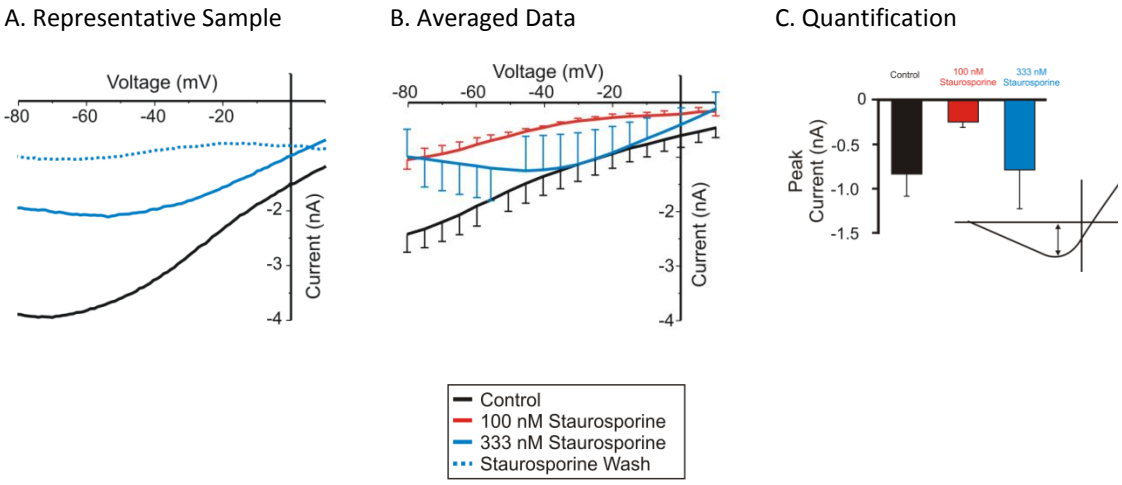


**Figure 3.18: The Protein Kinase C and Non-Specific Kinase Inhibitor Staurosporine Does Not Affect Proctolin-induced $I_{MI}$ Amplitude but Increases its Slope Conductance.** Low calcium saline (2 mM) contained 0.1 µM TTX, 10 µM PTX, 200 µM $CdCl_2$, 5 mM CsCl, and 20 mM TEA. Proctolin-induced $I_{MI}$ in control (**Black**), 100 nM (**Red**) and 333 nM (**Blue**) staurosporine. (A) Representative IV trace of proctolin-induced $I_{MI}$ in staurosporine (B) Averaged IV curves of proctolin-induced $I_{MI}$ in different concentrations of staurosporine.(C) A one-way ANOVA for staurosporine with covariate of application number showed that staurosporine was unable to alter $I_{MI}$ amplitude at -15 mV [Staurosporine; $F(2, 19) = 2.853$, $p = 0.083$. Application Number; $F(1, 19) = 3.947$, $p = 0.062$.] Error bars are SEM. Tukey test; *, $p < 0.05$.

**3.5 Other Phosphatases and Kinases.**

*The non-specific phosphatase inhibitor okadaic acid does not affect $I_{MI}$ slope or amplitude.*

Since kinase inhibitors did not affect $I_{MI}$ activation we wanted to test whether proctolin-induced $I_{MI}$ may be induced by de-phosphorylation. Therefore, we measured proctolin-induced $I_{MI}$ in different concentrations of the non-selective phosphatase inhibitor okadaic acid. We predicted that if proctolin activates $I_{MI}$ through a phosphatase-dependent pathway, then application of increasing concentrations of okadaic acid should decrease proctolin-induced $I_{MI}$. As illustrated in Figure 3.19, a paired t-test showed that okadaic acid was unable to alter $I_{MI}$ amplitude at -15 mV [$t(3) = -3.04$, $p = 0.056$.]. It is interesting to note that although this did not meet our criterion for statistical significance, the values was quite close. At this time it was unknown that desensitization was faster in low calcium than in normal calcium, so the same experiment was run in low calcium with the thinking that this may augment $I_{MI}$ and make any reductions in proctolin-induced $I_{MI}$ amplitude easier to detect.[13] We therefore ran the same experiment in low calcium. As illustrated in Figure 3.20, a one-way repeated measures ANOVA showed that slope was not significantly affected by

[13] In hindsight, it would have been better to run more experiments in the same conditions, but we did not know about low calcium desensitization at the time this decision was made.

increasing concentrations of okadaic acid [Okadaic Acid; F (3, 7) = 0.414, p = 0.748][14]. As shown in Figure 3.20, a one-way ANOVA with the covariate application number, showed that okadaic acid was unable to affect proctolin-induced $I_{MI}$ amplitude at -15 mV [Okadaic acid; F (1, 19) = 3.947, p = 0.062]. This data suggests that proctolin-induced $I_{MI}$ does not require phosphatases sensitive to okadaic acid.

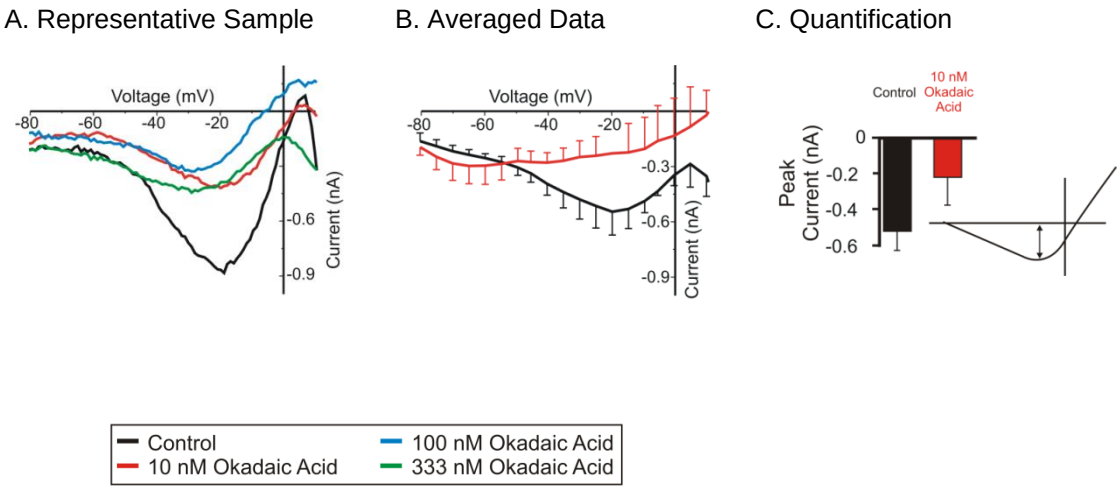


**Figure 3.19: The General Phosphatase Inhibitor Okadaic Acid Does Not Alter Proctolin-induced $I_{MI}$ Amplitude or Slope in Normal Calcium $I_{MI}$ Recording Saline.** Proctolin-induced $I_{MI}$ in Control (Black), or 10 nM okadaic Acid (Red). Saline contained 0.1 µM TTX, 10 µM PTX, 200 µM $CdCl_2$, 5 mM CsCl and 20 mM TEA ($I_{MI}$ recording saline).(A) Representative IV traces of proctolin-induced $I_{MI}$ in different concentrations of okadaic acid.(B) Averaged IV traces in control or 10 nM of okadaic Acid. (C) A paired t-test showed that okadaic acid was unable to alter $I_{MI}$ amplitude at -15 mV [t (3) = -3.04, p = 0.056.

[14] Unfortunately, we did not have proper application amplitude controls within the 6 month window to adjust for application number, so this data was compared to controls done 6 months previously in low calcium to adjust for desensitization. All other low calcium controls were done with controls within 1 month of the beginning and ends of the experiments. This analysis of covariance procedure was done for amplitude but not slope as slope was previously found to be stable.

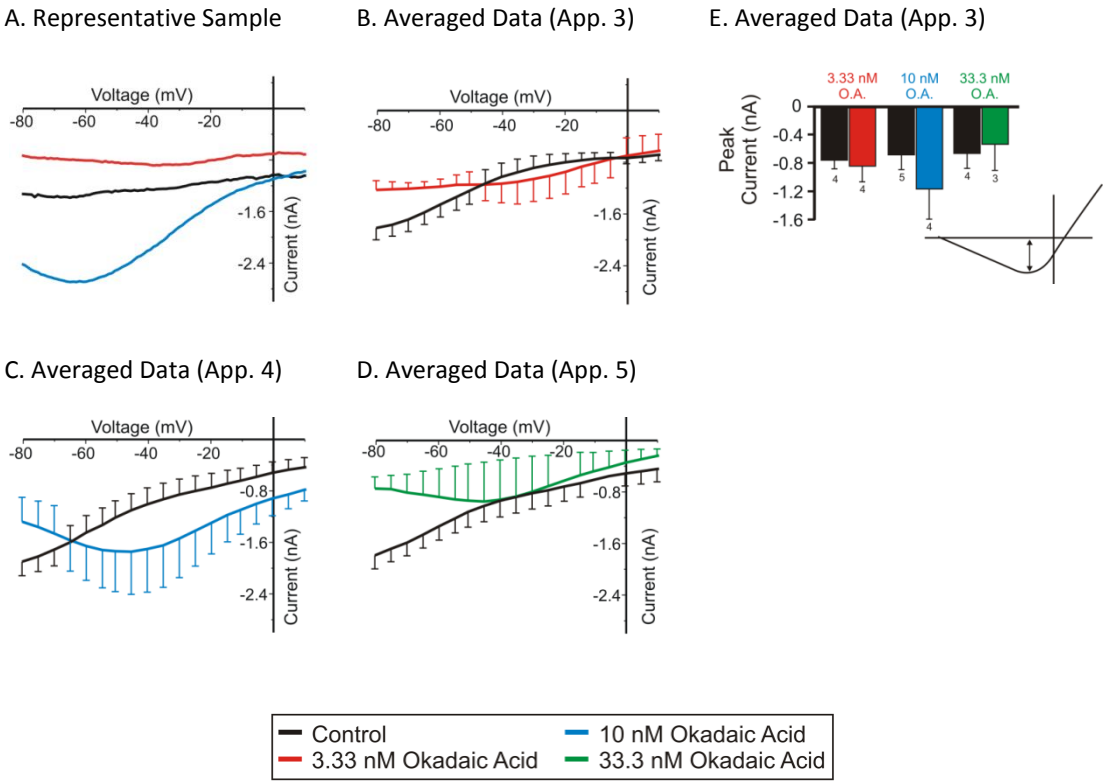


**Figure 3.20: The General Phosphatase Inhibitor Okadaic Acid Does Not Affect $I_{MI}$ Amplitude or Slope in Low Calcium.** Effect of okadaic acid on proctolin-induced $I_{MI}$ in Control (**Black**), 3.33 nM (**Red**),10 nM (**Blue**), and 33.3 nM (**Green**). Application controls used were similar only in amplitude and not in $I_{MI}$ slope, due to desensitization these controls were used for analysis of covariance for amplitude but not slope. 2 mM low calcium saline contained 0.1 µM TTX, 10 µM PTX, 200 µM $CdCl_2$, 5 mM CsCl and 20 mM TEA supplemented with 0.5% BSA ($I_{MI}$ low calcium recording Saline).(A) Representative IV curves for proctolin-induced $I_{MI}$. (B) Averaged traces for control application 3 vs 3.33 nM okadaic acid (Average Application #3.25). (C) ) Averaged IV curves for control application 4 vs 10 nM okadaic acid (Average Application #4.25).(D) Averaged traces for control application 5 vs 33.3 nM okadaic acid (Average Application #5.33). (E) A one-way ANOVA for okadaic acid with covariate application number showed that okadaic acid was not capable of altering $I_{MI}$ amplitude at -15mV[Okadaic Acid; $F(2, 19) = 2.853$, $p = 0.083$. Application number; $F(1, 19) = 3.947$, $p = 0.062$] Error bars are SEM.

*The tyrosine kinase inhibitor genistein does not alter proctolin-induced $I_{MI}$.*

To test the hypothesis that $I_{MI}$ is activated through a G-protein -independent pathway but is sensitive to SRC family kinases (similar to NaLCN activation by substance P in hippcampus and VTA (Lu et al., 2009)), we measured proctolin-induced $I_{MI}$ in various concentrations of the tyrosine kinase inhibitor genistein known to work in crustaceans at concentrations as low as 50 μM (Chuo et al., 2005; Uzdensky et al., 2005). We predicted that if proctolin-induced $I_{MI}$ was dependent upon tyrosine kinases, then we should observe a reduction in proctolin-induced $I_{MI}$ amplitude. This experiment was conducted in low calcium. As illustrated in Figure 3.21, a one-way ANOVA for genistein with the covariate application number, showed that genistein was unable to alter $I_{MI}$ amplitude at -15 mV [genistein; $F(1, 10) = .080$, $p = 0.783$. Application number; $F(1, 10) = 2.826$, $p = 0.124$.]. This data suggests that both proctolin-induced $I_{MI}$ activation and voltage dependence are not dependent on tyrosine kinases. If they are, their role is too small for detection.

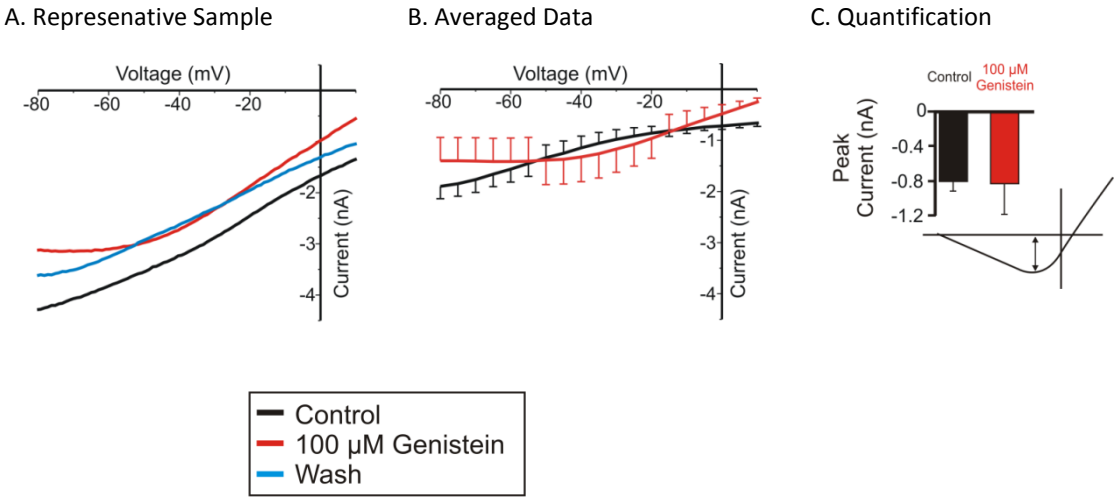


**Figure 3.21. The Tyrosine Kinase Inhibitor Genistein Does Not Affect Proctolin-induced $I_{MI}$ Slope or Amplitude.** Effect of Genistein on proctolin-induced $I_{MI}$. 2 mM low calcium saline contained 0.1 µM TTX, 10 µM PTX, 200 µM $CdCl_2$, 5 mM CsCl and 20 mM TEA supplemented with 0.5% BSA ($I_{MI}$ low calcium recording Saline).(A) Representative IV curves of genistein experiment. (B) Averaged IV curves of genistein experiments. (C) A one-way ANOVA for genistein with covariate application number showed that genistein was unable to alter $I_{MI}$ amplitude at -15 mV [Genistein; $F(1, 10) = .080$, $p = 0.783$. Application number; $F(1, 10) = 2.826$, $p = 0.124$.] Error bars are SEM.

*The SFK inhibitor dasatinib did not significantly alter $I_{MI}$ slope or amplitude.*

To further test the hypothesis that proctolin-induced $I_{MI}$ activates through a mechanism similar to NaLCN, we measured proctolin-induced $I_{MI}$ in different concentrations of the SFK inhibitor dasatinib in low calcium. This inhibitor has been used in culturerd insect cells before (Gossert et al., 2011),however, to this author's knowledge, this is its first reported use in crustacea. Figure 3.22 illustrates that 100 µM

dasatinib was unable to affect proctolin-induced $I_{MI}$ despite the extremely high concentrations that were used (IC50s is 2-5 nMs for SFKs in cultured human aortic smooth muscle cells (Chen et al., 2006)). A t-test showed that dasatinib was unable to alter proctolin-induced $I_{MI}$ amplitude at -15 mV [t (6) = -0.677, p = 0.523.]. Note that as all controls and experimental measurements were done on the second application, adjustment for desensitization was unneccesary. This data, the sensitivity of proctolin-induced $I_{MI}$ to G-protein inhibitors and activators, and the results of the genistein experiment argue against a NaLCN-like mechanism of activation. These results also argue against the involvement of tyrosine kinases as shown by genistein, staurosporine, and SFKs as shown by genistein and dasatinib.

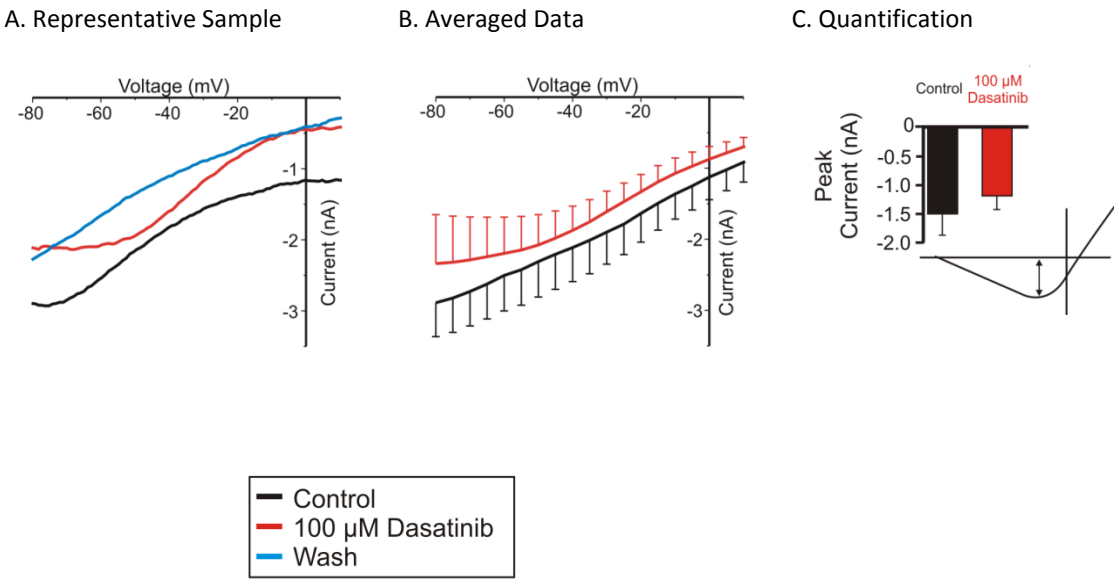


**Figure 3.22. The SRC Family Kinase Inhibitor Dasatinib Does not Affect Proctolin-induced $I_{MI}$ Slope or Amplitude.** Proctolin-induced $I_{MI}$ in the presence of the SFK inhibitor Dasatinib. 2 mM low calcium saline contained 0.1 µM TTX, 10 µM PTX, 200 µM $CdCl_2$, 5 mM CsCl and 20 mM TEA supplemented with 0.5% BSA ($I_{MI}$ low calcium recording Saline).(A) Representative IV curves for dasatinib experiment. (B) Averaged IV curves for all dasatinib experiments (C) A t-test showed that dasatinib was unable to alter proctolin-induced $I_{MI}$ amplitude at -15 mV [t (6) = -0.677, p = 0.523.] Error bars are SEM.

## 3.6: Calmodulin, and Calmodulin-Activated Proteins

*Many suspected voltage-dependence targets affected $I_{MI}$ activation.*

Many of the calmodulin activated proteins that we originally targeted for their suspected effects on voltage-dependence had significant effects on both voltage-dependence and activation. Here we will introduce these experiments focusing on how they might play a role in proctolin-induced $I_{MI}$ activation. We will also discuss how they effect voltage-dependence in more detail in Chapter 4. We find that the calmodulin inhibitor calmidizolium, the ryanodine receptor antagonist dantrolene, the CamKII inhibitor KN-93, and the myosin light chain kinase inhibitor (MLCK) ML-7 all play a dual role in reducing proctolin-induced $I_{MI}$ amplitude and increasing its slope conductance (i.e. reducing voltage dependence).

*Calmidizolium affects $I_{MI}$ slope and amplitude.*

In order to confirm the specificity of W7-induced linearization (that will be discussed in Chapter 4, also Swensen and Marder (2000)), we wished to select a calmodulin inhibitor that was not a napthasulfonamide such as W7, W9, W13, A2 and A7. The reasoning behind this is the assumption that the more different the chemical structure, the less chance of both inhibitors producing the same non-specific effect. We wanted to test relatively light molecules, which eliminated the peptide inhibitors of

calmodulin. When we tested the antipsychotic fluphenazine, which is a calmodulin inhibitor that has been used previously in crustaceans (Sedlmeier and Dieberg, 1983), it appeared to be toxic to the cells before concentrations relevant to calmodulin inhibition were reached (n = 3, data not shown). We therefore used the calmodulin inhibitor calmidazolium, and predicted that it should reduce $I_{MI}$ voltage dependence (increase slope) without affecting $I_{MI}$ amplitude. To our surprise, not only did calmidizolium increase proctolin-increased $I_{MI}$ slope as predicted, but unlike W7, it was an effective inhibitor of proctolin-induced $I_{MI}$. As illustrated in Figure 3.23, a one way repeated measures ANOVA showed that calmidizolium significantly decreased proctolin-induced $I_{MI}$ amplitude at -15 mV from -0.49 ± 0.10 nA (SEM; n = 6) in control, to -0.12 ± 0.07 nA (SEM; n = 4) in 1 µM of calmidizolium [Calmidizolium; $F(3, 9) = 6.382$, $p = 0.013$]. This was surprising at the time, as we had observed many negative results for proctolin-induced $I_{MI}$ activation, and our expectation that, if anything, calmodulin inhibitors would increase proctolin-induced $I_{MI}$ amplitude. As we did not observe any significant reduction by W7 in neuromodulator-induced $I_{MI}$, to explain why calmidizolium reduced proctolin-induced $I_{MI}$ amplitude, we hypothesized that this reduction may be due to intracellular calcium increase[15]. This is because, while both W7 and calmidazolium have been shown to inhibit calmodulin, only calmididizolium has been shown to be sufficient to mobilize intracellular calcium release through calmodulin-independent mechanisms

[15] Note that although caffeine experiments done in in figure 3.9 did not alter proctolin-induced $I_{MI}$ amplitude, the concentration analyzed (5 mM), is half that normally used to elicit intracellular calcium release in crustacea (Levi and Selverston 2006). However, as will be shown in Chapter 4 (Figure 4.9), larger concentrations used later, did not occlude Proctolin-induced $I_{MI}$ either, although the n of these experiments was somewhat low.

(Tornquist and Ekokoski, 1996; Harper and Daly, 2000). For example, in FRTL-5 (thyroid) cells, it has been shown that both calmidizolium and W7 attenuate thapsigargin induced increases in intracellular calcium[16] and ATP-induced calcium entry through a calmodulin-dependent mechanism into thyroid cells[17], but only calmidazolium is sufficient, by itself, to elicit increases in intracellular calcium from intracellular stores in a calmodulin-independent manner (Tornquist and Ekokoski, 1996). If this interpretation is correct, the reduction of proctolin-induced $I_{MI}$ amplitude by calmidizolium but not by W7 suggests that store-activated calcium is involved with proctolin-induced $I_{MI}$ activation.

[16] Thapsigargin is a $Ca^{++}$ ATPase blocker that transiently increases intracellular calcium due to lack of calcium uptake.

[17] Under the conditions tested in the study (low calcium) this effect was mediated via a CamKII calmodulin-dependent mechanism, but it was noted that there are other calmodulin-independent processes contributing to this in normal conditions.

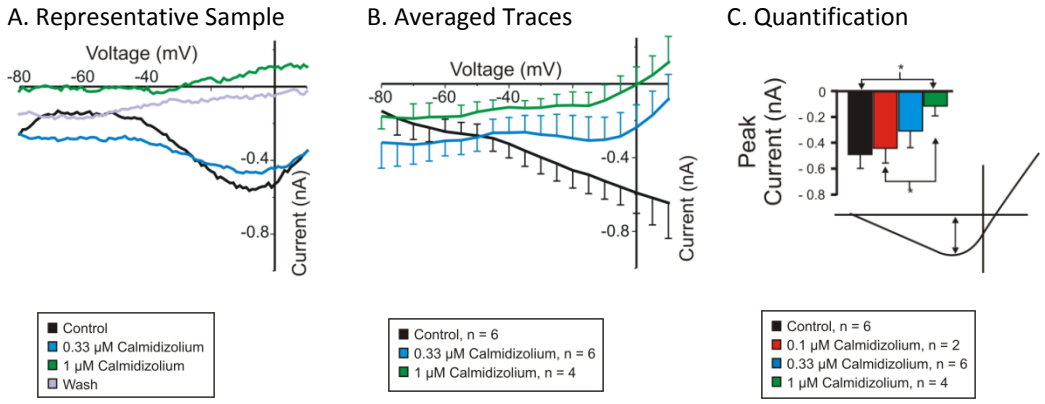


**Figure 3.23. The Calmodulin Inhibitor Calmidazolium Reduces Proctolin-induced $I_{MI}$ Voltage Dependence and Attenuates $I_{MI}$ Amplitude.** Saline contained 0.1 μM TTX, 10 μM PTX, 200 μM $CdCl_2$, 5 mM CsCl and 20 mM TEA. Proctolin-induced $I_{MI}$ in different concentrations of calmidazolium. (A)Representative IV curves from calmidazolium experiment. (B) Averaged IV curves for calmidazolium experiments. (C) A one-way repeated measures ANOVA showed that calmidazolium was capable of decreasing proctolin-induced $I_{MI}$ amplitude at -15 mV. [Calmidazolium; $F(3, 9) = 6.382$, $p = 0.013$].Error bars are SEM. Tukey test; *, $p < 0.05$.

*The ryanodine receptor antagonist dantrolene inhibits proctolin-induced $I_{MI}$, changes its voltage dependence, and left-shifts its reversal potential.*

In order to test the hypothesis that proctolin-induced $I_{MI}$ voltage dependence was modulated by intracellular calcium released from intracellular stores, we applied differing concentrations of the ryanodine receptor antagonist dantrolene. We predicted that increasing concentrations of dantrolene should increase $I_{MI}$ slope conductance. This is because we had hypothesized that intracellular calcium was mediating proctolin-induced $I_{MI}$ voltage dependence, and the reduced intracellular calcium from blockade of

ryanodine receptors should increase proctolin-induced $I_{MI}$ slope conductance. As illustrated in Figure 3.24, a paired t-test showed that dantrolene significantly decreased proctolin-induced $I_{MI}$ amplitude at -15 mV [ t(5) = -3.502 , p = 0.017.]. This agrees with the idea that calmidizolium may be acting by increasing intracellular calcium and proctolin-induced $I_{MI}$ is dependent on this. Tentatively, we propose an amplification process, where our results from dantrolene suggest that intracellular calcium is acting to inhibit proctolin-induced $I_{MI}$, while our results for calmidazolium are occluding proctolin-induced $I_{MI}$. Together these results suggest that proctolin-induced $I_{MI}$ signals through intracellular calcium.

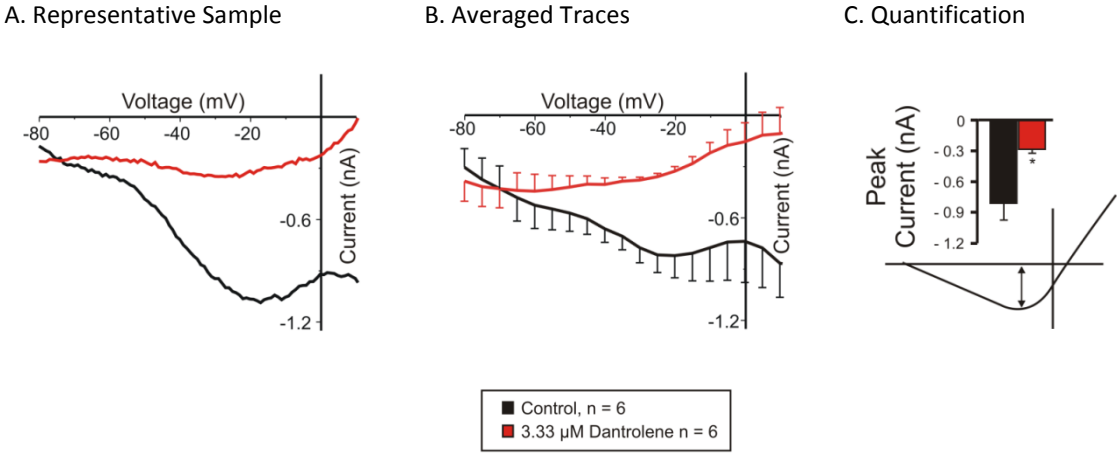


**Figure 3.24. The Ryanodine Antagonist Dantrolene Reduces Proctolin-Induced $I_{MI}$ Voltage Dependence and Amplitude.** Saline contained 0.1 µM TTX, 10 µM PTX, 200 µM $CdCl_2$, 5 mM CsCl and 20 mM TEA. Proctolin-induced $I_{MI}$ before (**Black**) and after (**Red**) application of 3.33 µM dantrolene. (A) Representative IV curve of Dantrolene experiment. (B) Averaged IV curves of dantrolene experiments] (C) A paired t-test showed that dantrolene significantly decreased proctolin-induced $I_{MI}$ amplitude at -15 mV [t(5) = -3.502 , p = 0.017.]*, $p < 0.05$. Error bars are SEM.

*The CamKII inhibitor KN-93 reduces proctolin-induced $I_{MI}$ amplitude and Increases $I_{MI}$ slope.*

We originally hypothesized, that the W7-induced reduction in voltage dependence may be due to lack of the activation of CamKII. This was by analogy with observations of calcium-dependent voltage dependence in the dogfish retina described by Shiells and Falk (2001). They found that cGMP activated currents could be switched from linear to voltage dependent states by CamKII phosphorylation (Shiells and Falk, 2001). It has also been demonstrated by Whithers et al. (1998), that a CamKII-like enzyme is present in the lobster nervous system (Withers et al., 1998). To test the hypothesis that the low calcium induced reduction in voltage dependence is due to loss of activated calmodulin and subsequent loss of CamKII activation, we applied varying concentrations of the CamKII inhibitor KN-93 and measured proctolin-induced $I_{MI}$. We predicted that KN-93 would increase proctolin-induced $I_{MI}$ slope while leaving its amplitude unchanged. As these experiments were done early on, the experiments were done at different concentrations with few replications. So, for statistical analysis they were grouped into a 'low dose', consisting of one preparation at 2 µM, and one at 4 µM. A 'high dose' condition consisted of one preparation at 10 µM and the other at 20 µM. While the remaining 3 were applied at 5 µM. As shown in Figure 3.25, a one way repeated measures ANOVA showed that KN-93 significantly decreased proctolin-induced $I_{MI}$ amplitude at -15 mV [KN-93; $F(3, 4) = 14.890$, $p = 0.012$.]. While there appears to be a genuine reduction in amplitude at concentrations up to 5 µM, it seems

that, in the high dose condition, $I_{MI}$ reversal potential is changing; it may be that our criterion for activation is not valid under these conditions, as it is made with the assumption that proctolin-induced $I_{MI}$ never has a reversal potential lower than -5 mV. It can be clearly seen, however, that in the high dose KN-93 condition, this is untrue. This is in contrast to the expected flatline of $I_{MI}$'s IV curve that was expected if CamKII was just mediating the signal from neuromodulator receptor to the effector/effector(s) mediating the current. For example, GDP-βS in normal calciumseems to 'flatten' proctolin-induced $I_{MI}$ (Figure 3.2A) which is what we expect for a modulator that is only acting between neuromodulator receptor and its effector. Similar results were obtained for overnight incubations in KN-93. As illustrated in Figure 3.26, overnight incubations in KN-93 reduced proctolin-induced $I_{MI}$ amplitude at -15 mV [KN-93; $F(1, 9) = 8.178$, $p = 0.019$. Application number; $F(1, 9) = 3.724$, $p = 0.086$. Interaction; $F(1, 9) = 1.230$, $p = 0.296$.] Strangely, these results are inconsistent with the findings from staurosporine (Figure 3.18). This is because staurosporine should inhibit CamKII at the concentrations tested (333nM) as the IC50 for CamKII inhibition is 20 nM in other systems (Meggio et al., 1995). Therefore, it is possible that KN-93 was acting nonspecifically. To confirm whether this was the case, the inactive isoform of KN-93, KN-92 should be tested. This is because it has been reported that KN-93 can cause CamKII–independent potassium channel block (Rezazadeh et al., 2006), and, therefore, it is not entirely implausible that it could be blocking some of the channels responsible for this current. This data suggests that CamKII may be involved, but there are inconsistenties between these results and

our staurosporine results insofar as proctolin-induced $I_{MI}$ activation is concerned.

Without KN-92 controls, conclusions are premature.

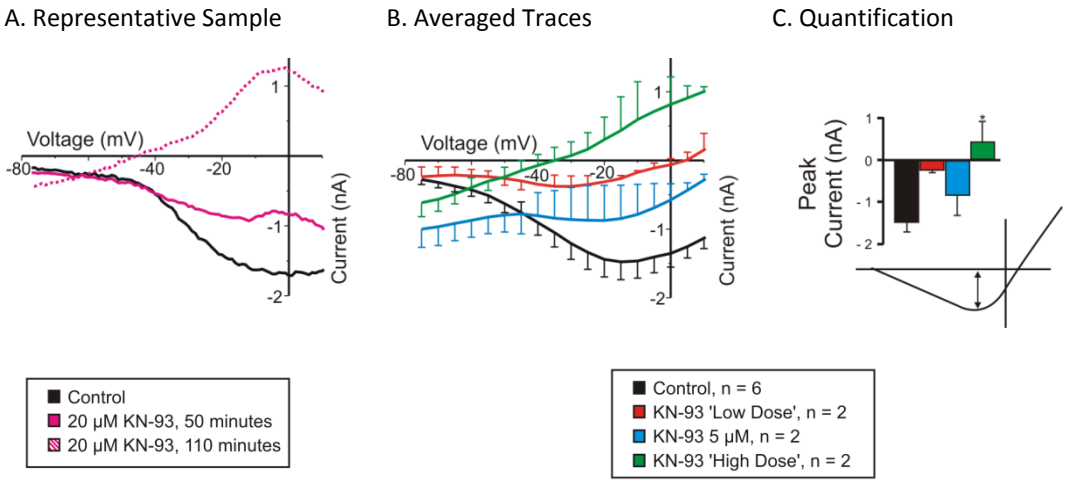


**Figure 3.25. The CamKII Inhibitor KN-93 Reduces $I_{MI}$ Voltage Dependence and Amplitude.** Saline contained 0.1 µM TTX, 10 µM PTX, 200 µM $CdCl_2$, 5 mM CsCl and 20 mM TEA. Proctolin-induced $I_{MI}$ in different concentrations of KN-93. For statistical analysis KN-93 was grouped into 'low dose' (2 µM-4 µM), 5 µM, and 'high dose' (10 µM- 20 µM). (A) Representative IV curve for KN-93 experiment.(B) Averaged IV curves for KN-93 experiments. (C) A one way repeated measures ANOVA showed that KN-93 significantly decreased proctolin-induced $I_{MI}$ amplitude at -15 mV [KN-93; $F(3, 4) = 14.890$, $p = 0.012$.]. Error bars are SEM. Tukey test; *, $p < 0.05$; ***, $p < 0.001$.

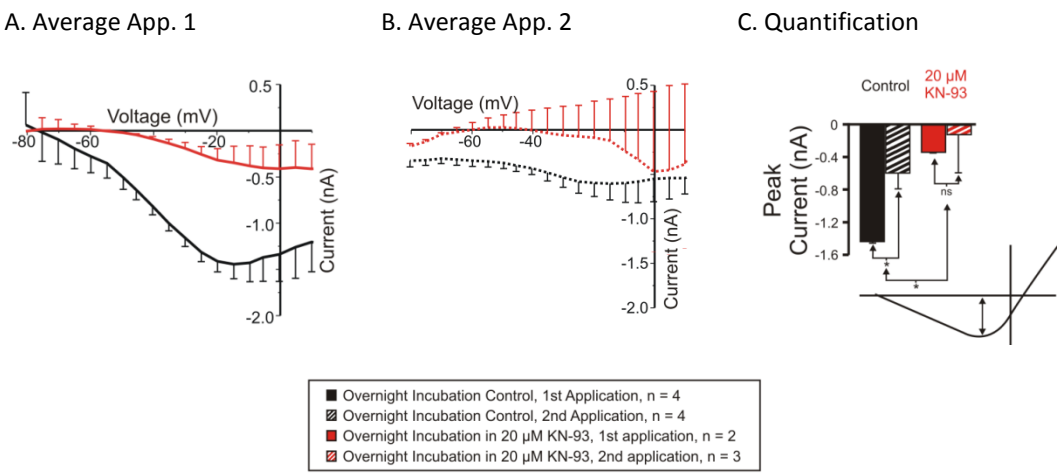


**Figure 3.26. Overnight Incubation in KN-93 Significantly Reduces Proctolin-Induced $I_{MI}$ Amplitude Without Affecting Voltage Dependence.** Preps either incubated in normal saline overnight or normal saline and 20 μM KN-93. When proctolin-induced $I_{MI}$ was measured, saline contained 0.1 μM TTX, 10 μM PTX, 200 μM $CdCl_2$, 5 mM CsCl and 20 mM TEA.(A) Averaged IV curves of application 1. (B) Averaged IV curves of application 2. (C) A two-way ANOVA showed that overnight incubation with KN-93 significantly altered proctolin-induced $I_{MI}$ amplitude at -15 mV versus overnight incubation alone [KN-93; $F(1, 9) = 8.178$, $p = 0.019$. Application number; $F(1, 9) = 3.724$, $p = 0.086$.Interaction; $F(1, 9) = 1.230$, $p = 0.296$.] Error bars are SEM. Tukey test; *, $p < 0.05$.

*The Myosin Light Chain Kinase (MLCK) inhibitor ML-7 affects both proctolin-induced $I_{MI}$ voltage dependence and activation.*

As there seems to be some involvement of calcium (as shown by dantrolene) and calmodulin-activated proteins (as shown by KN-93) with activation, we investigated whether calmodulin activated myosin light chain kinase was involved in proctolin-induced $I_{MI}$ activation. Originally we were examining this as a hypothesis that $I_{MI}$ voltage dependence is mediated by a calcium sensitive receptor, which has been proposed by some authors to be downstream of CaSR signalling (Conigrave et al., 2007), may affect

$I_{MI}$ voltage dependence. Therefore, we originally predicted that inhibitors of MLCK, such as ML-7, a specific MLCK inhibitor that has been used succesfully in crustaceans before (Chen et al., 2012), should increase proctolin-induced $I_{MI}$ slope in a dose-dependent manner. As depicted in Figure 3.27, a one-way repeated measures ANOVA showed that ML-7 decreased proctolin-induced $I_{MI}$ amplitude at -15 mV [ML-7; $F(3, 26)$ 4.468, $p = 0.012$.]. This suggests that MLCK is involved in both proctolin-induced $I_{MI}$ voltage dependence and activation. Again, staurosporine should theoretically inhibit MLCK, as it has been shown to have an IC50 of 21 nM in other systems (Meggio et al., 1995), it is possible that our results for staurosporine are being interpreted too strictly [Staurosporine; $F(2, 19) = 2.853$, $p = 0.083$. Application Number; $F(1, 19) = 3.947$, $p = 0.062$.]. However, we are erring on the side of caution due to the dose response relationship first decreasing than increasing, as this lack of consistency suggests that more careful study is needed before drawing strong conclusions are drawn. These results suggest involvement of MLCK with proctolin-induced $I_{MI}$ voltage dependence and activation.

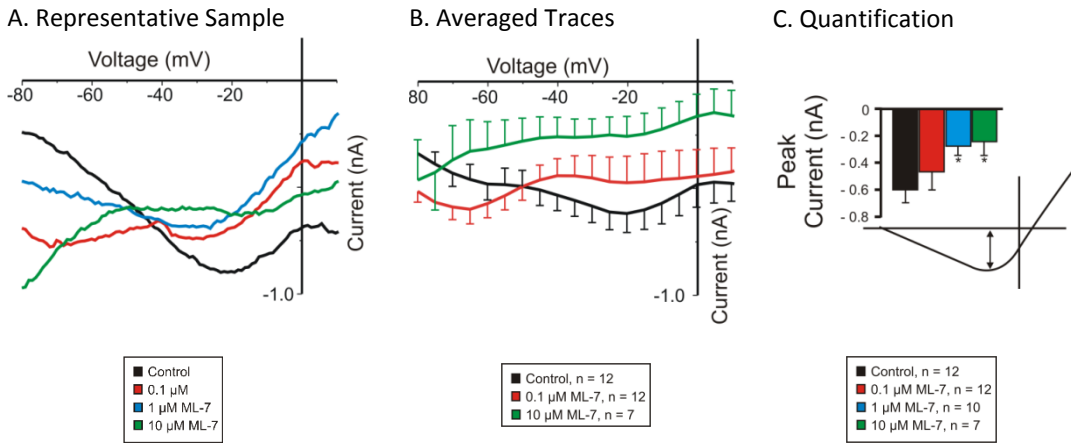


**Figure 3.27. The Myosin Light Chain Kinase Inhibitor (MLCK) ML-7 Reduces Proctolin-Induced $I_{MI}$ Amplitude.** Saline contained 0.1 µM TTX, 10 µM PTX, 200 µM $CdCl_2$, 5 mM CsCl and 20 mM TEA. Proctolin-induced $I_{MI}$ in presence of various concentrations of ML-7.(A) Representative IV traces for ML-7 experiment. (B) Averaged IV Traces for ML-7 experiments(1 µM omitted for clarity). (C) A one-way repeated measures ANOVA showed that ML-7 decreased proctolin-induced $I_{MI}$ amplitude at -15 mV [ML-7; $F(3, 26)$ 4.468, $p = 0.012$.] Error bars are SEM. Tukey; *, $p < 0.05$; ***, $p < 0.001$.

## 3.7: Discussion

*Proctolin-induced $I_{MI}$ is dependent on a G-protein that is sensitive to pertussis toxin in low-calcium.*

In this chapter, we have confirmed our suspicion that proctolin-induced $I_{MI}$ is mediated by G-protein signalling. Specifically, we have shown that proctolin-induced $I_{MI}$ is dependent on G-proteins through three key pieces of evidence. First, the G-protein inhibitor GDP-βS produced the expected inhibition of proctolin-induced $I_{MI}$ (Figure 3.2). Second, we have shown that pressure injection of the G-protein activator GTP-γS produced the predicted occlusion of proctolin-induced $I_{MI}$ (Figure 3.3). With these experiments alone, we have shown that proctolin activates $I_{MI}$ through a G-protein dependent mechanism, but we have not excluded the possibility for proctolin-induced $I_{MI}$ being modulated by monomeric G-proteins. By showing that proctolin-induced $I_{MI}$ is sensitive to pertussis toxin in low calcium, which to this author's knowledge, only ADP-rybosylates the alpha subunits of heterotrimeric subunits $G_I$, $G_O$, or $G_T$ (Katada, 2012), we have shown the first direct evidence that proctolin-induced $I_{MI}$ in the STG is mediated by G-protein coupled receptors. These results are in agreement with the results of Garcia et al., (2015), who show that the CCAP mRNA copy number is correlated with cell type responsiveness to CCAP (Garcia et al., 2015). This is also consistent with $I_{MI}$ being induced by the muscarinic agonist pilocarpine. These data do not exclude the possibility that neuromodulator receptors other than proctolin could signal through non-G-proteins, but they confirm that proctolin-induced $I_{MI}$ is signalling

through G-proteins in all conditions, and G-proteins that contain ADP-rybosylation sites in low calcium.

*Proctolin-induced $I_{MI}$ activation shows sensitivity to intracellular calcium signalling*

The differential effect of calmidizolium and W7 on proctolin-induced $I_{MI}$ activation, where both affect $I_{MI}$ voltage dependence, while only calmidazolium but not W7 affects activation, suggests that due to the agreement in both inhibitors activity--CaM modulates $I_{MI}$ voltage dependence, while calmidizolium (Figure 3.23) mediates its effect on proctolin-induced $I_{MI}$ amplitude through non-specific action. This non-CaM dependent effect by calmidazolium, which has been shown to be sufficient, in itself, to induce intracellular calcium release (Tornquist and Ekokoski, 1996; Harper and Daly, 2000), suggests that proctolin-induced $I_{MI}$ is either inhibited or occluded by release of intracellular calcium. This result is confirmed by the finding that dantrolene, a blocker of ryanodine receptors, also inhibits proctolin-induced $I_{MI}$ (Figure 3.24). Perhaps some interaction between internal calcium stores activates proctolin-induced $I_{MI}$. Together, these results suggest a dependency on intracellular calcium signalling for proctolin-induced $I_{MI}$ signalling.

*$I_{MI}$ is unlikely to signal directly through phosphatases, but there is evidence of dependence on calmodulin-activated kinases .*

We have tested the general kinase blocker staurosporine (Figure 3.18), the general tyrosine kinase blocker genistein (Figure 3.21), and the general phosphatase blocker okadaiac acid (Figures 3.19 & 3.20). Additionally, we have tested the more specific blockers: H89, KN-93, and ML-7. While most of our data (H89 during washout, KN-93, staurosporine, ML-7) suggests a role for kinases in modulation of proctolin-induced $I_{MI}$ voltage dependence, there was an issue of the lack of agreement between our staurosporine, ML-7 and KN-93 results for activation. As staurosporine blocks CamKII and MLCK with IC50s of 20 and 21 nM respectively (Meggio et al., 1995), our expectation was that we should see similar results. However, when analyzed including all results, staurosporine was quite close to statistical significance ($p = 0.083$) but did not meet our criterion. Normally, this would not be problematic, and would be interpreted as support for the findings of KN-93 and ML-7. However, the fact that staurosporine appears to first inhibit and then raise proctolin-induced $I_{MI}$ suggests that there could be nonlinear effects at play. As this is a promiscous kinase inhibitor, and the p-value was close to significance ($p = 0.083$) we interpret this result as supporting the hypothesis that proctolin-induced $I_{MI}$ activation is mediated by calmodulin-dependent kinases MLCK and CamKII, only in the context of our findings for ML-7 and KN-93. In support of this, if we had analyzed staurosporine only in control and 100 nM conditions our results

would have been significant [Staurosporine; F ( 1, 10) = 10.785, p = 0.008. Application number; F (1, 10) = 5.07, p = 0.048]. Note that this p value (0.008) is far below that required for 2 comparisions for experimentwise α of 0.05 which is only 0.025 (Ott and Longnecker, 2001)[18]. As it has been shown by other papers that CamKII is capable of inhibitory autophosphorylations (Elgersma et al., 2002), then perhaps CamKII could be regulated by other kinases thus explaining this biphasic response to staurosporine. In conflict with this interpretation though is the finding that the calmodulin inhibitor W7 does not affect proctolin-induced $I_{MI}$ amplitude.[19] As calmodulin is required for activation of both these kinases, it is difficult to imagine how activation could function in the presence of W7 without incorporation of additional calmodulin-activated elements. Similarly, the lack of modulation of proctolin-induced $I_{MI}$ by okadaic acid suggests that serine threonine phosphatases are not involved in the activation of proctolin-induced $I_{MI}$ which is counterintuitive, as one would expect sensitivity to kinases should confer sensitivity to general phosphatase inhibitors in some time scale (Golowasch and Paupardin-Tritsch, 1996) due to the irreversibility of phosphorylation in the absence of phosphastases in physiological conditions (Lehninger et al., 2000; Bruice, 2001; Lodish,

[18] This is the simplest application of the Bonferroni inequaltity where T1 error is $\alpha_E \leq m\alpha_1$. Where m =# comparisons, $\alpha_E$ = experimentwise T1 error rate, and $\alpha_1$ = error rate of individual experiments.

[19] As will be discussed in Chapter 4, W7 had a statististically significant, but biologically insignificant effect on proctolin-induced $I_{MI}$ amplitude (Figure 4.2), while it had no effect on CCAP-induced $I_{MI}$ amplitude (Figure 4.3).

2008)[20]. These results suggest that proctolin-induced $I_{MI}$ does not directly require dephosphorylation but there could be a role for phosphorylation in activation.

**Figure 3.28: Tentative Model for Proctolin-induced $I_{MI}$ Activation via Direct Calmodulin Activation.**

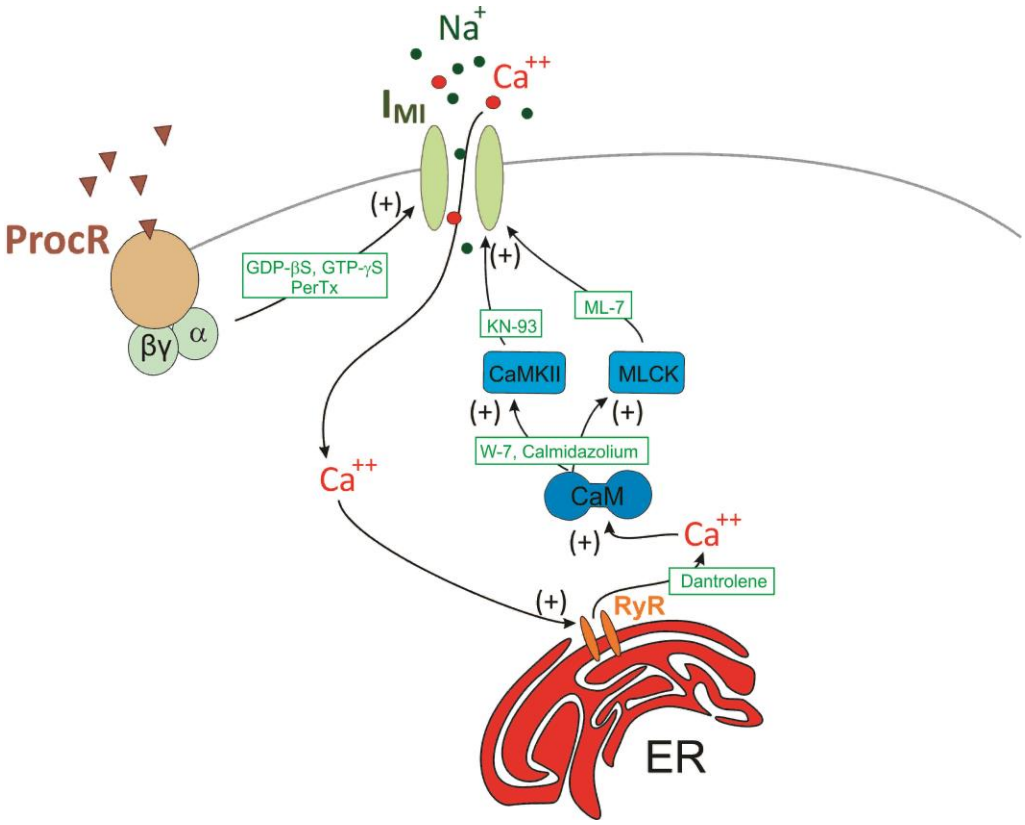


Figure 3.29: Tentative Model for Proctolin-induced $I_{MI}$ activation via Calmodulin Amplification.

[20] Lodish (2008) explicitly states this without citation. Lehinger et al., (2008) and Bruice (2001) put forth the principles to deduce this. One could lower pH (makes a better electrophile) and ATP, raise ADP and $P_I$ to unnatural conditions, and therefore reverse the reaction (phosphate is a good leaving group due to resonance stabilization); however, this is not the natural case and rarely observed.

*Cyclic nucleotides do not mediate proctolin-induced $I_{MI}$ signalling in the short term.*

Agonists for cAMP and cGMP made no difference in measured proctolin-induced $I_{MI}$. This suggests that cyclic nucleotides are not directly mediating proctolin-induced $I_{MI}$. Since these experiments used short incubation times, we do not rule out the enhancement of desensitization mechanisms that were observed several hours after application. There was, however, no statistically significant effect of 8-Br-cAMP on proctolin-induced $I_{MI}$ for up to one hour after application. This suggests that if these agents do affect proctolin-induced $I_{MI}$ these effects are very slow in nature, and not the primary means of activation, and more likely represent long term modulation of the receptor or effector. Supporting the conclusion that proctolin mediated $I_{MI}$ is not dependent on cAMP, is the finding that forskolin produced no change in measured current or voltage dependence. To test whether neuromodulator receptors signal through cGMP signalling, we applied the cell-permeable cGMP agonist 8-Br-cGMP which produced a significant difference current that was independent of voltage and therfore not '$I_{MI}$' -like in nature. There was no significant modulation of proctolin-induced $I_{MI}$ amplitude or voltage dependence leading us to conclude that cGMP signalling is not involved. Further, if proctolin-induced $I_{MI}$ is activated or inhibited by either cGMP or cAMP, we should be able to enhance or inhibit it by application of phosphodiesterase inhibitors. That is, if activated by nucleotides then application of caffeine should result in a reduction in proctolin-induced $I_{MI}$, while if it is inhibited by nucleotides, then caffeine should increase proctolin-induced $I_{MI}$. The unresponsiveness of proctolin-

induced $I_{MI}$ to the phosphodiesterase inhibitor caffeine suggests independently that niether of these mechanisms are involved. Together, these results suggest that cyclic nucleotides are not directly involved in either $I_{MI}$ signalling or voltage dependence.

*PLC signalling is unlikely, but no positive controls were found to suggest that inhibitors used were unambigiously working.*

As discussed in chapter one, our initial literature search found many $I_{MI}$-like currents, and proctolin-induced responses being mediated by PLC signalling, so we investigated this pathway carefully. We showed that both the PLC inhibitors edelfosine (Figure 3.16) and neomycin (Figure 3.17) did not produce significant inhibition of $I_{MI}$ with 1-2 hour incubations. In hindsight, the concentrations of edelfosine should have been higher (IC50 0.4-9.6 µM in fibroblasts (Powis et al., 1992)), as the IC50s used in Zhang et al. (2010) did not report positive results, while the positive results in Wong et al. (2007) used a higher concentration of 35 µM. Despite this, concentrations of neomycin (significant inhibition at 10 µM, IC50 = 30 µM (Schacht, 1976; Burch et al., 1986; Levi and Selverston, 2006)), a PLC inhibitor with a better established literature in invertebrate systems (Willoughby et al., 1999; Rivers et al., 2002; Wenzel et al., 2002; Vezenkov and Danalev, 2009; Brown et al., 2010), and this system (Levi and Selverston, 2006), at concentrations as high as 1000 µM and incubations of 1-3 hours produced no significant inhibition of proctolin-induced $I_{MI}$. These high concentrations strongly argue that proctolin-induced $I_{MI}$ does not utilize PLC signalling. Further, the finding that proctolin-induced $I_{MI}$ in low calcium is pertussis toxin (PTX) sensitive, is congruent with these

results. This is because if proctolin-induced $I_{MI}$ was mediated via PLC signalling, we would expect that it would not be sensitive to PTX, as PTX does not ADP-rybosylate $G_Q$ (Katada, 2012), the canonical signalling pathway for $PLC_\beta$. Although we did not find an effect of these agents on ionic currents, we expect that the extreme concentrations used, especially for neomycin, make it unlikely that PLC is involved with proctolin-induced $I_{MI}$. These results are in agreement with the findings of Swensen and Marder (2000) who found phorbol esters, and U73122 were ineffective at modulating neuromodulator induced $I_{MI}$ (Swensen and Marder, 2000). Together, these results suggest that proctolin-induced $I_{MI}$ does not signal through PLC signalling.

*$I_{MI}$ does not signal similarly to NaLCN of hippocampus, VTA and pancreas*.

The distinctive signalling pathway of NaLCN was a guiding hypothesis for this thesis, however, the results presented here have falsified this as proctolin-induced $I_{MI}$'s mechanism of activation. First, we have shown that neither the tyrosine kinase inhibitor genistein (Figure 3.21), nor the SFK inhibitor dasatinib (Figure 3.22) were able to significantly inhibit proctolin-induced $I_{MI}$. Second, proctolin-induced $I_{MI}$ does require G-protein signalling, which is not required by NaLCN signalling (Lu et al., 2009; Swayne et al., 2009; Lu et al., 2010; Swayne et al., 2010), as shown by its inhibition by pertussis toxin and GDP-βS, and occlusion by GTP-γS. Further, we have observed no significant changes in proctolin-induced $I_{MI}$ amplitude in NaLCN blockers such as $CdCl_2$ (NaLCN IC50

= 150 µM (Lu and Feng, 2012)) at 200 µM (all data shown here) and 400 µM (data not shown for low sample number), and $GdCl_3$ (NaLCN IC50 = 1.4 µM) that does not inhibit $I_{MI}$ in concentrations up to 1 mM (data not shown for low sample number). Additionally, we have tried iontophoresis of dsRNA's and shown that there was no significant difference in proctolin-induced depolarization in current clamp (Data not shown for low sample number). Therefore, we believe that we have conclusively falsified the hypothesis that proctolin-induced $I_{MI}$ signals through a G-protein independent, SFK-dependent mechanism that mediates NaLCN signalling in VTA, hippocampus and pancreas (Lu et al., 2009; Swayne et al., 2010; Lu and Feng, 2012). However, recent work in the STG transcriptome has shown the presence of the NaLCN ortholog in *Daphnia pulex* (Schulz., DJ, unpublished data), however, its function is unknown.

*Model for Proctolin-induced $I_{MI}$ Activation.*

We propose two tentative models for proctolin-induced $I_{MI}$ signalling illustrated in figure 3.28 & 3.29. The first model, illustrated in figure 3.28, assumes direct activation through calmodulin, while the second model, suggests amplification by calmodulin. Both models incorporate a dependence on G-protein signalling as shown by PtX, GDP-βS, and GTP-γS results. A dependence on intracellular calcium as shown by dantrolene and calmidazolium results. A dependence on calmodulin, as shown by W7 and calmidazolium, and a dependency on calmodulin activated kinases as shown by ML-7 and KN-93 results. The key difference is whether calmodulin acts to directly activate

proctolin-induced $I_{MI}$ or amplify the signal. Both models at this point show inconsistencies, but these two will be described as tentative models for $I_{MI}$ activation.

*General Model:*

(1) Proctolin –induced $I_{MI}$ is mediated by G-protein that shows pertussis sensitivity in low calcium, as shown by PTX, GDP-βS inhibition and GTP-γS occlusion.

(2) This G-protein activates intracellular calcium release from internal stores or calcium channels protected from bath calcium concentrations. This is supported by the finding that dantrolene inhibits (occludes) proctolin-induced $I_{MI}$, and as dantrolene inhibits ryanodine receptors (Zhao et al., 2001), this suggests both an initial source of calcium and connection to the ER is needed.

As proctolin-induced $I_{MI}$ is still present in low calcium, it suggests that this requirement is more than likely mediated by intracellular calcium release. An alternative would be activation of calcium channels that are resistant to $Cd^{++}$ ion but they would have to be somewhat protected from bath calcium concentrations as if they were not calcium influx could not initiate calcium induced calcium release. In contrast, as illustrated in figure 3.28, it has been suggested by Zhao et al., (2011) that $I_{MI}$ could be permeable to calcium itself due to its enhancement of the LP to PD synapse. Therefore, it could be possible that $I_{MI}$ is in close proximity to ER membrane, which in turn acts to amplify the signal. This model is more plausible, as the more ubiquitious mechanism of intracellular calcium mobilization, PLC signalling, showed no evidence for modulation of

proctolin-induced $I_{MI}$ activation as shown by neomycin and edelfosine. Unfortunately, it has yet to be explained how $I_{MI}$ persists without attenuation in low calcium in this model. So either through direct calcium influx via $I_{MI}$, G-protein activation of calcium channels, or possibly close coupling to the ER such as the case demonstrated by STIM1-ORA1 coupling (Garcia-Alvarez et al., 2015). While there are many examples of G-proteins coupling directly to ion channels such as GIRKS, and calcium channels (Imoto et al., 1988; Schreibmayer et al., 1996), the coupling of ER to plasma membrane is more often associated with muscle. However, it has been shown that calcium sensing proteins such as those from the STIM family may have important consequences for neurons as well (Garcia-Alvarez et al., 2015). These proteins are single transmembrane domain proteins with EF hand domains found in the ER, which oligerimize to couple the plasma membrane to ER membrane when calcium is low (Garcia-Alvarez et al., 2015). Not only do these proteins have important consequences for calcium homeostasis in neurons through capacitive calcium entry (store operated calcium entry) (Van Eldik and Watterson, 1998; Putney, 2005, 2009; Garcia-Alvarez et al., 2015), and TRPC regulation (Freichel et al., 2014; Zholos, 2014), but these proteins have also have important consequences for signal transduction in neurons. This is supported by the finding that the phosphorylation of AMPAR subunits can be regulated by the ER calcium sensor/ plasma membrane STIM2 (Garcia-Alvarez et al., 2015). Although this model was originally inspired by muscle, these findings from neuron suggest that intracellular calcium stores can be in quite close proximity to our receptor to initiate calcium

induced calcium release. This close proximity allows initiation of proctolin-induced $I_{MI}$ signalling while application of dantrolene and calmidzazolium functionally decouple proctolin-induced $I_{MI}$ from intracellular calcium increases and therefore reduce proctolin-induced $I_{MI}$ amplitude.

3. Calcium induces calcium release as shown by dantrolene and calmidazolium in both models.

4. Intracellular calcium activates calmodulin (Figure 3.27) (supported by calmidazolium but not by W7(Chapter 4)) or acts to amplify $I_{MI}$ activation (Figure 3.28).5. Calmodulin activates MLCK and CamKII (both figures). While a CamKII like-protein has been directly identified (Withers et al., 1998) in this system, there is no direct evidence currently for MLCK. However, the finding that proctolin-induced $I_{MI}$'s voltage dependence is surprisingly sensitive to extremely low concentrations of ML-7(Chapter 4), where non-specific action is less likely, coupled to its ubiquitous nature and presence in many other crustacean systems (Saitoh et al., 1987; Yamamoto et al., 1998; Chen et al., 2012; Chung et al., 2013; Taengchaiyaphum et al., 2013), suggests that an ML-7-sensitive analogue is present in the STG.

*A note on $I_{MI}$ activation mechanisms and statistical modelling suggested in this chapter:*

Although only three statistical hypotheses were tested in this thesis: 1. A substance affects $I_{MI}$ amplitude. 2. A substance affects $I_{MI}$ voltage dependence. 3. A substance affects both. It is important to note that a growing problem in statistical

hypothesis testing today comes when a hypothesis is made after the data is collected (i.e. 'post-hoc theorizing'). This is when a hypothesis is claimed to be confirmatory research when in fact it any hypothesis made after the fact is technically exploratory research until new data is collected (Payne and Dyer, 1975; Wagenmakers et al., 2012). P values from research where this mistake is made are dubious theoretically and empirically have been shown to be less meaningful. This is especially true as the ratio between independent variables and number of obversations increases due to the increasing hypotheses and therefore multiple comparisons that are present {Wagenmakers, 2012 #94377;Payne, 1975 #94181}. Therefore, it is especially important to define what experiments are exploratory and confirmatory in nature (Payne and Dyer, 1975).Therefore, while the data put forth from figures 3.2-3.22 can be claimed to be confirmatory research as the hypothesis was clear before hand, strictly speaking the data from figures 3.23-3.25 were unexpected and must be caveated as being exploratory research, and must be replicated before strong conclusions are drawn.

## Appendix A: Effects for G-protein modulators

*Brief introduction.*

Many of the pharmaceutical agents used in this thesis have not been studied in the STG of *Cancer borealis* so this section represents a compendium of results from the applications of these pharmaceutical agents as one of the primary difficulties of this study was determining even if a substance would be effective. Most importantly, in the event of a negative result, it is helpful to have a positive control to ascertain whether a substance was active. Likewise, in the event of a positive result, possible confounds must be examined. In either case, it is good to have a working knowledge of what the effects of these agents are in this system. Therefore, the effects of these agents on commonly studied parameters of ionic currents in this system were surveyed.

**Effects for G-protein modulators**

*Is GTP-γS mediated reduction in proctolin-induced $I_{MI}$ amplitude inhibition due to occlusion or inhibition?*

In order to investigate whether GTP-γS was truly activating $I_{MI}$, we examined the effect of some G-protein modulators on membrane resting potential. We predicted that if GTP-γS was activating $I_{MI}$, we would expect a depolarization of resting membrane potential (RMP) due to constitutive activation of $I_{MI}$. In contrast to our expectation, as shown in Figure A3.5, GTP-γS significantly hyperpolarized RMP from -55 ± 1.4 mV to -61.100 ±2.1 mV (SEM; $n_{Control} = 11$ $n_{GTP\text{-}\gamma S} = 5$; $p = 0.03$). Despite this hyperpolarization shown with GTP-γS, GDP-βS and PTX did not significantly alter membrane resting potential (Figures A3.3, A3.7). It is unclear what caused this hyperpolarization as Figures A3.5 and A3.6 demonstrate that the only other effect attributable to GTP-γS alone was a drop in input resistance of 42 ± 11% (SEM; $n_{Control} = 11$ $n_{GTP\text{-}\gamma S} = 5$; $p = 0.042$). Since neither pertussis nor GDP-βS had a significant effect on RMP, it is difficult to interpret what this GTP-γS hyperpolarization represents and whether it is related to $I_{MI}$ or another unknown neuromodulator effector. This lack of the expected depolarization, suggests that if GTP-γS is activating $I_{MI}$, it is not activating this current alone. Therefore, this result cannot be interpreted as occlusion independently of other results.

*The effect of pressure Injection and TEA on cell health*

In order to control for what the effects of pressure injection and inclusion of TEA, we examined the consequences of using 500 mM KCl and 500mM KCl + 20 mM TEA, before and after the pressure injection procedure of the test substances, on several commonly measured parameters in our system. Figure A3.1 shows that pressure injection of 500 KCl alone had no significant effects on transient or steady state $I_{HTK}$, $I_A$, $R_{IN}$, $I_H$ or $V_{rest}$ (Compare red solid to red striped). Unsurprisingly, inclusion of 20 mM TEA, reduced transient (A3.1A) and steady state $I_{HTK}$(A3.1B) and $I_A$, but left $R_{IN}$ (A3.1D) and $I_H$ (A3.1E) unaffected. These results are consistent with TEA blocking potassium currents more non-specifically when internally applied (Armstrong, 1971; Connor and Stevens, 1971; Hoshi et al., 1990; Johnston and Wu, 1995). These results, especially the finding that $R_{IN}$, and $V_{rest}$ were unaffected by either TEA or pressure injection, suggest that cell health was intact in these experiments. Further, as shown in Figure A3.1A, the finding that TEA immediately inhibits transient $I_{HTK}$ (Tukey; within before, $p = 0.062$) and then inhibits it further upon pressure injection(Tukey; within after, $p < 0.001$) , suggests that $I_{HTK}$ inhibition is not immediately saturated. Further pressure injection reduces $I_{HTK}$ more, and therefore $I_{HTK}$ inhibition can be used to calibrate the efficacy of our pressure injections across experiments. This way, we have a relative measure of how much drug containing solution was injected. If $I_{HTK}$ inhibition were immediately saturated, we would not have this calibration mechanism. All cells were pressure injected until the 50%

criterion for transient $I_{HTK}$ was reached. In $I_{MI}$ recording saline, TEA significantly inhibited $I_A$ at +20 mV (Figure 3.2B).

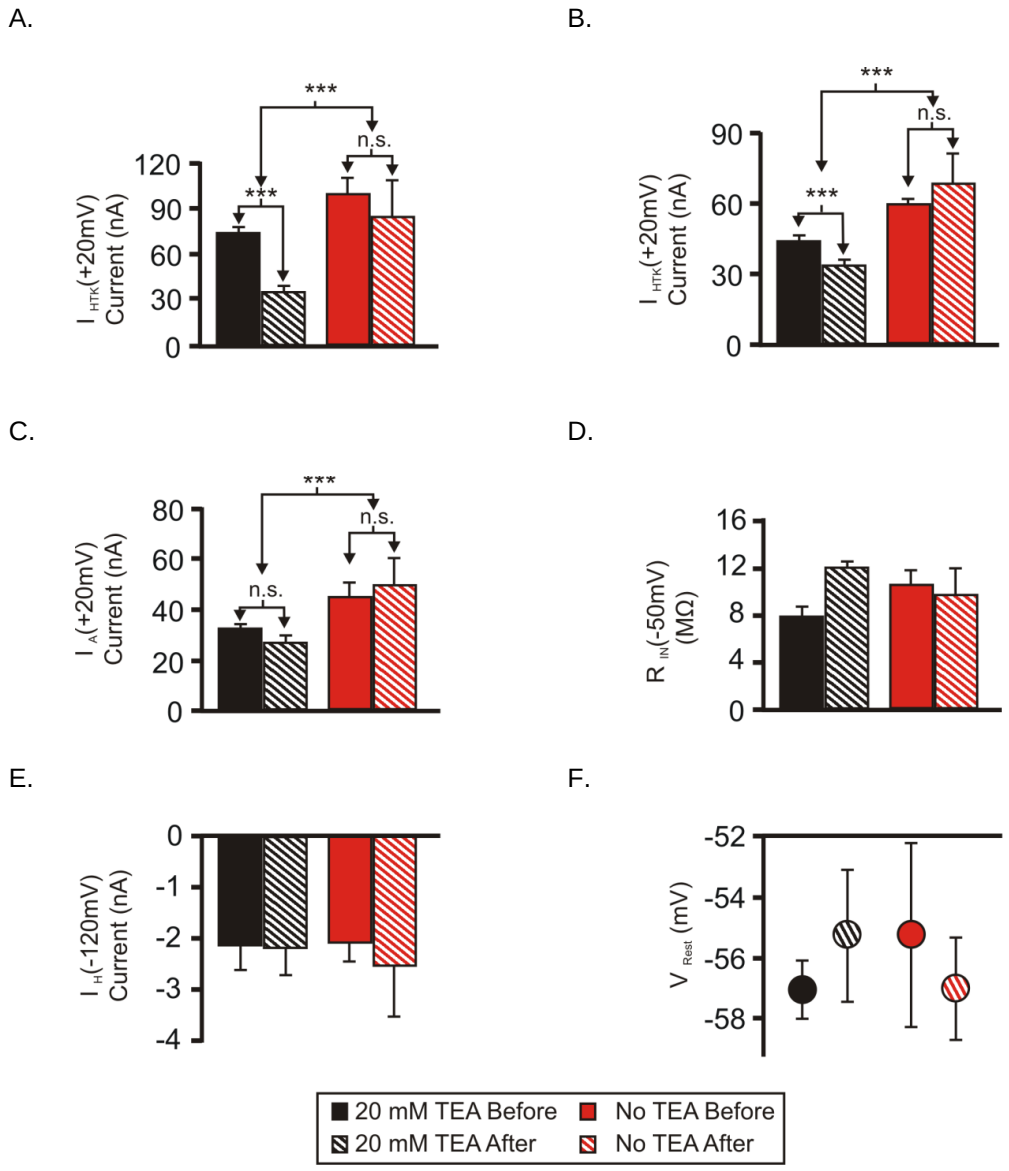


**Figure A3.1: Pressure Injection of 20 mM Tetraethylammonium (TEA) Only Affects Potassium Currents.** Saline contained 0.1 μM TTX. Current injection pipettes included either 500 mM KCL (No TEA, **Red**, n = 4) or the same with 20 mM TEA (TEA, **Black**, n = 12.)The conditions shown are before pressure injection (**Solid**) and after pressure injection (*Striped*). (A) Including 20 mM TEA (**Black**) vs 500 KCl alone (**Red**) in the injection pipette reduced transient $I_{HTK}$ at +20 mV. A 2-way repeated measures ANOVA showed that TEA and pressure injection reduced $I_{HTK}$ at +20 mV as main effects. [TEA; $F(1, 14) = 20.407$, $p = 4.82 \times 10^{-4}$. Pressure Injection; $F(1, 14) = 10.270$, $p = 0.006$. Interaction; $F(1, 14) = 1.838$, $p = 0.197$.] (B) Including TEA in pipette reduced $I_{HTK}$ steady state at +20 mV. A 2-way repeated measures

ANOVA showed that TEA reduced $I_{HTK}$ steady state at +20 mV as a main effect, and significantly interacted with time.[TEA; F (1, 14) = 36.334, p = 3.103 x $10^{-5}$. Pressure Injection; F (1, 14) = 0.0355, p = 0.853. Interaction; F (1, 14) = 5.195, p = 0.039.] (C) TEA reduced the transient A current ($I_A$) at +20 mV. A 2 way repeated measures ANOVA showed that TEA reduced the $I_A$ as a main effect. [TEA; F (1, 14) = 11.437, p = 0.004. Pressure Injection; F (1, 14) = 0.0226, p = 0.883. Interaction; F (1, 14) = 3.698, p = 0.075.] (D) Neither TEA nor pressure injection affected input resistance ($R_{IN}$) measured at -50 mV. A 2-way repeated measures ANOVA showed no significant main effects or interactions. [TEA; F (1, 14) = 0.0123, p = 0.913. Pressure Injection; F (1, 14) = 2.087, p = 0.171. Interaction; F (1, 14) = 4.419, p = 0.056.] (E) TEA and pressure injection did not affect the H current ($I_H$). A 2-way repeated measures ANOVA showed no significant main effects or interactions for $I_H$. [TEA; F (1, 14) = 0.119, p = 0.735. Pressure Injection; F (1, 14) = 0.092, p = 0.766. Interaction; F (1, 14) = 0.183, p = 0.676.] (F) TEA and pressure injection did not affect $V_{Rest}$. A 2-way repeated measures ANOVA showed no significant main effects or interactions. [TEA; F (1, 14) = 8.8 x $10^{-5}$, p = 0.993. Pressure Injection; F (1, 14) = 8.0 x $10^{-5}$, p = 0.993. Interaction; F (1, 14) = 0.901, p = 0.358.] All graphs show means, error bars SEM, Tukey post hoc tests: * , p < 0.05, **, p < 0.01, *** p < 0.001.

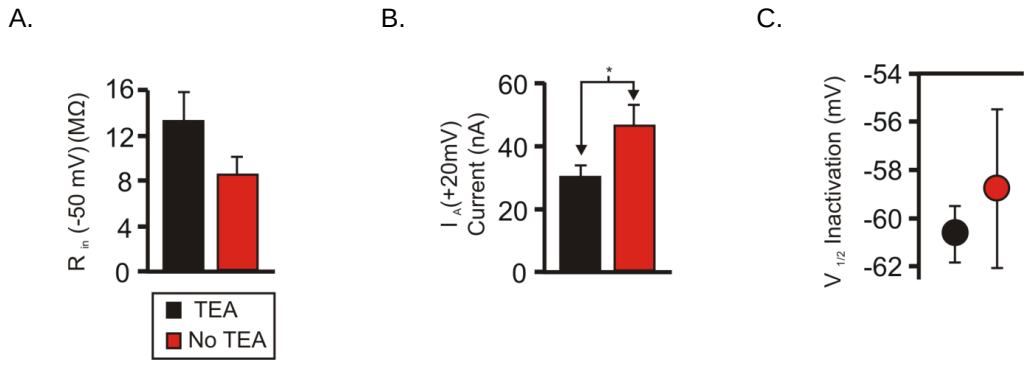


**Figure A3.2: Pressure Injection of TEA Reduces $I_A$ in $I_{MI}$ Recording Solution.** Pressure injection of either 20 mM TEA + 500 mM KCl (**Black**, n = 10) or 500 mM KCl alone (**Red**, n = 4). Saline contained 0.1 µM TTX, 10 µM PTX, 200 µM $CdCl_2$, 5 mM CsCl and 20 mM TEA ($I_{MI}$ recording saline).Measurements are after pressure injection. (A) A t-test showed that inclusion of TEA in injection pipette did not significantly alter input resistance at -50 mV in $I_{MI}$ recording saline [ t (12) = 1.138, p = 0.277]. (B) A t-test showed that inclusion of TEA in injection pipette significantly reduced $I_A$ amplitude at +20 mV [ t (12) = -2.427, p = 0.039]. (C) A t-test showed that $I_A$ $V_{1/2}$ inactivation was not significantly altered by inclusion of 20 mM TEA in $I_{MI}$ recording saline [t (12) = -0.69, p = 0.503.]Error bars are SEM.

*Pressure injection of GDP-βS, significantly increases both steady state $I_{HTK}$ and $R_{IN}$.*

A sign that GDP-βS had an effect over pressure injection of TEA alone, is shown by the ability of GDP-βS to significantly increase both steady state $I_{HTK}$ (+21 ± 6%; $n_{control}$ = 13, $n_{GDP\text{-}\beta S}$ = 8, p = 0.047; Figure A1.3B), and $R_{IN}$ (+54 ± 10 %; SEM; $n_{control}$ = 13, $n_{GDP\text{-}\beta S}$ = 8, p = 0.003; Figure A1.3D). These results, along with the inhibition of proctolin-induced $I_{MI}$, suggest that GDP-βS was active.

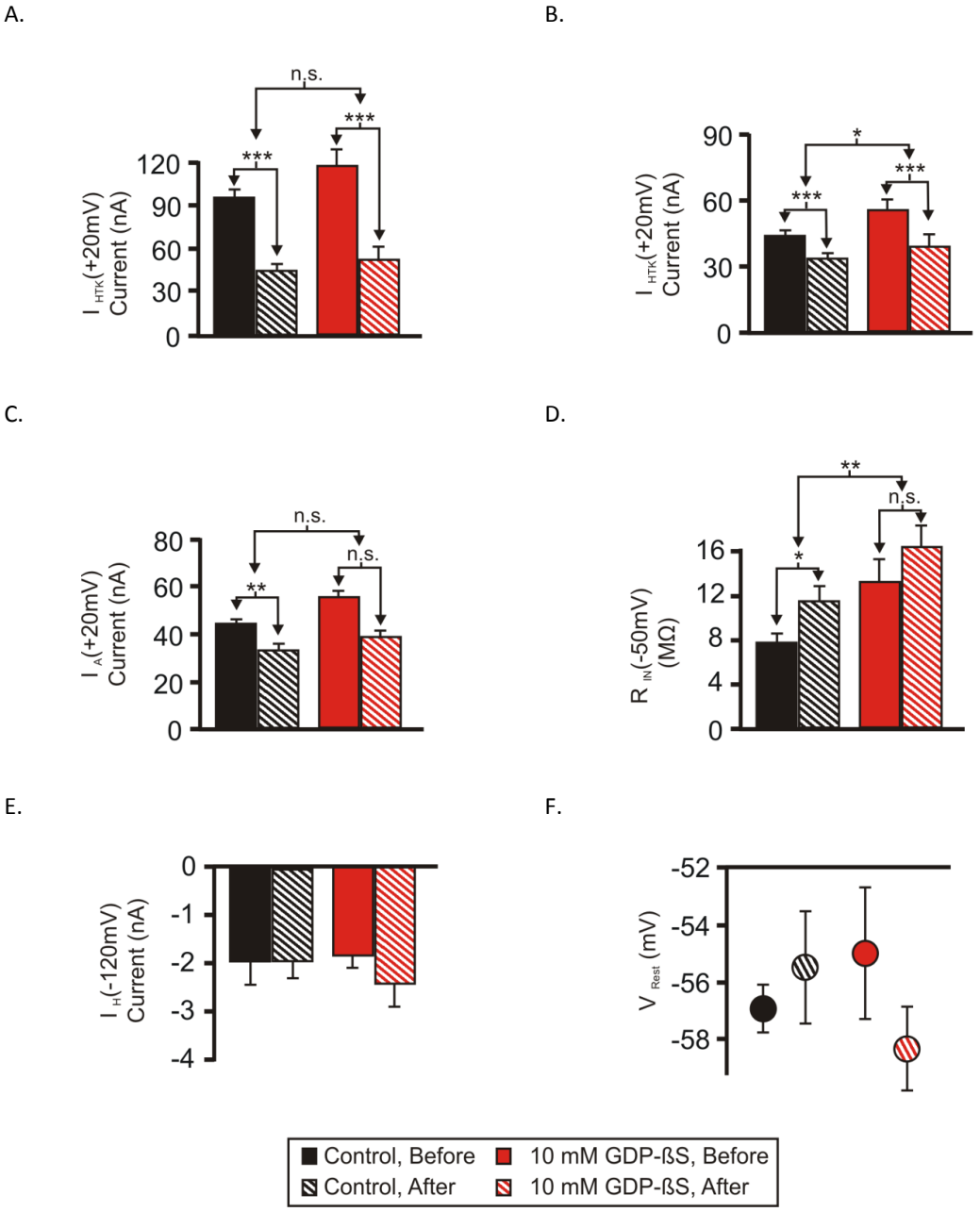


**Figure A3.3: Pressure Injection of the G-protein Inhibitor GDP-βS Increases Input Resistance at -50 mV, Increases $I_{HTK}$ steady state and $I_A$, but does not Affect Other Measured Ionic Currents.** Saline contained 0.1 μM TTX. Current injection pipettes included 500 mM KCL + 20 mM TEA (Control, **Black**, n = 13) or the same plus 10 mM GDP-βS (**Red**, n = 8). Conditions are before pressure injection (**Solid**) and after pressure injection (*Striped*). (A) A 2-way repeated measures ANOVA showed that Pressure injection of TEA, but not GDP-βS, inhibited transient $I_{HTK}$ (+20 mV). [GDP-βS; F (1, 19) = 2.900, p = 0.105. Pressure Injection; F (1,

19) = 189.318, $p < 10^{-8}$. Interaction; F (1, 19) = 2.846, p = 0.108.].(B) A 2-way repeated measures ANOVA showed that pressure injection of TEA was capable of reducing $I_{HTK}$ steady state while GDP-βS, was capable of increasing it [GDP-βS; F (1, 19) = 4.509, p =0.047. Pressure Injection; F (1, 19) = 47.405, $p = 1.4 \times 10^{-6}$. Interaction; F (1, 19) = 1.794, p = 0.196.] (C) A 2-way repeated measures ANOVA showed that pressure injection of TEA, but not GDP-βS, inhibited $I_A$ (+20 mV) [GDP-βS; F (1, 19) = 0.0186, p = 0.893. Pressure Injection; F (1, 19) = 12.107, p = 0.003. Interaction; F (1, 19) = 0.0417, p = 0.840.] (D) A 2-way repeated measures ANOVA showed that both pressure injection of TEA and GDP-βS increased $R_{IN}$ at -50 mV [GDP-βS; F (1, 19) = 11.548, p = 0.003. Pressure Injection; F (1, 19) = 7.447, p = 0.013. Interaction; F (1, 19) = 0.0554, p = 0.817.] (E) A 2-way repeated measures ANOVA showed that neither pressure injection of TEA, or GDP-βS was capable of changing $I_H$ at-120 mV. [GDP-βS; F (1, 19) = 0.125, p = 0.728. Pressure Injection; F (1, 19) = 0.613, p = 0.443. Interaction; F (1,19) = 0.664, p = 0.425.] (F) A 2-way repeated measures ANOVA showed that neither pressure injection or GDP-βS were capable of altering $V_{Rest}$. [GDP-βS; F (1, 19) = 0.0431, p = 0.838. Pressure Injection; F (1, 19) = 0.498, p = 0.489. Interaction; F (1, 19) = 2.975, p = 0.101.] Error bars SEM, Tukey post hoc tests: * , p < 0.05, **, p < 0.01, *** p < 0.001.

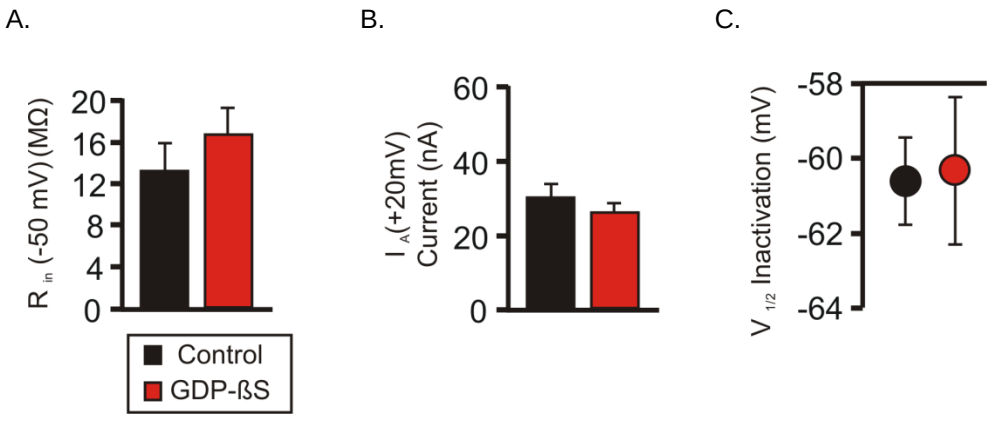


**Figure A3.4. Pressure Injection of GDP-βS Does not Affect $I_A$, $R_{IN}$ or $I_A$ $V_{1/2}$ Inactivation in $I_{MI}$ Recording Solution.** Pressure injection of either 20 mM TEA + 500 mM KCl (**Black**, n = 10) or the same with 10 mM GDP-βS (**Red**, n=4). Saline contained 0.1 μM TTX, 10 μM PTX, 200 μM $CdCl_2$, 5 mM CsCl and 20 mM TEA ($I_{MI}$ recording saline).Measurements are after pressure injection. (A) A t-test showed that GDP-βS did not change $R_{IN}$ at -50 mV [t (16) = -1.006, p = 0.329.] (B) A t-test showed that GDP-βS did not change $I_A$ at +20 mV [t (16) = 0.962, p = 0.350.] (C) A t-test showed that GDP-βS did not change $I_A$ $V_{1/2}$ inactivation [t (16) = -0.133, p = 0.896.] Error bars are SEM.

*Pressure injection of GTP-γS, significantly decreases $R_{IN}$ and Hyperpolarizes RMP.*

Evidence that GTP-γS was affecting LP activity over and beyond pressure injection is that pressure injection of this activator significantly reduced input resistance (-42 ± 11%; SEM; $n_{control}$ = 11, $n_{GDP\text{-}\beta S}$ = 5, p = 0.042; Figure A1.5D) and hyperpolarized LP from -55 ± 1.4mV to -61.100 ± 2.1mV (SEM; $n_{Control}$ = 11 $n_{GTP\text{-}\gamma S}$ = 5; p = 0.03; Figure A1.5E). Interestingly, this effect on $R_{IN}$ is opposite of the response of GDP-βS suggesting that this effect is on $R_{IN}$ is consistent. This result is intuitive, as the most naïve explanation of GPCRs would be the opening of channels consequently reducing $R_{IN}$. This together with GTP-γS's occlusion of proctolin-induced $I_{MI}$ versus control injections, suggests that GTP-γS was active.

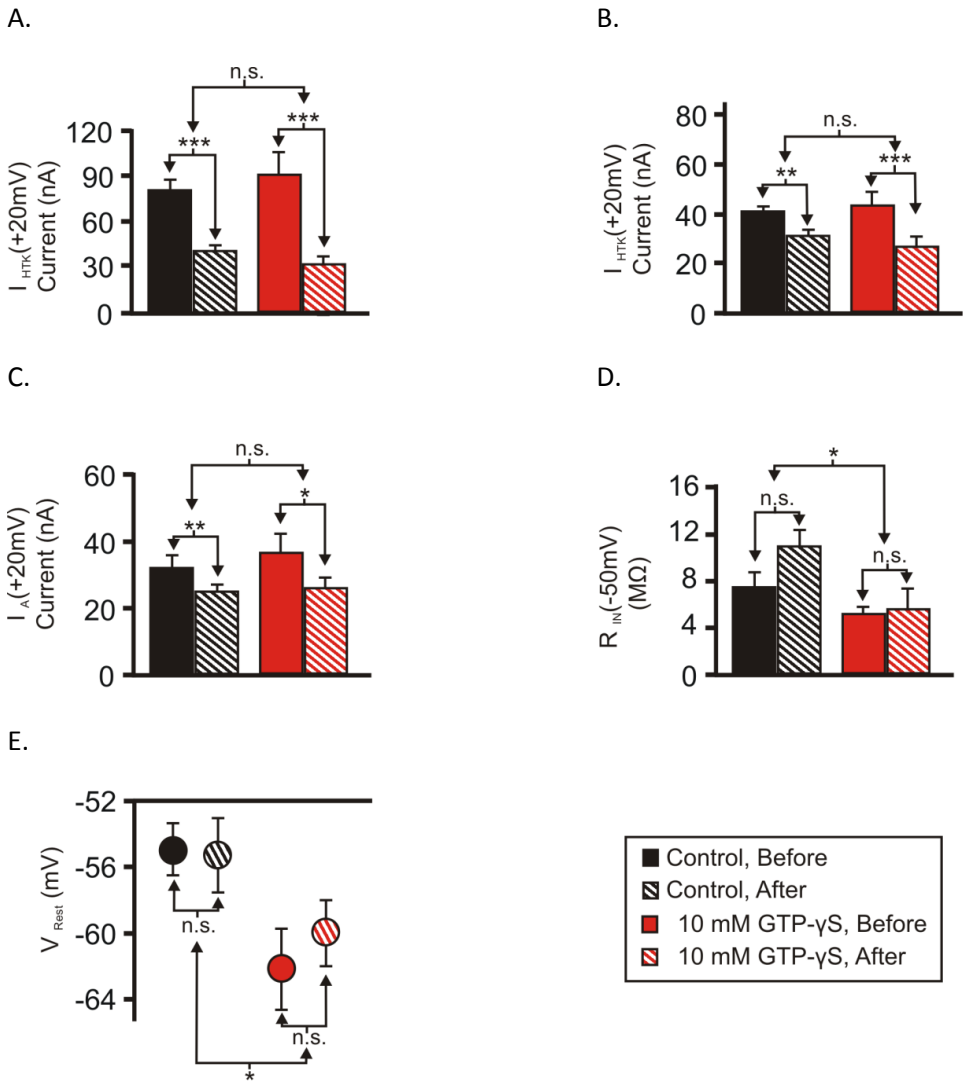


**Figure A3.5. GTP-γS Did Not Affect Ionic Currents but Lowered Input Resistance and Hyperpolarized Resting Membrane Potential (RMP).** Saline contained 0.1 μM TTX. Current injection pipettes included 500 mM KCL + 20 mM TEA (Control, **Black**, n = 11) or the same plus 10 mM GTP-γS (**Red**, n = 5). Conditions are before pressure injection (**Solid**) and after pressure injection (*Striped*). (A) A 2-way repeated measures ANOVA showed that pressure injection of TEA, but not GTP-γS, inhibited transient $I_{HTK}$ at +20 mV [GTP-γS; F (1, 14) = 0.0189, p = 0.893. Pressure Injection; F (1, 14) = 75.901, p = 5.00 x $10^{-7}$. Interaction; F (1, 14) = 1.819, p = 0.199.] (B) A 2-way repeated measures ANOVA showed that pressure injection of TEA, but not GTP-γS,

inhibited steady state $I_{HTK}$ [GTP-γS; F (1, 14) = 0.0461, p = 0.833. Pressure Injection; F (1, 14) = 34.665, p = 3.951 x $10^{-5}$. Interaction; F (1, 14) = 2.279, p = 0.153.] (C) A 2-way repeated measures ANOVA showed that pressure injection of TEA, but not GTP-γS, inhibited $I_A$ at +20 mV [GTP-γS; F (1, 14) = 0.410, p = 0.533. Pressure Injection; F (1, 14) = 15.349, p = 0.002. Interaction; F (1, 14) = 0.169, p = 0.687.] (D) A 2-way repeated measures ANOVA showed that pressure injection of GTP-γS, but not pressure injection alone, was capable of reducing input resistance at -50 mV.[GTP-γS; F (14, 1) = 4.994, p = 0.042. Pressure Injection; F (1, 14) = 3.871, p = 0.069. Interaction; F (14, 1) = 2.188, p = 0.161.] (E) A 2-way repeated measures ANOVA showed that pressure injection of GTP-γS, but not pressure injection alone, was capable of reducing $V_{rest}$. [GTP-γS; F (1, 14) = 5.810, p = 0.030. Pressure Injection; F (1, 14) = 0.185, p = 0.673. Interaction; F (14, 1) = 0.361, p = 0.557.] Error bars SEM, Tukey post hoc tests: * , p < 0.05, **, p < 0.01, *** p < 0.001.

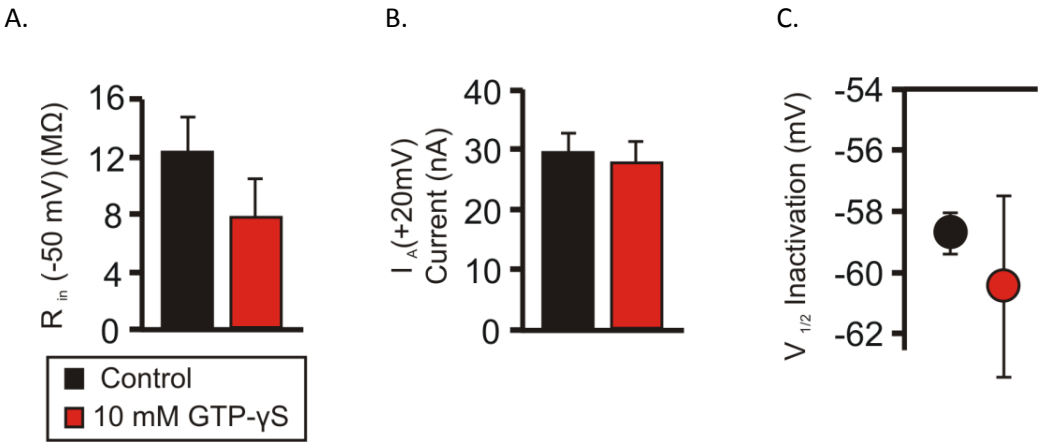


**Figure A3.6: Pressure Injection of GTP-γS Does not Affect $I_A$, $R_{IN}$ or $I_A$ $V_{1/2}$ Inactivation in $I_{MI}$ Recording Solution.** Pressure injection of either 20 mM TEA + 500 mM KCl (**Black**, n = 9) or the same with 10 mM GTP-γS (**Red**, n = 5). Saline contained 0.1 μM TTX, 10 μM PTX, 200 μM $CdCl_2$, 5 mM CsCl and 20 mM TEA ($I_{MI}$ recording saline).Measurements are after pressure injection. (A) A Mann-Whitney rank sum test showed that $R_{IN}$ at -50 mV was not significantly altered by GTP-γS in $I_{MI}$ recording saline [Mann Whitney U-test; $Mdn_{Control}$ = 13.15, $Mdn_{GTP-γS}$ = 3.57; $n_{Control}$ = 9, $n_{GTP-γS}$ = 5; U = 12, p = 0.182.] (B) A t-test showed that GTP-γS had no effect on $I_A$ at+20 mV [t (12) = 0.431, p = 0.674.] (C) A Mann-Whitney rank rum test showed that $I_A$ $V_{1/2}$ inactivation was not significantly altered by GTP-γS in $I_{MI}$ recording saline [Mann Whitney U-test; $Mdn_{Control}$ = -58.29, $Mdn_{GTP-γS}$ = -62.66; $n_{Control}$ = 9, $n_{GTP-γS}$ = 5; U = 19, p = 0.689.] All graphs show means. Error bars are SEM.

*Pressure injection of pertussis toxin (PTX), significantly decreases both transient and steady state $I_{HTK}$, and shifts $I_A$ $V_{1/2}$ inactivation to more hyperpolarized potentials.*

In contrast to GDP-βS, injection of PTX significantly decreased $I_{HTK}$ steady state (-15 ± 4%; SEM; $n_{control} = 9$, $n_{Pertussis} = 9$, $p = 0.031$; Figure A1.7B). Likewise, PTX significantly decreased transient $I_{HTK}$ compared to pressure injection alone (-28 ± 5% SEM; $n_{control} = 9$, $n_{GDP\text{-}\beta S} = 9$, $p = 0.002$; Figure 20A). The inhibition of these two currents cannot be explained by disproportionate-pressure injection. This is because we have observed, in some cases, that pressure injection of TEA inhibits $I_A$. Therefore we assume that at high levels of TEA pressure injection, $I_A$ eventually decreases.[21] Therefore, if we were overzealous in our pressure injection procedure, we would expect to see a reduction in pertussis $I_A$ vs control injected $I_A$. However, this was not the case, as PTX $I_A$ and control $I_A$ were not significantly different in either TTX (A3.7C) or $I_{MI}$ recording saline (A3.8B). This suggests that the difference in both steady state and transient $I_{HTK}$ cannot be due to differences in injection of TEA. Although it is a difficult argument to make when using TEA in the electrodes, it suggests this reduction of both steady state and transient $I_{HTK}$ are most likely due to PTX and not differences in pressure injection. Therefore we argue that PTX significantly reduced transient and steady state $I_{HTK}$. Figure A3.8C shows that pressure injection of PTX significantly hyperpolarized $I_A$ $V_{1/2}$ inactivation from -58.44 ± 2.06 mV to -64.73 ± 1.437 (SEM; $n_{control} = 7$, $n_{Pertussis} = 9$; [ $t(14) = -2.354$, $p = 0.034$.]) These results, together with the inhibition of proctolin-induced $I_{MI}$, suggest that pertussis was active compared to pressure injection alone.

[21] Although much less sensitive to TEA pressure injection than $I_{HTK}$, $I_A$ is significantly inhibited by TEA pressure injection. This is shown by Figure A3.3C (compare solid black-to-black stripes) and also shown in Figure A3.2B despite the finding that it was not technically significant when measured in 3.1C (Tukey within TEA; $p = 0.057$).

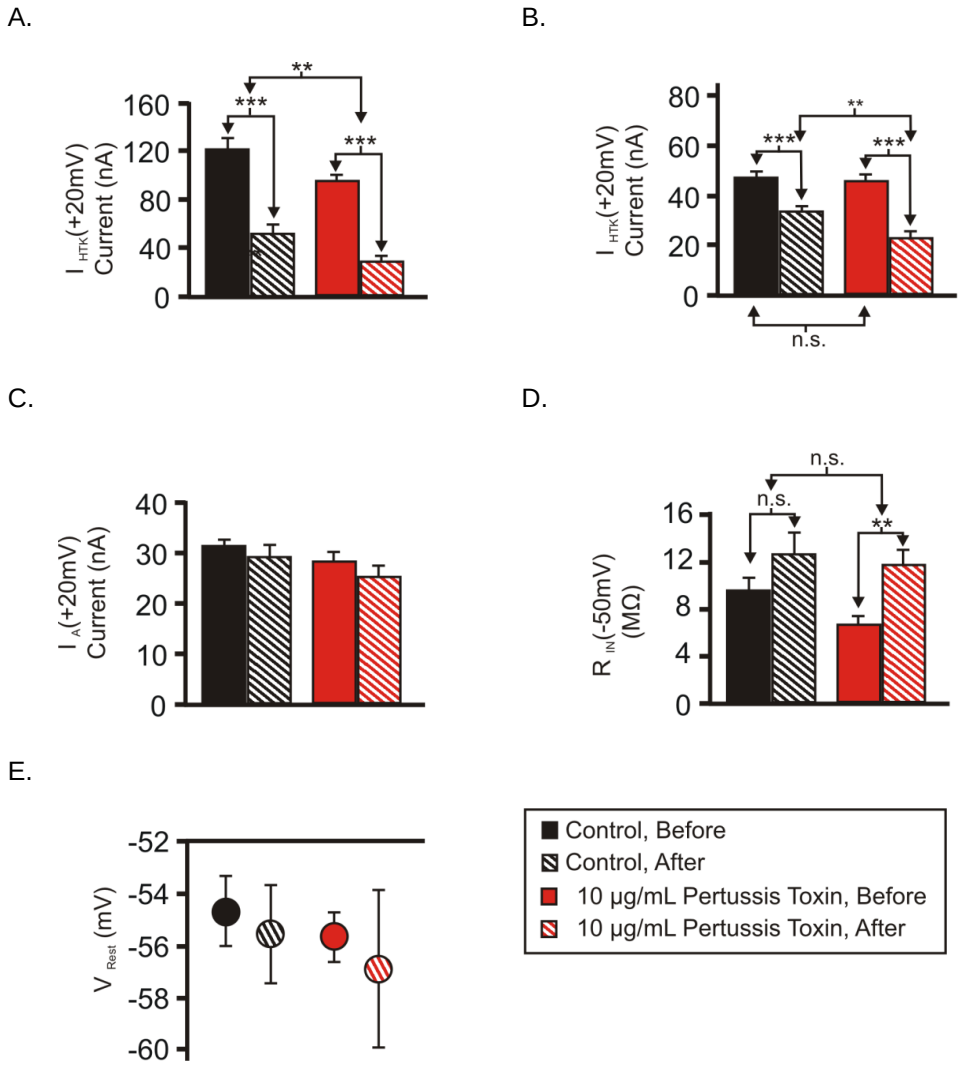


**Figure A3.7: Pertussis Toxin Inhibits Both $I_{HTK}$ Transient and Steady State but Leaves Other Currents Unaffected in TTX.** Saline contained 0.1 µM TTX. Current injection pipettes included 500 mM KCL + 20 mM TEA (Control, **Black**, n = 9) or the same plus 10 µg/ mL of Pertussis Toxin A protomer (**Red**, n = 9). Conditions are before pressure injection (**Solid**) and after pressure injection (*Striped*). (A) A 2-way repeated measures ANOVA showed that both pressure injection and pertussis toxin inhibited transient $I_{HTK}$ at +20 mV as main effects.[Pertussis; F (1, 16) = 13.731, p = 0.002. Pressure Injection; F (1, 16) = 232.314, $p < 10^{-8}$. Interaction; F (1, 16) = 0.140, p = 0.713.] (B) A 2-way repeated measures ANOVA showed that both pressure injection and pertussis toxin inhibited steady state $I_{HTK}$ as main effects with a significant interaction. [Pertussis; F (1, 16) = 5.578, p = 0.031. Pressure Injection; F (1, 16) = 90.405, p = 6.0 x $10^{-8}$. Interaction; F (1, 16) = 5.541, p = 0.032.] (C) A 2-way repeated measures ANOVA showed that neither pressure injection nor Pertussis toxin were capable of altering $I_A$ at

+20 mV. [Pertussis; F (1, 16) = 2.661, p = 0.122. Pressure Injection; F (1, 16) = 2.575, p = 0.128. Interaction; F (1, 16) = 0.0930, p = 0.764.] (D) A 2-way repeated measures ANOVA showed that pressure injection but not Pertussis toxin was capable of increasing $R_{IN}$ at -50 mV. [Pertussis; F (1, 16) = 1.920, p = 0.185. Pressure Injection; F (1, 16) = 12.837, p = 0.002. Interaction; F (1, 16) = 0.825, p = 0.377.] (E) A 2-way repeated measures ANOVA showed that neither pressure injection nor Pertussis toxin was capable of changing $V_{rest}$. [Pertussis; F (1, 16) = 0.275, p = 0.607. Pressure Injection; F (1, 16) = 0.379, p = 0.547. Interaction; F (1, 16) = 0.00945, p = 0.924.] Error bars are SEM. Tukey post hoc tests: * , p < 0.05, **, p < 0.01, *** p < 0.001.

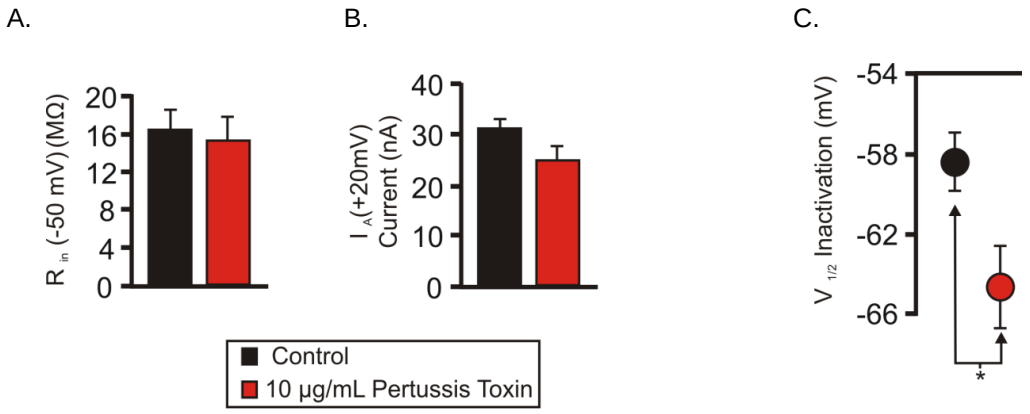


**Figure A3.8: Pressure Injection of Pertussis Toxin Shifts $I_A$ $V_{1/2}$ Inactivation to More Hyperpolarized Voltages.** Pressure injection of either 20 mM TEA + 500 mM KCl (**Black**, n = 7) or the same with 10 µg/mL of Pertussis Toxin Protomer A. (**Red**, n = 9). Saline contained 0.1 µM TTX, 10 µM PTX, 200 µM $CdCl_2$, 5 mM CsCl and 20 mM TEA. ($I_{MI}$ recording saline).Measurements are after pressure injection. (A) A t-test showed that Pertussis Toxin did not affect $R_{IN}$ at -50 mV. [t (14) = -0.367, p = 0.729.] (B) A t-test showed that Pertussis Toxin did not affect $I_A$ at +20 mV. [t (14) = -1.852, p = 0.085.] (C) A t-test showed that Pertussis Toxin significantly hyperpolarized $I_A$ $V_{1/2}$ inactivation [t (14) = -2.35, p = 0.034.] Error bars are SEM.*, p < 0.05.

## Appendix B: Effects for Cyclic Nucleotide Agents

*Effect of cyclic nucleotide neuromodulators on $R_{IN}$ and $I_A$.: Ionic currents are stable for long term recording in $I_{MI}$ recording saline.* In standard $I_{MI}$ recording saline (0.1 µM TTX, 10 µM PTX, 200 µM $CdCl_2$, 5 mM CsCl and 20 mM TEA), the only currents that were measured were $I_{MI}$, $I_A$ and $R_{IN}$. To exclude the trivial possibility that these agents were simply ineffective, or non-specific we examined whether a given agent affected $R_{IN}$ or $I_A$. We first had to establish the stability of these variables in long term incubations of $I_{MI}$ recording saline. Figure B3.1 shows that neither $R_{IN}$ at -50 mV or $I_A$ at +20 mV were significantly changed in 5 hour incubations in $I_{MI}$ recording saline [statistics in Figure B3.1]. Therefore, when applying signal transduction modulators, the variable measure taken before drug application can serve as its own control as any changes in $R_{IN}$ and $I_A$ are directly attributable to changes brought on by the drug. In this way, a more powerful repeated measures or paired t-test design, where each preparation serves as its own control, can be used rather than comparing across preparations.

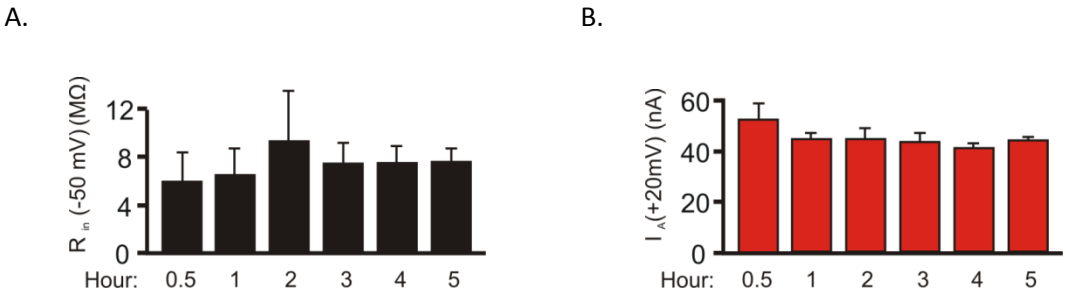


**Figure B3.1. Long Term Incubation in $I_{MI}$ Recording Saline Does not affect $R_{IN}$ (-50 mV) or $I_A$ (+20 mV).** Saline contained 0.1 µM TTX, 10 µM PTX, 200 µM $CdCl_2$, 5 mM CsCl and 20 mM TEA ($I_{MI}$ recording Saline). (A) Stability of $R_{IN}$ at -50 mV. (**Black**, n = 3) at various times during proctolin measurement in $I_{MI}$ recording saline. A one way repeated measures ANOVA showed that incubation time did not affect $R_{IN}$ at -50 mV.[Time; F (5, 10) = 0.901, p = 0.517.] (B) Stability of $I_A$ at +20 mV (**Red**, n = 3). A one way repeated measures ANOVA showed that incubation time did not affect $I_A$ at +20 mV.[Time; F (5, 10) = 1.478, p = 0.280.] Error bars are SEM.

*Neither forskolin nor 8-Br-cAMP affected $I_A$ or $R_{IN}$.*

Despite the use by previous authors of 8-Br-cAMP in this system at concentrations ranging from 0.1-10mM (Flamm et al., 1987; Harris-Warrick, 1989; Ouyang et al., 2007; Ballo et al., 2010a; Zhang et al., 2010), at 500 µM this agonist showed no significant effect on $I_{MI}$ (Figure 3.7) and was unable to elicit a significant difference current (Figure 3.6). Further, as illustrated in Figure B3.2, this drug was unable to affect either $R_{IN}$ [t (3) = -0.369, p = 0.732.], or $I_A$ [t (3) = -0.709, p = 0.529]. This is surprising, as it had been reported previously in *Panularis interruptus* that lower concentrations of 8-Br-cAMP could significantly depolarize $I_A$ activation (Zhang et al., 2010). For this reason we examined the effect of 500 µM 8-Br-cAMP on $V_{1/2}$ activation of

$I_A$. No change was observed for $I_A$ $V_{1/2}$ activation ($\mu_{Control}$ = 3.51 ± 0.91 mV, $\mu_{8\text{-}Br\text{-}cAMP}$ = 2.65 ± 1.47; ncontrol = 4, $n_{8\text{-}Br\text{-}cAMP}$=4; SEM; p=0.373). However, these measurements were taken before proctolin-induced $I_{MI}$, so, 10-20 minutes of incubation time may not have been enough for them to reach full effect. In contrast to the lack of any postive results with 8-Br-cAMP, 10 µM forskolin was capable of producing a significant difference current in voltages from -50 mV to -80 mV (Figure 3.8). Surprisingly, again ( Figure B3.3) we found that forskolin was unable to affect either $R_{IN}$ at -50 mV [t (3) = -0.305, p = 0.781], or $I_A$ [t (3) = 2.400, p = 0.096] at the same voltage. The resistance result seems incongruent with the difference current results, as it seems that anything that produces a positive sloping difference current should by default reduce $R_{IN}$, or equivalently increase leak. Perhaps since $R_{IN}$ was measured at -50 mV, a region where statistical significance is just beginning in the difference current, coupled with the use of ANOVA for the difference current vs a less powerful t-test for the resistance measurement can explain some of this discrepeancy. It has been reported previously that forskolin is non-specific and can inhibit the A-current in this system (Harris-Warrick, 1989). Although this was not significant in our hands, it is possible that our earlier experiments, as mentioned earlier, did not employ long enough application times to exert full efficacy. Also Harris-Warrick used 50 µM of forskolin to exert these nonspecific effects and perhaps 10 µM of forskolin was not enough to produced these effects (Harris-Warrick, 1989).These results suggest that there is no direct evidence other than the literature precedent (Flamm et al., 1987; Harris-Warrick, 1989; Ouyang et al., 2007;

Ballo et al., 2010a, b) that 8-Br-cAMP was active. Interestingly, the area where forskolin produced a significant difference current, is where one would expect a difference due to $I_H$. This is because $I_H$ begins to activate at voltages negative to -50 mV (Golowasch and Marder, 1992a). As $I_H$ can be enhanced in PD axon through cAMP dependent mechanisms (Ballo et al., 2010a), this could be evidence of the specificity of forskolin. This is inconsistent, however, with the claim that $I_H$ is completely blocked by 5 mM CsCl (Golowasch and Marder, 1992a), in which all of our $I_{MI}$ recordings and difference currents were done. However, it has never been observed whether the pharmacological milieu used for recording $I_{MI}$ could electrotonically shorten the axon, increasing residual $I_H$ not normally observable in these neurons. The negative results of these two agonists, coupled with a literature precedent for the use of these agonists in this system, suggests that $I_{MI}$ is not critically dependent on cAMP signalling.

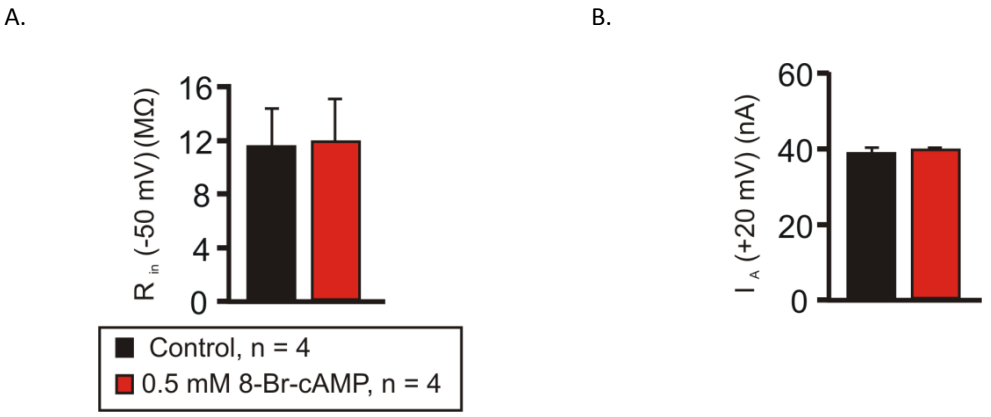


**Figure B3.2. The cAMP Agonist 8-Br-cAMP Does Not Affect Either $R_{IN}$ or $I_A$ in $I_{MI}$ Recording Saline.** Saline contained 0.1 µM TTX, 10 µM PTX, 200 µM $CdCl_2$, 5 mM CsCl and 20 mM TEA ($I_{MI}$ recording Saline).(A) A paired t-test showed that application of 8-Br-cAMP did not affect $R_{IN}$ at -50 mV. [t (3) = -0.369, p = 0.732.] (B) A paired t-test showed that 8-Br-cAMP did not alter $I_A$ at +20 mV. [t (3) = -0.709, p = 0.529.] Error bars are SEM.

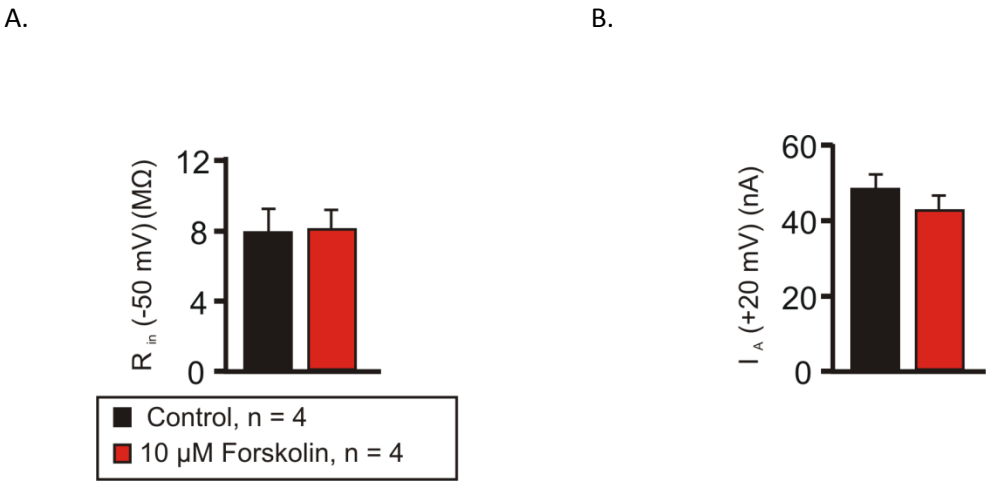


**Figure B3.3: 20 Minute Application of the Adenylyl Cyclase Agonist Forskolin Does Not Affect Either $R_{IN}$ or $I_A$ in $I_{MI}$ Recording Saline.** Saline contained 0.1 µM TTX, 10 µM PTX, 200 µM $CdCl_2$, 5 mM CsCl and 20 mM TEA ($I_{MI}$ recording Saline).(A) A paired t-test showed that application of 10 µM Forskolin did not affect $R_{IN}$ at -50 mV. [t (3) = -0.305, p = 0.781] (B) A paired t-test showed that 10 µM forskolin did not alter $I_A$ at +20 mV. [t (3) = 2.400, p = 0.096] Error bars are SEM.

*8-Br-cGMP Inhibits $I_A$.*

As illustrated in Figure B3.4, a 1 way ANOVA showed that 8-Br-cGMP significantly inhibited $I_A$ at +20 mV [8-Br-cGMP; F (2, 5) = 7.210, p = 0.034.]. It is interesting, however, that this inhibition seemed to saturate at 500 µM, as 1000 µM did not produce further inhibition. In contrast, a 1 way ANOVA showed that 8-Br-cGMP had no effect on $R_{IN}$ [8-Br-cGMP; F (2, 5) = 7.210, p = 0.034]. These results, coupled with the finding that 8-Br-cGMP was capable of producing a significant difference current, suggest that 8-Br-cGMP was active.

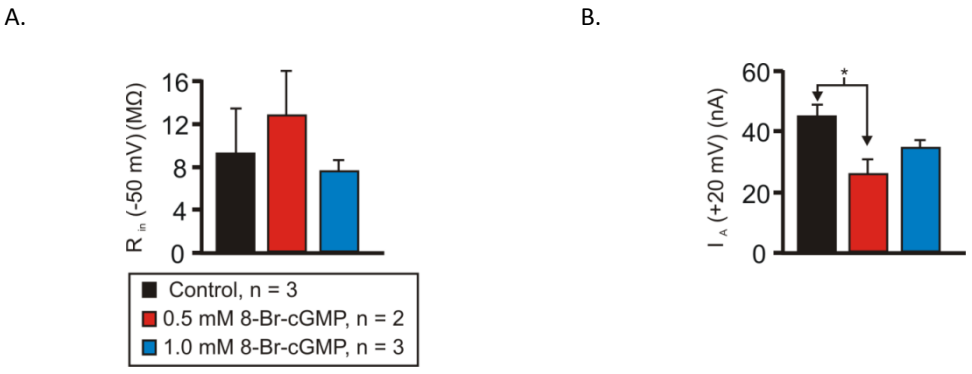


**Figure B3.4: The cGMP Agonist 8-Br-cGMP Does not affect $R_{IN}$ (-50 mV) but May Reduce $I_A$ (+20 mV) in $I_{MI}$ Recording Saline.** Saline contained 0.1 µM TTX, 10 µM PTX, 200 µM $CdCl_2$, 5 mM CsCl and 20 mM TEA ($I_{MI}$ recording Saline). (A) A one way ANOVA showed that different concentrations of 8-Br-cGMP did not affect $R_{IN}$ at -50 mV. [ 8-Br-cGMP; F (2, 5) = 0.564, p = 0.601.] (B) A one way ANOVA showed that different concentrations of 8-Br-cGMP were capable of reducing IA at +20 mV. [8-Br-cGMP; F (2, 5) = 7.210, p = 0.034.] Error bars are SEM. Tukey; * $p < 0.05$.

*The PKA antagonist H89 inhibits $I_A$.* As shown in Figure B3.5, a paired t-test showed that the PKA antagonist H89 significantly inhibited $I_A$ [t (4) = 4.865, p = 0.008.]. This is consistent with the report of Zhang et al., (2010) who report a depolarizing shift in $I_A$ activation when LP cells of *Panularis interruptus* are exposed to H89 (Zhang et al., 2010). There was no change however in $R_{IN}$ at -50 mV [$Mdn_{Control}$ = 5.25, ; $Mdn_{H89}$ = 5.25; n = 5; Z = -1.289, p = 0.250.]. This inhibition of $I_A$, along with the finding that H89 was capable of modulating $I_{MI}$ slope, suggests that H89 was active in our system.

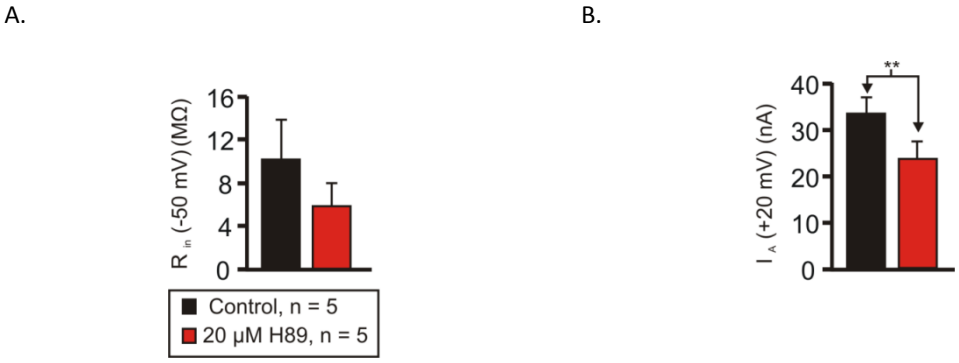


**Figure B3.5: The PKA Antagonist H89 Does not Affect RIN (-50 mV) but Reduces IA (+20 mV).** Saline contained 0.1 µM TTX, 10 µM PTX, 200 µM $CdCl_2$, 5 mM CsCl and 20 mM TEA ($I_{MI}$ recording Saline).(A) A Wilcoxon signed rank test showed that H89 was unable to change $R_{IN}$ at -50 mV.[$Mdn_{Control}$ = 5.25, ; $Mdn_{H89}$ = 5.25; n = 5; Z = -1.289, p = 0.250.](B) A paired t-test showed that H89 was capable of significantly reducing $I_A$ at +20 mV.[t (4) = 4.865, p = 0.008.] Means shown. Error bars are SEM.

## Appendix C: Effects of PLC Pharmaceutical Agents

*Edelfosine did not affect either $R_{IN}$, $I_A$ (+20mV) or $I_A$ $V_{1/2}$ inactivation.*

In order to determine *if C. borealis* cells are sensitive to edelfosine, we measured $I_A$ at +20 mV and $R_{IN}$ at -50 mV, with the hypothesis that PLC signalling may affect these measurements. More importantly, we wished to see if edelfosine did anything at the concentrations used in our experiments. Figure C3.1 shows that Edelfosine was incapable of affecting either $R_{IN}$ at -50 mV, $I_A$ at +20 mV, and V1/2 inactivation. The same was observed for $I_{A\_MAX}$, $I_{A\ \_V1/2}$ activation, and $V_{Rest}$ (Data not shown). Although there is precedent for use of this drug in our system (Zhang et al., 2010), this result was negative as well. Other than its use in non-STG crustacean systems (Kashiwagi et al., 2000; Wong et al., 2007), or on crustacean proteins expressed in HEK-293 cells (Clark et al., 2004), we have neither direct literature precedent or positive evidence that this drug was working correctly at the concentrations (10-20µM) and incubations (1-3 hours) that we used.

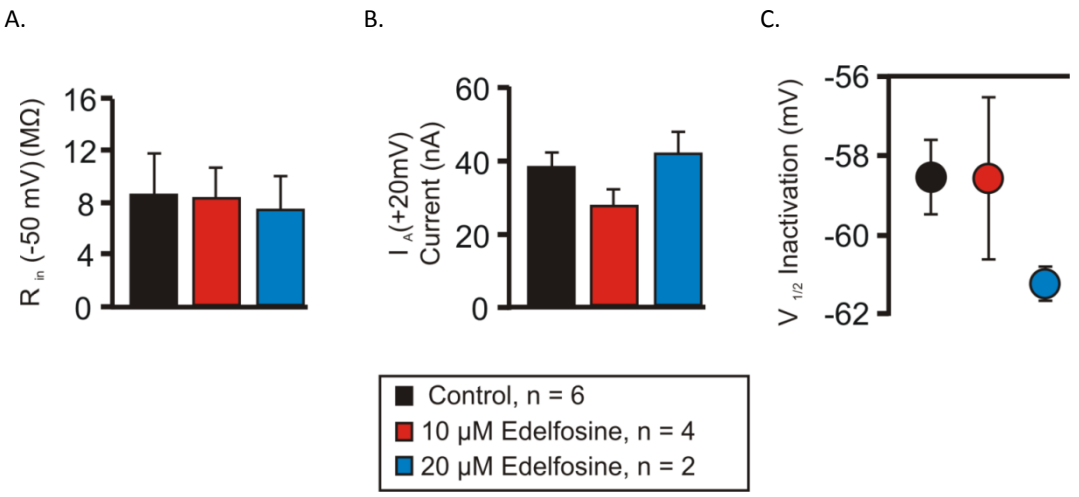


**Figure C3.1: The PLC Inhibitor Edelfosine Does Not Affect $R_{IN}$ (-50 mV), $I_A$ (+20 mV), or $I_A$ Inactivation.** Saline contained 0.1 μM TTX, 10 μM PTX, 200 μM $CdCl_2$, 5 mM CsCl and 20 mM TEA ($I_{MI}$ recording Saline) (A) A one-way repeated measures ANOVA showed that Edelfosine was unable to alter $R_{IN}$ at -50 mV [Edelfosine; F (2, 4) = 0.249, p = 0.791.] (B) A one-way repeated measures ANOVA showed that Edelfosine was unable to alter $I_A$ at +20 mV [Edelfosine; F (2, 4) = 2.372, p = 0.209.] (C) A one-way repeated measures ANOVA showed that Edelfosine was unable to alter $I_A$ $V_{1/2}$ inactivation [Edelfosine; F (2, 4) = 0.131, p = 0.881.] Error bars are SEM.

*Extended Periods in low calcium do not affect $R_{IN}$ at -50 mV or $I_A$ at +20 mV.*

As several experiments were run in long term incubations of low calcium $I_{MI}$ recording saline, we wanted to see whether $R_{IN}$ at -50 mV and $I_A$ at +20 mV would be stable in these long incubations. If they changed over time, we would not be able to use them as positive controls or we would have to adjust for time in low calcium with an analysis of covariance. Figure C3.2 shows that neither $R_{IN}$ at -50 mV nor $I_A$ at +20 mV significantly changed over 3 hours in low calcium $I_{MI}$ recording saline. The same was

found for $I_A$ $V_{1/2}$ activation (n = 5 to 2 hours), $I_{AMAX}$ (n =5 to 2 hours), $I_A$ at +20 mV, and $I_A$ $V_{1/2}$ inactivation (n = 2, only to 2 hours (Data not shown)). $V_{1/2}$ inactivation was not measured in later preparations due to the observed instability of cells in low calcium at voltages less than -80 mV. $V_{Rest}$, however, slowly depolarized with incubation but was only significantly different from the first half hour after five hours of incubation. This suggests that $I_A$ (+20 mV) and $R_{IN}$ (-50 mV) are stable during incubation in low calcium $I_{MI}$ recording saline, and therefore experiments in low calcium $I_{MI}$ recording saline can be measured before and after drug condition without accounting for low calcium incubation. When considering changes in $V_{Rest}$ however, analysis of covariance for incubation time should be considered when measuring over long periods.

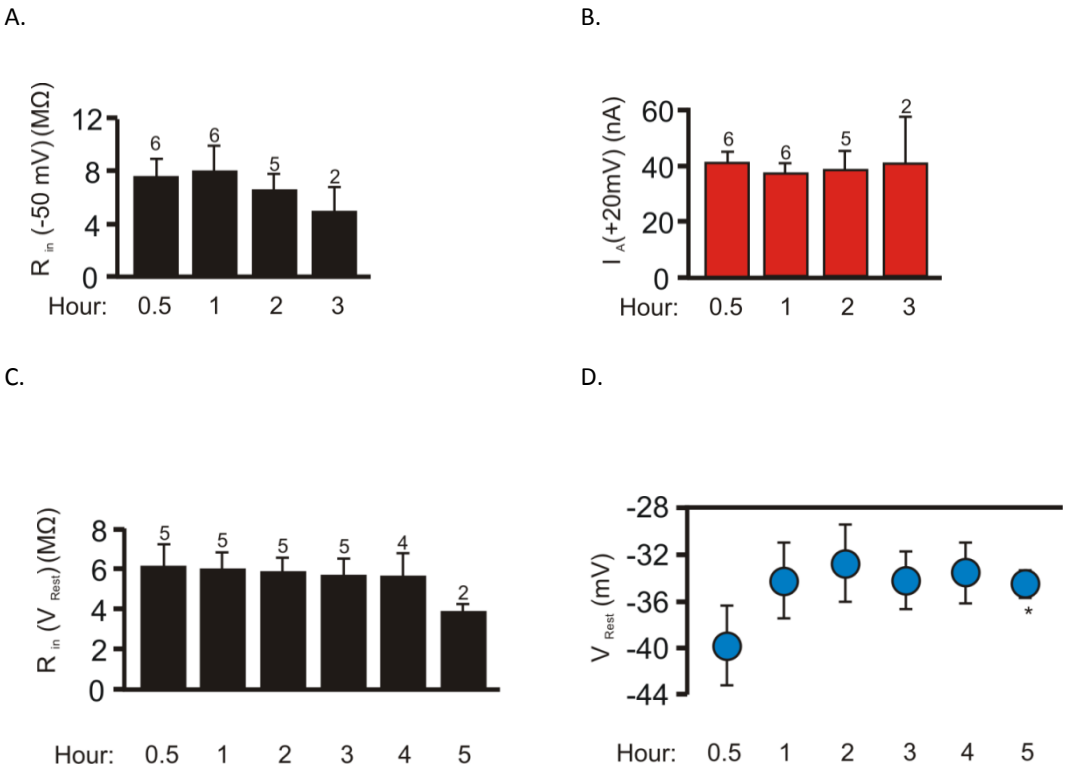


**Figure C3.2. $R_{IN}$ (-50) and $I_A$ (+20) are Stable in 2 mM Low Calcium $I_{MI}$ Recording Saline.** 2 mM low calcium saline contained 0.1 µM TTX, 10 µM PTX, 200 µM $CdCl_2$, 5 mM CsCl and 20 mM TEA supplemented with 0.5% BSA ($I_{MI}$ low calcium recording Saline). (A) A one-way repeated measures ANOVA showed there was no change in $R_{IN}$ at -50 mV for up to 3 hours incubation in low calcium $I_{MI}$ recording saline [Incubation Time; F (3, 9) = 0.624, p = 0.617]. (B) A one-way repeated measures ANOVA showed there was no change in IA at +20 mV for up to 3 hours incubation in low calcium $I_{MI}$ recording saline [Incubation Time; F (3, 9) = 0.452, p = 0.722].(C) A one-way repeated measures ANOVA showed that $R_{IN}$ at $V_{Rest}$ was not influenced by incubation in low calcium $I_{MI}$ recording saline [Incubation Time; F (5, 16) = 0.221, p = 0.948].(D) A one-way repeated measures ANOVA showed that $V_{Rest}$ was significantly altered by incubation in low calcium $I_{MI}$ recording saline [Incubation Time; F (5, 16) = 3.486, p = 0.025]. Error bars are SEM. Tukey post-hoc test; *, $p < 0.05$.

*Neomycin was unable to alter $R_{IN}$ or $V_{Rest}$.*

Due to instability at low voltages in low calcium, we did not do any voltage clamp measurements for neomycin other than $I_{MI}$. Figure C3.3 shows that while incubation time was capable of altering both $V_{Rest}$ and $R_{IN}$, neomycin had no effect [Statistics in Figure C3.3]. Note that $R_{IN}$ is different from previous measurements as it was measured from $V_{Rest}$ and not measured at -50 mV. These results suggest that we do not have an internal positive control for neomycin inhibiting PLC, other than the literature precedent in other invertebrate systems (Willoughby et al., 1999; Rivers et al., 2002; Wenzel et al., 2002; Vezenkov and Danalev, 2009; Brown et al., 2010).

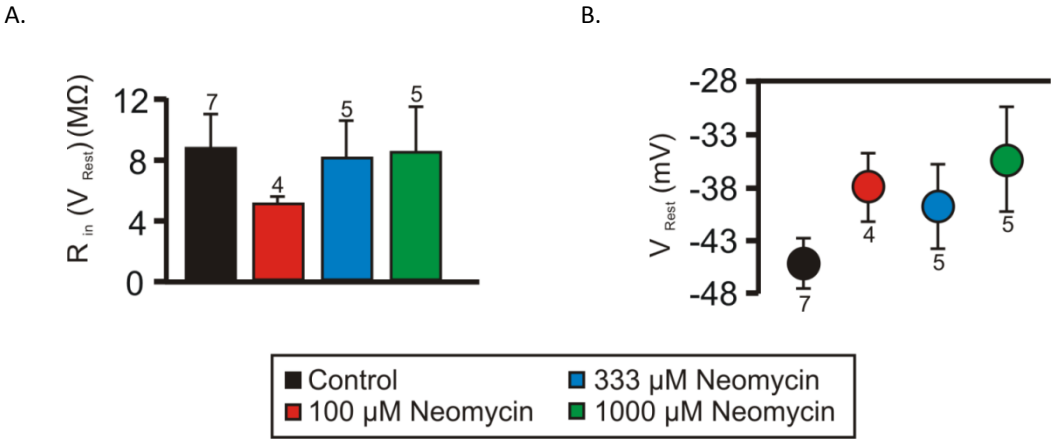


**Figure C3.3. The PLC Inhibitor Neomycin Does Not Affect $R_{IN}$ or $V_{Rest}$.** 2 mM low calcium saline contained 0.1 µM TTX, 10 µM PTX, 200 µM $CdCl_2$, 5 mM CsCl and 20 mM TEA supplemented with 0.5% BSA ($I_{MI}$ low calcium recording Saline).(A) A one-way ANOVA for neomycin with covariate incubation time, showed that neomycin did not significantly alter $R_{IN}$ at $V_{Rest}$ [Neomycin; F (3, 34) = 1.99, p = 0.133. Incubation Time; F (1, 34) = 7.103, p = 0.012]. (B) A one-way ANOVA for neomycin with covariate incubation time showed that neomycin did not significantly alter $V_{Rest}$ [Neomycin; F (3, 34) = 1.001, p = 0.40. Incubation Time; F (1, 34) = 11.33, p = 0.002]. Error bars are SEM.

*The PKC and general kinase inhibitor staurosporine did not affect the ionic currents or their activation.*

As Illustrated in Figure C3.4, in *Cancer* saline with 0.1 µM TTX, staurosporine did not affect $I_{HTK}$ at +20 mV, $I_A$ at + 20 mV, $R_{IN}$ at -50mV, $V_{MID}$ for $I_{HTK,}$ or $I_A$, or $V_{Rest}$. Similar results were found for peak $I_{HTK}$ and $I_A$ (Data not shown). In low calcium $I_{MI}$ recording saline, ionic currents were not recorded. As illustrated in Figure C3.5, staurosporine in $I_{MI}$ did not affect either $R_{IN}$ at $V_{Rest}$, or $V_{Rest}$. This is interesting as it seems to be in direct conflict with our results from H89 (B3.5), which suggests that either staurosporine does

not inhibit PKA effectively in this system, or that H89 is acting on a staurosporine-resistant kinase and not PKA. If staurosporine had not affected $I_{MI}$, these negative results would be problematic, but as staurosporine significantly altered $I_{MI}$ slope (Figure 3.18), it suggests that staurosporine was active in this system.

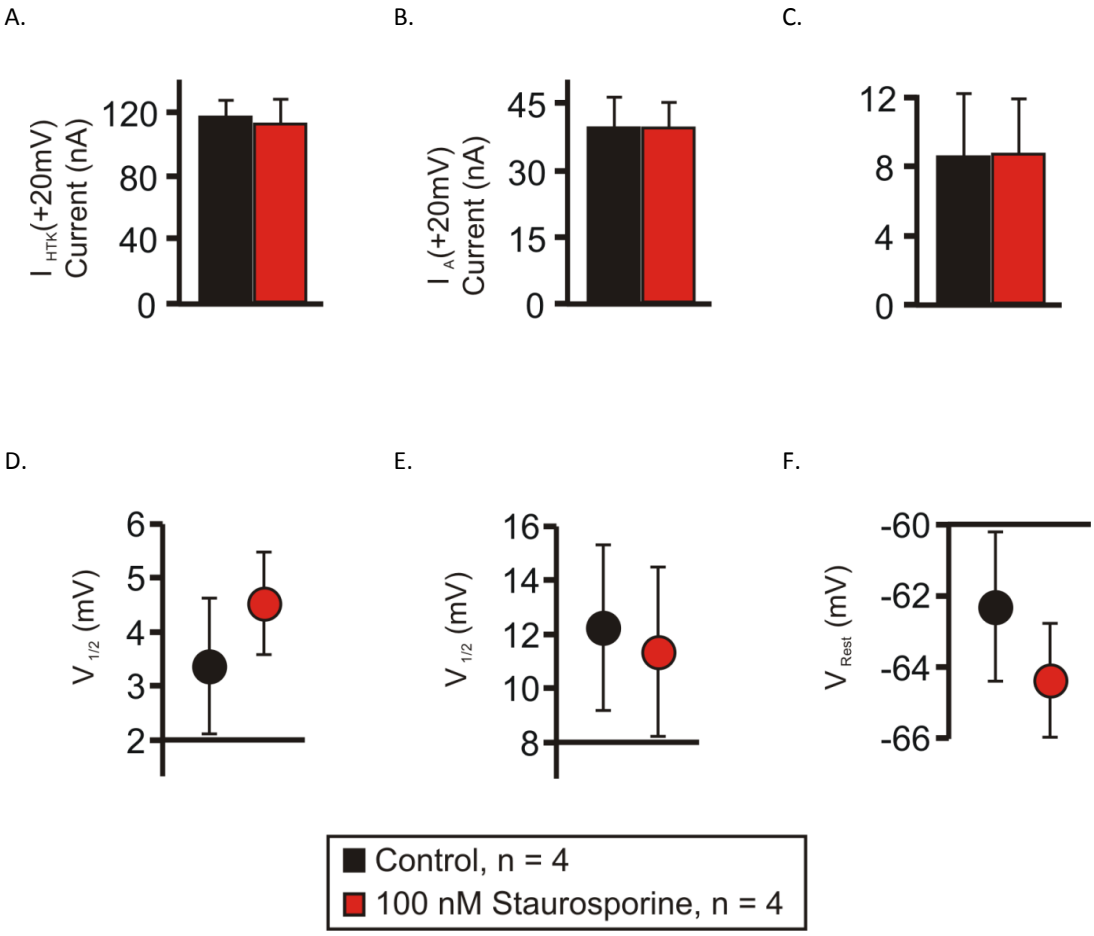


**Figure C3.4. The PKC and General Kinase Inhibitor Staurosporine Does not Affect $I_{HTK}$(+20 mV), $I_A$ (+20 mV), $R_{IN}$(-50 mV), $I_{HTK}$ $V_{1/2}$, $I_A$ $V_{1/2}$, or $V_{Rest}$ in TTX.** Measurements for control (**Black**) or 45 minutes in 100 nM of staurosporine (**Red**). Saline contained 0.1 µM TTX.(A) A paired t-test showed that staurosporine was unable to alter $I_{HTK}$ at +20 mV [t (3) = 0.304, p = 0.781.] (B) A paired t-test showed that staurosporine was unable to alter $I_A$ at + 20 mV [t (3) = -0.006, p = 0.995.](C) A paired t-test showed that staurosporine was unable to alter $R_{IN}$ at -50 mV [t (3) = -0.140, p = 0.897.] (D) A paired t-test showed that staurosporine was unable to alter $I_{HTK}$ $V_{1/2}$ activation [t (3) = -2.439, p = 0.093.] (E) A paired t-test showed that staurosporine was unable to alter $I_A$ $V_{1/2}$ activation [t (3) = - 0.442, p = 0.688.] F) A paired t-test showed that staurosporine was unable to alter $V_{Rest}$ [t (3) = 2.569, p = 0.083.] Error bars are SEM.

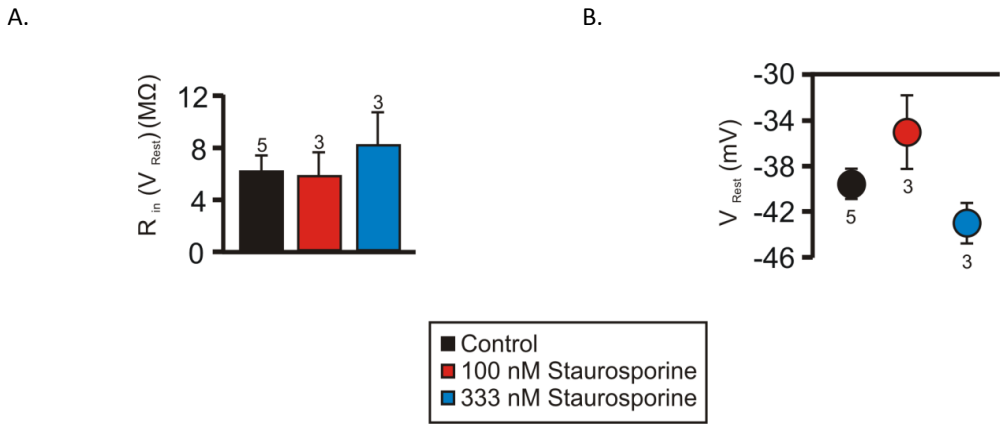


**Figure C3.5: The PKC and General Kinase Inhibitor Staurosporine Has No Effect On $R_{IN}$ or $V_{Rest}$ in $I_{MI}$ Recording Saline.** 2 mM low calcium saline contained 0.1 µM TTX, 10 µM PTX, 200 µM $CdCl_2$, 5 mM CsCl and 20 mM TEA supplemented with 0.5% BSA ($I_{MI}$ low calcium recording Saline). (A) A one-way ANOVA for staurosporine with covariate incubation time showed that staurosporine was unable to significantly alter RIN at VREST [Staurosporine; F (2, 35) = 2.130, p = 0.134. Incubation time; F (1, 35) = 2.09, p = 0.157.] (B) A one-way ANOVA for staurosporine with covariate incubation time showed that staurosporine was unable to significantly alter $V_{REST}$ [Staurosporine; F (2, 35) = 2.93, p = 0.067. Incubation time; F (1, 35) = 3.347, p = 0.067.] Error bars are SEM.

## Appendix D: Effects of phosphatase and tyrosine kinase inhibitors

*Okadaic acid affects $I_A$ in the STG.*

As many of the drugs used in this study have not been tested in this system, we examined the effects these modulators may be having on ionic currents. Figure D3.1 shows that in normal calcium $I_{MI}$ recording saline, increasing concentrations of okadaic acid decreases both $I_A$ at +20 mV and $R_{IN}$ at -50 mV. In agreement with this, estimated peak $I_A$ current was also found to significantly decrease (72.54 ± 6.11 nA for control to 58.95 ± 10.08 nA in 100 nM; SEM ; p = 0.002). Interestingly, the stepwidth of $I_A$ steady-state activation also significantly decreased (data not shown). Similarly, in low calcium $I_{MI}$ recording saline, both $I_A$ at +20 mV (Figure D3.2) and estimated peak $I_A$ (data not shown) both increased in okadaic acid. In agreement with this, $I_A$ $V_{1/2}$ activation was significantly hyperpolarized. Unlike in normal calcium, $R_{IN}$ at -50 mV in low calcium was unaffected by increasing concentrations of okadaic acid. These data suggest that okadaic acid was active in this system.

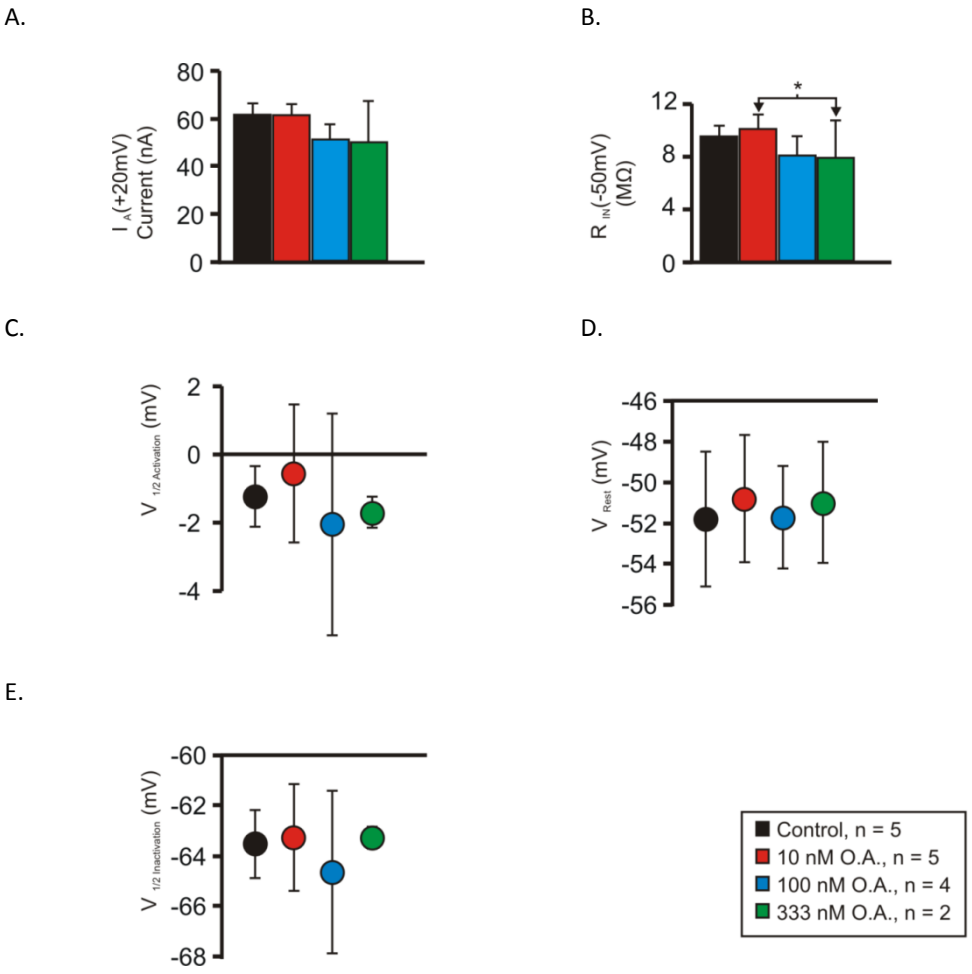


**Figure D3.1: The Non-specific Phosphatase Inhibitor Okadaic Acid Affects $I_A$ and $R_{IN}$ in Normal Calcium $I_{MI}$ Recording Saline.** Effects of okadaic acid on ionic currents. Saline contained 0.1 µM TTX, 10 µM PTX, 200 µM $CdCl_2$, 5 mM CsCl and 20 mM TEA.O.A. = Okadaic acid. (A) A one-way repeated measures ANOVA showed that okadaic Acid significantly altered $I_A$ at +20 mV [O.A.; F (3, 8) = 4.452, p = 0.041.] N was too low to distinguish means in post-hoc testing. (B) A one-way repeated measures ANOVA showed that okadaic acid significantly altered $R_{IN}$ at -50 mV [O.A.; F (3, 8) = 6.243, p = 0.017.] (C) A one-way repeated measures ANOVA showed that okadaic acid was unable to alter $I_A$ $V_{MID}$ of $I_A$ activation [O.A.; F (3, 8) = 1.484, p = 0.291.] (D) A one-way repeated measures ANOVA showed that okadaic acid was unable to alter $V_{Rest}$ [O.A.; F (3, 8) = 1.125, p = 0.391.] (E) A one-way repeated measures ANOVA showed that okadaic acid was unable to alter $I_A$ $V_{1/2}$ inactivation. [O.A.; F (3, 8) = 2.027, p = 0.189.] Error bars are SEM. Tukey test; * $p < 0.05$.

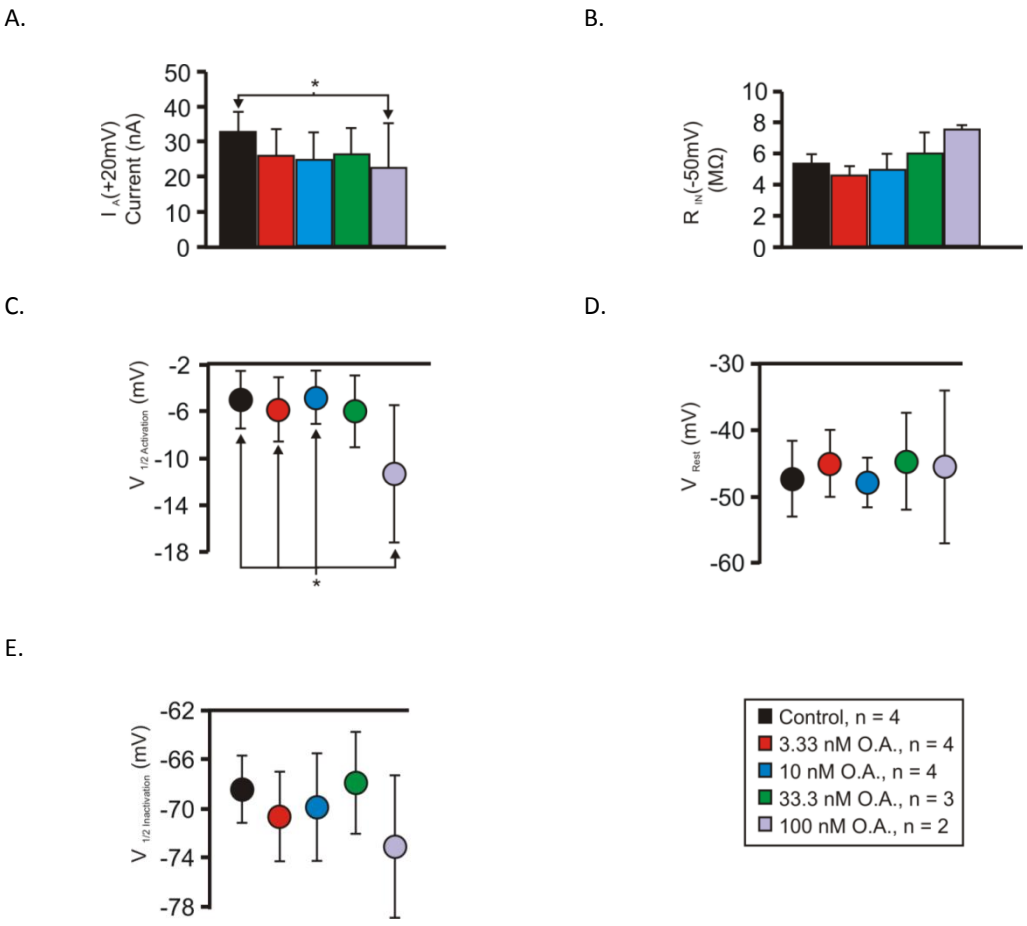


**Figure D3.2: The Non-specific Phosphatase Inhibitor Okadaic Acid Affects IA Amplitude and V1/2 Activation in Low Calcium $I_{MI}$ Recording Saline.** Effects of okadaic acid on ionic currents. 2 mM low calcium saline contained 0.1 µM TTX, 10 µM PTX, 200 µM $CdCl_2$, 5 mM CsCl and 20 mM TEA and was supplemented with 0.5% BSA. O.A. = Okadaic acid. (A) A one-way repeated measures ANOVA showed that okadaic acid significantly altered $I_A$ at +20 mV [O.A.; F (4, 9) = 3.830, p = 0.044.] (B) A one-way repeated measures ANOVA showed that okadaic acid did not significantly alter $R_{IN}$ at -50 mV [O.A.; F (4, 9) = 2.120, p = 0.160.] (C) A one-way repeated measures ANOVA showed that okadaic acid significantly altered $I_A$ $V_{1/2}$ activation [O.A.; F (4, 9) = 9.745, p = 0.002.] (D) A one-way repeated measures ANOVA showed that okadaic acid did not significantly alter $V_{Rest}$ [O.A.; F (4, 9) = 1.197, p = 0.376.] (E) A one-way repeated measures ANOVA showed that okadaic acid did not significantly alter $I_A$ $V_{1/2}$ inactivation [O.A.; F (4, 9) = 2.302, p = 0.137.]

*The tyrosine kinase inhibitor genistein reversibly changes $I_A$ activation and inactivation in 2 mM low calcium.*

In seach of indications that genistein was working, we examined the effect of genistein on ionic currents in TTX (data not shown because only one experiment was conducted) and low calcium (Figure A3.21). Both in TTX, and low calcium $I_{MI}$ recording saline, genistein appeared to reversibly inhibit $I_A$. As illustrated in Figure D3.3, the inhibition was not significant for $I_A$ at +20 mV [t (2) = 3.614, p = 0.069], but the effect was very consistent; this may be a result of the low n (n = 3) of the positive controls. Further, despite the low n of these positive controls, $I_A$ inactivation was significantly hyperpolarized [t (2) = 8.984, p = 0.012] and the $I_A$ activation step width was significantly increased [t (2) = -14.896, p = 0.004]. Although not studied in this system, there have been more specific studies linking genistein (more specifically EGFR and SFKs) to modulation of KV4.3 (inactivating voltage-dependent potassium channels) in human cardiac myocytes and HEK-293 cells (Zhang et al., 2012b). This suggests that the effect of genistein may be specific to tyrosine kinase inhibition. This data suggests that genistein was active in our system.

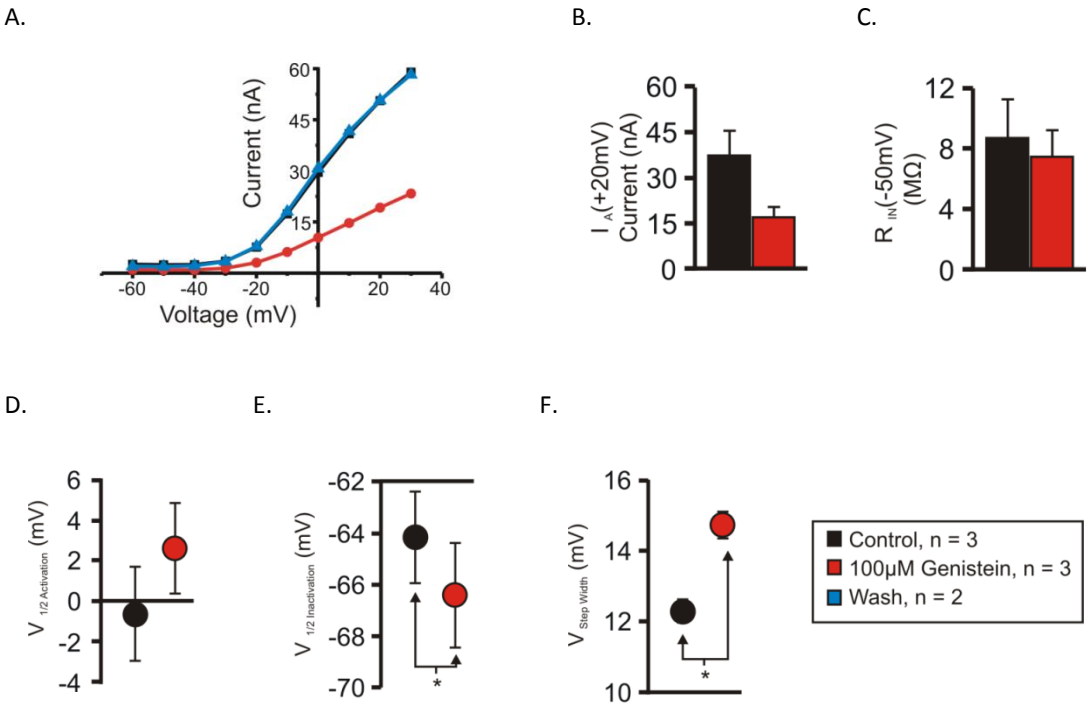


**Figure D3.3: The Tyrosine Kinase Inhibitor Genistein Reversibly Affects A-Current Activation and Inactivation in Low Calcium $I_{MI}$ Recording Saline.** 2 mM low calcium saline contained 0.1 μM TTX, 10 μM PTX, 200 μM $CdCl_2$, 5 mM CsCl and 20 mM TEA and was supplemented with 0.5% BSA. (A) Representative IV curve for IA in control (**Black**), 100 μM genistein (**Red**) and washout (**Blue**). (B) A paired t-test showed that genistein did not reduce IA +20 mV [t (2) = 3.614, p = 0.069] (C) A paired t-test showed that $R_{IN}$ at -50 mV was not significantly affected by genistein [t (2) = 1.085, p = 0.391]. (D) A paired t-test showed that $I_A$ $V_{1/2}$ activation was not affected by genistein [t (2) = -1.985, p = 0.186].(E) A paired t-test showed that genistein significantly hyperpolarized $I_A$ $V_{1/2}$ inactivation [t (2) = 8.984, p = 0.012].(F) A paired t-test showed that genistein significantly increased $I_A$ step width [t (2) = -14.896, p = 0.004]. Error bars are SEM. *, $p < 0.05$.

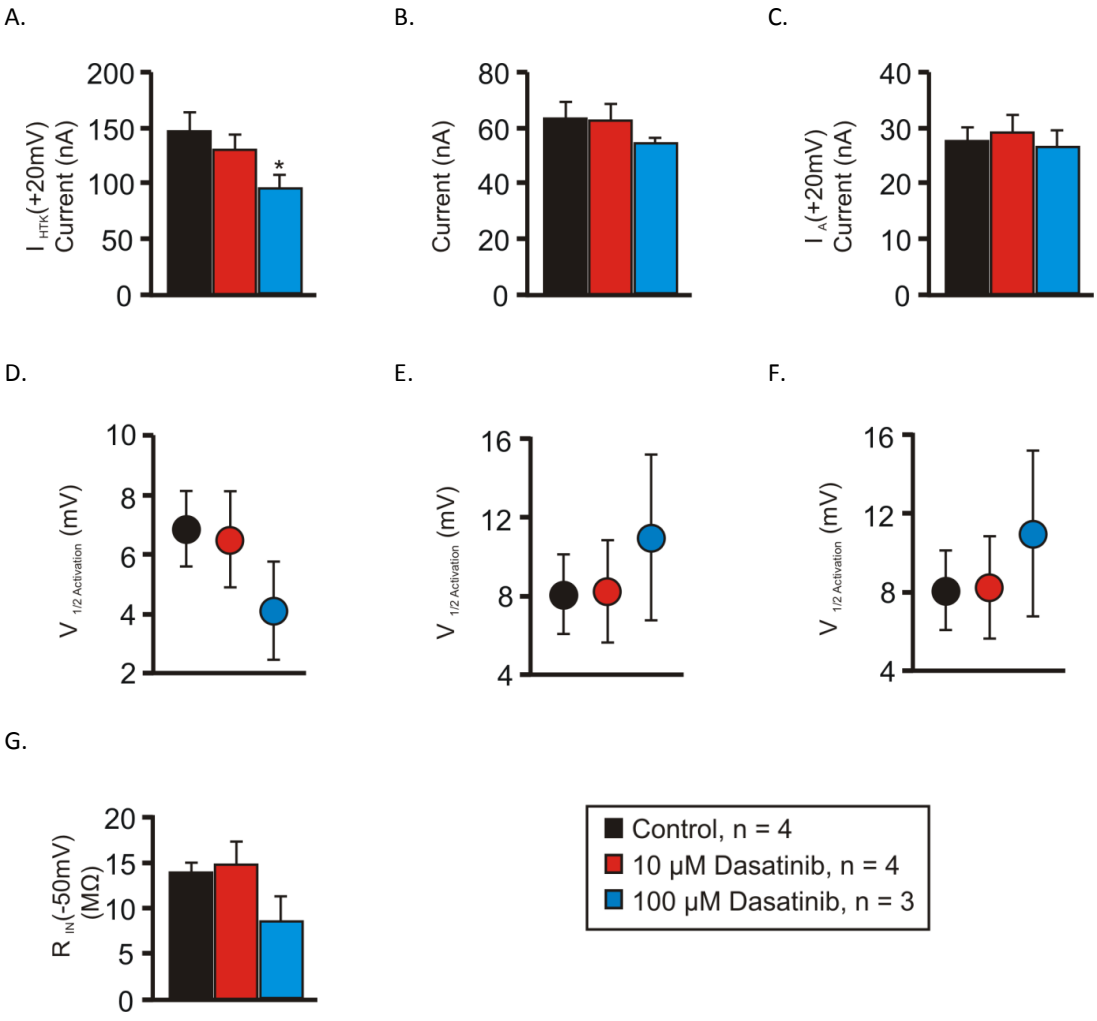


**Figure D3.4: The SFK Inhibitor Dasatinib Inhibits the Transient High Threshold Potassium Current (IHTK).** Saline Contained 0.1 μM TTX. (A) A one-way repeated measures ANOVA showed that dasatinib significantly reduced transient $I_{HTK}$ at + 20 mV [Dasatinib; F (2, 5) = 12.800, p = 0.011]. (B) A one-way repeated measures ANOVA showed that dasatinib was unable to affect steady-state $I_{HTK}$ at + 20 mV [Dasatinib; F (2, 5) = 1.228, p = 0.368]. (C) A one-way repeated measures ANOVA showed that dasatinib was unable to affect $I_A$ at + 20 mV [Dasatinib; F (2, 5) = 0.802, p = 0.499].(D) A one-way repeated measures ANOVA showed that dasatinib was unable to affect transient $I_{HTK}$ $V_{1/2}$ activation [Dasatinib; F (2, 5) = 0.825, p = 0.490]. (E) A one-way repeated measures ANOVA showed that dasatinib was unable to affect steady-state $I_{HTK}$ $V_{1/2}$ activation [Dasatinib; F (2, 5) = 1.757, p = 0.264].(F) A one-way repeated measures ANOVA showed that dasatinib was unable to affect $I_A$ $V_{1/2}$ activation [Dasatinib; F (2, 5) = 0.652, p = 0.560]. (G) A one-way repeated measures ANOVA showed that dasatinib was unable to affect $R_{IN}$ at -50mV [Dasatinib; F (2, 5) = 2.497, p = 0.177].Error bars are SEM. Tukey post-hoc test; *, p

< 0.05.

*The SFK inhibitor dasatinib inhibits transient $I_{HTK}$.*

As shown in Figure D3.4, dasatinib inhibited transient but not steady state $I_{HTK}$ in 0.1 µM TTX. Similarly, the maximal transient $I_{HTK}$ current was significantly inhibited (data not shown). As shown in Figure D3.5, dasatinib inhibited $I_A$ at +20 mV but only when measured in low calcium $I_{MI}$ recording saline. Although a paired t-test showed that this inhibition was statistically significant[t (3) = 5.200, p = 0.014.], an 8 ± 15 % (SEM) inhibition is questionable as to its biological relevance. Together, these results suggest that dasatinib was active in this system.

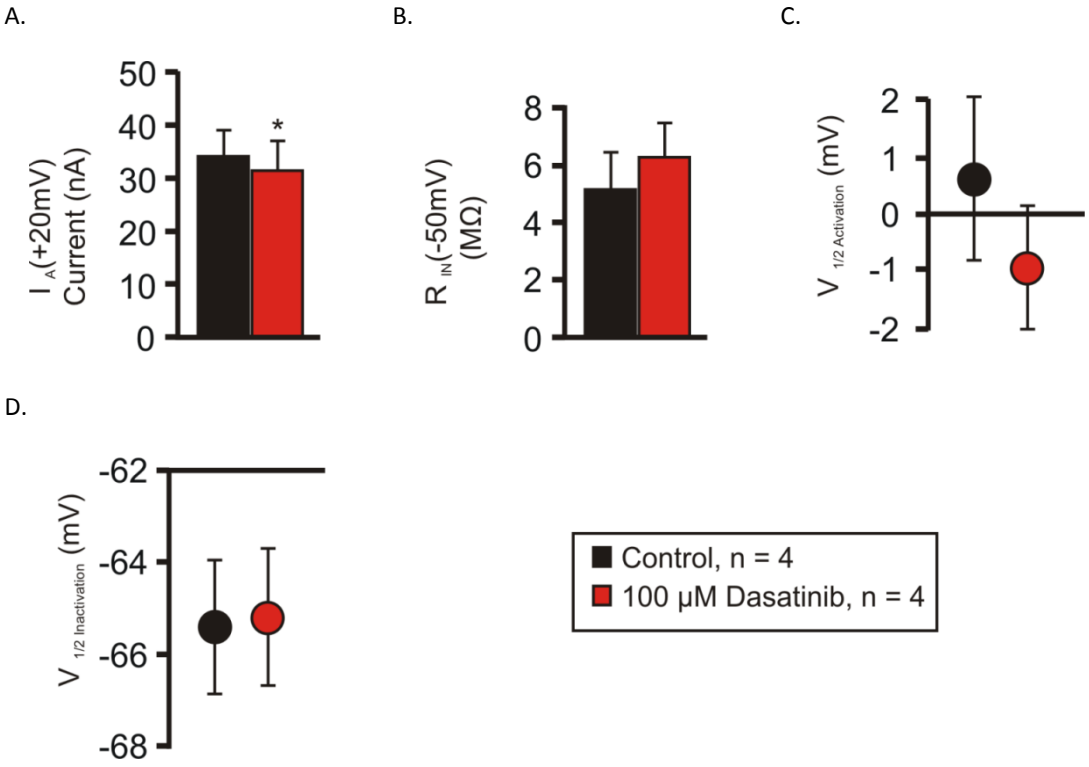


**Figure D3.5: The SFK Inhibitor Dasatinib Produces a Statistically Significant, but Biologically Insignificant Inhibition of $I_A$ at +20 mV.** 2 mM low calcium saline contained 0.1 μM TTX, 10 μM PTX, 200 μM $CdCl_2$, 5 mM CsCl and 20 mM TEA and was supplemented with 0.5% BSA. (A) A paired t-test showed that dasatinib significantly reduced $I_A$ at + 20 mV [t (3) = 5.200, p = 0.014.] (B) A paired t-test showed that dasatinib did not significantly reduce $R_{IN}$ at -50 mV [t (3) = -2.263, p = 0.452.] (C) A paired t-test showed that dasatinib did not significantly reduce $I_A$ $V_{1/2}$ activation. [t (3) = 1.315, p = 0.280.](D) A paired t-test showed that dasatinib did not significantly reduce $I_A$ $V_{1/2}$ inactivation. [t (3) = -0.565, p = 0.612.] Error bars are SEM. *. P < 0.05

## Appendix E: Effects of calmodulin (Cam) and Cam-activated inhibitors and activators.

*Calmidazolium depolarizes $V_{Rest}$ but does not change $I_A$ or $R_{IN}$.*

As illustrated in Figure E3.1, calmidazolium depolarized $V_{Rest}$ but did not affect either $I_A$ at + 20 mV or $R_{IN}$ at -50 mV [statistics in Figure E3.1]. As calmidazolium increased proctolin-induced $I_{MI}$ slope conductance, and, as it will be shown, so does the calmodulin inhibitor W7, this inhibitor was working in our system. Further, the agreement of the two inhibitors both acting to reduce proctolin-induced $I_{MI}$ voltage dependence, suggests that the voltage dependence effect is specific to calmodulin. This is because they both have very different chemical structures as one is a naphthasulfanamide (W7)(Inagaki et al., 1986), while the other is a more complicated molecule without the napthalene moeity[22] (Bruice, 2001). Presumably, it would be unlikely that these very different molecules produce the same non-specific effect.

[22] Naphtha moiety from Bruice (2001)
Calmidazolium structure from chemspider: [CSID:2435, http://www.chemspider.com/Chemical-Structure.2435.html (accessed 22:15, Apr 30, 2015)

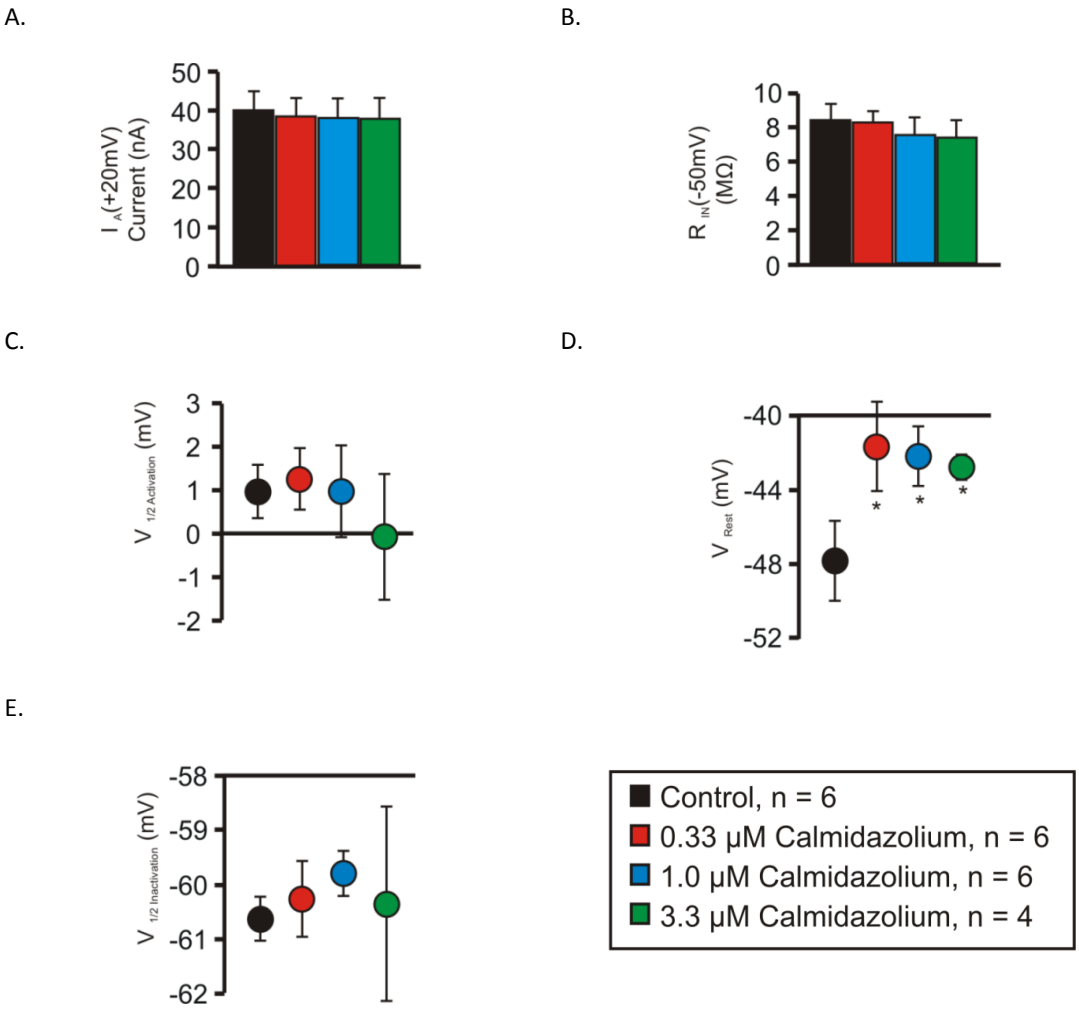


**Figure E3.1. The Calmodulin Inhibitor Calmidazolium Depolarizes $V_{Rest}$ but does not Affect $R_{IN}$ or $I_A$ in $I_{MI}$ Recording Saline.** Saline contained 0.1 μM TTX, 10 μM PTX, 200 μM $CdCl_2$, 5 mM CsCl and 20 mM TEA. 20 minute incubations in calmidazolium. (A)A one-way repeated measures ANOVA showed that calmidazolium did not affect $I_A$ at +20 mV [Calmidazolium; F (3, 13) = 1.450, p = 0.274] (B)A one-way repeated measures ANOVA showed that calmidazolium did not affect $R_{IN}$ at -50 mV [Calmidazolium; F (3, 13) = 0.382, p = 0.768] (C) A one-way repeated measures ANOVA showed that calmidazolium did not affect $I_A$ at $V_{1/2}$ activation [Calmidazolium; F (3, 13) = 0.102, p = 0.957] (D) A one-way repeated measures ANOVA showed that calmidazolium changed $V_{Rest}$ [Calmidazolium; F (3, 13) = 7.542, p = 0.004] (E) A one-way repeated measures ANOVA showed that calmidazolium did not change $I_A$ $V_{1/2}$ inactivation[Calmidazolium; F (3, 13) = 0.282, p = 0.838] Error bars are SEM. Tukey; *, p < 0.05.

*The ryanodine receptor antagonist dantrololene reduces $R_{IN}$ and $I_A$, but only at high concentrations.*

As illustrated in Figure E3.2, the ryanodine receptor antagonist dantrolene inhibited $I_A$ at + 20 mV and $R_{IN}$ at -50 mV but only at 33 µM.The inhibition of IA although statistically significant [Dantrolene; F (3, 11) = 5.811, p = 0.012.], as mentioned before is probably not biologically relevant due to its small dimunation. A post hoc Tukey test showed that mean $I_A$ at +20 mV was reduced from 45.7 ± 6.2 nA to 44.6 ± 7.0 nA in 33 µM dantrolene (p = 0.015). Due to our disbelief of being able to detect such a small effect, we scrutinized this data. This data was not transformed and passed equal variance test but failed normality testing. To ensure the result was not due to non-normally distributed results a rank transform was done. Rerunning the results on rank transformed data yielded the same result [Dantrolene; F (3, 11) = 6.304, p = 0.010.]. A post hoc Tukey test showed that mean rank score for $I_A$ at +20 mV was reduced from 10.2 ± 2.7 Rank (nA) to 9.5 ± 3.3 Rank (nA) in 33 µM dantrolene (p = 0.013). Although surprising that we could detect such a small finding, it is reiterated that the biological significance is questionable. Nevertheless, an effect was observed. Note that these concentrations are much higher than the 3.33 µM required to reduce proctolin-induced $I_{MI}$ voltage dependence and activation (Figure 3.24). This suggests that ryanodine was working in our system.

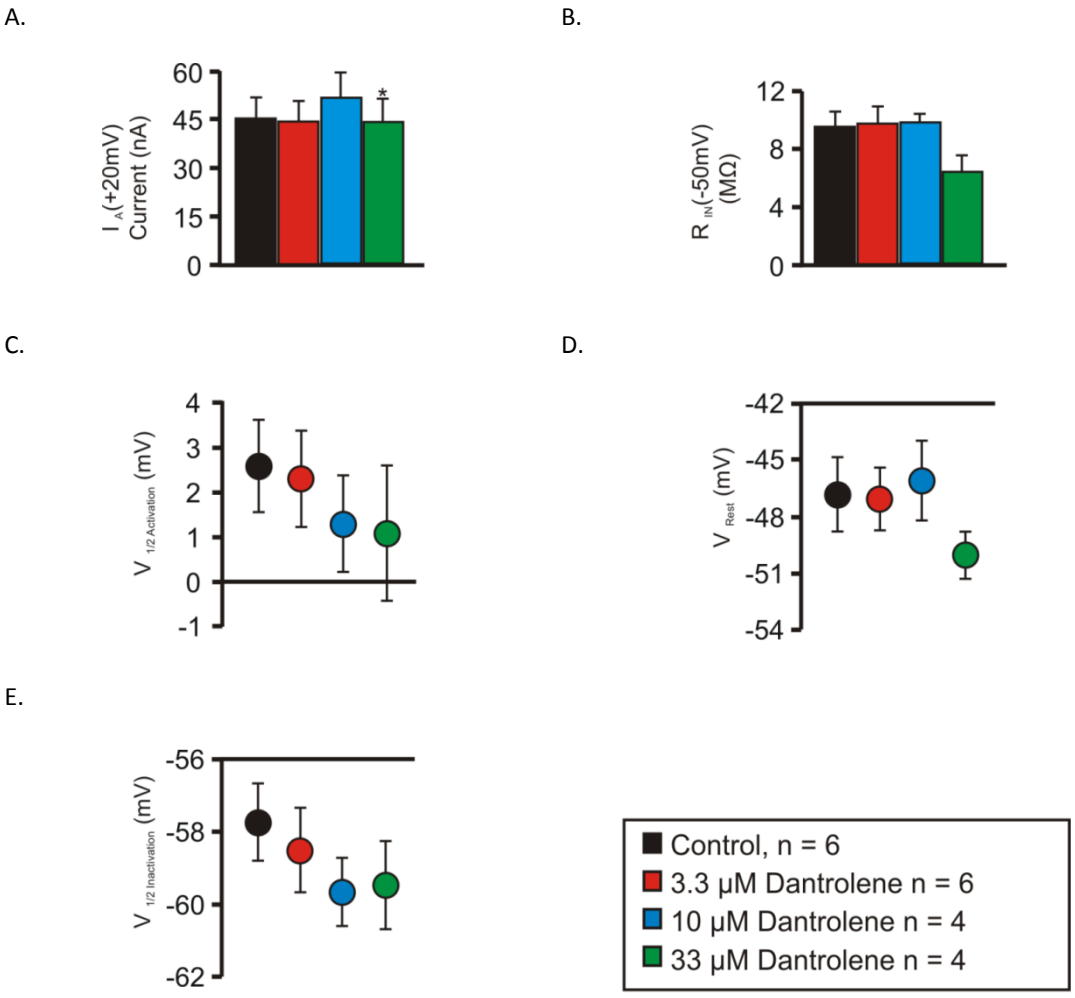


**Figure E3.2. The Ryanodine Receptor Antagonist Dantrolene Reduces IA and RIN at High Concentrations In $I_{MI}$ Recording Saline.** Saline contained 0.1 μM TTX, 10 μM PTX, 200 μM $CdCl_2$, 5 mM CsCl and 20 mM TEA. 20-45 minute incubation of Dantrolene.(A) A one-way repeated measures ANOVA showed that dantrolene reduced $I_A$ at +20 mV [Dantrolene; F (3, 11) = 5.811, p = 0.012.] (B) A one-way repeated measures ANOVA showed that dantrolene reduced $R_{IN}$ at -50 mV [Dantrolene; F (3, 11) = 4.324, p = 0.03.] (Tukey tests could not distinguish means.) (C) A one-way repeated measures ANOVA showed that dantrolene did not affect $I_A$ $V_{1/2}$ activation [Dantrolene; F (3, 11) = 0.712, p = 0.565.](D) A one-way repeated measures ANOVA showed that dantrolene did not affect $V_{Rest}$ [Dantrolene; F (3, 11) = 1.770, p = 0.211.] (E) A one-way repeated measures ANOVA showed that dantrolene did not affect $I_A$ $V_{1/2}$ inactivation [Dantrolene; F (3, 11) = 0.500, p = 0.690.] Error bars are SEM. Tukey; *, $p < 0.05$.

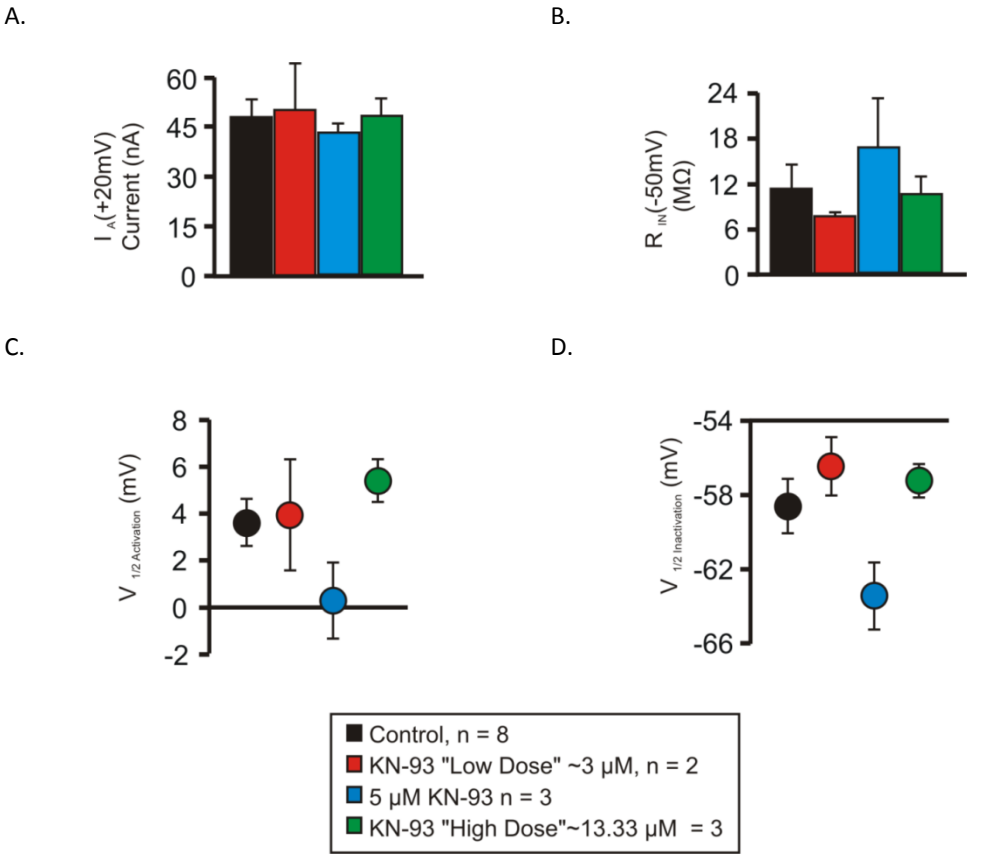


**Figure E3.3. The CamKII Inhibitor KN-93 Affects $R_{IN}$ Nonlinearly but does Not Affect $I_A$ in $I_{MI}$ Recording Saline.** Saline contained 0.1 μM TTX, 10 μM PTX, 200 μM CdCl2, 5 mM CsCl and 20 mM TEA. 20 minute incubation of KN-93. Preps were grouped into low dose and high dose conditions for statistical analyses. 'Low Dose' contains one prep at 2μM and one at 4μM KN-93. 'High Dose' contains 2 preps at 10 μM and one at 20μM KN-93.(A) A one-way repeated measures showed that KN-93 had no effect on $I_A$ at +20 mV [KN-93; F (3, 5) = 1.416, p = 0.341.] (B) A one-way repeated measures showed that KN-93 had a nonlinear effect on $R_{IN}$ at -50 mV [KN-93; F (3, 5) = 5.538, p = 0.048.]Tukey test did not distinguish means.(C) A one-way repeated measures showed that KN-93 had no effect on $I_A$ $V_{1/2}$ activation [KN-93; F (3, 5) = 0.490, p = 0.705.](D) A one-way repeated measures showed that KN-93 had no effect on $I_A$ $V_{1/2}$ inactivation [KN-93; F (3, 5) = 0. 0.432, p = 0.740.]Error bars are SEM.

*KN-93 produces a nonlinear change in $R_{IN}$ when applied directly but does not affect $I_A$.*

As illustrated in Figure E3.3, KN-93 produced a nonlinear response on $R_{IN}$. The sample number was too low to distinguish individual means, but due to the inconsistency of the effect it is hard to interpret whether this is meaningful. The effect on $I_{MI}$ voltage dependence and proctolin-induced $I_{MI}$ suggests that KN-93 worked in this system with acute applications.

*Overnight Incubations in 20 µM KN-93 do not affect transient or steady state $I_{HTK}$, $I_A$, $R_{IN}$, or $V_{Rest}$.*

As illustrated in Figures E3.4 and E3.5, overnight incubations in 20 µM KN-93, had no significant effects on both transient and steady state $I_{HTK}$, activation and inactivation of $I_A$, $R_{IN}$ at -50 mV, or $V_{REST}$; both in TTX (E3.4); and in $I_{MI}$ recording saline (E3.5). The only negative result we are hesitant to claim no effect for, is for $I_A$ inactivation. This is because although this did not meet our criterion for statistical significance, its p value of 0.057, coupled with the low sample number of these experiments, may suggest a smaller effect that this study is not concerned with. The finding that KN-93 incubations significantly affected proctolin-induced $I_{MI}$ suggests that KN-93 was working. Whether it was working specifically can be tested with application of the inactive isoform KN-92 as a control for nonspecific effects (not performed here).

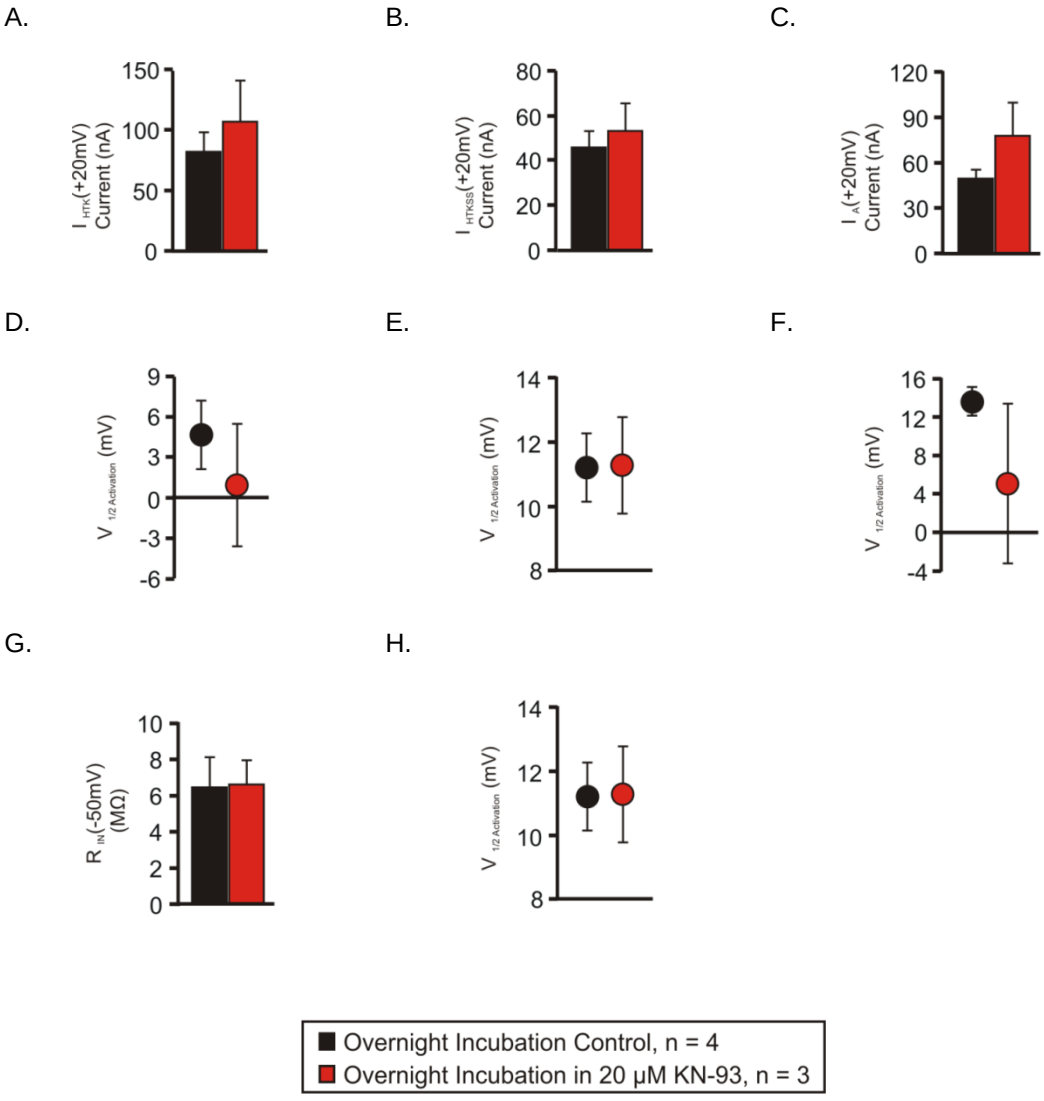


**Figure E3.4. The CamKII Inhibitor KN-93 does not Significantly Change Transient $I_{HTK}$, Steady State $I_{HTK}$, $I_A$, $R_{IN}$ or $V_{Rest}$ with Overnight Incubation.** Preps were incubated in *Cancer* saline (**Black**) or 20 μM KN-93 (**Red**) in *Cancer* saline. Currents measured in 0.1 μM TTX. (A) A t-test showed KN-93 was not significantly different from incubation control for transient $I_{HTK}$ at +20 mV [t (5) = 0.737. p = 0.494]. (B) A t-test showed KN-93 was not significantly different from incubation control for steady state $I_{HTK}$ at +20 mV [t (5) = 0.544. p = 0.610]. (C) A t-test showed KN-93 was not significantly different from incubation control for $I_A$ at +20 mV [t (5) = 1.441. p = 0.209]. (D) A t-test showed that KN-93 did not significantly shift transient $I_{HTK}$ $V_{1/2}$ activation [t (5) = -0.770. p = 0.476]. (E) A t-test showed that KN-93 did not significantly shift steady state $I_{HTK}$ $V_{1/2}$ activation [t (5) = 0.0385. p = 0.973]. (F) A t-test showed that KN-93 did not significantly shift steady state $I_A$ $V_{1/2}$ activation [t (5) = -1.187, p = 0.289]. (G) A t-test showed that KN-93 did not significantly change $R_{IN}$ at -50 mV [t (5) = 0.0756, p = 0.943]. (H) A t-test showed that KN-93 did

not significantly change $V_{Rest}$ [t (5) = -0.325, p = 0.759].Error bars are SEM.

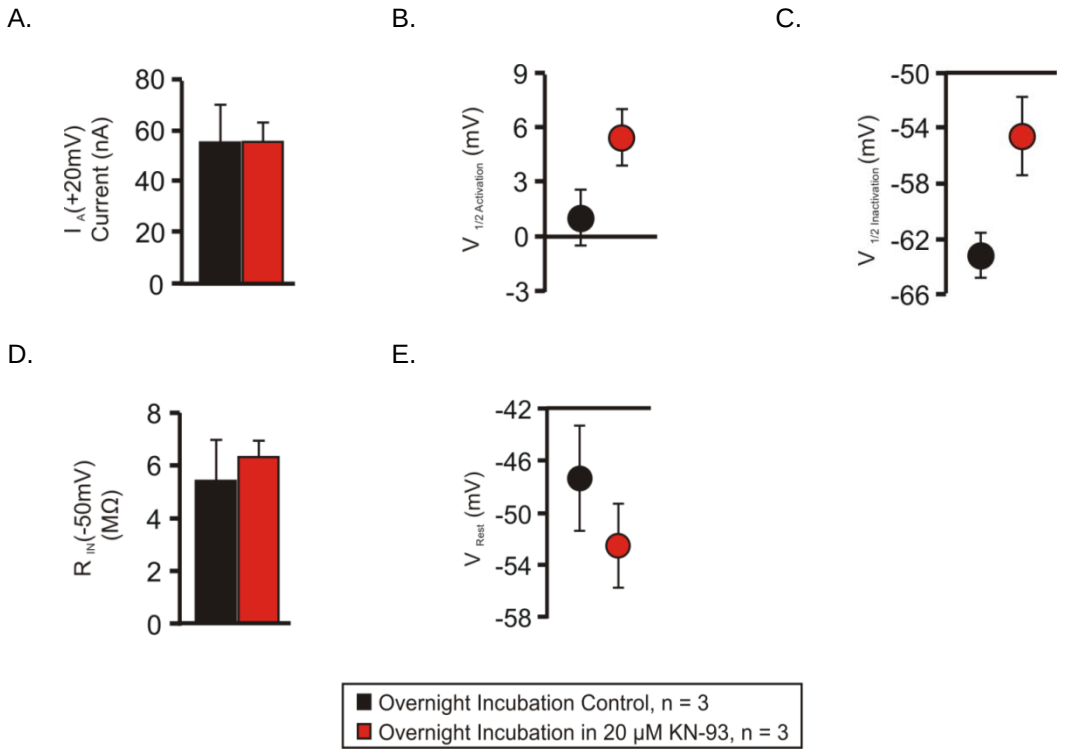


**Figure E3.5. Overnight Incubation in the CamKII inhibitor KN-93 does not Affect $I_A$, $R_{IN}$ or $V_{Rest}$ in $I_{MI}$ Recording Saline.** Preps were incubated in *Cancer* saline (**Black**) or 20 µM KN-93 (**Red**) in *Cancer* saline. Currents measured in 0.1 µM TTX, 10 µM PTX, 200 µM CdCl2, 5 mM CsCl and 20 mM TEA.(A) A t-test showed that KN-93 had no effect on $I_A$ at +20 mV [t (4) = 0.0238, p = 0.982.] .(B) A t-test showed that KN-93 had no effect on $I_A$ $V_{1/2}$ activation [t (4) = 2.008 , p = 0.115.] (C) A t-test showed that KN-93 had no effect on $I_A$ $V_{1/2}$ Inactivation [t(4) = 2.655 , p = 0.057.] (D) A t-test showed that KN-93 had no effect on $R_{IN}$ at -50 mV [t (4) = 0.560, p = 0.605.] (E) A t-test showed that KN-93 had no effect on $V_{Rest}$ [t (4) = -1.005, p = 0.372.] Error bars are SEM.

*The MLCK inhibitor ML-7 reduces $I_A$ by reducing maximal conductance and hyperpolarizing $V_{1/2}$ inactivation.*

As illustrated in Figure E3.6, increasing concentrations of ML-7 reduced $I_A$ at +20 mV, $I_A$ maximal conductance and hyperpolarized $I_A$ inactivation. This means that not only is the maximal current increased, but for the same voltage, less of this current will be available as it is inactivated due to the hyperpolarization of $V_{1/2}$ inactivation. These results, combined with the findings that ML-7 altered proctolin-induced $I_{MI}$ voltage dependence and amplitude at -15 mV suggests that ML-7 was active in these experiments.

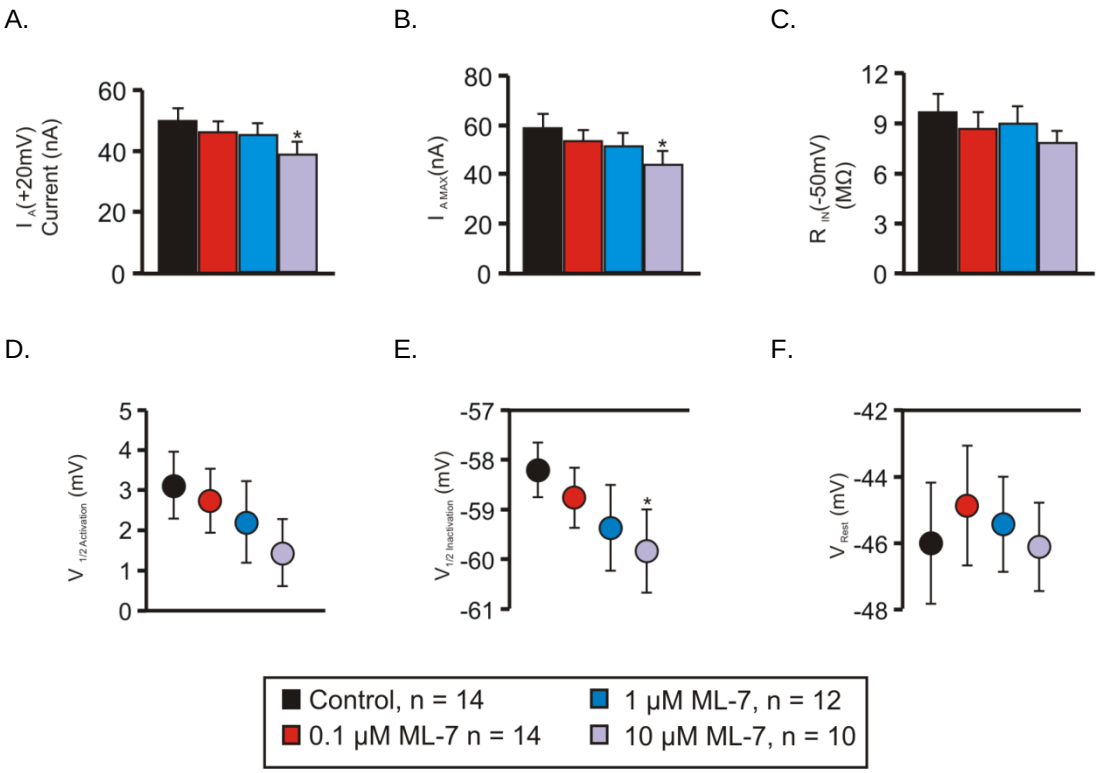


**Figure E3.6. The MLCK Inhibitor ML-7 Reduces $I_A$ by Reducing Maximal Conductance and Hyperpolarizing $I_A$ Inactivation.** Saline Contained 0.1 μM TTX, 10 μM PTX, 200 μM $CdCl_2$, 5 mM CsCl and 20 mM TEA. 20-50 minute incubations in ML-7. (A) A one-way repeated measures ANOVA showed that ML-7 significantly reduced $I_A$ at +20 mV [ML-7; F (3, 33) = 4.944, p = 0.006.] (B) A one-way repeated measures ANOVA showed that ML-7 significantly reduced $I_A$ maximum [ML-7; F (3, 33) = 5.285, p = 0.004.] (C) A one-way repeated measures ANOVA showed that ML-7 did not significantly alter $R_{IN}$ at -50mV [ML-7; F (3, 33) = 2.545, p = 0.073.] (D) A one-way repeated measures ANOVA showed that ML-7 did not significantly alter $I_A$ $V_{1/2}$ activation [ML-7; F (3, 33) = 1.683, p = 0.190.] (E) A one-way repeated measures ANOVA showed that ML-7 significantly altered $I_A$ $V_{1/2}$ inactivation [ML-7; F (3, 33) = 5.552, p = 0.003.] (F) A one-way repeated measures ANOVA showed that ML-7 did not significantly alter $V_{Rest}$ [ML-7; F (3, 33) = 0.747, p = 0.532.] Error bars are SEM. Tukey test; *, $p < 0.05$.

# Chapter 4: $I_{MI}$ Voltage Dependence

## 4.1 Introduction

In this chapter, we address the mechanism of neuromodulator-induced $I_{MI}$ voltage dependence that is dependent on extracellular calcium. We first examine the results of Golowasch and Marder (1992) who showed that at a holding potential of -40 mV divalent ions produce inhibition of proctolin-induced $I_{MI}$. We wish to determine whether this block is voltage dependent or voltage independent, as a voltage dependent block would support an NMDA-like mechanism of voltage dependence (Golowasch and Marder, 1992b). We then hypothesize that the observed augmentation of neuromodulator-induced $I_{MI}$ by W7 as shown by Swensen and Marder (2000) is consistent with a reduction in voltage dependence. We demonstrate that this is similar to the loss observed when extracellular calcium is reduced. This is demonstrated by applying various calmodulin inhibitors and showing that they increase proctolin-induced $I_{MI}$ slope (i.e. reduce voltage dependence) which in turn suggests a dependence on intracellular calcium. In order to confirm the hypothesis that $I_{MI}$ voltage dependence relies upon internal calcium signaling, we attempt to rescue voltage dependence by application of calmodulin agonists in the presence of low calcium. We then examine the role of calmodulin-activated proteins in an attempt to determine whether these downstream targets of calmodulin are responsible for $I_{MI}$ voltage dependence. Finally,

upon failure of calmodulin activators to rescue voltage dependence in the presence of low calcium, we propose the calcium sensitive receptor (CaSR) hypothesis (hypothesis two of Chapter 1). We support this hypothesis by four lines of evidence. First, we show that the CaSR antagonist NPS-2143 increases proctolin-induced $I_{MI}$ slope. Second, we show G-proteins are involved with proctolin-induced $I_{MI}$ voltage dependence. Third, we determine that signaling pathways, suspected of being downstream of CaSR, appear to modulate proctolin and CCAP-induced $I_{MI}$. Fourth, we show that W7-induced linearization of CCAP-induced $I_{MI}$ is prevented by preincubation in endocytosis inhibitors.

## 4.2 Divalents Block Proctolin-induced $I_{MI}$ Uniformly and Do not Restore Proctolin-induced $I_{MI}$ Voltage Dependence.

Golowasch and Marder (1992) demonstrated that with a holding potential of -40 mV, certain divalents could inhibit proctolin-induced $I_{MI}$. We wanted to determine whether this inhibition was voltage dependent. If this were true, it could represent restoration of voltage dependence and therefore support the NMDA hypothesis. We measured proctolin-induced $I_{MI}$ in low calcium and different concentrations of $Ba^{++}$. We predicted that if proctolin-induced $I_{MI}$'s voltage dependence was based on an NMDA-like mechanism, then we should observe a voltage dependent block. This should restore proctolin-induced $I_{MI}$ slope to negative values. If there were not an NMDA-like mechanism, we predicted that the block would be voltage independent. Slope should also decrease but is not expected to 'overshoot' and become negative. Most importantly, this decrease should be uniform (voltage-independent). Therefore, any sign of negative slope in 1 mM $Ca^{++}$ would support an NMDA-like mechanism. To be consistent with this paper, we quantified proctolin-induced $I_{MI}$ at -40 mV for the divalents tested. Note that for reasons previously discussed, we suggest that proctolin-induced $I_{MI}$ voltage dependence and amplitude are not independent at this voltage.

*$Ba^{++}$ does not produce voltage dependent block in one mM low $Ca^{++}$ saline*.

As illustrated in Figure 4.1, 10 mM $Ba^{++}$ was capable of reducing proctolin-induced $I_{MI}$ at -40 mV. Note that for 10 mM, this block by $Ba^{++}$ is independent of voltage.

Although the IV-relation is somewhat curvilinear, there is no sign of negative slope being restored at 10 mM $Ba^{++}$. A one-way ANOVA, with covariate application number, showed that $Ba^{++}$ did not alter proctolin-induced $I_{MI}$ slope [$Ba^{++}$; F (2, 10) = 1.543, p = 0.261. Application number; F (1, 10) = 3.955, p = 0.075]. Note that the p value for application number is much lower than that for $Ba^{++}$. This means that in this particular set of experiments any of this 'curviness' would have to be attributed first to chance, then to application number, and then to $Ba^{++}$. A one-way ANOVA for $Ba^{++}$ with covariate application number showed that $Ba^{++}$ inhibited proctolin-induced $I_{MI}$ amplitude at -40 mV [$Ba^{++}$ ; F (2, 10) = 4.164, p = 0.048. Application number; F (1, 10) = 12.694, p = 0.005.]. Again, the effect for application number is much bigger than the effect for $Ba^{++}$. This data suggests that $Ba^{++}$ blocks proctolin-induced $I_{MI}$ in a voltage independent manner. Similar results were observed for $Co^{++}$, and $Mn^{++}$, however, not enough data was collected from these experiments to adjust them statistically for application number in low calcium; they were therefore omitted.

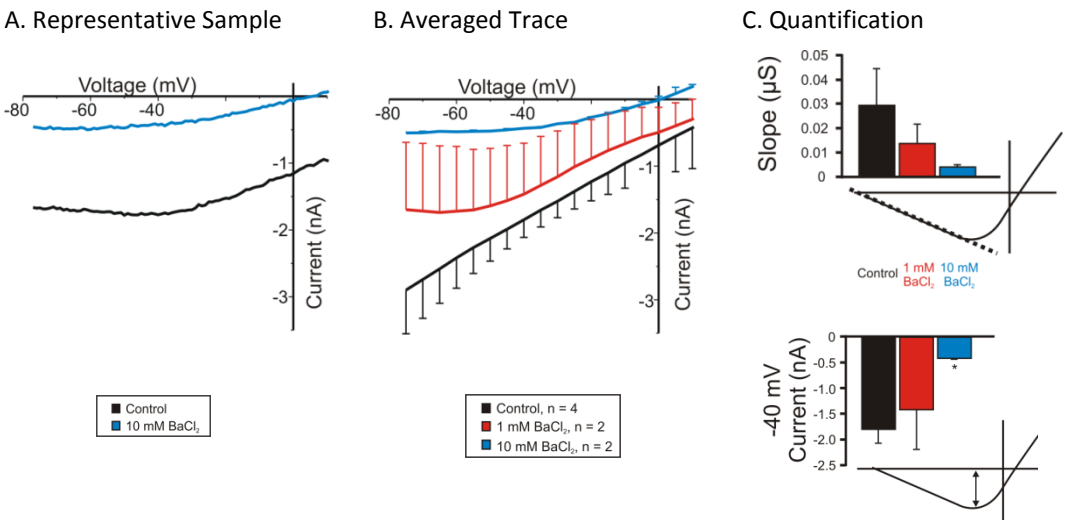


**Figure 4.1. $Ba^{++}$ Inhibits Proctolin-induced $I_{MI}$ Amplitude at -40 mV but does Not Affect Slope.** 1 mM low calcium saline contained 0.1 µM TTX, 10 µM PTX, 200 µM $CdCl_2$, 5 mM CsCl and 20 mM TEA. This experiment had no BSA. Proctolin-induced $I_{MI}$ in different concentrations of $Ba^{++}$.Note that amplitude was quantified at -40 mV and not -15 mV.(A) Representative IV curve of $Ba^{++}$ experiment.(B) Averaged IV curves of proctolin-induced $I_{MI}$ for $Ba^{++}$ experiments. Average application number for traces is 3.5.(C) A one way ANOVA for $Ba^{++}$ with covariate application number showed that $Ba^{++}$ did not alter proctolin-induced $I_{MI}$ slope [$Ba^{++}$ ; $F(2, 10) = 1.543$, $p = 0.261$. Application number; $F(1, 10) = 3.955$, $p = 0.075$] (D) A one way ANOVA for $Ba^{++}$ with covariate application number showed that $Ba^{++}$ inhibited proctolin-induced $I_{MI}$ amplitude at -40 mV [$Ba^{++}$ ; $F(2, 10) = 4.164$, $p = 0.048$. Application number; $F(1, 10) = 12.694$, $p = 0.005$.] Error bars are SEM. Tukey test; *, $p < 0.05$.

## 4.3 Calmodulin inhibitors Reduce $I_{MI}$ voltage dependence

*The calmodulin inhibitor W7 increased neuromodulator-induced $I_{MI}$ slope*

Swensen and Marder (2000) showed that W7 increases the amplitude of $I_{MI}$, but that this effect was stronger at hyperpolarized voltages. We therefore originally interpreted this as consistent with calmodulin mediating neuromodulator-induced $I_{MI}$ voltage dependence. As calmodulin is a calcium sensor, we hypothesized that in low extracellular calcium, a smaller inward flux of calcium leads to less available activated calmodulin. In this state, we assumed a reduction of voltage dependence and therefore a more linear IV relation would result. When extracellular calcium was raised, there would be an increase in activated calmodulin. This activated calmodulin would interact with channels mediating $I_{MI}$ itself, or through activation of calmodulin-activated proteins, switch $I_{MI}$ from a linear to a voltage dependent current. Therefore, we predicted that voltage ramps in the presence of calmodulin inhibitors should increase proctolin-induced $I_{MI}$ slope, or equivalently reduce voltage dependence. As shown in Figure 4.2, a one-way repeated measures ANOVA showed that increasing concentrations of W7 increased proctolin-induced $I_{MI}$ slope. [W7; $F(4, 19) = 15.972$, $p = 6.96 \times 10^{-6}$.] Application of W7 increased proctolin-induced $I_{MI}$ slope from -0.0217±0.00374 µS (SEM; n = 12) in control to 0.0131± 0.00417 in 100 µM of W7[23]. This suggested that our hypothesis was correct and that calmodulin was somehow mediating

[23] As shown in figure 4.2C, this result was obtained in step protocols as well (n = 2) suggesting this was not an artifact of protocol used.

proctolin-induced $I_{MI}$ voltage dependence. A small but significant diminution of proctolin-induced $I_{MI}$ at -15 mV was observed 10 µM W7 [W7; F (4, 19) = 3.243, p = 0.035.], consistent with the observations on CaM-dependent mechanisms described in chapter thee.

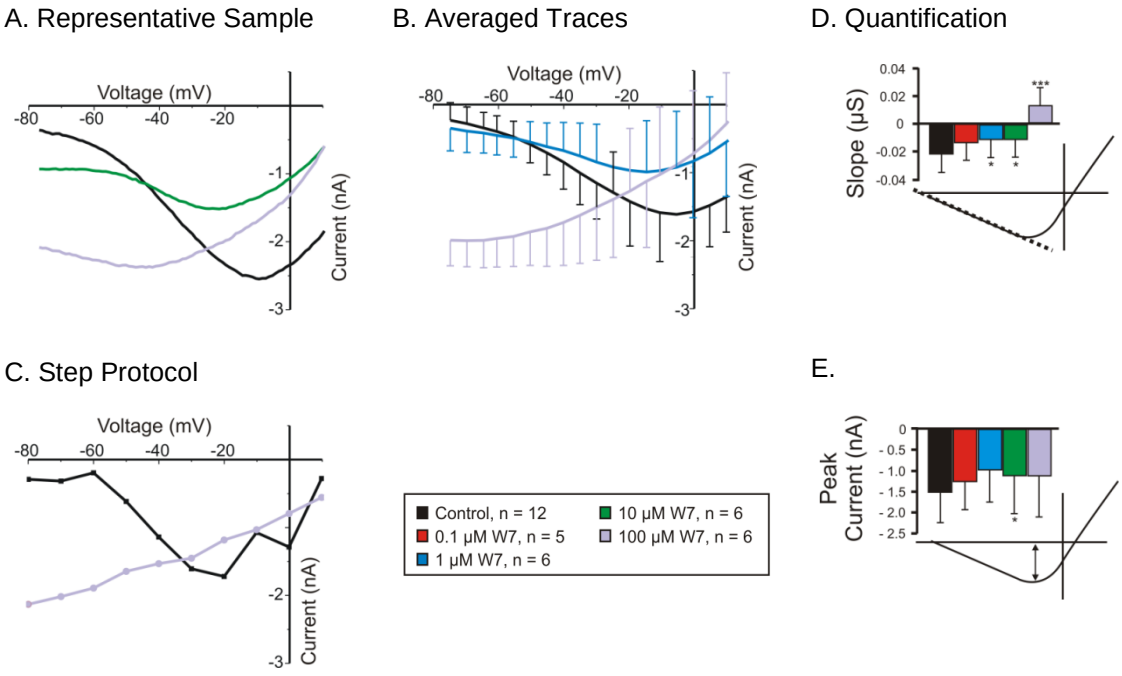


**Figure 4.2. The Calmodulin Inhibitor W7 Increases Proctolin-induced $I_{MI}$ Slope.** Saline contained 0.1 µM TTX, 10 µM PTX, 200 µM $CdCl_2$, 5 mM CsCl and 20 mM TEA. Proctolin-induced $I_{MI}$ in different concentrations of W7.(A) Representative IV curves of a W7 experiment. (B) Averaged IV curves across W7 experiments. (C) W7 experiment where a step protocol was used instead of a ramp protocol. Note the same result is obtained. (D) Quantification of W7 data shown in B. A one-way repeated measures ANOVA showed that W7 changed proctolin-induced $I_{MI}$ slope [W7; F (4, 19) = 15.972, p = 6.96 x $10^{-6}$.] (E). A one-way repeated measures ANOVA showed that W7 changed proctolin-induced $I_{MI}$ amplitude at -15 mV [W7; F (4, 19) = 3.243, p = 0.035.] Error bars are SEM. Tukey test; *, p < 0.05; ***, p < 0.001.

Upon establishing the effect of W7 on proctolin-induced $I_{MI}$, we sought to determine if the effect of W7-induced reduction in voltage dependence was generalizable to other neuromodulators, so we examined the effect of W7 on CCAP-induced $I_{MI}$ slope. As illustrated in Figure 4.3, a paired t-test showed that W7 significantly increased CCAP-induced $I_{MI}$ slope from -0.0131 ± 0.0030 µS in control to -0.0030 ± 0.003 µS in 33.3 µM of W7 [t (5) = -2.625, p = 0.047]. In this experiment, a paired t-test showed that W7 had no effect on CCAP-induced $I_{MI}$ amplitude at -15 mV [t (5) = -0.435, p = 0.681.] Together, these results suggested to us a model for $I_{MI}$ voltage dependence based on activated calmodulin. In this model, calcium activated calmodulin mediates $I_{MI}$ voltage dependence. Therefore, when extracellular calcium is reduced there is less calcium influx to the cell. Less calcium influx results in less activated calmodulin, which in turn leads to less voltage dependence.

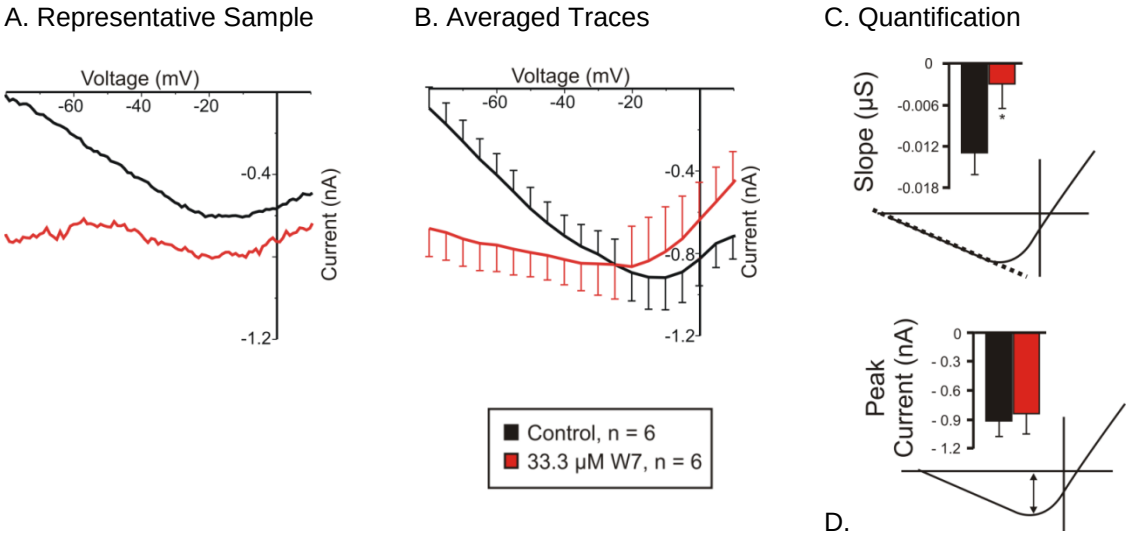


**Figure 4.3.The Calmodulin Inhibitor W7 Also Increases CCAP-Induced $I_{MI}$ Slope.** Saline contained 0.1 µM TTX, 10 µM PTX, 200 µM $CdCl_2$, 5 mM CsCl and 20 mM TEA. CCAP-induced $I_{MI}$ in absence (**Black**) or presence (**Red**) of 33.3 µM W7. (A) Representative IV curves of a W7 experiment. (B) Averaged IV curves for CCAP-induced $I_{MI}$ experiments in W7. (C) A paired t-test showed that W7 significantly increased CCAP-induced $I_{MI}$ slope [t (5) = -2.625, p = 0.047.] . (D) A paired t-test showed that W7 did not affect CCAP-induced $I_{MI}$ amplitude at -15 mV [t (5) = -0.435, p = 0.681.]. Error bars are SEM. *, p < 0.05.

*Confirmation of calmodulin's involvement in proctolin-induced $I_{MI}$ voltage dependence.*

As briefly alluded to in Chapter 3, we wanted to confirm the involvement of calmodulin on $I_{MI}$ voltage dependence using a variety of pharmacological inhibitors. This is because it has been shown that many pharmacological inhibitors can have nonspecific effects that have nothing to do with the pharmacological activity for which they are intended. Previously mentioned examples include 'specific' inhibitors such as H89 (Davies et al., 2000) and KN-93 (Rezazadeh et al., 2006). Therefore, we searched for

calmodulin inhibitors that were as different in chemical structure from W7 as possible. As W7 is a naphthasulfonamide (Inagaki et al., 1986), this eliminated inhibitors such as A3, A7, W9, W13 etc. We had had some confusion as to whether some membrane permeable peptide inhibitors were working as they did not produce any positive results in the past (CALP1, see below). Thus, our preference was not to use agents with large molecular weights such as CALP3. We tried the antipsychotic fluphenazine, a calmodulin antagonist that has been used with some success in crayfish (Sedlmeier and Dieberg, 1983). Unfortunately, this left cells depolarized and leaky, even at concentrations way below those required for calmodulin inhibition[24]. This left us with calmidazolium. As illustrated in Figure 3.23 & 4.4, calmidazolium both reduced proctolin-induced $I_{MI}$ (Chapter 3) and significantly increased proctolin-induced $I_{MI}$ slope [Calmidazolium; $F(3, 9) = 5.244$, $p = 0.023$]. Although the sample number was not high enough to distinguish individual means, the trend is clear and is in agreement with the finding from the previously mentioned W7 experiments. This experiment confirms that calmodulin inhibition increases proctolin-induced $I_{MI}$ slope. Also, notice that this cannot be explained simply by inhibition, where one would expect slope to drop to zero. Instead, as illustrated in Figure 4.4, slope actually goes from negative to positive, suggesting that this is different from a pure reduction in amplitude which would stop at 0 µS. This data, together with the W7 results, suggests that both of these molecules are mediating their

[24] Multiple cells and not just LP seemed to die around 100 µM of fluphenazine (n = 3).We were attempting to reach 1000 µM as shown in crayfish by Sedlmeier and Dieberg (1983). We therefore abandoned this approach.

effect on neuromodulator-induced $I_{MI}$ voltage dependence through the inhibition of calmodulin. The effects of these calmodulin inhibitors on voltage dependence are unlikely to be nonspecific, as they do not share the same chemical structure yet produce the same effect on voltage dependence.

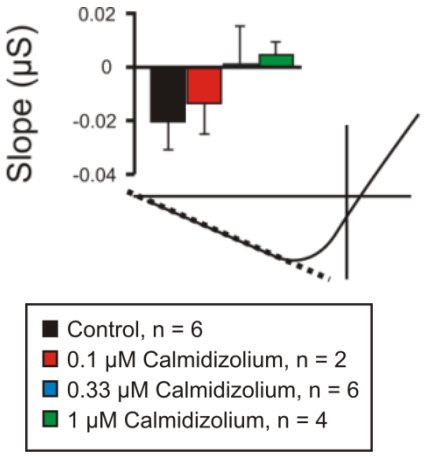


**Figure 4.4: The Calmodulin Inhibitor Calmidazolium Increases Proctolin-induced $I_{MI}$ Slope.** Saline contained 0.1 µM TTX, 10 µM PTX, 200 µM $CdCl_2$, 5 mM CsCl and 20 mM TEA. Slope conductance of proctolin-induced $I_{MI}$ in different concentrations of Calmidazolium. A one-way repeated measures ANOVA showed that calmidazolium was capable of increasing proctolin-induced $I_{MI}$ slope [Calmidazolium; $F(3, 9) = 5.244$, $p = 0.023$].

*The calcium chelator BAPTA-AM does not affect proctolin-induced $I_{MI}$ slope or amplitude.*

In order to test the hypothesis that calmodulin switched proctolin-induced $I_{MI}$ from a linear to a voltage dependent state, we tested the membrane permeable calcium chelator BAPTA-AM. We predicted that intracellular calcium chelation should leave less activated calmodulin. Less activated calmodulin in turn should lead to a reduction in voltage dependence for proctolin-induced $I_{MI}$, specifically, it should increase measured proctolin-induced $I_{MI}$ slope. Figure 4.5 shows that 30 µM of the BAPTA-AM, a concentration shown to work in the cardiac ganglion of *Cancer borealis* (Ransdell et al.,

2012)[25], was unable to alter proctolin-induced $I_{MI}$ slope [t (2) = 0.943, p = 0.445.]. Similarly, a paired t-test showed that BAPTA-AM had no effect on proctolin-induced $I_{MI}$ amplitude [t (2) = -0.419, p = 0.716]. These experiments were done at higher and lower concentrations, but due to low replications for this (n = 1 for 10, 50 and 100), and the following BAPTA-AM incubation experiments, these experiments were not included in the statistical analysis. From our observations with some of the higher concentrations, there could be a non-significant reduction on proctolin-induced amplitude, but in none of these experiments was an increase in proctolin-induced $I_{MI}$ slope observed. These results were in direct conflict with our hypothesis that the reduction of voltage dependence, induced by reduction in extracellular calcium, is mediated by a reduction in active calmodulin.

[25] Randsell et al, (2012) show that while transient $I_{HTK}$ is unresponsive to BAPTA-AM, a phenomenon where application of the $I_A$ blocker 4-AP increases measured transient $I_{HTK}$ is blocked by preincubation in BAPTA-AM.

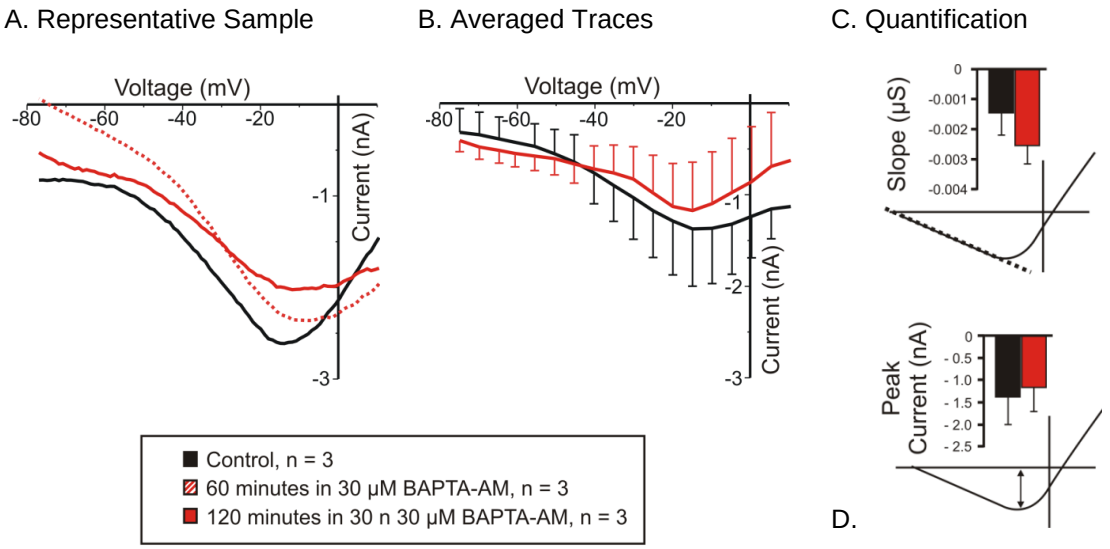


**Figure 4.5. The Membrane Permeable Calcium Chelator BAPTA-AM does Not Alter Proctolin-induced $I_{MI}$ Amplitude or Voltage Dependence.** Saline contained 0.1 µM TTX, 10 µM PTX, 200 µM $CdCl_2$, 5 mM CsCl and 20 mM TEA. Proctolin-induced $I_{MI}$ in absence (**Black**) or presence (**Red**) of 30 µM BAPTA-AM. Data was quantified after 2 hours of incubation in BAPTA-AM. (A) Representative IV curves of a BAPTA-AM experiment. (B) Averaged IV curves of BAPTA-AM experiments. (C) A paired t-test showed that BAPTA-AM had no effect on proctolin-induced $I_{MI}$ slope [t (2) = 0.943, p = 0.445.] (D) A paired t-test showed that BAPTA-AM had no effect on proctolin-induced $I_{MI}$ amplitude at -15 mV [t (2) = -0.419, p = 0.716.] Error bars are SEM.

*Overnight incubation in BAPTA-AM does not affect proctolin-induced $I_{MI}$ slope.*

As we could not be certain that BAPTA-AM was permeating the membrane, we needed either a positive control or a means of ensuring that enough time had passed so that BAPTA-AM could permeate the cell membrane. We thought a good positive control would be to look for a reduction of the transient $I_{HTK}$. The majority of this current is a calcium-dependent potassium current that is dependent on other calcium currents (Golowasch and Marder, 1992a). However, counterintuitively, it has been shown that, in

the *Cancer borealis* cardiac ganglion, this current is insensitive to BAPTA-AM (Ransdell et al., 2012). We decided to try overnight incubations in BAPTA-AM to ensure that the calcium chelator had enough time to permeate the membrane. This experiment is illustrated in Figure 4.6. A two-way ANOVA for application number and BAPTA-AM showed that application number, but not BAPTA-AM was capable of altering proctolin-induced $I_{MI}$ slope [BAPTA-AM; $F(2, 17) = 0.983$, $p = 0.342$. Application number; $F(1, 17) = 6.690$, $p = 0.019$.]. Similarly, it was found that BAPTA-AM did not alter proctolin-induced $I_{MI}$ amplitude at -15 mV [BAPTA-AM; $F(2, 17) = 0.242$, $p = 0.788$. Application number; $F(1, 17) = 4.820$, $p = 0.042$.]. It is possible that the effect of BAPTA-AM is too small to detect with the limited sample number used, or that the concentration of BAPTA-AM was not effectively chelating calcium. Although not meeting our criterion for statistical significance, a Tukey test showed that within application 1, there was p of 0.098, for 100 µM of BAPTA-AM vs control for proctolin-induced $I_{MI}$ slope. This suggests that we could see results at higher concentrations of BAPTA-AM. Unfortunately, however, we have observed precipitation of BAPTA-AM at concentrations above 50 µM. This suggests that raising concentrations further would be of little use due to BAPTA-AM precipitation in our high salinity solutions. The only alternative would be to increase the sample number massively in the 100 µM condition. It is therefore believed that this method of study is unreasonable without finding a way to prevent BAPTA-AM precipitation and therefore test higher concentrations. Future work should consider direct pressure injection of the non-ester form of BAPTA, which, although much more

technically demanding, in addition to its enhanced solubility may also reap the benefit of producing more localized calcium chelation[26]. Since these experiments were incubated overnight, if BAPTA-AM could not permeate in this period, it would seem that no amount of time would be enough for BAPTA-AM to permeate the cell membrane. These data are consistent with the findings for two-hour applications of BAPTA-AM, but do not support the hypothesis that a calcium dependent pathway is mediating the loss in voltage dependence in low external calcium.

[26] Injection of BAPTA has shown to modulate calcium responses in the STG before but it is unclear whether this was completely effective. For example, Levi and Selverston (1991) show in LG/MG neurons that oscillation period is increased by BAPTA injection but frequency is counterintuitively unaffected.The authors also claim this is due to a reduction in calcium-dependent potassium current but never measure this directly. Similarly Zhang et al., (1995) show that EGTA injections appear to stop fast oscillatory activity but not slow oscillatory activity, but do not statistically quantify this. While Levi and Selverston (1991) cite Zhang et al., (1995) to support this claim, this citation is misleading as Zhang et al., (1995) never show direct evidence to support this with BAPTA injection itself, and only show this through indirect literature precedent and in the context of the finding that photolysis of caged calcium induces fast oscillatory activity. These studies never tested BAPTA and caged-calcium directly together and are in conflict with the findings of this thesis and Randsell et al., (2012) where $I_{HTK}$ was directly measured. As all of these studies at best show that some physiological activity can be modulated by BAPTA, but at worst demonstrate the persistence of calcium associated activity in this system (Transient $I_{HTK}$), it is difficult to determine the efficacy of this agent without calcium imaging studies.

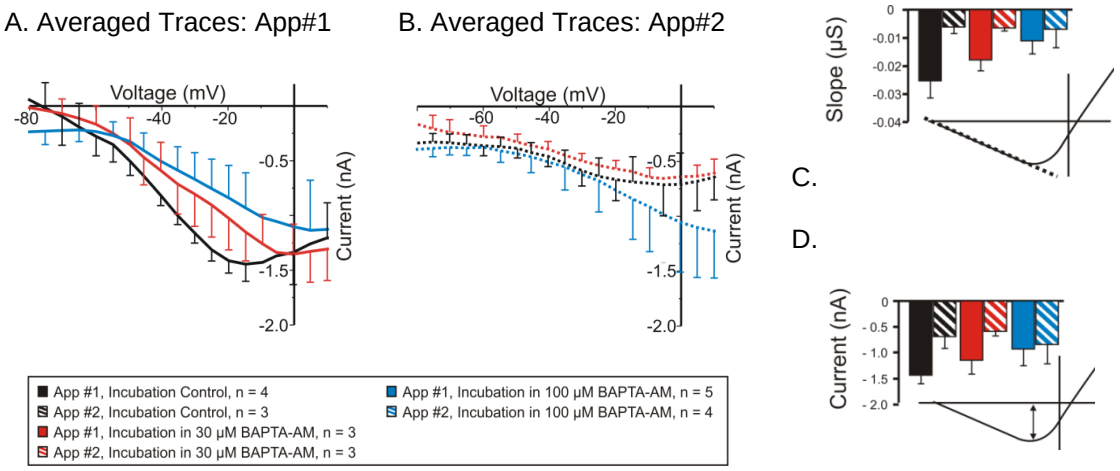


**Figure 4.6. Overnight Incubation in the Membrane-Permeable Calcium Chelator BAPTA-AM does Not Alter Proctolin-induced $I_{MI}$ Slope or Amplitude.** Preparations were incubated overnight in normal *Cancer* saline in various concentrations of BAPTA-AM. First two applications of proctolin-induced $I_{MI}$ were measured in normal calcium *Cancer* saline that contained 0.1 µM TTX, 10 µM PTX, 200 µM $CdCl_2$, 5 mM CsCl and 20 mM TEA. (A) Averaged IV curves of first measurement of proctolin-induced $I_{MI}$. (B) Averaged IV curves of second measurement of proctolin-induced $I_{MI}$.(C) A two-way ANOVA for factors application number and BAPTA-AM showed that application number, but not BAPTA-AM was capable of altering proctolin-induced $I_{MI}$ slope [BAPTA-AM; $F(2, 17) = 0.983$, $p = 0.342$. Application number; $F(1, 17) = 6.690$, $p = 0.019$.] . (D) A two-way ANOVA for factors application number and BAPTA-AM showed that application number, but not BAPTA-AM was capable of altering proctolin-induced $I_{MI}$ amplitude at -15 mV [BAPTA-AM; $F(2, 17) = 0.242$, $p = 0.788$. Application number; $F(1, 17) = 4.820$, $p = 0.042$.] Error bars are SEM.

*The ryanodine receptor antagonist dantrolene increases proctolin-induced $I_{MI}$ slope conductance and reduces amplitude.*

To test the hypothesis that changes in proctolin-induced $I_{MI}$ voltage induced by extracellular calcium reduction are mediated through reduced calcium influx and in turn are mediated by decreased activation of calmodulin, we tested the ryanodine receptor antagonist dantrolene. This antagonist, inhibits RYR1, and RYR3 isoforms of the

ryanodine receptor (Zhao et al., 2001), and has been shown to directly reduce calcium levels in barnacle muscle fiber (Hainaut and Desmedt, 1974). We predicted that ryanodine would decrease intracellular calcium and therefore increase proctolin-induced $I_{MI}$ slope and not necessarily affect $I_{MI}$ amplitude. As discussed in Chapter 3, dantrolene did significantly reduce proctolin-induced $I_{MI}$ amplitude. Consistent with our hypothesis, as shown in Figure 4.7, dantrolene also increased proctolin-induced $I_{MI}$ slope from -0.008 ± 0.003 µS in control to 0.002 ± 0.002 µS in 3.3 µM dantrolene. Note that since this slope is positive, it cannot be explained by a decrease in proctolin-induced $I_{MI}$ alone. These results support the hypothesis that a reduction in voltage dependence induced by extracellular calcium reduction is due to the lack of activated calmodulin. This is because dantrolene is expected to reduce intracellular calcium, which should lead to reduced activation of calmodulin and therefore reduce voltage dependence.

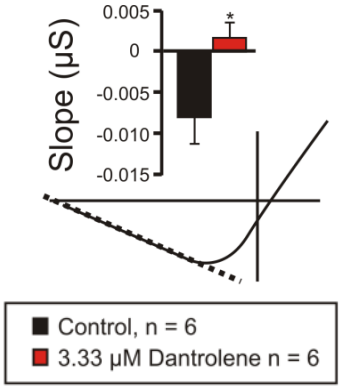


**Figure 4.7. The Ryanodine Receptor Antagonist Dantrolene Increases Proctolin-Induced $I_{MI}$ Slope Conductance.** Saline contained 0.1 µM TTX, 10 µM PTX, 200 µM $CdCl_2$, 5 mM CsCl and 20 mM TEA. A paired t-test showed that dantrolene significantly increased proctolin-induced $I_{MI}$ slope [t(5) = -4.230, p = 0.008.

*Summary of the effect of calmodulin activators on proctolin-induced $I_{MI}$ voltage dependence.*

We hypothesized that low calcium induced reduction in voltage dependence was due to loss of activated calmodulin. We showed that both calmidazolium and W7 increase proctolin-induced $I_{MI}$ slope and therefore reduce its voltage dependence. These data suggest that $I_{MI}$ voltage dependence is at least in part dependent on calmodulin. Our prediction that the calcium chelator BAPTA-AM would reduce activated calmodulin, and therefore increase proctolin-induced $I_{MI}$ slope was incorrect or at least limited by the efficacy of BAPTA-AM in our hands. As discussed in the appendix, we found that BAPTA-AM both hyperpolarized $I_A$ inactivation and had the expected effect of reducing synaptic activity. Although it is possible that not enough calcium was chelated or the calmodulin mediating proctolin-induced $I_{MI}$ voltage dependence is in close proximity to a calcium channel microdomain, it is surprising that we could detect other effects that these experiments were not originally designed to measure. Despite this, we found no significant change in proctolin-induced $I_{MI}$ slope. Dantrolene, on the other hand, produced the predicted effect but also shared an unexpected activity that was also demonstrated with calmidazolium. These agents not only increased proctolin-induced $I_{MI}$ slope, but also had the effect of reducing proctolin-induced $I_{MI}$ amplitude. This is perplexing as theoretically these agents should produce opposing effects as dantrolene should tend to decrease intracellular calcium while calmidazolium should act to increase it. We also observed that dantrolene shifted proctolin-induced $I_{MI}$ reversal potentials to more hyperpolarized voltages but could not statistically quantify this. These data imply that calmodulin is necessary for proctolin-induced $I_{MI}$ voltage dependence, but it is still

unclear whether calmodulin is sufficient for proctolin-induced $I_{MI}$ voltage dependence. This is due to the various confounding effects of drugs that did work such as calmidazolium and dantrolene, coupled with a lack of effect for drugs that theoretically should be just as efficacious such as BAPTA-AM. In the next section, we will examine whether calmodulin is sufficient for proctolin-induced $I_{MI}$ voltage dependence by trying to rescue voltage dependence in low calcium.

## 4.4 Calmodulin Activators do Not Restore $I_{MI}$ Voltage Dependence in Low Calcium

Upon establishing that W7 did indeed reduce proctolin-induced $I_{MI}$ voltage dependence in a manner that was similar to lowering extracellular calcium, we interpreted this as evidence that lowering calcium works by reducing activated calmodulin: the reduced level of activated calmodulin is now unavailable to switch $I_{MI}$ from a linear to a voltage –dependent state. Therefore, we predicted that if we applied calmodulin activators in the presence of low calcium, we should be able to restore voltage dependence.

*The membrane permeable calmodulin activator CALP1, does not restore voltage dependence in low calcium.*

CALP1 is a synthetic, membrane-permeable peptide that is designed to interact with the EF-hand domains of calmodulin and therefore activate calmodulin in lieu of calcium (Manion et al., 2000). It should therefore bypass any requirement for calcium binding. We predicted that application of this peptide activator should restore proctolin-induced $I_{MI}$ voltage dependence in low calcium. As illustrated in Figure 4.8, a one-way ANOVA showed that CALP1 did not significantly alter proctolin-induced $I_{MI}$ slope [CALP1; $F(3, 16) = 1.077$, $p = 0.387$]. Similarly, a one-way ANOVA showed that CALP1 did not alter proctolin-induced $I_{MI}$ amplitude at -15 mV [CALP1; $F(3, 16) = 0.437$, $p = 0.729$]. These results were surprising in that they did not support our hypothesis that reduction

in voltage dependence related to reduced external calcium concentration was due to loss of activated calmodulin. Knowing that CALP1 has a relatively high MW (842.09), we thought that maybe 1-2 hours was not enough time for this molecule to permeate the cell membrane. We therefore repeated the same experiment where we incubated preparations overnight with either normal saline or the same with CALP1. On the following day, proctolin-induced $I_{MI}$ was measured in low calcium $I_{MI}$ recording saline. As shown in Figure 4.9, overnight incubation in CALP1 did not alter proctolin-induced $I_{MI}$ slope [t (3) = 0.441, p = 0.689] or amplitude at -15 mV [t (3) = 0.777, p = 0.494]. These data suggested either that our hypothesis was incorrect or CALP1 was ineffective in our system.

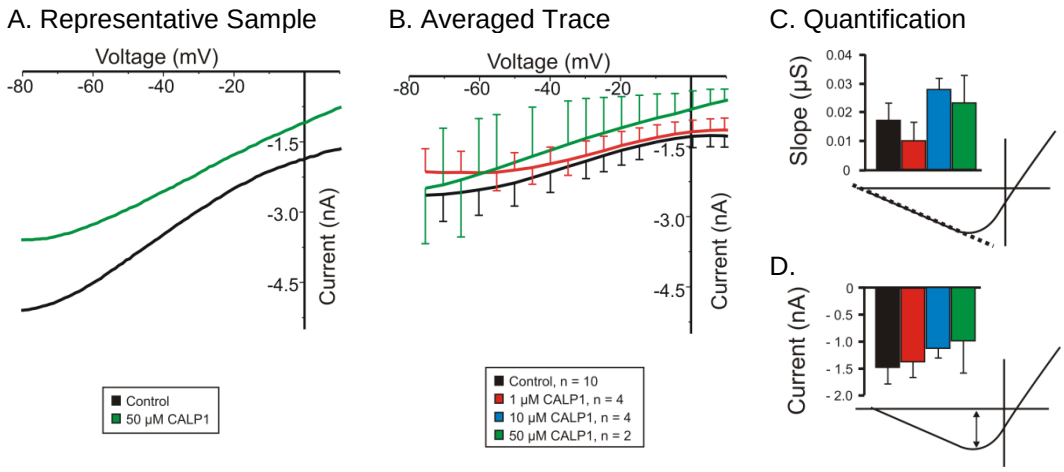


**Figure 4.8. CALP1 Does not Alter Proctolin-Induced $I_{MI}$ Slope or Restore Normal Voltage Dependence in Low Calcium.** 2 mM low calcium saline contained 0.1 µM TTX, 10 µM PTX, 200 µM $CdCl_2$, 5 mM CsCl and 20 mM TEA. (A) Representative IV curves from a CALP1 experiment. (B) Averaged IV curves from CALP1 experiments. (C) A one-way ANOVA showed that CALP1 did not alter proctolin-induced $I_{MI}$ slope [CALP1; F (3, 16) = 1.077, p = 0.387] (D) A one-way ANOVA showed that CALP1 did not alter proctolin-induced $I_{MI}$ amplitude at -15 mV [CALP1; F (3,

16) = 0.437, p = 0.729] Error bars are SEM.

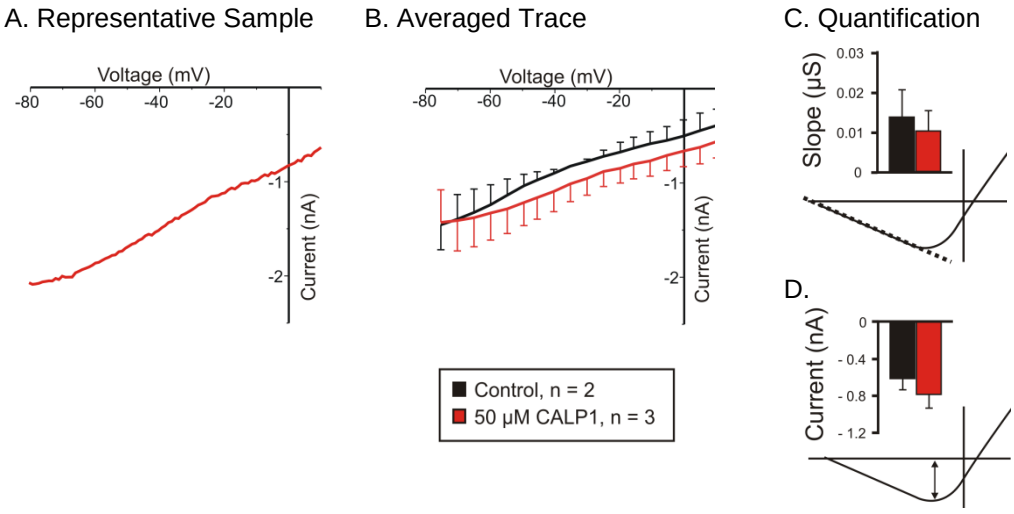


**Figure 4.9. Overnight Incubation in CALP1, does Not Decrease Proctolin-Induced $I_{MI}$ Slope or Restore Normal Voltage Dependence in Low Calcium.** Overnight incubation in normal saline (**Black**) or the same plus 50 µM CALP1 (**Red**). Proctolin-induced $I_{MI}$ was measured in 2 mM low calcium saline that contained 0.1 µM TTX, 10 µM PTX, 200 µM $CdCl_2$, 5 mM CsCl and 20 mM TEA supplemented with 0.1% BSA. (A) Representative IV curve from overnight incubation in 50 µM CALP1. (B) Averaged IV curves from CALP1 experiments. (C) A t-test showed that CALP1 did not alter proctolin-induced $I_{MI}$ slope [t (3) = 0.441, p = 0.689.] (D) A t-test showed that CALP1 did not alter proctolin-induced $I_{MI}$ amplitude at -15 mV [t (3) = 0.777, p = 0.494.] Error bars are SEM.

*The Calcium ionophore A21387 does not alter proctolin-induced $I_{MI}$ at -15 mV but increases proctolin-induced $I_{MI}$ slope.*

In order to test the hypothesis that $I_{MI}$ voltage dependence is due to calmodulin, we applied the calcium ionophore A21387. We predicted that A21387 would restore voltage dependence. We reasoned that it should enhance permeability to calcium, raising intracellular calcium levels, resulting in more activated calmodulin and, therefore, a decrease in proctolin-induced $I_{MI}$ slope (positive slope becomes negative;

i.e. a sign that voltage dependence is restored). As shown in Figure 4.10, a one-way ANOVA for A21387 with covariate application number showed that A21387 significantly decreased proctolin-induced $I_{MI}$ slope [A21387; $F(1, 18) = 8.99$, $p = 0.008$. Application number; $F(1, 18) = 0.461$, $p = 0.506$], but did not significantly increase proctolin-induced $I_{MI}$ amplitude at -15 mV [A21387; $F(1, 18) = 1.08$, $p = 0.313$. Application number; $F(1, 18) = 2.76$, $p = 0.114$]. Despite confirmation of the predicted decrease in proctolin-induced $I_{MI}$ slope, in none of the 5 preparations for these experiments did we observe an instance where the slope became more negative (steeper) than the control application. This suggests that the decrease in slope was due to a decrease in overall current and did not actually reflect restoration of negative slope conductance. This suggests that this change in slope was voltage-independent and did not support our hypothesis that activated calmodulin mediated proctolin-induced $I_{MI}$ voltage dependence.

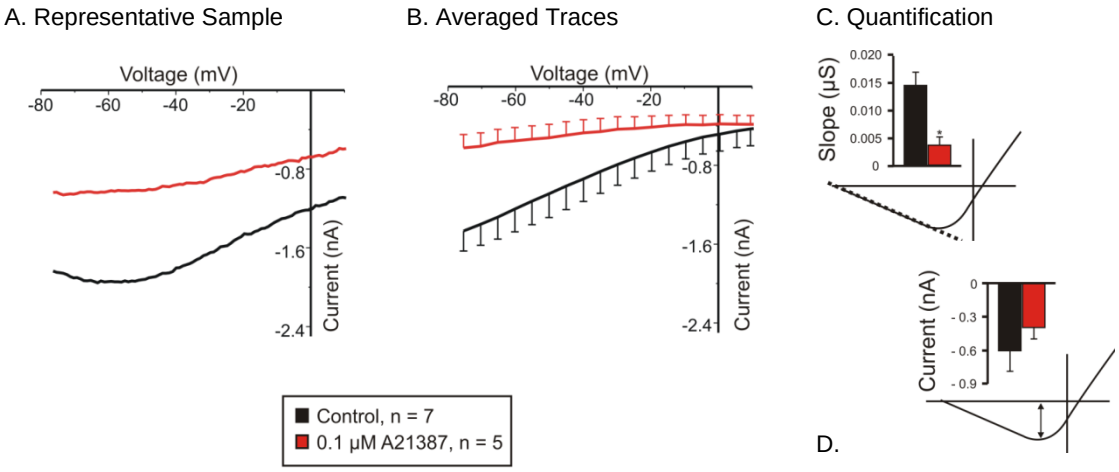


**Figure 4.10. The Calcium Ionophore A21387 Decreases Proctolin-Induced $I_{MI}$ Slope but does not Restore Normal Voltage Dependence or Affect Amplitude at -15 mV.** 2 mM low calcium saline contained 0.1 µM TTX, 10 µM PTX, 200 µM $CdCl_2$, 5 mM CsCl and 20 mM TEA supplemented with 0.1% BSA. Proctolin-induced $I_{MI}$ in the absence (**Black**) or presence of 0.1 µM A21387 (**Red**).(A) Representative IV curves of an A21387 experiment. (B) Averaged IV curves of A21387 experiments. (C) A one-way ANOVA for A21387 with covariate application number showed that A21387 significantly altered Proctolin-induced $I_{MI}$ slope [A21387; F (1, 18) = 8.99, p = 0.008. Application number; F (1, 18) = 0.461, p = 0.506] (D) A one-way ANOVA for A21387 with covariate application number showed that A21387 did not significantly alter proctolin-induced $I_{MI}$ amplitude at -15 mV [A21387; F (1, 18) = 1.08, p = 0.313. Application number; F (1, 18) = 2.76, p = 0.114.]Error bars are SEM. Tukey test; *, $p < 0.05$.

*The intracellular calcium release agent caffeine does not restore proctolin-induced $I_{MI}$ voltage dependence in low calcium.*

In order to test our hypothesis that calcium-activated calmodulin was responsible for proctolin-induced $I_{MI}$ voltage dependence, we predicted that application of 20 mM caffeine, a nonspecific intracellular calcium release agent (Ganitkevich and

Isenberg, 1992; Ribeiro and Sebastiao, 2010), should restore proctolin-induced $I_{MI}$ voltage dependence. As this agent has been verified with calcium imaging to produce changes of intracellular calcium of up to 60% in the soma of STG neurons of lobster at concentrations as low as 10 mM (Levi et al., 2003), we are confident that if an intracellular store release is possible in 2 mM low calcium, 20 mM caffeine should be sufficient to raise intracellular calcium(Levi et al., 2003). As shown in Figure 4.11, a t-test showed that caffeine did not significantly change proctolin-induced $I_{MI}$ slope [t (3) = 1.665, p = 0.195.][27]. Similarly, a t-test showed that caffeine did not significantly change proctolin-induced $I_{MI}$ amplitude at -15 mV [t (3) = -0.680 , p = 0.545.]. Additionally, as illustrated in figure 4.12, in normal calcium, a one way ANOVA for caffeine with analysis of covariance for application number showed that 5 mM caffeine had no significant effect on $I_{MI}$ slope. [Caffeine; F (1, 8) = 0.245, p = 0.634. Application Number; F (1, 8) = 3.567, p = 0.096.][28] Although the power was low for these experiments, due to low sample number, it is in agreement with the findings from our A21387 experiment that negative $I_{MI}$ slope was not restored. Another experiment was conducted with an inhibitor of sarcoplasmic endoplasmic reticulum ATPase (SERCA), thapsigargin. This agent should theoretically raise calcium levels and restore proctolin-induced $I_{MI}$ voltage dependence, but similar results were observed in that voltage dependence was no restored (Figure A4.1). This experiment was only run once. Together, these results

[27] These experiments were designed to test the Voltage dependence hypothesis.
[28] These experiments were designed to test activation by cyclic nucleotides.

suggest that these calcium release agents do not restore proctolin-induced $I_{MI}$ voltage dependence.

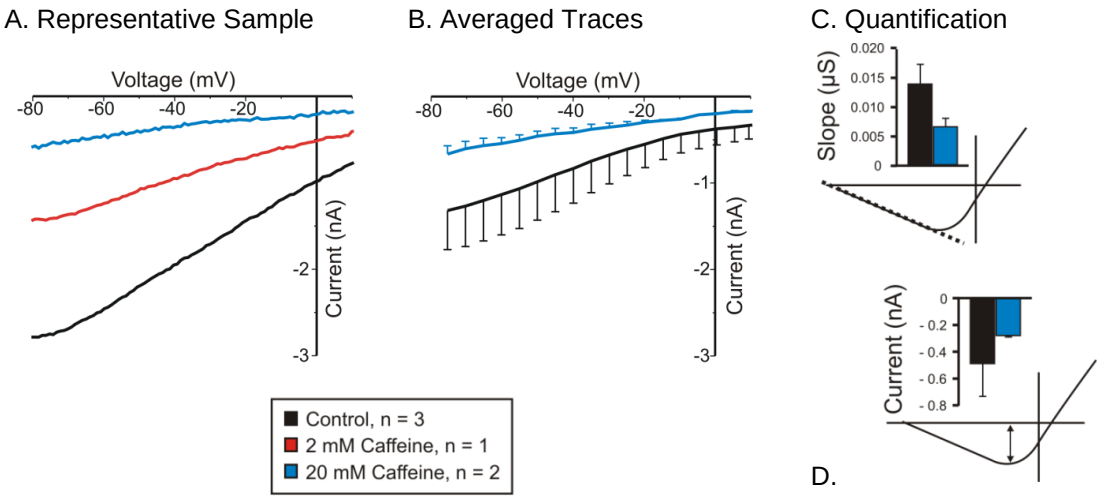


**Figure 4.11. The Intracellular Calcium Release Agent Caffeine Does Not Significantly Decrease Proctolin-Induced $I_{MI}$ Slope or Restore Voltage Dependence in Low Calcium $I_{MI}$ Recording Saline.** 2 mM low calcium saline contained 0.1 µM TTX, 10 µM PTX, 200 µM $CdCl_2$, 5 mM CsCl and 20 mM TEA supplemented with 0.1% BSA. Some Error bars smaller than line.(A) Representative IV curve from a caffeine experiment. (B) Averaged IV curves for proctolin-induced $I_{MI}$ caffeine experiments.(C) A t-test showed that caffeine did not significantly change proctolin-induced $I_{MI}$ slope [ t (3) = 1.665, p = 0.195.] (D) A t-test showed that caffeine did not significantly change proctolin-induced $I_{MI}$ amplitude at -15 mV [ t (3) = -0.680 , p = 0.545.] Error bars are SEM.

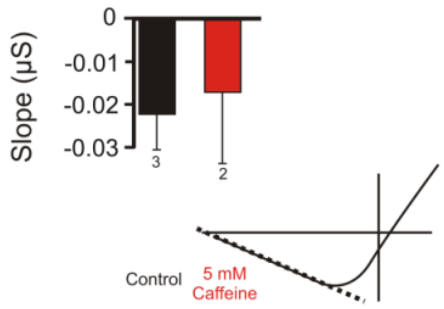


**Figure 4.12. Caffeine Does not Alter Proctolin-induced $I_{MI}$ slope in normal Calcium.** Saline contained 0.1 µM TTX, 10 µM PTX, 200 µM $CdCl_2$, 5 mM CsCl and 20 mM TEA. A one way ANOVA for caffeine with analysis of covariance for application number showed that caffeine had no significant effect on $I_{MI}$ slope. [Caffeine; F (1, 8) = 0.245, p = 0.634. Application Number; F (1, 8) = 3.567, p = 0.096.] Error bars are SEM.

*Summary of the effect of calmodulin activators on proctolin-induced $I_{MI}$ voltage dependence.*

CALP1, caffeine, and A21387 were all incapable of rescuing proctolin-induced $I_{MI}$ voltage dependence. A21387 did significantly decrease proctolin-induced $I_{MI}$ slope but in all samples (n = 5), not one instance was observed where a portion of negative slope conductance more negative than its control measurement was observed. This suggests that A21387 was increasing internal calcium concentrations but not restoring proctolin-induced $I_{MI}$ voltage dependence. CALP1 was applied for 1-2 hour incubations, overnight incubations and even through pressure injection (Figure 4A.1). In all of these experiments, not one instance was observed where proctolin-induced $I_{MI}$ voltage dependence was restored in low calcium. Although we are less confident about the results of CALP1 than A21387, due to a lack of CALP1 affecting any of the properties measured, these results argue against our original hypothesis that activated calmodulin is necessary and sufficient for proctolin-induced $I_{MI}$ voltage dependence. We also

observed that neither 20 mM caffeine (a concentration double that required to produce sustained increases in the soma of lobster STG neurons (Levi et al., 2003)), nor thapsigargin were capable of restoring proctolin-induced $I_{MI}$ voltage dependence. However, due to the low sample number, these results should only be interpreted in the context of our results from CALP1 and A21387 to show that other methods had been tried. All of these results lead us to conclude that although calmodulin may be necessary for proctolin-induced $I_{MI}$ voltage dependence as shown by calmidazolium and W7, it is not sufficient for $I_{MI}$ voltage dependence. This is because calmodulin activators and agents that increase intracellular calcium (and presumably activate calmodulin) cannot restore proctolin-induced $I_{MI}$ voltage dependence in low calcium. In later sections we explore the hypothesis that calmodulin-activated proteins may differentially control proctolin-induced $I_{MI}$ voltage dependence and help us explain the conflicting results between calmodulin inhibitors in normal calcium and calmodulin activators in low calcium. The experiments done in this section can be claimed to be confirmatory rather than exploratory, as the hypotheses and predictions tested were made prior to data analysis with explicit predictions (W7, Calmidazolium, Dantrolene and A21387, Low calcium caffeine[29]).

[29] Normal calcium was exploratory

## 4.5 Other Tested Agents that Had No Effect on Proctolin-Induced $I_{MI}$ Slope.

As discussed in Chapter 3, we had accumulated substantial data for different second messenger pathways and wished to determine if there were interactions between these pathways and proctolin-induced $I_{MI}$ voltage dependence. As these experiments were originally designed to test activation and not voltage dependence, as discussed in Chapter 3, this data must be caveated as exploratory rather than confirmatory (Payne and Dyer, 1975; Wagenmakers et al., 2012).

*Cyclic nucleotide modulators do not alter proctolin-induced $I_{MI}$ slope*

In our experiments to establish an activation mechanism for proctolin-induced $I_{MI}$, as illustrated in figure 4.13, we found that neither the cyclic amp analogue 8-Br-cAMP applied at 500 µM [ 8-Br-cAMP; F (1, 10) = 0.187, p = 0.675. Application number; F (1, 10) = 4.562, p = 0.058. Interaction; F (1, 10) = 1.025, p = 0.335.], nor the adenyl cyclase agonist forskolin applied at 10 µM [Forskolin; F (1, 12) = 2.944, p = 0.112. Condition; F (1, 12) = 1.027, p = 0.331. Interaction; F (1, 12) = 0.103, p = 0.754.] significantly altered proctolin-induced $I_{MI}$ slope. Therefore we conclude that at least in the short term, cAMP signaling is not involved with proctolin-induced $I_{MI}$ voltage dependence.

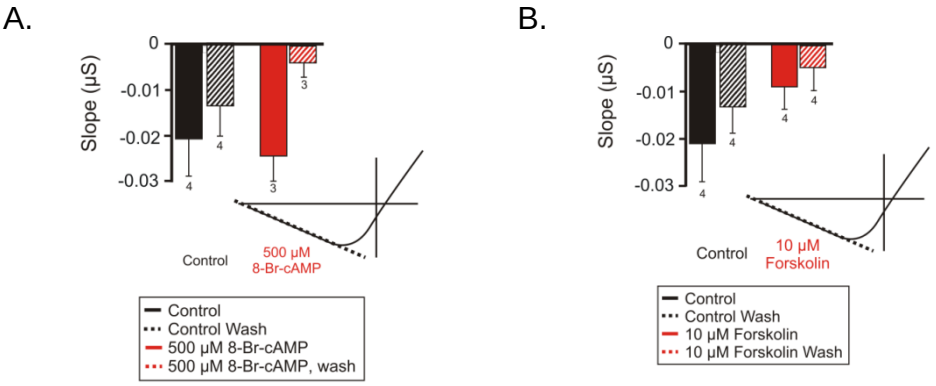


**Figure 4.13. Neither the cAMP Agonist 8-Br-cAMP nor the Adenyl Cyclase Agonist Forskolin Alter Proctolin-induced $I_{MI}$ Slope.** *Saline contained 0.1 μM TTX, 10 μM PTX, 200 μM $CdCl_2$, 5 mM CsCl and 20 mM TEA.. Slope of proctolin-induced $I_{MI}$ for proctolin applications during agonist application (**Solid**) or after washout (**Striped**) in either control (**Black**) or agonist conditions (**Red**). (A) A 2-way ANOVA showed neither 8-Br-cAMP nor application number significantly changed proctolin-induced $I_{MI}$ slope. [8-Br-cAMP; F (1, 10) = 0.187, p = 0.675. Application number; F (1, 10) = 4.562, p = 0.058. Interaction; F (1, 10) = 1.025, p = 0.335.] (B) A 2-way ANOVA showed that neither forskolin nor condition (during vs wash) had a significant effect on $I_{MI}$ slope. Error bars are SEM.*

In our experiments to characterize the activation mechanism of proctolin-induced $I_{MI}$, as illustrated in figure 4.14. we found that applications of the cGMP agonist 8-Br-cGMP did not alter proctolin-induced $I_{MI}$ slope at concentrations up to 1 mM [F (2, 9) = 0.278, p = 0.764.]. Therefore, we conclude that cGMP does not play a role in proctolin-induced $I_{MI}$ voltage dependence.

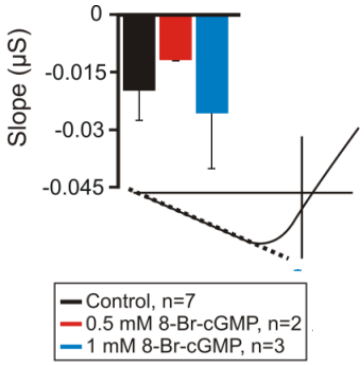


**Figure 4.14. The cGMP Agonist 8-Br-cGMP Does not Affect Proctolin-induced $I_{MI}$ Slope.** Saline contained 0.1 µM TTX, 10 µM PTX, 200 µM $CdCl_2$, 5 mM CsCl and 20 mM TEA.. Slope conductance of proctolin-induced $I_{MI}$ for control (**Black**), 0.5 mM (**Red**), and 1 mM (**Blue**) 8-Br-cGMP. A 1-way ANOVA showed that application of 8-Br-cGMP had no significant effect on $I_{MI}$ slope. [F (2, 9) = 0.278, p = 0.764.] Error bars are SEM.

In contrast to our findings for the previously described modulators of cyclic nucleotides, when we applied the PKA inhibitor H89, we did not find effects in proctolin-induced $I_{MI}$ in the short term, but we did find effects in the long term. As illustrated in figure 4.15, a 2-way ANOVA showed that H89 but not time (During vs Wash) was capable of significantly increasing $I_{MI}$ slope. [H89; F (1, 17) = 6.340, p = 0.022. Time; F (1, 17) = 1.681, p = 0.212. Interaction; F (1, 17) = 0.512, p = 0.484]. However, a Tukey test showed that the only significant difference within conditions was between washout of control, and washout of H89 (p = 0.041) Due to this long incubation requirement, and the finding that it only occurs in the wash, makes it difficult to differentiate whether the effect is due to a compensatory mechanism exposed by incubation, or due to the slow effect of the drug. As it has been shown in lobster that H89 can modulate the effect of dopamine on the A-current in 20 minutes (Zhang et al., 2010), and we saw no short-term response with either 8-Br-cAMP or forskolin, we suggest that this a compensatory response rather than a direct role for PKA mediating $I_{MI}$ voltage dependence. However,

both confirmatory experiments of the same type, with additional control incubations that are not washed out will have to be done before strong conclusions can be drawn.

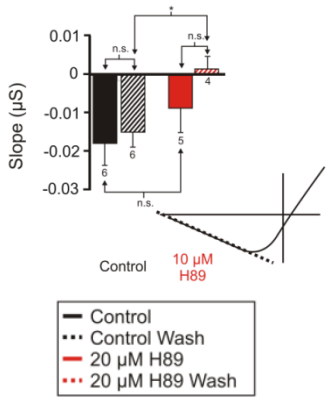


**Figure 4.15. Incubations of the PKA Inhibitor H89 has no Acute Affects on Proctolin-Induced $I_{MI}$ Slope but Washout Appears to Alter Slope.** Saline contained 0.1 µM TTX, 10 µM PTX, 200 µM $CdCl_2$, 5 mM CsCl and 20 mM TEA.. Slope of proctolin-induced $I_{MI}$ for proctolin applications during H89 application (**Solid**) or after washout (*Striped*) in either control (**Black**) or agonist conditions (**Red**). A 2-way ANOVA showed that H89 but not time (During vs Wash) was capable of significantly increasing $I_{MI}$ slope. [H89; F (1, 17) = 6.340, p = 0.022. Time; F (1, 17) = 1.681, p = 0.212. Interaction; F (1, 17) = 0.512, p = 0.484] Error bars are SEM. Tukey test; *, p < 0.05.

*PLC signaling does not alter proctolin-induced $I_{MI}$ slope.*

We examined the effect of PLC inhibitors on the voltage-dependence of proctolin-induced $I_{MI}$. As classical PLC signaling through PLC is associated with increases in intracellular calcium (Schwertz et al., 1984; Cheng et al., 2002; Gomperts et al., 2002; Levi and Selverston, 2006; Alberts, 2008; Lodish, 2008), we predicted that proctolin-induced $I_{MI}$ voltage dependence should increase (i. e. slope should become more negative) in the presence of these inhibitors. As shown in figure 4.16, a one-way ANOVA showed that the PLC inhibitor edelfosine had no significant effect on proctolin-induced $I_{MI}$ slope [Edelfosine; F (2, 9) = 0.475, p = 0.637.] Similarly, we examined the PLC inhibitor neomycin, but it was originally hypothesized that this agonist should increase

$I_{MI}$ voltage dependence as it was initially examined for its activity as a CaSR agonist.[30] Therefore, these experiments were initially carried out in low calcium. As shown in figure 4.17, a one way ANOVA for neomycin with analysis of covariance for application number showed that neither neomycin or application number were capable of significantly altering $I_{MI}$ slope. [Neomycin; $F(3, 18) = 0.865$, $p = 0.477$. Application number; $F(1, 18) = 2.601$, $p = 0.124$.]. This suggests that PLC signaling is not involved in proctolin-induced $I_{MI}$ voltage dependence in low calcium conditions. These results with along with those from edelfosine suggest that proctolin-induced $I_{MI}$ voltage dependence does not depend on PLC signaling.

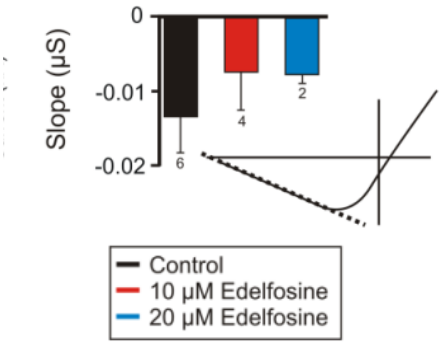


**Figure 4.16. The PLC Inhibitor Edelfosine Does not Affect Proctolin-induced $I_{MI}$ Slope.** Saline contained 0.1 µM TTX, 10 µM PTX, 200 µM $CdCl_2$, 5 mM CsCl and 20 mM TEA.. Slope conductance of proctolin-induced $I_{MI}$ for control (**Black**), 10 µM (**Red**), and 20 µM (**Blue**) Edelfosine. A one-way ANOVA showed that edelfosine had no significant effect on proctolin-induced $I_{MI}$ slope [Edelfosine; $F(2, 9) = 0.475$, $p = 0.637$.] Error bars are SEM.

[30] As will be discussed later in the chapter, we wanted to know if CaSR agonists could restore proctolin-induced $I_{MI}$ voltage dependence. We initially examined neomycin as it has been shown to be a potent CaSR agonist at 200 µM in intestinal crypts of rat (Cheng et al., 2002; Chakravarti et al., 2012), and cultured neocortical cells of mice (Vyleta and Smith, 2011) . Confoundingly, however, neomycin is an important well documented PLC inhibitor (Schacht, 1976; Schwertz et al., 1984; Burch et al., 1986; Pina-Chable et al., 1998; Levi and Selverston, 2006), which along with $G_i$ is the common mechanism of CaSR signaling in many systems (Cheng et al., 2002; Huang et al., 2010). Despite this, it has been claimed in the same paper that a neomycin-induced CaSR response is mediated through PLC signaling without discussion of why neomycin has no effect on CASR-eliciterd responses relative to other agonists (Cheng et al., 2002) .

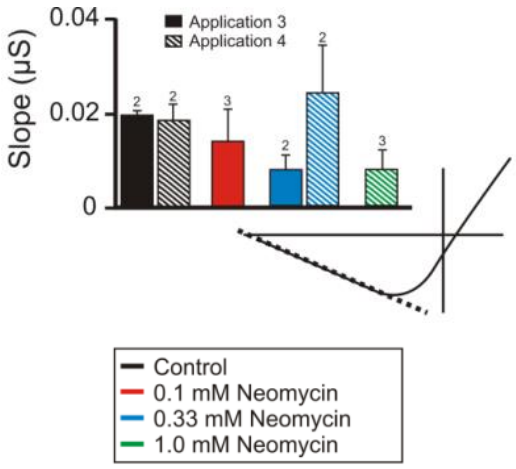


**Figure 4.17. The PLC Inhibitor/ CaSR Agonist Neomycin does not Affect Proctolin-induced $I_{MI}$ Slope.** 2 mM Low $CaCl_2$ Saline contained 0.1 µM TTX, 10 µM PTX, 200 µM $CdCl_2$, 5 mM CsCl and 20 mM TEA supplemented with 0.5% BSA. Slope conductance of proctolin-induced $I_{MI}$ for control (**Black**), 0.1 mM (**Red**), 0.33 mM (**Blue**) , and 1 mM (**Green**) neomycin, at either application 3 (**Solid**) or application 4 (*striped*). A one way ANOVA for neomycin with analysis of covariance for application number showed that neither neomycin or application number were capable of significantly altering $I_{MI}$ slope. [Neomycin; F (3, 18) = 0.865, p = 0.477. Application number; F (1, 18) = 2.601, p = 0.124.] Error bars are SEM.

*Effect of Kinase and Phosphotase inhibitors on proctolin-induced $I_{MI}$ slope.*

We examined the effect of numerous kinase and phosphatase inhibitors on proctolin-induced $I_{MI}$ slope. We examined whether the general kinase inhibitor staurosporine was capable of altering proctolin-induced $I_{MI}$. As shown in figure 4.18, A one-way ANOVA for staurosporine with covariate of application number showed that staurosporine significantly decreased proctolin-induced $I_{MI}$ slope (increased voltage dependence) [Staurosporine; F (2, 19) = 3.708, p = 0.044. Application Number; F (1, 19) = 0.002, p = 0.961.]A Fischer's least squared difference[31] test showed that this was significant for 333 nM staurosporine (p = 0.015) but not for 100 nM (p = 0.393). This is an interesting result as it implies inhibition of an unidentified kinase may restore, or

[31] Tukey test is not permitted with a covariate in SPSS.

prevent reductions in voltage dependence induced by incubation in low calcium. However, due to the exploratory[32] nature and low sample number of these experiments, further replication with larger samples and more specific kinase inhibitors will be needed before strong conclusions are drawn.

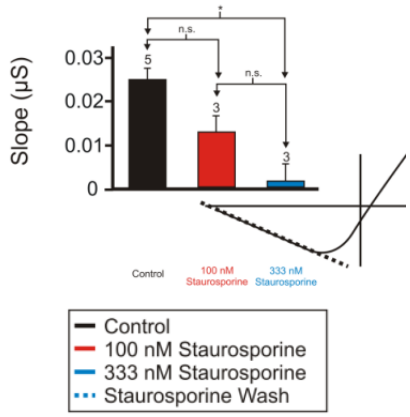


**Figure 4.18. The PKC/ General Kinase Inhibitor Staurosporine Decreases Proctolin-induced $I_{MI}$ Slope.** 2 mM Low $CaCl_2$ Saline contained 0.1 µM TTX, 10 µM PTX, 200 µM $CdCl_2$, 5 mM CsCl and 20 mM TEA supplemented with 0.5% BSA. Slope conductance of proctolin-induced $I_{MI}$ for control (**Black**), 0.1 µM (**Red**), 0.33 µM (**Blue**), and 1 µM (**Green**) staurosporine. A one-way ANOVA for staurosporine with covariate of application number showed that staurosporine significantly decreased proctolin-induced $I_{MI}$ slope [Staurosporine; $F(2, 19) = 3.708$, $p = 0.044$. Application Number; $F(1, 19) = 0.002$, $p = 0.961$.] Error bars are SEM. Tukey test; *, $p < 0.05$.

As the general kinase inhibitor staurosporine increased voltage dependence, it implies that kinases may be mediating reductions in proctolin-induced $I_{MI}$ voltage dependence. Therefore, one might expect that phosphatases would, at least in the long run, mediate restoration of voltage dependence by dephosphorylation. Therefore, their inhibition by nonspecific phosphatase inhibitors should theoretically reduce voltage dependence. As shown in figure 4.19A, superficially this appeared to be the case with the general phosphatase inhibitor okadaic acid in normal calcium. However, a paired t-test showed that okadaic acid was unable to alter $I_{MI}$ slope [$t(3) = -2.71$, $p = 0.073$.]. Assuming the difference in means of this exploratory experiment was not due to

[32] This experiment was designed to test Proctolin-induced $I_{MI}$ activation and its effect on voltage dependence was found after analysis.

chance, a power calculation of an experiment with α = 0.05, shows that this effect could be detected using a sample number of 10 (adding 6 additional replications). This would be consistient with the findings of staurosporine, but due to the low sample number and low observed power (0.412), we cannot make any inferences at this time. Despite the borderline significance found in normal calcium, as shown in figure 4.19B, A one-way repeated measures ANOVA showed that okadaic acid was unable to affect proctolin-induced $I_{MI}$ slope in low calcium [Okadaic Acid; F (3, 7) = 0.414, p = 0.748]. These results tentatively suggest that an unidentified kinase may act to reduce proctolin-induced $I_{MI}$ voltage dependence.

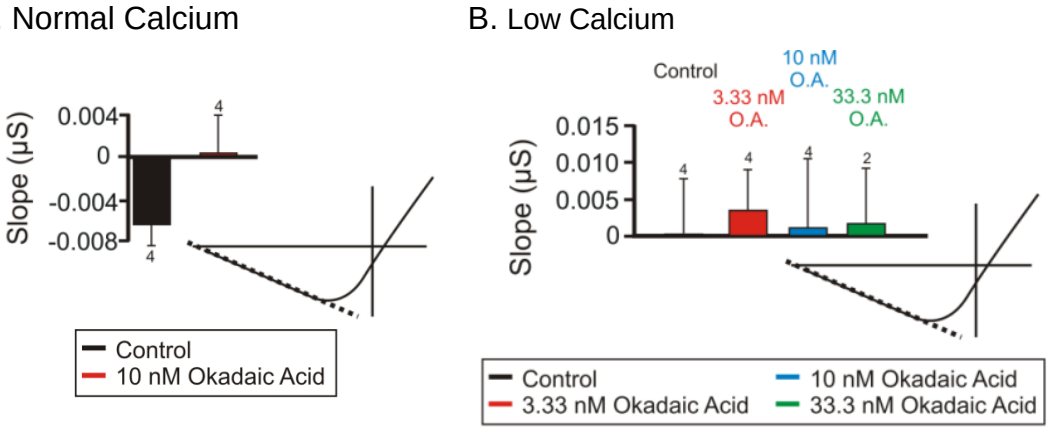


**Figure 4.19. The General Phosphatase Inhibitor Okadaic Acid does not Alter Proctolin-induced $I_{MI}$ Slope.** Saline contained 0.1 µM TTX, 10 µM PTX, 200 µM $CdCl_2$, 5 mM CsCl and 20 mM TEA (A) Normal Calcium proctolin-induced $I_{MI}$ in presence or absence of Okadaic Acid. A paired t-test showed that okadaic acid was unable to alter $I_{MI}$ slope [t (3) = -2.71, p = 0.073.] (B) 2 mM $CaCl_2$ proctolin induced $I_{MI}$ supplemented with 0.5% BSA in different concentrations of Okadaic Acid. A one-way repeated measures ANOVA showed that okadaic acid was unable to affect proctolin-induced $I_{MI}$ slope [Okadaic Acid; F (3, 7) = 0.414, p = 0.748] Error bars are SEM

Similar to the findings for tyrosine kinase and SFK inhibitors on activation, we found no effect of the tyrosine kinase inhibitor genistein or the SFK inhibitor dasatinib

on the slope of proctolin induced $I_{MI}$. As illustrated in figure 4.20, A one-way ANOVA for genistein with covariate application number showed that genistein was unable to alter $I_{MI}$ slope [Genistein; F (1, 10) = 2.587, p = 0.139. Application number; F (1, 10) = 0.131, p = 0.725.]. Similarly, as shown in figure 4.21, a t-test showed that dasatinib was unable to alter proctolin-induced $I_{MI}$ slope [t (6) = -0.370, p = 0.724.] As these experiments were only done in low calcium, they suggest that tyrosine kinases and SFKs do not increase proctolin-induced $I_{MI}$ voltage dependence but the hypothesis that they reduce voltage dependence has not been tested as this would have to be tested in normal calcium.

The results for staurosporine and okadaic acid in normal calcium may suggest a role for kinases, but due to lack of their robustness, lack of specificity of the substances used, and their apparent contradiction to results found for inhibitors of calmodulin-activated kinases (which tend to reduce voltage dependence as discussed in the next section) suggest these results should be interpreted with caution.

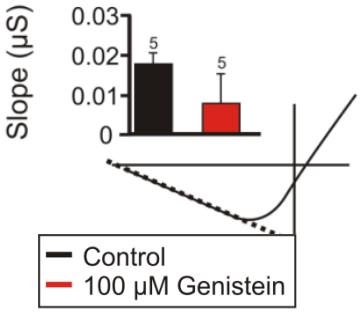


**Figure 4.20. The Tyrosine Kinase Inhibitor Genistein does not Alter Proctolin-induced $I_{MI}$ Slope.** 2 mM Low $CaCl_2$ Saline contained 0.1 µM TTX, 10 µM PTX, 200 µM $CdCl_2$, 5 mM CsCl and 20 mM TEA supplemented with 0.5% BSA. Slope conductance of proctolin-induced $I_{MI}$ for control (**Black**), or 100 µM (**Red**) Genistein. A one-way ANOVA for genistein with covariate application number showed that genistein was unable to alter $I_{MI}$ slope [Genistein; $F(1, 10) = 2.587$, $p = 0.139$. Application number; $F(1, 10) = 0.131$, $p = 0.725$.] Error bars are SEM.

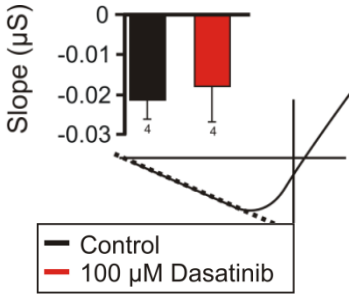


**Figure 4.21. The SFK Inhibitor Dasatibib does not Alter Proctolin-induced $I_{MI}$ Slope.** 2 mM Low $CaCl_2$ Saline contained 0.1 µM TTX, 10 µM PTX, 200 µM $CdCl_2$, 5 mM CsCl and 20 mM TEA supplemented with 0.5% BSA. Slope conductance of proctolin-induced $I_{MI}$ for control (**Black**), or 100 µM (**Red**) Dasatinib. A t-test showed that dasatinib was unable to alter proctolin-induced $I_{MI}$ slope [$t(6) = -0.370$, $p = 0.724$.] Error bars are SEM.

## 4.6 Calmodulin Activated Proteins.

For a long time we suspected that, calmodulin-activated proteins may play a role in $I_{MI}$ voltage dependence. This was due to our W7 findings and descriptions in a series of papers by Shiells and Falk on the dogfish retina. These studies showed that CamKII is the target of calcium-mediated voltage dependence in the 'on'-bipolar cells of the dogfish retina (Shiells and Falk, 2001). Upon finding that calmodulin activators did not restore proctolin-induced $I_{MI}$ voltage dependence, we hypothesized that different calmodulin-activated pathways could have opposing roles on proctolin-induced $I_{MI}$ voltage dependence. If these opposing pathways had different sensitivities and/or requirements for calmodulin, this could explain the asymmetry[33] in our results. For both of these reasons, we examined the role that calmodulin-activated proteins had in regulating proctolin-induced $I_{MI}$ voltage dependence.

*The calcineurin inhibitor cyclosporine does not alter proctolin-induced $I_{MI}$ amplitude or voltage-dependence.*

In order to test the hypothesis that dephosphorylation by calcineurin (a calmodulin-activated phosphatase) mediated a switch of proctolin-induced $I_{MI}$ from a linear to a voltage dependent state, we applied the calcineurin inhibitor cyclosporine (Weiser and Shenolikar, 2003; Heindorff and Baumann, 2014)[34]. This inhibitor has been

[33] This asymmetry being the finding that calmodulin inhibitors decreased $I_{MI}$ voltage dependence in normal calcium, but calmodulin activators were unable to restore voltage dependence in low calcium
[34] Note that Okadaic Acid does not affect calcineurin/PP2B

used successfully in the cardiac ganglion of *Cancer borealis* at concentrations of 2 µM (Ransdell et al., 2012). We predicted that when measuring proctolin-induced $I_{MI}$, we should see an increase in proctolin-induced $I_{MI}$ slope. Data in these experiments were binned into a 5 µM condition, and a 'high dose' condition consisting of two 10 µM experiments and one 20 µM experiment for statistical analysis. As shown in figure 4.22, a one-way repeated measures ANOVA showed that cyclosporine had no significant effect on proctolin-induced $I_{MI}$ slope [Cyclosporine; $F(2, 3) = 0.529$, $p = 0.636$.]. Similarly, a one-way repeated measures ANOVA showed that cyclosporine did not alter proctolin-induced $I_{MI}$ amplitude at -15 mV [Cyclosporine; $F(2, 3) = 1.022$, $p = 0.459$.]. We did observe one example of reduced voltage dependence but this result was never replicated. This data suggests that calcineurin is not responsible for proctolin-induced $I_{MI}$ slope changes observed in low calcium and the presence of calmodulin inhibitors.

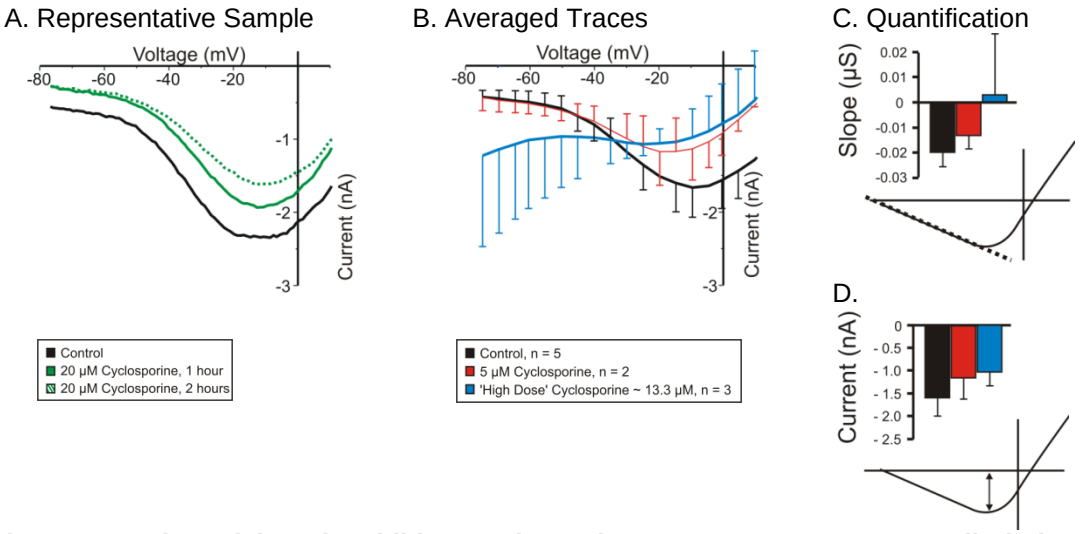


**Figure 4.22. The Calcineurin Inhibitor Cyclosporine Does not Increase Proctolin-induced $I_{MI}$ Slope.** Saline contained 0.1 μM TTX, 10 μM PTX, 200 μM $CdCl_2$, 5 mM CsCl and 20 mM TEA. Proctolin-induced $I_{MI}$ in control (**Black**), 5 μM Cyclosporine (**Red**), and a high dose of cyclosporine (**Blue**). High dose was 2 preparations at 10 μM of cyclosporine and 1 preparation at 20 μM grouped together for statistical analysis. (A) Representative IV Curve of proctolin-induced $I_{MI}$ during a cyclosporine experiment before (**Black**) and after 1 hour (**Green**) and 2 hours (***Green***) of incubation in cyclosporine (B) Averaged IV curves of proctolin-induced $I_{MI}$ for cyclosporine experiments after 2 hours of incubation.(C) A one-way repeated measures ANOVA showed that cyclosporine did not alter proctolin-induced $I_{MI}$ slope [Cyclosporine; $F(2, 3) = 0.529$, $p = 0.636$.] (D) A one-way repeated measures ANOVA showed that cyclosporine did not alter proctolin-induced $I_{MI}$ amplitude at -15 mV [Cyclosporine; $F(2, 3) = 1.022$, $p = 0.459$.] Error bars are SEM.

*The CamKII inhibitor KN93 reduces proctolin-induced $I_{MI}$ voltage dependence*

One of our initial hypotheses as to the mechanism of proctolin-induced $I_{MI}$ voltage dependence was similar to the CamKII-dependent phosphorylation of cyclic-nucleotide gated channels in 'on'-bipolar cells of the dogfish retina, as described in Chapter 1 (Shiells and Falk, 2001). We therefore predicted that incubation of cells with KN-93 would reduce proctolin-induced $I_{MI}$ voltage dependence. As shown in Figure 4.23, a one way repeated measures ANOVA showed that KN-93 indeed significantly increased proctolin-induced $I_{MI}$ slope [KN-93; $F(3, 4) = 157.497$, $p = 1.32 \times 10^{-4}$.]. There were several confounding factors, however, that accompanied this increase in slope. First, was the previously discussed decrease in proctolin-induced $I_{MI}$ amplitude. Second, there is an apparent shift in reversal potential. Although we could not measure this in control groups, and therefore could not use a hypothesis-testing statistic, it is obvious from figure 3.25B that the reversal potential that was not measureable in control, is now clearly measurable. This reversal potential in the 'high dose condition' was $V_{Reversal} = -43.58 \pm 9.29$ mV (n = 3; ± SD). This is in contrast to the reversal measured for control applications that did reverse shown in figure 2.6, of 10.77 ± 9.8 mV (n = 43; ± SD).[35] As shown in figure 4.24A, similar results were obtained in overnight incubations of KN-93 for amplitude and slope, but conspicuously missing is the shift in reversal potential.

[35] As discussed in Chapter 2, this estimate as negatively biased, as reversals positive to +20 mV had to be excluded.

Strangely, KN-93's effect on slope and amplitude seems to be an order of magnitude less than that observed for the short-term incubations despite longer incubation times. A third issue during these experiments was an observed increase in oscillatory activity during the measurement of proctolin-induced $I_{MI}$ which was accompanied by an increased leakiness of the cell. These data suggest a role for CamKII in proctolin-induced $I_{MI}$ in activation, voltage-dependence, and measured reversal potential. Staurosporine, a substance thought to inhibit CamKII at nanomolar concentrations (IC50 = 20 nM; (Meggio et al., 1995)), does not seem to produce a comparable decrease in amplitude, although as discussed in Chapter 3, this result could be combination of low sample number and differential kinase inhibition. These results, although interesting in implicating a role for CamKII in both proctolin-induced $I_{MI}$ voltage dependence and activation, need to be examined with the inactive isoform KN-92 to ensure this substance is acting specifically. These data indicate CamKII has multiple effects on proctolin-induced $I_{MI}$, but they do not support the original hypothesis that CamKII only modulates $I_{MI}$ voltage dependence as originally hypothesized.

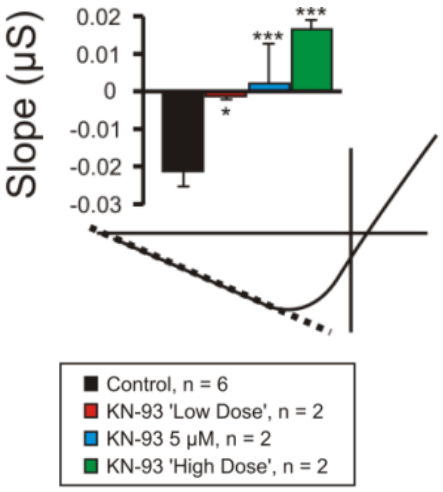


**Figure 4.23. The CamkII Inhibitor KN-93 Increases Proctolin-induced $I_{MI}$ Slope.** Saline contained 0.1 µM TTX, 10 µM PTX, 200 µM $CdCl_2$, 5 mM CsCl and 20 mM TEA. Slope conductance of Proctolin-induced $I_{MI}$ in different concentrations of KN-93. For statistical analysis, KN-93 was grouped into 'low dose' (2 µM-4 µM), 5 µM, and 'high dose' (10 µM- 20 µM).. A one way repeated measures ANOVA showed that KN-93 significantly increased proctolin-induced $I_{MI}$ slope [KN-93; $F(3, 4) = 157.497$, $p = 1.32 \times 10^{-4}$.] Error bars are SEM. Tukey test; *, $p < 0.05$. ***, $p < 0.001$.

A. Averaged App #2

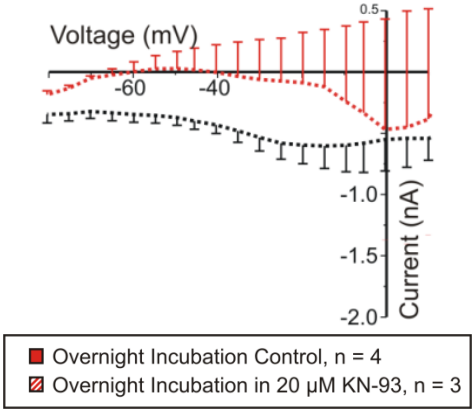


B. Quantification

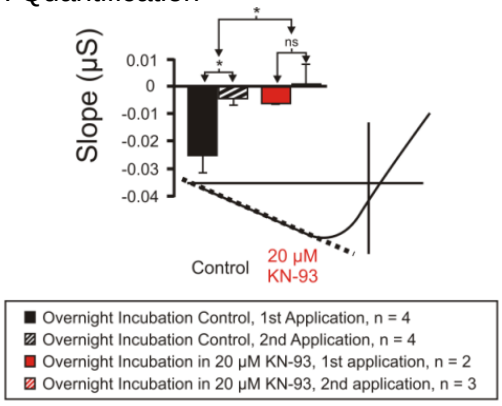


**Figure 4.24. Overnight Incubation in the CamkII Inhibitor KN-93 Increases Proctolin-induced $I_{MI}$ Slope.** Preparations either incubated in normal saline overnight or normal saline and 20 µM KN-93. When proctolin-induced $I_{MI}$ was measured, saline contained 0.1 µM TTX, 10 µM PTX, 200 µM $CdCl_2$, 5 mM CsCl and 20 mM.(A) Averaged IV curves of application 2. (B) A two-way ANOVA showed that overnight incubation with KN-93 significantly altered proctolin-induced $I_{MI}$ slope versus overnight incubation alone [KN-93; $F(1, 9) = 5.325$, $p = 0.046$. Application number; $F(1, 9) = 6.653$, $p = 0.030$. Interaction; $F(1, 9) = 1.655$, $p = 0.230$] Error bars are SEM. Tukey test; *, $p < 0.05$.

*Summary of the effect of inhibitors of calmodulin-activated proteins on proctolin-induced $I_{MI}$ voltage dependence*

Possible targets of calmodulin include CamKII as shown by the increase in proctolin-induced slope during application of KN-93, and MLCK (This will be reviewed more in the next section). The calcineurin inhibitor, cyclosporine did not produce a significant change in proctolin-induced $I_{MI}$ slope and calcineurin is therefore unlikely to be the mechanism by which calmodulin induces proctolin-induced $I_{MI}$ voltage dependence unless this substance is completely ineffective in bath application which is unlikely as this has been used successfully in the cardiac ganglion of the same species at 2 µM (Ransdell et al., 2012). Another reason we believe cyclosporine was active was that it was shown to modulate maximal $I_A$ conductance (see appendix). Therefore, we conclude that calcineurin is not the mechanism by which calmodulin mediates proctolin-induced $I_{MI}$ voltage dependence. The case for involvement of intracellular calcium, CamKII and MLCK, however, seems much more complicated, as all three of the substances used to inhibit these pathways seem to affect proctolin-induced $I_{MI}$ voltage dependence and amplitude. In the next section, we discuss a hypothesis to explain at least some of the results so far observed.

## 4.6 Calcium Sensing Receptor: A New Hypothesis to Explain Proctolin-induced $I_{MI}$ Voltage Dependence.

*Asymmetry of the effect of calmodulin inhibitors and activators in proctolin-induced $I_{MI}$ voltage dependence shows that activated calmodulin is necessary, but not sufficient for $I_{MI}$ voltage dependence.*

As we had shown that calmodulin inhibitors such as calmidazolium and W7 could increase proctolin-induced $I_{MI}$ slope, which is interpreted as reducing voltage dependence, we found it surprising that proctolin-induced $I_{MI}$ voltage dependence could not be restored in low calcium by application of calmodulin activators. As previously mentioned, A21387, CALP1 and caffeine all failed to restore proctolin-induced $I_{MI}$ voltage dependence. Although it was possible that there were different sensitivities to calmodulin distributed amongst many calmodulin-activated proteins, at the time we had very little evidence to support this. At the same time, however, we had evidence to support the idea that calmodulin was necessary but not sufficient for proctolin-induced $I_{MI}$ voltage dependence. As reviewed in Chapter 1, we found an interesting current that we initially suspected of mediating $I_{MI}$: NaLCN. NaLCN is a sodium and calcium-permeable leak current regulated by the calcium sensing receptor (CaSR) (Lu et al., 2007). Although this current is linear in the examples known to date (chapter 1), it could be envisaged that the CaSR in *Cancer borealis* may instead induce a voltage dependent inhibition. We suggest that LP cells actively sense extracellular calcium via CaSR. In this model, neuromodulator-induced $I_{MI}$ receives input from two branches, a G-protein

dependent, calmodulin dependent activation pathway as discussed in chapter 3, and a voltage-dependence pathway mediated by the CaSR. This is illustrated in Figure 4.25.

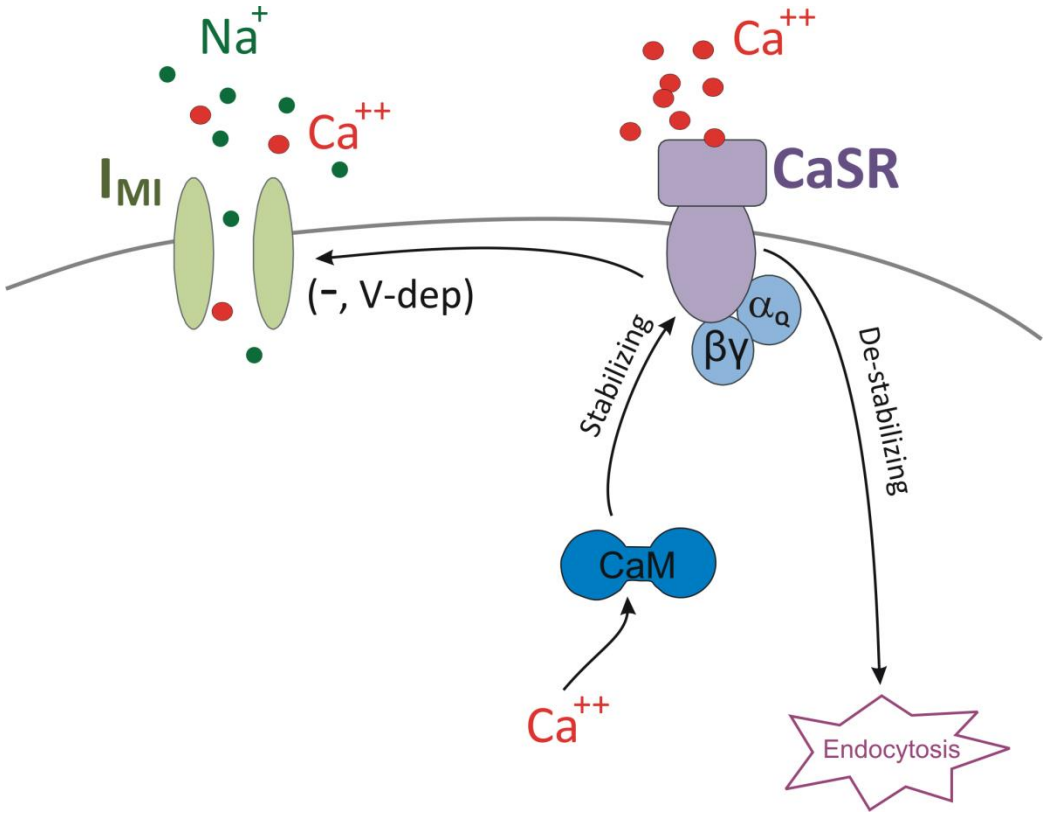


**Figure 4.25. A model for CaSR mediation of $I_{MI}$ voltage dependence.**

In this model, CaSR actively senses extracellular calcium and in its presence sends a 'voltage-dependence' signal to $I_{MI}$ channels. This then switches proctolin-induced $I_{MI}$ from a linear to voltage dependent state. This is supported by our experimental findings as follows. First, it is proposed that the reduction in voltage dependence observed in low calcium in the short run is due to a lack of calcium ligand and, therefore, CaSR signaling. This lack of signal leads to $I_{MI}$'s linear state when extracellular calcium is

reduced. Second, in other systems, CaSR requires activated calmodulin to be stabilized in the membrane or it becomes endocytosed (Huang et al., 2010; Huang et al., 2011). Therefore, when calmodulin inhibitors such as W7 and calmidazolium are applied, CaSR becomes destabilized and is then endocytosed. Without CaSR, the voltage dependence signal is lost. This explains our observations that calmodulin inhibitors reduce proctolin-induced $I_{MI}$ voltage dependence and that calmodulin activators do not restore voltage dependence. Calmodulin inhibitors cause endocytosis of CaSR, which causes the reduction in voltage dependence in normal calcium. Calmodulin activators in low calcium do nothing to change the fact that there is still low calcium extracellularly. They may stabilize CaSR but have no effect extracellularly. This loss of ligand accounts for the reduction in voltage dependence in low calcium rather than anything to do with calmodulin. This hypothesis makes many testable predictions that we will now examine.

*The specific CaSR antagonist NPS-2143 increases proctolin-induced $I_{MI}$ slope, suggesting a role for CaSR in proctolin-induced $I_{MI}$ voltage dependence.*

To directly test our hypothesis that CaSR mediates proctolin-induced $I_{MI}$ voltage dependence, we measured proctolin-induced $I_{MI}$ in the presence of the specific CaSR antagonist NPS-2143. This antagonist has been shown to block CaSR selectively with an IC50 of 43 nM, but even at concentrations as high as 3 µM, it does not inhibit other closely related GPCR family members such as mGluR1 (Nemeth et al., 2001). We predicted that if proctolin-induced $I_{MI}$ voltage dependence was mediated by CaSR, then NPS-2143 should increase proctolin-induced $I_{MI}$ slope. As shown in Figure 4.26,

application of NPS-2143 increased proctolin-induced $I_{MI}$ slope conductance without altering proctolin-induced $I_{MI}$ amplitude at -15 mV. A one-way repeated measures ANOVA showed that NPS-2143 significantly increased proctolin-induced $I_{MI}$ slope [NPS-2143; $F(4, 22) = 3.314$, $p = 0.029$]. In contrast, a one-way repeated measures ANOVA showed that NPS-2143 did not significantly alter proctolin-induced $I_{MI}$ amplitude at -15 mV [NPS-2143; $F(4, 22) = 1.085$, $p = 0.388$]. These experiments directly implicate CaSR in mediating proctolin-induced $I_{MI}$ voltage dependence.

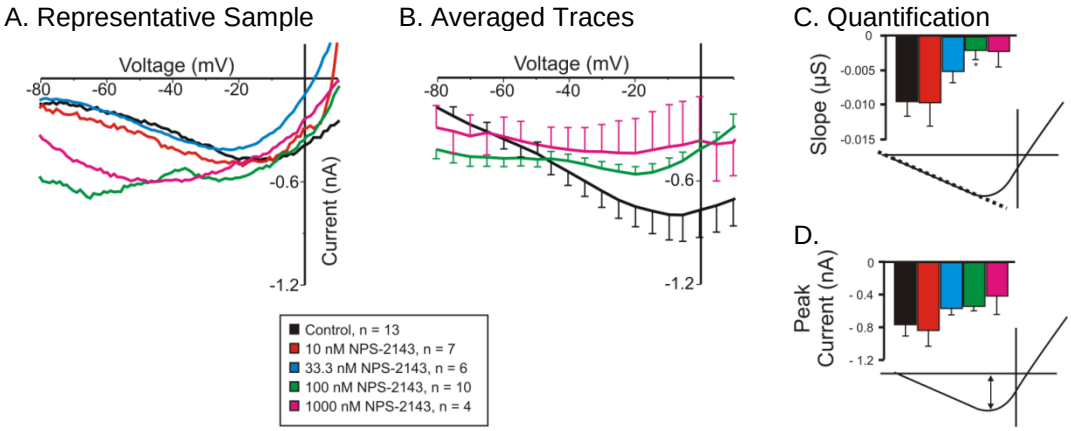


**Figure 4.26. The Specific CaSR Antagonist NPS-2143 Increases Proctolin-Induced $I_{MI}$ Slope in Normal Calcium without Altering Amplitude.** Saline contained 0.1 µM TTX, 10 µM PTX, 200 µM $CdCl_2$, 5 mM CsCl and 20 mM TEA. (A) Representative IV curves of a NPS-2143 experiment. (B) Averaged IV curves of NPS-2143 experiments. (C) A one-way repeated measures ANOVA showed that NPS-2143 significantly increased proctolin-induced $I_{MI}$ slope [NPS-2143; F (4, 22) = 3.314, p = 0.029.] (D) A one-way repeated measures ANOVA showed that NPS-2143 did not significantly alter proctolin-induced $I_{MI}$ amplitude at -15 mV [NPS-2143; F (4, 22) = 1.085, p = 0.388.] Error bars are SEM. Tukey; *, $p < 0.05$.

*Pressure injection of GDP-βS increases proctolin-induced $I_{MI}$ slope in low calcium.*

If CaSR were modulating voltage dependence of proctolin-induced $I_{MI}$, one would expect that since CaSR is a GPCR (Huang et al., 2010), injection of inhibitors of G-proteins should increase proctolin-induced $I_{MI}$ voltage dependence. As discussed in Chapter 3, proctolin-induced $I_{MI}$ was almost completely abolished by GDP-βS in normal calcium (Figure 3.2A). Figure 4.27A and 2-way ANOVA also showed that in addition to the effect of $Ca^{++}$, GDP-βS was capable of significantly increasing $I_{MI}$ slope conductance [Calcium; F (1, 30) = 43.661, p = 2.6 x 10-7. GDP-βS; F (1, 30) = 7.509, p=0.01). Interaction; F (1, 30) = 0.291, p = 0.594]. A Tukey test showed that pooling all data, GDP-βS significantly increased proctolin-induced $I_{MI}$ slope from 2.62 ± 1.63 nS to 7.26 ± 1.97

nS ($p = 0.01$). Although we did not have the statistical resolution to examine this difference within low calcium, notice that this increase in conductance cannot be explained purely by inhibition as seen in the normal calcium situation. This is because inhibition could not produce overshoot of the conductance beyond control values (instead it would bring the conductance to 0), and this is exactly what is seen here. Although exploratory, this data suggests that GDP-βS reduced proctolin-induced $I_{MI}$ voltage dependence. This supports the hypothesis that proctolin-induced $I_{MI}$ voltage dependence is regulated by a G-protein dependent mechanism. In contrast to this result, we expected that if GDP-βS reduced $I_{MI}$ voltage depednendence, than application of the G-protein agonist GTP-γS should increase voltage dependence. Despite this, as shown in figure 4.27B,) a 2 way ANOVA showed that calcium, but not GTP-γS was capable of altering $I_{MI}$ slope. [Calcium; $F(1, 22) = 23.702$, $p = 7.25 \times 10^{-5}$. GTP-γS ; $F(1, 22) = 0.0113$, $p = 0.916$. Interaction ; $F(1, 22) = 1.285$, $p = 0.269$.] Additionally, as CaSR is usually mediated via a Gi or Gq alpha subunit (Huang et al., 2010), we would expect pertussis toxin to reduce proctolin-induced $I_{MI}$ voltage dependence in normal calcium if CaSR was mediated by $G_i$. As shown in figure 4.27C a 2-way ANOVA showed that calcium, but not pertussis was capable of increasing $I_{MI}$ slope. [Calcium; $F(1, 22) = 40.026$, $p = 2.29 \times 10^{-6}$. Pertussis; $F(1, 22) = 3.830$, $p = 0.063$. Interaction; $F(1, 22) = 0.170$, $p = 0.684$.]. While the GDP-βS result supports our hypothesis,as CaSR is a GPCR, and in the context of our NPS-2143 result, we interpret these results as evidence that proctolin-induced $I_{MI}$'s voltage dependence is influenced by a CaSR-like GPCR with the

caveat that this response is not Gi mediated. Interestingly, we did not see the expected increase in slope from GTP-γS.

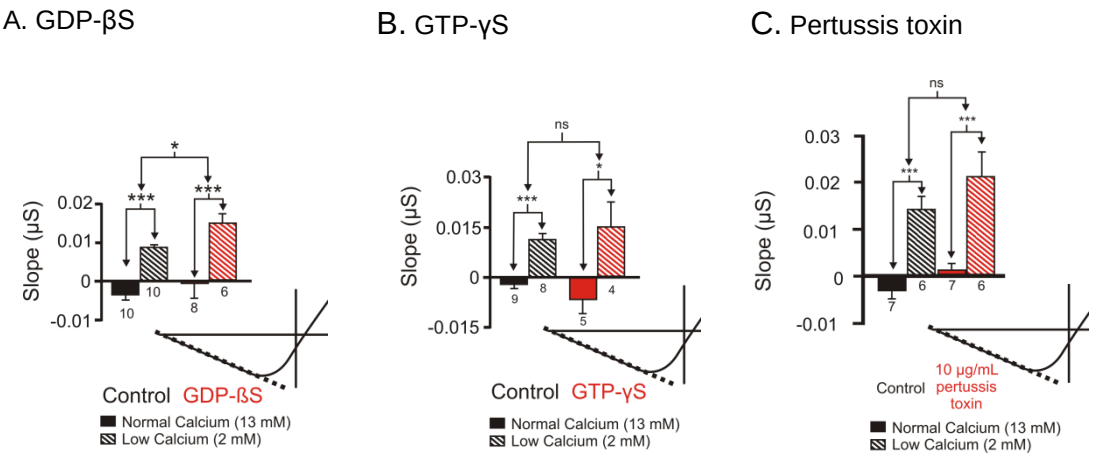


**Figure 4.27: Effects of G-protein Modulators on Proctolin-induced $I_{MI}$ Slope.** 10 mM GDP-βS, 10 mM GTP-γS, or 10μg/ mL Pertussis toxin were pressure injected in 500 mM KCl and 20 mM TEA solution (**Red**). Control solutions (**Black**) were 500 mM KCl and 20 mM TEA. Currents were measured in 13 mM $CaCl_2$,(**Solid**) or 2 mM $CaCl_2$ (*Stripes*) All recording electrodes used 20 mM KCl and 0.6 M $K_2SO_4$.(A) A 2-way ANOVA showed that both calcium and GDP-βS were capable of changing $I_{MI}$ slope conductance [Calcium; $F(1, 30) = 43.661$, $p = 2.6 \times 10^{-7}$. GDP-βS; $F(1, 30) = 7.509$, $p=0.01$). Interaction; $F(1, 30) = 0.291$, $p = 0.594$]. (B) A 2 way ANOVA showed that calcium, but not GTP-γS was capable of altering $I_{MI}$ slope. [Calcium; $F(1, 22) = 23.702$, $p = 7.25 \times 10^{-5}$. GTP-γS ; $F(1, 22) = 0.0113$, $p = 0.916$. Interaction ; $F(1, 22) = 1.285$, $p = 0.269$.] (C) A 2-way ANOVA showed that calcium, but not pertussis was capable of increasing $I_{MI}$ slope. [Calcium; $F(1, 22) = 40.026$, $p = 2.29 \times 10^{-6}$. Pertussis; $F(1, 22) = 3.830$, $p = 0.063$. Interaction; $F(1, 22) = 0.170$, $p = 0.684$.] Error bars are SEM. Tukey; *, $p < 0.05$. ***, $p < 0.001$.

*The βγ-subunit inhibitor gallein increases proctolin-induced $I_{MI}$ slope, suggesting a specific pathway for voltage dependence signaling.*

Although our GDP-βS results suggest that a G-protein sensitive to GDP-βS (Figure 4.26A) but insensitive to PTX (Figure 4.26C) may be mediating proctolin-induced $I_{MI}$

voltage dependence, we found it impossible to locate adequate G-protein modulators of pertussis-insensitive $G_q$ [36]. With $G_i$ eliminated by our pertussis results, $G_q$ has been shown to be the most common pertussis-insensitive α-subunit downstream of CaSR in many preparations (Saidak et al., 2009; Huang et al., 2010; Conigrave and Ward, 2013). However, we found that application of the membrane permeable βγ-subunit inhibitor gallein did affect $I_{MI}$ slope. As shown in Figure 4.28, a one-way repeated measures ANOVA showed that gallein significantly increased proctolin-induced $I_{MI}$ slope [Gallein; $F(2, 16) = 4.445$, $p = 0.029$]. In contrast, a one-way repeated measures ANOVA showed that gallein did not significantly change proctolin-induced $I_{MI}$ amplitude at -15 mV [Gallein; $F(2, 16) = 2.337$, $p = 0.129$]. In the context of the negative findings for pertussis, cyclic nucleotides and PLC signaling pathways (Gilman, 1987; Tang and Gilman, 1991)[37], these results suggest that proctolin-induced $I_{MI}$ voltage dependence is directly modulated by the G-protein βγ-subunit.

[36] A substance named YM-254890 has been shown by Kawasaki et al. (2003) to inhibit $G_q$, but several email attempts at contacting the author failed. Since then less exotic but less powerful analogs of YM-254890 have been synthesized (Rensing et al., 2015) that might be tested.

[37] These papers suggest βγ can have an inhibitory effect on α subunits by themselves, but then we would expect changes in $I_{MI}$ due to PLC and nucleotide signaling making the most parsimonious explanation that of direct $G_{\beta\gamma}$ signaling.

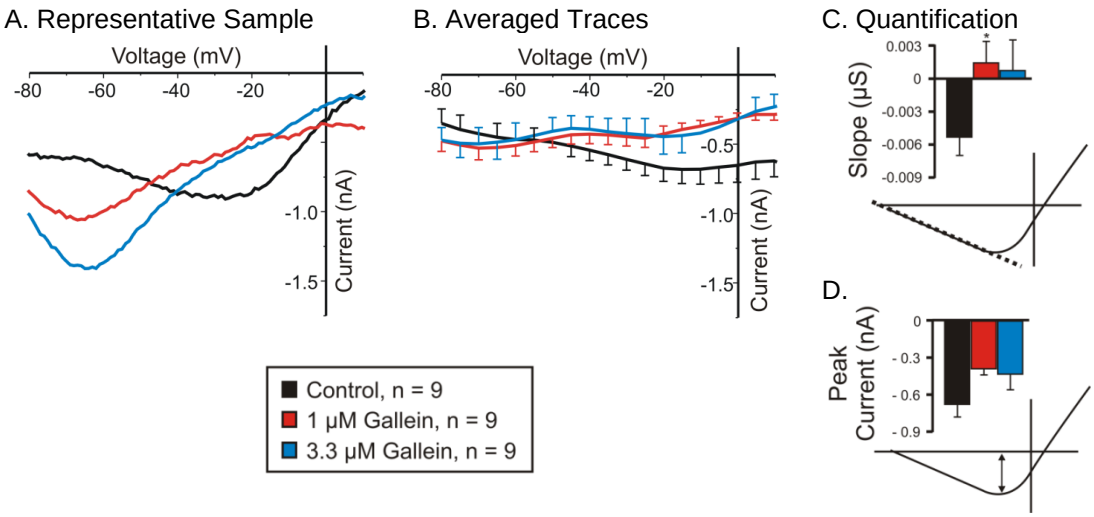


**Figure 4.28. The βγ-Subunit Inhibitor Gallein Increases Proctolin-Induced $I_{MI}$ Slope Conductance.** Saline contained 0.1 µM TTX, 10 µM PTX, 200 µM $CdCl_2$, 5 mM CsCl and 20 mM TEA. (A) Representative IV curve of proctolin-induced $I_{MI}$ in gallein. (B) Averaged IV curves of proctolin-induced $I_{MI}$ for gallein experiments.(C) A one-way repeated measures ANOVA showed that gallein significantly changed proctolin-induced $I_{MI}$ slope [Gallein; $F(2, 16) = 4.445$, $p = 0.029$.] .(D) A one-way repeated measures ANOVA showed that gallein did not significantly change proctolin-induced $I_{MI}$ amplitude at -15 mV [Gallein; $F(2, 16) = 2.337$, $p = 0.129$.] Error bars are SEM. Tukey; *, $p < 0.05$.

*Does CaSR signal through MLCK?*

To test the hypothesis that proctolin-induced $I_{MI}$ voltage dependence may be mediated through CaSR, we examined downstream pathways of CaSR signaling. CaSR is normally mediated via $G_i$ or $G_q$ dependent pathways in other systems (Cheng et al., 2002; Conigrave et al., 2007; Saidak et al., 2009; Conigrave and Hampson, 2010; Huang et al., 2010; Conigrave and Ward, 2013). Since PTX ADP-ribosylates $G_i$ (Katada, 2012), and PTX did not change proctolin-induced $I_{MI}$ slope (Figure 4.27) and cyclic nucleotides also do not affect voltage-dependence (Figure 4.13 & 4.14), we thought $G_q$ may be a

possible candidate for this pathway. However, the inhibition of PLC by edelfosine and neomycin has no significant effect on proctolin-induced $I_{MI}$ slope (Figure 4.16 & 4.17). As we had no direct assays for testing $G_q$, we examined the effect of second messengers thought to be downstream of CaSR signaling. An example of this is given by Conigrave et al., (2007) who proposed that MLCK might be downstream of CaSR signaling. As naphthasulfonamides such as W7 have been shown to inhibit MLCK independently of calmodulin inhibition (Inagaki et al., 1986; Saitoh et al., 1987), we thought MLCK was a good target that may mediate proctolin-induced $I_{MI}$ voltage dependence. We predicted, a priori, that with application of the MLCK inhibitor, ML-7, proctolin-induced $I_{MI}$ slope conductance would increase without change to its amplitude. As depicted in Figure 4.29, a one-way repeated measures ANOVA, showed that, as predicted, ML-7 increased proctolin-induced $I_{MI}$ slope [ML-7; $F(3, 26) = 7.503$, $p = 8.92 \times 10^{-4}$]. As discussed in chapter 3, higher concentrations also led to a reduction in proctolin-induced $I_{MI}$ amplitude at -15 mV. There have, however, been reports of ML-7 inhibiting processes thought to be mediated by CamKII at concentrations such as 10 µM, which are higher than that required for MLCK inhibition (Chung et al., 2013). As ML-7 has been shown to have $K_I$s for MLCK in the range of 0.3 µM (Saitoh et al., 1987), we therefore interpret the increase in proctolin-induced $I_{MI}$ slope at 0.1 µM--a concentration where amplitude is not affected--as being consistent with MLCK inhibition, and the high ML-7 concentration effects on amplitude as being consistent with a CamKII mediated effect. A control with KN-92 (which inhibits CamKII, not MLCK) was not performed but should complement

these results. This is because if KN-92 is ineffective as expected, it would suggest a role for CamKII in activation and a role for MLCK[38] in voltage dependence. This is consistent with the hypothesis that proctolin-induced $I_{MI}$ voltage dependence is mediated by CaSR via MLCK signaling.

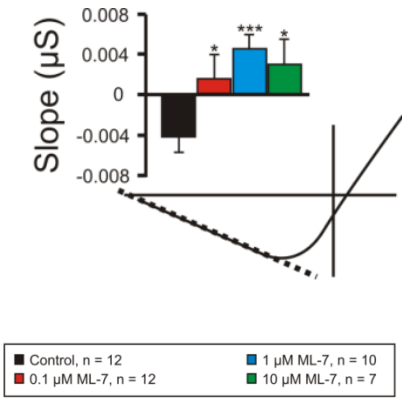


**Figure 4.29: The MLCK Inhibitor ML-7 Increases Proctolin-induced $I_{MI}$ Slope Conductance.** Saline contained 0.1 µM TTX, 10 µM PTX, 200 µM $CdCl_2$, 5 mM CsCl and 20 mM TEA. A one-way repeated measures ANOVA showed that ML-7 increased proctolin-induced $I_{MI}$ slope [ML-7; $F(3, 26) = 7.503$, $p = 8.92 \times 10^{-4}$.] (D) Error bars are SEM. Tukey; *, $p < 0.05$. ***, $p < 0.001$.

*Can endocytosis inhibitors prevent W7-induced increases in CCAP-induced $I_{MI}$?*

If calmodulin inhibition's effects on slope is due to destabilization of CaSR on the membrane as suggested earlier and suggested by Huang et al., (2010), then preincubation in the endocytosis inhibitor dynasore should prevent the increase in $I_{MI}$ slope conductance caused by W7. In these experiments, we used CCAP, as it was thought to produce larger $I_{MI}$ responses[39] at the time. We measured CCAP-induced $I_{MI}$ before application of drugs and in three distinct drug conditions. First, we measured

[38] i.e. MLCK may be acting non-specifically at higher concentrations.
[39] However, this was found not to be the case as a t-test showed there were no significant differences at application 2. [$t(6) = 0.846$, $p = 0.460$]. Mean proctolin amplitude = -1.5 ± 0.5 nA. Mean CCAP amplitude = -1.0 ± 0.2 nA.

CCAP-induced $I_{MI}$ after 45-60 minutes of incubation in 33 µM of W7. Second, we measured CCAP-induced $I_{MI}$ after 45-80 minute incubations in 33 µM of the endocytosis inhibitor dynasore. Then we measured CCAP-induced $I_{MI}$ after we added 33 µM of Dynasore for 20 minutes and then incubated in 33 µM of W7 plus 33 µM of dynasore for 45-60 minutes. As illustrated in Figure 4.30, a two-way ANOVA for factors dynasore and W7 showed changes in CCAP-induced $I_{MI}$ slope [dynasore; $F(1, 32) = 4.317$, $p = 0.046$. W7; $F(1, 32) = 14.934$, $p = 5.12 \times 10^{-4}$.Interaction; $F(1, 32) = 2.109$, $p = 0.156$]. There are some interesting Tukey comparisons for CCAP-induced $I_{MI}$ slope to note that are listed for clarity:

*W7 increases slope (becomes less negative, loses voltage dependence).*

1. Control (**Black)** vs W7 (**Red**), as expected, W7 significantly increased CCAP-induced $I_{MI}$ slope from -11.3 ± 1.3 nS in control (**Black**) to -0.4 ± 1.6 nS in W7 (**Red**) ($p < 0.001$). This means that W7 is reducing CCAP-induced $I_{MI}$ voltage dependence.

*W7 has no effect when preincubated in dynasore.*

2. When preincubated with dynasore (**Blue** vs **Green**), W7 (**Green**) did not significantly increase CCAP-induced $I_{MI}$ slope relative to dynasore alone (**Blue**) ($p = 0.129$). This suggests that dynasore prevented W7-induced changes in CCAP-induced $I_{MI}$ slope. This supports our hypothesis that W7-induced reduction in voltage dependence is due to the

endocytosis of the CaSR receptor because W7 does not affect slope when preincubated in dynasore. This means the expected reduction in voltage dependence was blocked by preincubation in dynasore.

An alternative explanation for this data would be that dynasore had an effect opposite of W7. This could oppose the effect of W7 and that the two cancel one another out. This interpretation however, is incorrect. This is because a Tukey test showed that there was no significant difference between control (**Black**) and dynasore only (**Blue**) ($p = 0.624$). These data strongly support our hypothesis that W7-induced reduction in voltage dependence is due to endocytosis of CaSR.

*W7 affects CCAP-induced $I_{MI}$ amplitude when preincubated in dynasore.*

There was an unexpected result on CCAP-induced $I_{MI}$ amplitude at -15 mV. A two-way ANOVA for factors dynasore and W7 showed significant changes in CCAP-induced $I_{MI}$ amplitude at -15 mV [dynasore; $F(1, 32) = 0.000115$, $p = 0.991$. W7; $F(1, 32) = 8.738$, $p = 0.006$. Interaction; $F(1, 32) = 1.472$, $p = 0.234$.]. Consistent with our previous findings of W7 not affecting CCAP-induced amplitude, a Tukey test showed that when dynasore was not present, W7 did not affect CCAP-induced amplitude at -15 mV ($p = 0.178$; Figure 4.30F; compare **Black** to **Red**). In contrast, when dynasore was present, a Tukey test showed that W7 significantly reduced the absolute value of CCAP-induced $I_{MI}$ amplitude ($p = 0.011$; Figure 4.30F; compare **Blue** to **Green**)

This result is interesting but it is unclear why calmodulin inhibition should have differential effects when endocytosis is blocked. This is surprising as it is striking, that when measuring proctolin-induced $I_{MI}$ in W7 at voltages at or below -40 mV, how much W7 effect changes a barely perceptible current into a huge inward current.Therefore, the last thing we would suspect was that W7 could inhibit this current. These data strongly support the hypothesis that W7-induced reduction in voltage dependence is due to endocytosis of a CaSR-like receptor.

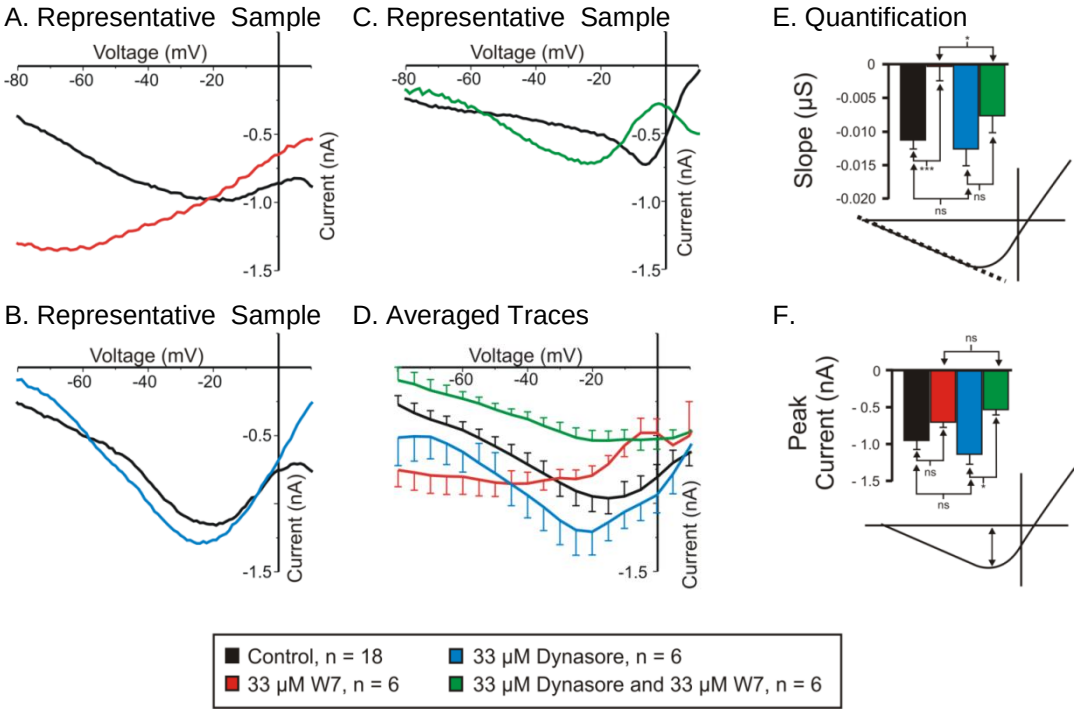


**Figure 4.30. Preincubation in the Endocytosis Inhibitor Dynasore Prevents W7-induced Increases in Slope of CCAP-induced $I_{MI}$.** Saline contained 0.1 µM TTX, 10 µM PTX, 200 µM $CdCl_2$, 5 mM CsCl and 20 mM TEA. CCAP-induced $I_{MI}$ was measured before (**Black**) and after exposure to the following: 1) 33 µM W7 for 45-65 minutes (**Red**). 2) Dynasore for 45-80 minutes (**Blue**).3)20 minutes in 33 µM Dynasore, then 45-60 minutes of in 33 µM Dynasore plus 33 µM W7 (**Green**).(A) Representative IV curve of W7 experiment. (B) Representative IV Curve of a dynasore experiment.(C) Representative IV curves of a dynasore and W7 experiment. (D) A two-way ANOVA for factors dynasore and W7 showed changes in CCAP-induced $I_{MI}$ slope [dynasore; $F(1, 32) = 4.317$, $p = 0.046$. W7; $F(1, 32) = 14.934$, $p = 5.12 \times 10^{-4}$.Interaction; $F(1, 32) = 2.109$, $p = 0.156$.] Tukey Comparisons to Note: 1. Within no Dynasore: Control (**Black)** vs (**Red**) W7 significantly increased CCAP-induced $I_{MI}$ slope ($p < 0.001$). 2. Within Dynasore: Dynasore only (**Blue**) vs Dynasore plus W7 (**Green**). W7 did not significantly increase CCAP-induced $I_{MI}$ slope ($p = 0.129$).3. Within no W7: Control (**Black**) vs Dynasore (**Blue**). Dynasore did not alter CCAP-induced $I_{MI}$ slope by itself ($p = 0.624$) 4.Within 33 µM W7: W7 (**Red**) vs W7 plus Dynasore (**Green**). Preincubation in dynasore increased CCAP-induced $I_{MI}$ slope ($p = 0.03$)(prevented W7 effect).(E) A two-way ANOVA for factors dynasore and W7 showed significant changes in CCAP-induced $I_{MI}$ amplitude at -15 mV [dynasore; $F(1, 32) = 0.000115$, $p = 0.991$. W7; $F(1, 32) = 8.738$, $p = 0.006$.Interaction; $F(1, 32) = 1.472$, $p = 0.234$.] Error bars are SEM. Tukey; *, $p < 0.05$; ***, $p < 0.001$.

*Summary of evidence for CaSR*

We propose that neuromodulator-induced $I_{MI}$ voltage dependence is due to active sensing of extracellular calcium by a CaSR-like receptor. Activation of this receptor switches neuromodulator-induced $I_{MI}$ from a linear to a voltage dependent state. This hypothesis was originally proposed due to the inconsistency between calmodulin inhibitors reducing voltage dependence in normal calcium while calmodulin activators were unable to restore voltage dependence in low calcium. We provide several pieces of evidence to support this model. First, the specific CaSR antagonist NPS-2143, increases proctolin-induced $I_{MI}$ slope in a dose dependent manner (Figure 426). Second, pressure injection the G-protein inhibitor GDP-βS increases proctolin-induced $I_{MI}$ slope, which suggests that G-proteins increase proctolin-induced $I_{MI}$ voltage dependence (Figure 4.27). Third, exposure to the MLCK inhibitor ML-7 increases proctolin-induced $I_{MI}$ slope (Figure 4.29) , which suggests a signaling mechanism consistent with CaSR signaling mechanisms proposed by other authors (Conigrave et al., 2007). Fourth, our results show that the βγ-subunit inhibitor gallein is capable of increasing proctolin-induced $I_{MI}$ slope (Figure 4.28). This suggests that the βγ-subunit may mediate proctolin-induced voltage dependence perhaps directly. Fifth, but most importantly, we have found that preincubation in the endocytosis inhibitor dynasore prevents W7-induced changes in CCAP-induced $I_{MI}$ (Figure 4.30). This suggests that endocytosis is required for W7-induced changes in voltage-dependence, and explains the lack of effect of calmodulin activators observed in low calcium.

## 4.7 Conclusions:

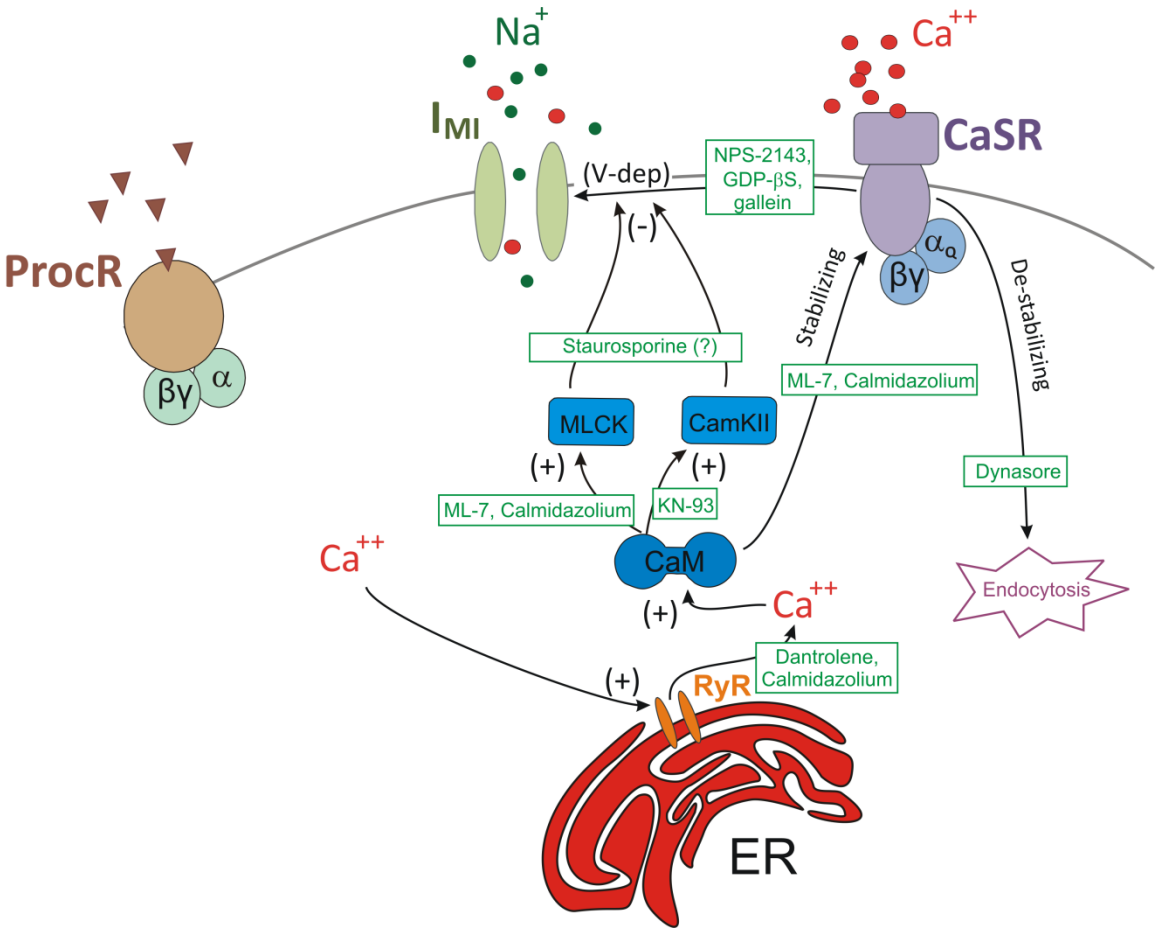


**Figure 4.31: Model of CaSR Modulation of $I_{MI}$ Voltage Dependence.**

In this chapter, we have attempted to explain the reduction in $I_{MI}$ voltage-dependence in low calcium. We have shown that calmodulin inhibitors W7 and calmidazolium are capable of increasing neuromodulator-induced $I_{MI}$ slope. This suggested a role for calmodulin in $I_{MI}$ voltage dependence. It was found, however, that calmodulin activators could not restore proctolin-induced $I_{MI}$ voltage dependence in low calcium, inconsistent with a role of activated calmodulin exclusively mediating $I_{MI}$

voltage dependence. We therefore proposed that a calcium-sensing receptor (CaSR) mediated $I_{MI}$ voltage dependence consistent with a reduction in voltage dependence in low calcium simply due to the loss of the receptor's ligand (i. e. $Ca^{++}$). (Figure 4.16)

*Can anything restore neuromodulator-induced voltage dependence in low calcium?*

Although we have provided a large body of evidence that implicates CaSR in at least the regulation of $I_{MI}$ voltage dependence, we still have been unsuccessful in restoring voltage dependence in low calcium conditions. One experiment we would like to try is the application of selective CaSR agonists in the absence of extracellular $Ca^{++}$ with the prediction that they should restore neuromodulator-induced $I_{MI}$ voltage dependence. However, the calcium concentration in this system is much higher than in systems where more is known about CaSR. For example, neomycin has been shown to be an effective agonist of CaSR in systems with lower calcium concentrations such as the intestinal crypts of the rat (Cheng et al., 2002). As shown in Figure 4.17, proctolin-induced $I_{MI}$ slope was unresponsive to concentrations of neomycin up to 1000 µM of neomycin. Although this would be a large concentration for this agonist in other systems, this may not be sufficient concentration for this agonist in this system. This is because it has been shown that the efficacy of CaSR agonists are regulated by osmolarity (Fellner and Parker, 2004). Using the CaSR agonist spermine in cells from the rectal gland of the shark, for example, Fellner et al., (2004) has shown that a 1 ± 0.3% increase in osmolarity led to 62 ± 8% reduction in spermine-induced responses mediated by CaSR. Considering our system is normally bathed in 13 mM $CaCl_2$, in

conjunction with this extreme modulation of CaSR agonists by osmolarity, suggests that proper dose-response curves of these agonists must be constructed. Unfortunately, this is no easy task, as our hypothesis predicts that long-term incubations in low calcium should theoretically lead to permanent increases in neuromodulator-induced $I_{MI}$ slope due to CaSR endocytosis. Therefore, to do these experiments properly, only first applications in low calcium can be considered[40]. As only the first low calcium measurement can be used, this will have to be compared to preparations other than the test preparation. Therefore, a repeated measures procedure cannot be used and statistical power suffers as a result. This, in conjunction with construction of full dose response curves makes these studies a very difficult undertaking indeed. This is without consideration of the non-specific effects from CaSR agonism of spermine, $GdCl_3$ and neomycin. For example, neomycin at micromolar concentrations inhibits PLC and PLA (Schacht, 1976; Burch et al., 1986). This is far below the several millimolar concentrations expected to produce significant modulations of neuromodulator-induced $I_{MI}$ voltage dependence. We predict that in short incubations (less than an hour) in low calcium, application of selective CaSR agonists should be able to restore voltage dependence--if our hypothesis is correct.

[40] I have observed normal voltage dependence restored several times for incubations in 2 mM low calcium up to one hour, but I am unsure of the effects beyond this period, and therefore proper controls would have to be done on the effects of long term incubations in low calcium on voltage dependence before using multiple applications.

*Loose ends, unexplained pharmaceutical agents that play a role in $I_{MI}$ voltage dependence.*

Several agents we tested for $I_{MI}$ activation showed modulation of neuromodulator-induced $I_{MI}$ slope that, at first glance, do not seem to fit into our model of $I_{MI}$ voltage dependence. H89 for example, does not affect proctolin-induced $I_{MI}$ amplitude or slope during its application. Upon washout, however, there was a significant change in voltage dependence but not activation (Figure 3.13). Another example is given by the general kinase inhibitor staurosporine. This, however, may, in the context of our model, yield an interesting explanation. Staurosporine at 333 nM, was the only substance we found that reduced proctolin-induced $I_{MI}$ slope (i.e. restore voltage dependence), and at least some samples with negative slope conductance. If our hypothesis is correct, and CaSR is regulated by the mechanism proposed by Huang et al. (2010), then, binding of calmodulin prevents endocytosis due to its covering a phosphorylation site from PKC. When in low calcium, calmodulin does not cover this site, PKC phosphorylates this site, and that targets the receptor for endocytosis. Staurosporine potently inhibits PKC (Meggio et al., 1995; Huang et al., 2010), and should therefore lead to less phosphorylation of CaSR. This should lead in turn to an increase in the CaSR population, and increased residual signaling in low calcium relative to control. This residual signaling partially restores voltage dependence. A complementary experiment would predict that incubation in PKC activators should increase slope (decrease voltage dependence) in the presence of normal calcium.

*Future Directions*

Although we have provided evidence to support our model of CaSR mediating neuromodulator-induced voltage dependence, there is still much that remains to be understood. The use of molecular-genetic approaches to study the CaSR receptor would unambiguously confirm its presence in our system. Another important issue is that the W7-induced reduction in voltage dependence has only been established for CCAP and proctolin-induced $I_{MI}$. Although it is assumed that since these neuromodulators converge to the same current (Swensen and Marder, 2000), and that they both lose voltage dependence when exposed to W7, they should generalize to other receptors that activate $I_{MI.}$ An example against this was discussed in chapter 2, as the modulation of voltage dependence by calcium for proctolin-induced $I_{MI}$ seems to have differences when compared to CCAP-induced $I_{MI}$ voltage dependence. Another issue that was beyond the scope of this thesis is why inhibition of CamKII produced the unexpected result of shifting neuromodulator-induced $I_{MI}$ reversal potential. In addition, upon availability of more specific $G_q$ inhibitors such as YM-254890, our hypothesis that this pathway is mediated by $G_q$ can be tested.

As pharmacology is usually not black and white, it would be interesting to see if genetic tools such as dsRNA KO of CaSR could be used to support our hypothesis. We would predict that dsRNAs for CaSR should increase neuromodulator-induced slope. The problem with this approach is that there is little known about CaSR in this system and one of the requirements of dsRNA KO of CaSR would be to know the sequence of CaSR

before applying this approach. To do this, degenerate oligonucleotides could be constructed from the conserved regions of other invertebrate systems where more is known about CaSR. Then, PCR could be employed to see if these mRNAs were present in this system. Upon identification and sequencing, dsRNAs could be constructed and injected to KO CaSR. We predict this should produce and increase in neuromodulator-induced $I_{MI}$ slope (decreased voltage dependence).We still do not understand why KN-93 not only seemed to regulate voltage dependence and activation, but also seemed to shift reversal potential as well. Our protocol was constructed around the assumption that the $I_{MI}$-reversal potential was centered around 0 mV (Golowasch and Marder, 1992b; Swensen and Marder, 2000), but in our hands, this value seems closer to 10.8 ± 9.8 mV (SD) and we believe this result is an underestimate as we could not include reversal potentials higher than +20 mV. This makes it difficult for us to say anything definitive about the shifts we have observed other than they are hyperpolarized relative to control.

*Appendix F: Other Calcium/calmodulin activators that failed to restore proctolin-induced $I_{MI}$ voltage dependence in low calcium.*

*Individual samples show that bath application of thapsigargin and intracellular pressure injection of CALP1 did not restore proctolin-induced $I_{MI}$ voltage dependence.*

Many experiments were too low in sample number to provide any real insight as to the voltage dependence mechanism but were included here for to let the reader know that the method had been tried.

*CALP1 pressure injection did not restore voltage dependence.*

It could be argued that CALP1 was not permeating the membrane, to show that we had tried intracellular pressure injection of these experiments a sample was included and illustrated in Figure F4.1. This experiment was repeated four times, but only twice was proctolin-induced $I_{MI}$ measured due to cell death, and one time these responses did not fully reverse so this response was not processed. It was found that CALP1 tended to 'foam' and make stable pressure injection difficult. Although not valid for the main body of the text, the conclusion is the same, as it had no obvious effect. Note that as proctolin-induced $I_{MI}$ is measured in $CdCl_2$, which in our hands does not wash, only a night and day effect could be interpreted from this.

*Thapsigargin did not restore voltage dependence.*

Another molecule that failed to restore voltage dependence is shown in figure F4.2. This result shows a similar result to all other calcium activators tested in low calcium: they failed to rescue voltage dependence.

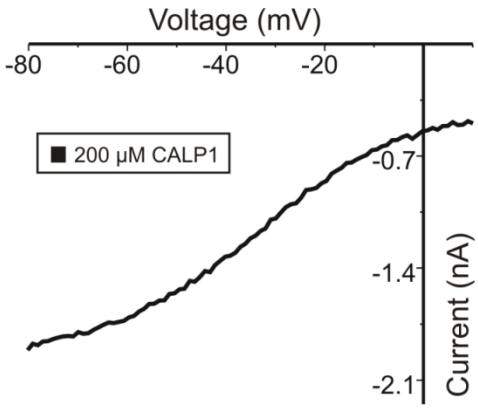


**Figure F4.1. Individual Samples Show CALP1 does not Restore Proctolin-Induced $I_{MI}$ Voltage Dependence in Low Calcium.** 2 mM low calcium saline contained 0.1 µM TTX, 10 µM PTX, 200 µM $CdCl_2$, 5 mM CsCl and 20 mM TEA supplemented with 0.5% BSA. Pressure injection of CALP1, 20 mM TEA and 500 mM KCl, did not restore voltage dependence when exposed to low calcium.

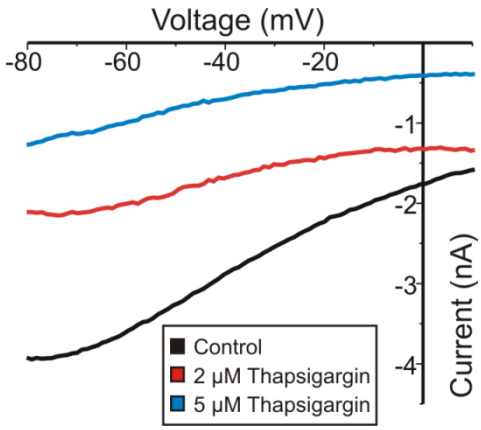


**Figure F4.2. Individual Samples Show Thapsigargin does not Restore Proctolin-Induced $I_{MI}$ Voltage Dependence in Low Calcium.** 2 mM low calcium saline contained 0.1 µM TTX, 10 µM PTX, 200 µM $CdCl_2$, 5 mM CsCl and 20 mM TEA supplemented with 0.1% BSA. Application of the SERCA blocker thapsigargin did not restore voltage dependence when exposed in to low calcium.

## Appendix G: Calmodulin Inhibitors

*The calmodulin inhibitor W7 reduced transient and steady-state $I_{HTK}$, and $I_A$, depolarizes $V_{Rest}$, but does not affect $R_{IN}$.*

As the W7 effect on neuromodulator-induced $I_{MI}$ was an important finding of this thesis, we wanted to know if it affected the other ionic currents. As illustrated in Figure G4.1, W7 significantly reduced transient and steady-state $I_{HTK}$, $I_A$, and depolarized $V_{Rest}$. At high concentrations, W7 significantly depolarized $V_{1/2}$ activation for both steady state and transient $I_{HTK}$. W7 also hyperpolarized $I_A$ $V_{1/2}$ activation. W7 increased maximal conductance for transient but not steady state $I_{HTK}$. This suggests that the mechanism of calmodulin inhibition of steady-state $I_{HTK}$ is specific to depolarizing its $V_{1/2}$ activation therefore requiring more depolarization for a given current. It will be interesting to see if this result is reversed in the presence of calmodulin activators. W7 also significantly reduced $I_A$ maximal conductance. These results suggest that W7 is having many effects on the ionic currents in this system. Theoretically, this should not affect $I_{MI}$ measurement. This is because neuromodulator-induced $I_{MI}$ was measured in the presence of 20 mM TEA, blocking both steady state and transient $I_{HTK}$, with a holding potential of -40 mV, where $I_A$ is also blocked *(Golowasch and Marder, 1992a)*, and therefore changes in these currents should not alter measured neuromodulator-induced $I_{MI}$ in these conditions. These data suggest W7 is active in this system. The effect on $I_A$, is probably not specific to calmodulin, as this effect was not observed for calmidazolium (Figure E3.1). As shown in Figure G4.2, when measured in $I_{MI}$ recording saline, W7

altered $V_{1/2}$ activation, $I_A$ at +20 mV, and hyperpolarized $I_A$ $V_{1/2}$ inactivation. $V_{Rest}$ and $R_{IN}$ were unchanged suggesting that TEA may have mitigated whatever was responsible for W7-induced depolarization of $V_{Rest}$ when it was measured in TTX. These data along with the effect on proctolin and CCAP-induced $I_{MI}$ suggests that W7 was working in this system. The agreement between the effect of calmidazolium and W7, both affecting $I_{MI}$ slope, suggests calmodulin specificity. The finding that W7 but not calmidazolium affects $I_A$, suggests that this effect is through non-specific action. The same can be said for the reduction of proctolin-induced $I_{MI}$ amplitude that we suggest is acting through intracellular calcium release as argued in Chapter 3.

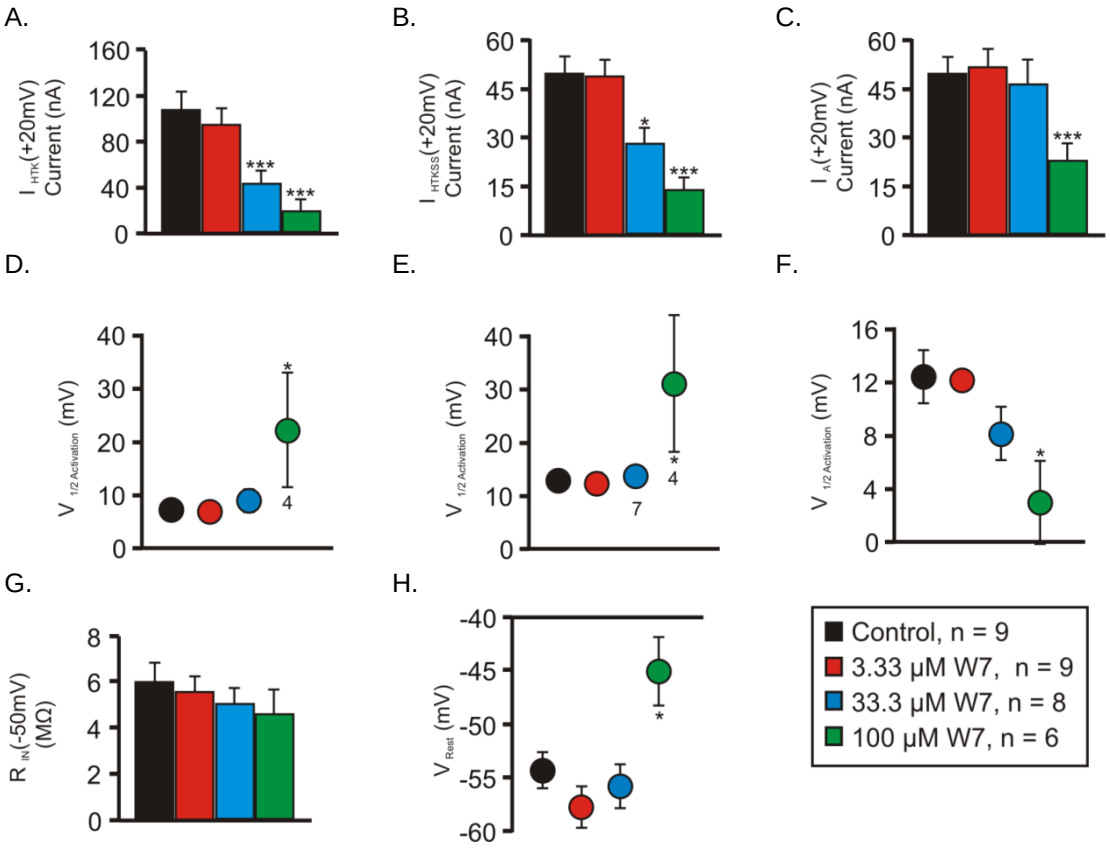


**Figure G4.1. The Calmodulin Inhibitor W7 Reduces Transient and Steady State $I_{HTK}$, $I_A$, $V_{Rest}$ but does not Affect $R_{IN}$.** Experiments in 0.1 µM TTX and various concentrations of W7. Many error bars smaller than symbols. Some $V_{mid}$ activations did not converge to a fit and therefore had to be excluded from analysis; adjusted n listed below error bars. (A) A one-way repeated measures ANOVA showed that W7 significantly reduced transient $I_{HTK}$ at +20 mV [W7; F (3, 20) = 15.823, p = 1.657 x $10^{-5}$.] (B) A one-way repeated measures ANOVA showed that W7 significantly reduced steady-state $I_{HTK}$ at +20 mV [W7; F (3, 20) = 19.336, p = 3.98 x $10^{-6}$.] (C) A one-way repeated measures ANOVA showed that W7 significantly reduced $I_A$ at +20 mV [W7; F (3, 20) = 22.841, p = 1.14 x $10^{-6}$.] (D) A one-way repeated measures ANOVA showed that W7 significantly changed transient $I_{HTK}$ $V_{1/2}$ activation [W7; F (3, 18) = 4.180, p = 0.021.] (E) A one-way repeated measures ANOVA showed that W7 significantly changed steady-state $I_{HTK}$ $V_{1/2}$ activation [W7; F (3, 17) = 3.370, p = 0.043.] (F) A one-way repeated measures ANOVA showed that W7 significantly changed $I_A$ $V_{1/2}$ activation [W7; F (3, 20) = 4.784, p = 0.011.] (G) A one-way repeated measures ANOVA showed that W7 did not significantly change $R_{IN}$ at -50 mV [W7; F (3, 20) = 0.879, p = 0.469.] (H) A one-way repeated measures ANOVA showed that W7 did significantly changed $V_{Rest}$ [W7; F (3, 20) = 10.178, p = 2.79 x $10^{-4}$.] Error bars are SEM. Tukey; *, p < 0.05; ***, p < 0.001.

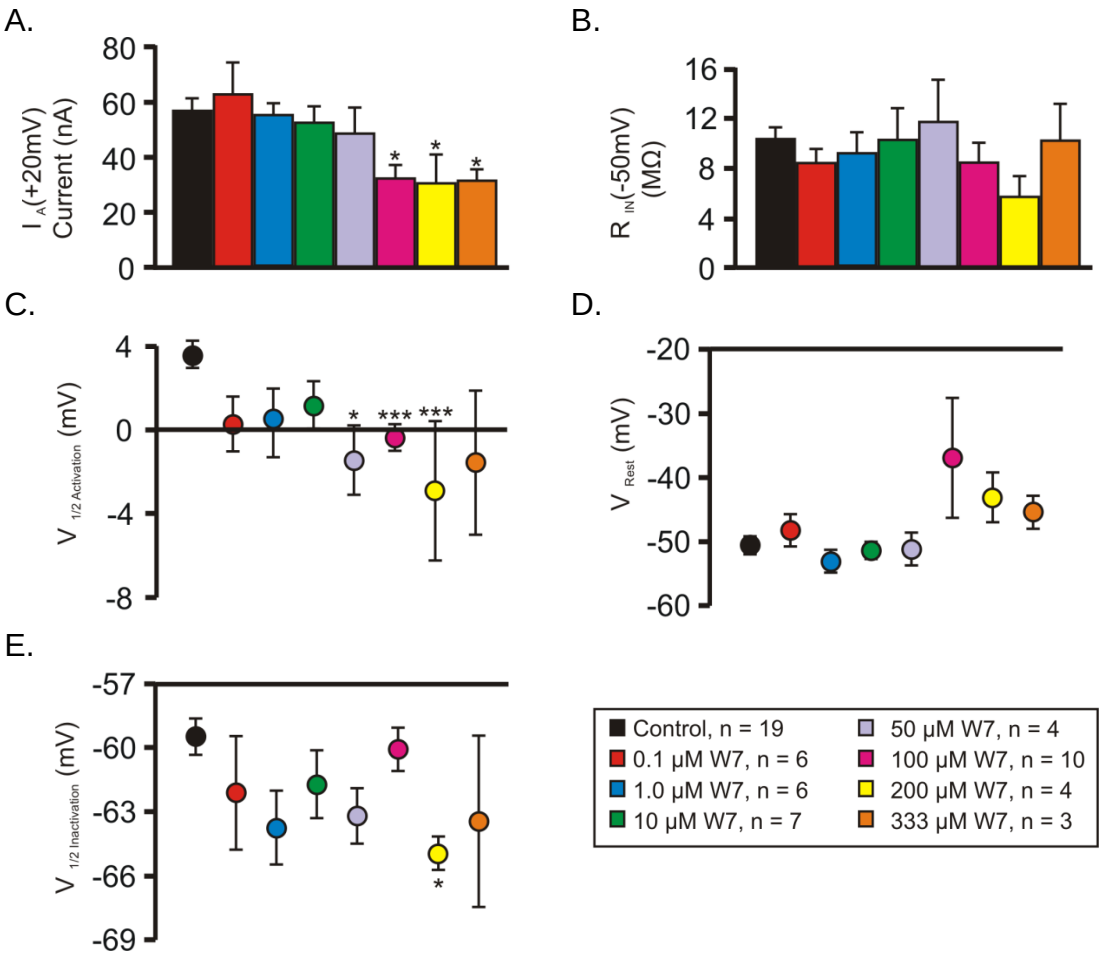


**Figure G4.2. The Calmodulin Inhibitor W7 Alters $I_A$ Amplitude, Activation and Inactivation but does not Alter $V_{Rest}$ or $R_{IN}$ in $I_{MI}$ Recording Saline.** Saline Contained 0.1 μM TTX, 10 μM PTX, 200 μM $CdCl_2$, 5 mM CsCl and 20 mM TEA. Some error bars smaller than symbols. (A) A one-way repeated measures ANOVA showed that W7 significantly decreased $I_A$ at +20 mV [W7; F (7, 33) = 7.037, p = 3.723 x $10^{-5}$. ] (B) A one-way repeated measures ANOVA showed that W7 did not significantly alter $R_{IN}$ at -50 mV [W7; F (7, 33) = 1.988, p = 0.087.] (C) A one-way repeated measures ANOVA showed that W7 significantly altered $I_A$ $V_{1/2}$ activation [W7; F (7, 33) = 8.188, p = 9.09 x x$10^{-6}$.] (D) A one-way repeated measures ANOVA showed that W7 did not significantly alter $V_{Rest}$ [W7; F (7, 33) = 2.061, p = 0.076.] (D) A one-way repeated measures ANOVA showed that W7 did significantly alter $I_A$ $V_{1/2}$ inactivation [W7; F (7, 33) = 3.677, p = 0.005.]

*Effects of BAPTA-AM incubations on ionic currents, $V_{Rest}$ and $R_{IN}$*

As BAPTA-AM did not affect proctolin-induced $I_{MI}$, we wanted to find out whether BAPTA-AM affected other properties of LP cells. As shown in Figure G4.3, in $I_{MI}$ recording saline, 1-2 hour incubations in BAPTA-AM significantly hyperpolarized $V_{1/2}$ inactivation [BAPTA-AM; $F(3, 9) = 13.628$, $p = 0.013$.], but did not affect $I_A$ activation or amplitude at +20 mv, $R_{IN}$ or $V_{Rest}$. When incubated overnight and these properties were measured in 0.1 µM TTX, as shown in Figure G4.4, a one-way ANOVA showed that BAPTA-AM decreased $I_A$ maximal conductance [BAPTA-AM; $F(2, 11) = 4.669$, $p = 0.034$]. Although we expected to see reduced transient $I_{HTK}$, this did not occur. This is consistent with the lack of $I_{HTK}$ reduction after BAPTA-AM application reported by Randsell et al., (2012) in the cardiac ganglion (Ransdell et al., 2012). Similarly, when these overnight incubated cells were measured in $I_{MI}$ recording saline, $I_A$ at +20 mV was reduced and $V_{1/2}$ inactivation was hyperpolarized (Figure G4.5). Another support that BAPTA-AM was working is shown in Figure G4.6, which shows that overnight incubation reduced the size of the largest detected PY→LP synapse [BAPTA-AM; $F(2, 12) = 5.889$, $p = 0.012$]. These results suggest that BAPTA-AM was active in this system.

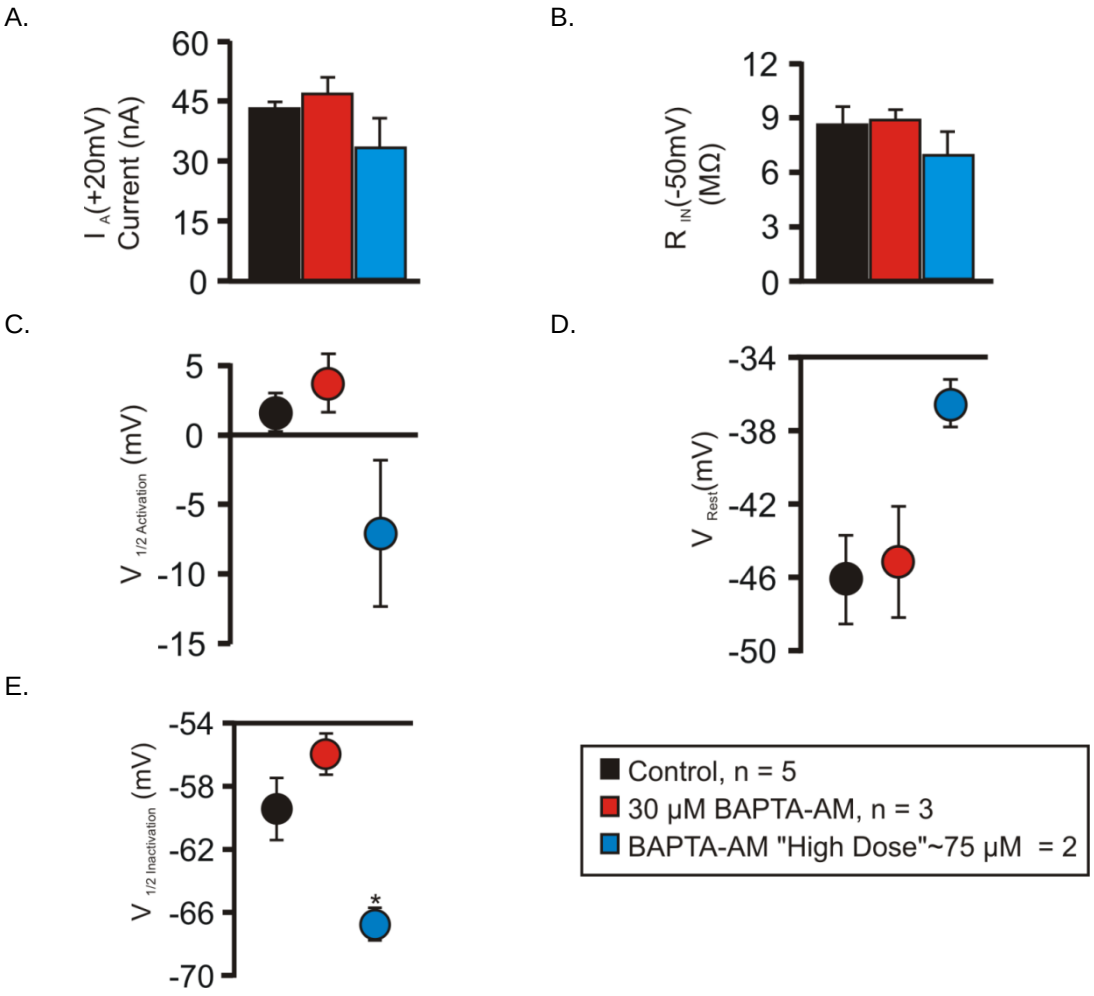


**Figure G4.3. 1-2 Hour Incubations of BAPTA-AM May Hyperpolarize IA V1/2 Inactivation but Do Not Affect Other IA Parameters, RIN or VRest.** Saline Contained 0.1 μM TTX, 10 μM PTX, 200 μM $CdCl_2$, 5 mM CsCl and 20 mM TEA. We noticed significant precipitation at concentrations of BAPTA-AM higher than 50 μM, thus these concentrations were grouped into a 'high dose condition' (1 prep at 50 μM and 1 prep at 100 μM) for statistical analysis. Average incubation time 105 minutes. (A) A one-way repeated measures showed that BAPTA-AM did not significantly affect $I_A$ at + 20 mV [BAPTA-AM; $F(3, 9) = 0.934$, $p = 0.484$.] (B) A one-way repeated measures showed that BAPTA-AM did not significantly affect $R_{IN}$ at -50 mV [BAPTA-AM; $F(3, 9) = 1.981$, $p = 0.283$.] (C) A one-way repeated measures showed that BAPTA-AM did not significantly affect $I_A$ $V_{1/2}$ activation [BAPTA-AM; $F(3, 9) = 4.155$, $p = 0.137$.] (D) A one-way repeated measures showed that BAPTA-AM did not significantly affect $V_{Rest}$ [BAPTA-AM; $F(3, 9) = 1.553$, $p = 0.344$.] (E) A one-way repeated measures showed that BAPTA-AM did significantly affect $V_{1/2}$ inactivation [BAPTA-AM; $F(3, 9) = 13.628$, $p = 0.013$.] Error bars are SEM. Tukey test ; *, $p < 0.05$.

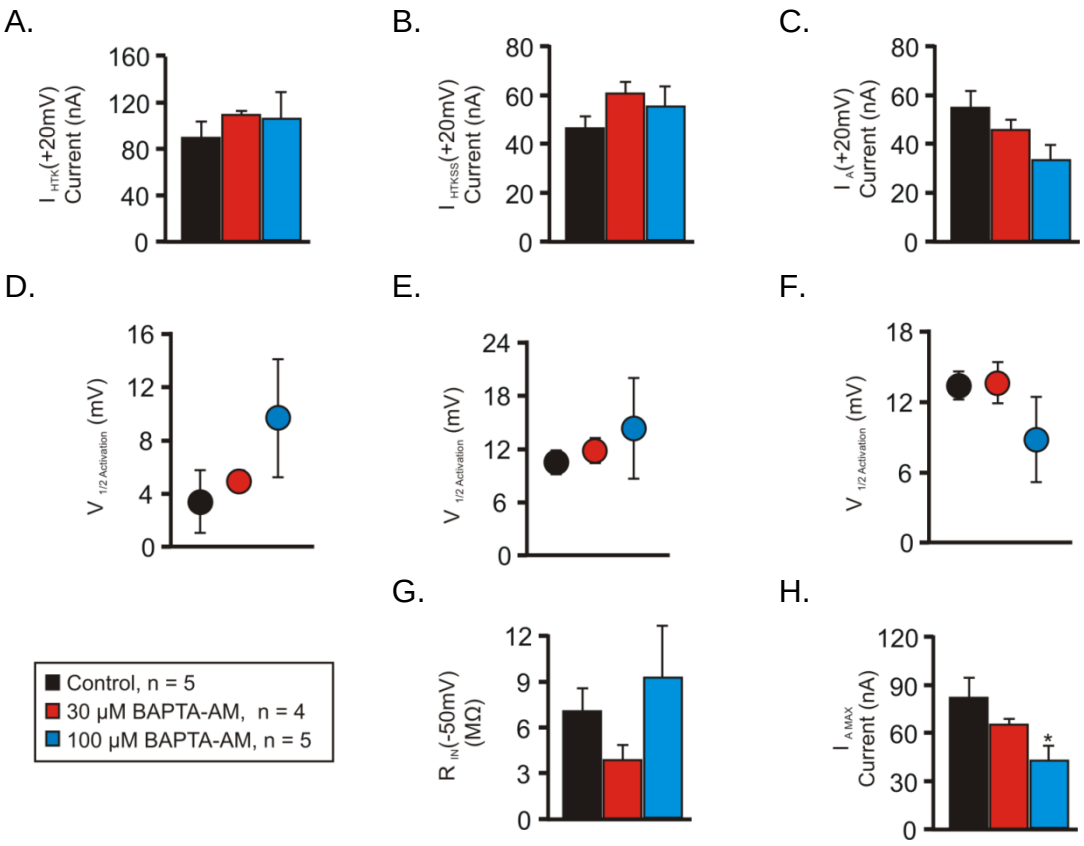


**Figure G4.4. Overnight Incubation in BAPTA-AM Decreases $I_A$ Max, but Does not Affect Other Properties Measured.** Preparations were incubated overnight in normal saline or the same in different concentrations of BAPTA-AM. When currents were measured saline contained 0.1 µM TTX. Some error bars smaller than symbols. (A) A one-way ANOVA showed that BAPTA-AM did not significantly change transient $I_{HTK}$ at +20 mV [BAPTA-AM; F (2, 11) = 0.404, p = 0.677]. (B) A one-way ANOVA showed that BAPTA-AM did not significantly change steady state $I_{HTK}$ at +20 mV [BAPTA-AM; F (2, 11) = 1.387, p = 0.290]. (C) A one-way ANOVA showed that BAPTA-AM did not significantly change $I_A$ at +20 mV [BAPTA-AM; F (2, 11) = 3.522, p = 0.066]. (D) A one-way ANOVA showed that BAPTA-AM did not significantly change transient $I_{HTK}$ $V_{1/2}$ activation [BAPTA-AM; F (2, 11) = 1.148, p = 0.352]. (E) A one-way ANOVA showed that BAPTA-AM did not significantly change steady state $I_{HTK}$ $V_{1/2}$ activation [BAPTA-AM; F (2, 11) = 0.305, p = 0.743]. (F) A one-way ANOVA showed that BAPTA-AM did not significantly change $I_A$ $V_{1/2}$ activation [BAPTA-AM; F (2, 11) = 1.194, p = 0.340]. (G) A one-way ANOVA showed that BAPTA-AM did not significantly change $R_{IN}$ at -50 mV [BAPTA-AM; F (2, 11) = 1.341, p = 0.301]. (H) A one-way ANOVA showed that BAPTA-AM significantly changed $I_{A\ MAX}$ [BAPTA-AM; F (2, 11) = 4.669, p = 0.034].Error bars are SEM. Tukey test; *, $p < 0.05$.

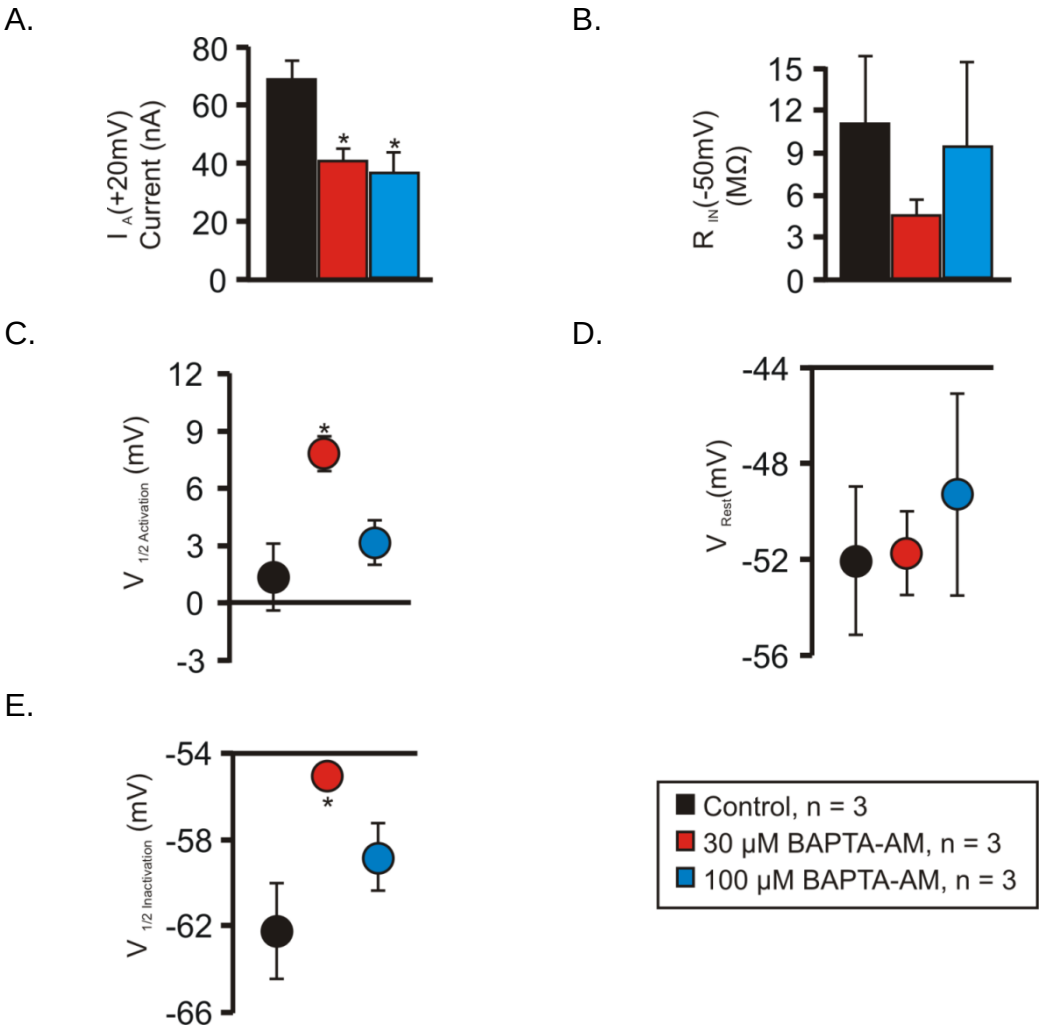


**Figure G4.5. Overnight Incubation with BAPTA-AM Reduces $I_A$, and Hyperpolarizes $I_A$ $V_{1/2}$ Inactivation in $I_{MI}$ Recording Saline.** Preparations were incubated overnight in normal saline or the same in different concentrations of BAPTA-AM. When currents were measured saline contained 0.1 μM TTX, 10 μM PTX, 200 μM $CdCl_2$, 5 mM CsCl and 20 mM TEA. Some error bars smaller than symbols.(A) A one-way ANOVA showed that BAPTA-AM significantly reduced $I_A$ at +20 mV [BAPTA-AM; F (2, 6) = 8.710, p = 0.017.] (B) A one-way ANOVA showed that BAPTA-AM did not significantly alter $R_{IN}$ at -50 mV [BAPTA-AM; F (2, 6) = 0.613, p = 0.573.] (C) A one-way ANOVA showed that BAPTA-AM significantly altered $I_A$ $V_{1/2}$ activation [BAPTA-AM; F (2, 6) = 7.479, p = 0.023.] (D) A one-way ANOVA showed that BAPTA-AM did not significantly alter $V_{Rest}$ [BAPTA-AM; F (2, 6) = 0.230, p = 0.801.] (E) A one-way ANOVA showed that BAPTA-AM significantly altered $I_A$ $V_{1/2}$ inactivation [BAPTA-AM; F (2, 6) = 5.255, p = 0.048.]Error bars are SEM. Tukey test; *, $p < 0.05$.

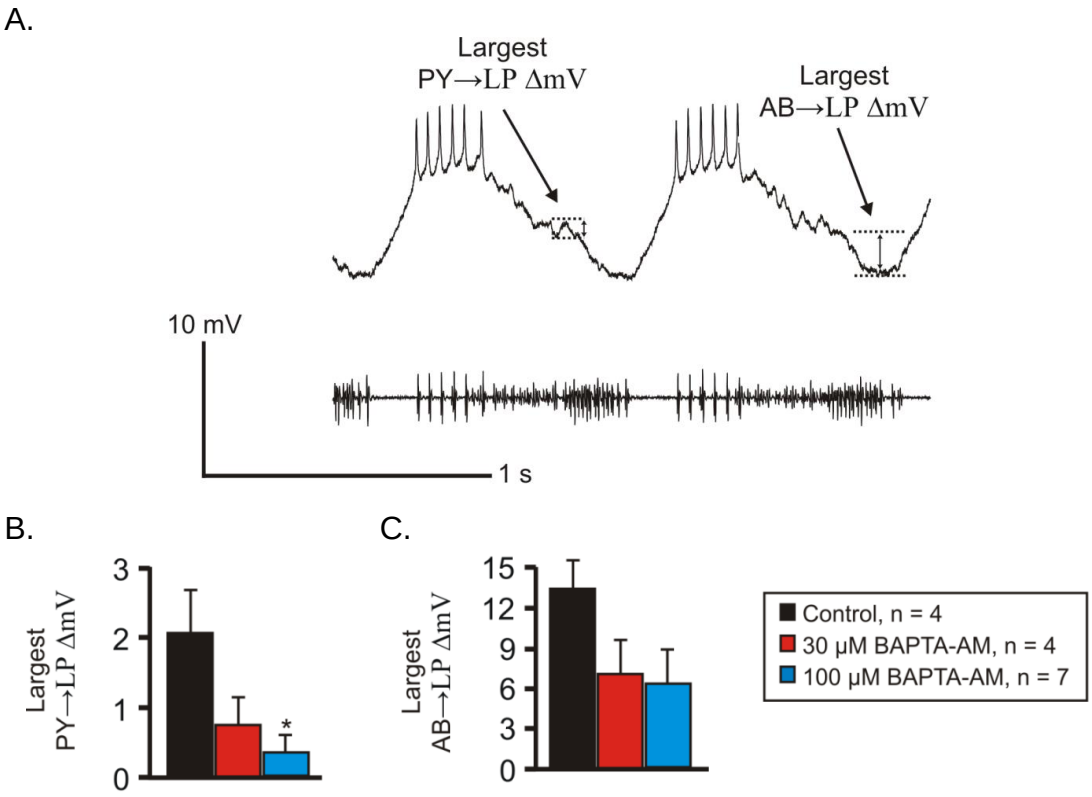


**Figure G4.6. Overnight Incubation In BAPTA-AM Reduces but does not Abolish Synapses.** Experiment in normal saline after overnight incubation in different concentrations of BAPTA-AM. (A) Quantification method of either largest synapse from PY or largest synapse from AB. (B) A one-way ANOVA showed that BAPTA-AM significantly reduced largest PY→LP synapse [BAPTA-AM; $F(2, 12) = 5.889$, $p = 0.012$] (C) A one-way ANOVA showed that BAPTA-AM did not significantly reduce largest AB→LP synapse [BAPTA-AM; $F(2, 12) = 2.190$, $p = 0.155$]. Error bars are SEM. Tukey test; * $p < 0.05$.

*CALP1 did not affect transient and steady state $I_{HTK}$, $I_A$, $V_{Rest}$, or $R_{IN}$.*

As CALP1, did not affect proctolin-induced $I_{MI}$, we wanted to determine whether this drug was effective in our system. As illustrated in Figures G4.7-G4.9, CALP1 did not affect $I_{HTK}$, $I_A$, $R_{IN}$ or $V_{Rest}$ in either incubation condition (overnight vs 1-2 hours), or measurement solution (0.1 µM TTX or $I_{MI}$ recording saline). We also tried pressure injection of CALP1, which had no effect on proctolin-induced $I_{MI}$ voltage dependence (Figure A4.1). Although we tried to test this substance as thoroughly as possible, we have no evidence to say definitively whether CALP1 was having an effect or not.

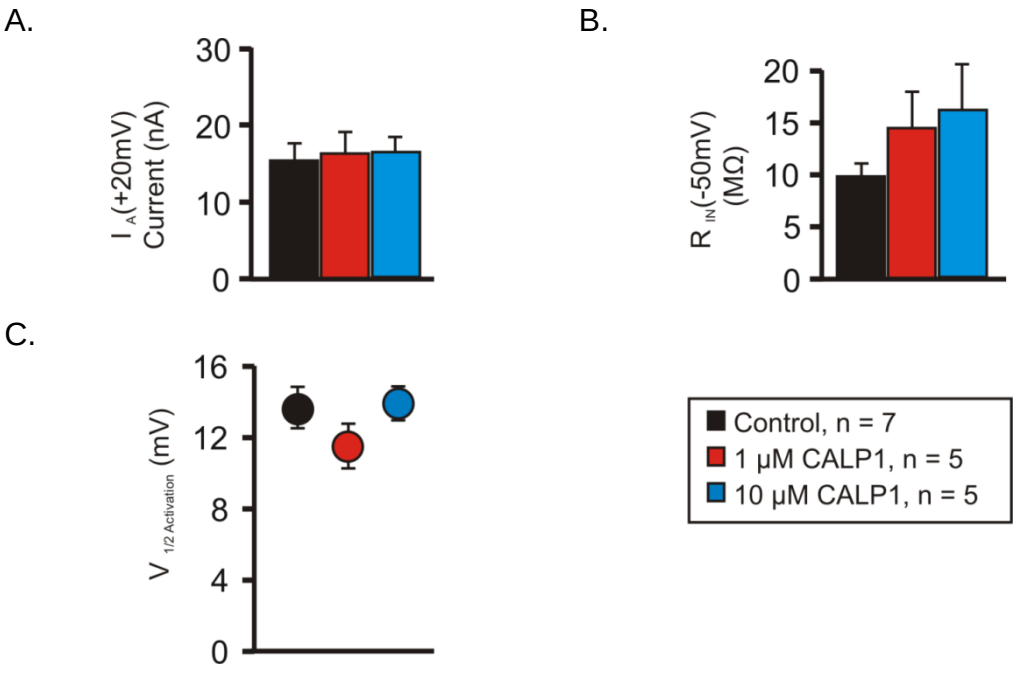


**Figure G4.7. 1-2 Hour Incubations of up to 10 µM CALP1 Did Not Affect $I_A$ at +20 mV or $R_{IN}$ at -50 mV.** 2 mM low calcium saline contained 0.1 µM TTX, 10 µM PTX, 200 µM $CdCl_2$, 5 mM CsCl and 20 mM TEA supplemented with 0.1% BSA. (A) A one-way repeated measures ANOVA showed that CALP1 did not significantly alter $I_A$ at +20 mV [CALP1; F (2, 8) = 0.434, p = 0.662. (B) A one-way repeated measures ANOVA showed that CALP1 did not significantly alter $R_{IN}$ at -50 mV [CALP1; F (2, 8) = 2.384, p = 0.154.] (C) A one-way repeated measures ANOVA showed that CALP1 did not significantly alter $I_A$ $V_{1/2}$ activation [CALP1; F (2, 8) = 0.335, p = 0.725.] Error bars are SEM.

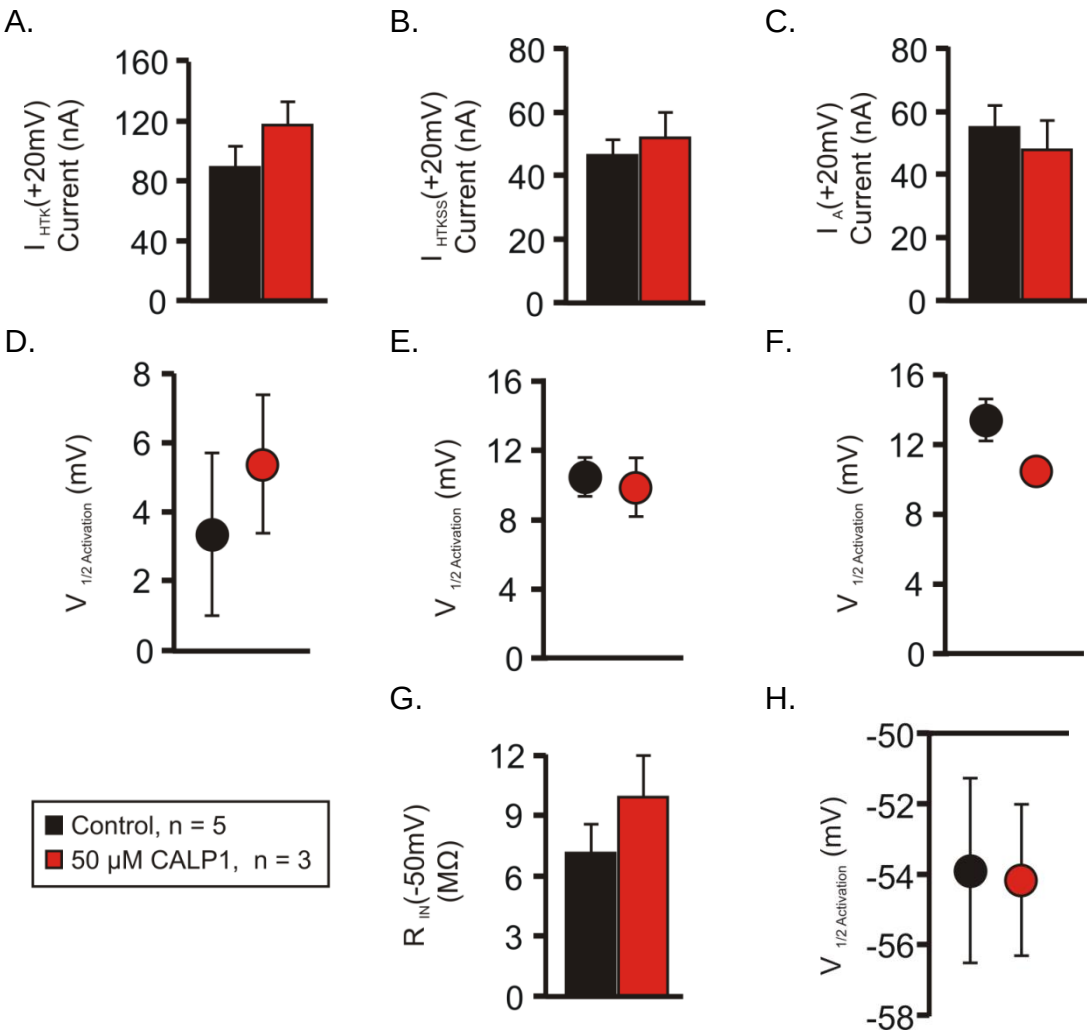


**Figure G4.8. Overnight Incubations in CALP1 do not Affect Ionic Currents, $V_{Rest}$, or $R_{IN}$ when Measured in TTX.** Preparations were incubated overnight in normal saline (**Black**) or the same with 50 μM CALP1 (**Red**). Currents were measured in the presence of 0.1 μM TTX. (A) A t-test showed that CALP1 did not alter transient $I_{HTK}$ at +20 mV [t (6) = -1.345, p = 0.227.] (B) A t-test showed that CALP1 did not alter steady state $I_{HTK}$ at +20 mV [t (6) = -0.599, p = 0.571.] (C) A t-test showed that CALP1 did not alter $I_A$ at +20 mV [t (6) = 0.623 , p = 0.556.] (D) A t-test showed that CALP1 did not alter transient $I_{HTK}$ $V_{1/2}$ activation [t (6) = -1.345, p = 0.227.] (E) A t-test showed that CALP1 did not alter steady state $I_{HTK}$ $V_{1/2}$ activation [t (6) = 0.316, p = 0.763.] (F) A t-test showed that CALP1 did not alter steady state $I_A$ $V_{1/2}$ activation [t (6) = 1.849, p = 0.114.]. (G) A t-test showed that CALP1 did not alter $R_{IN}$ at -50 mV [t (6) = -1.194 , p = 0.277).] (H) A t-test showed that CALP1 did not alter $V_{Rest}$ [t (6) = 0.0692 , p = 0.947).] Error bars are SEM.

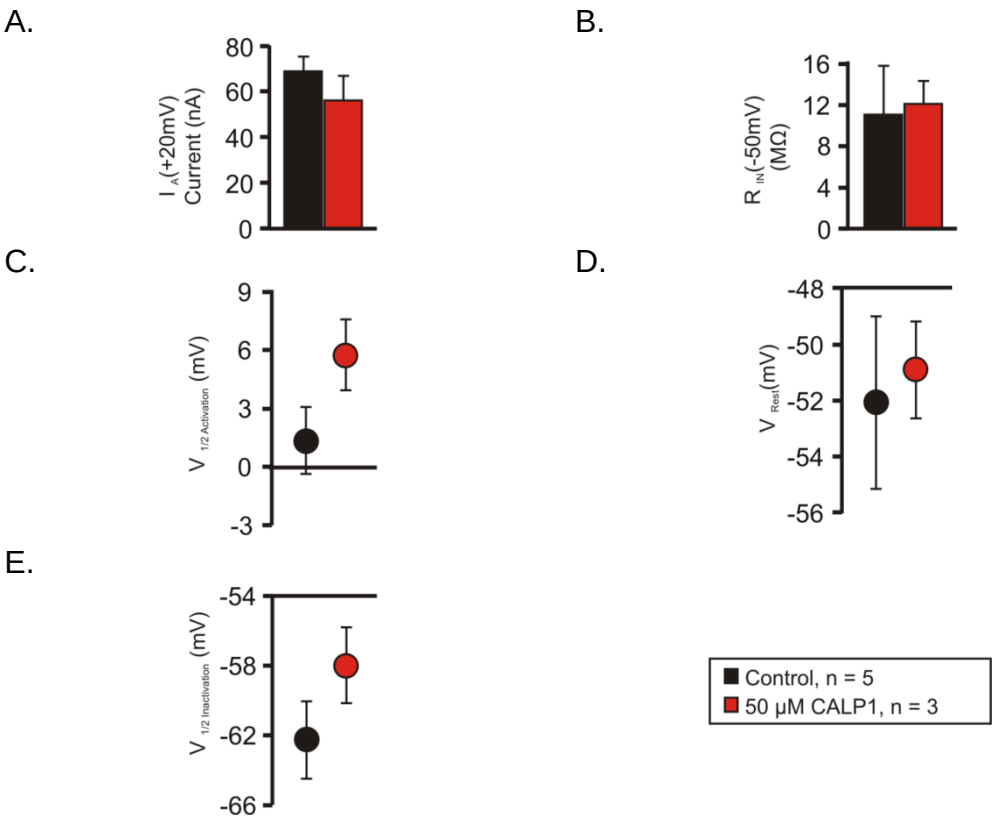


**Figure G4.9. Overnight Incubations in CALP1 do Not Affect Ionic Currents, $R_{IN}$ or $V_{Rest}$.** Preps were incubated in either normal saline or the same plus 50 μM CALP1. At time of current measurement, saline contained 0.1 μM TTX, 10 μM PTX, 200 μM $CdCl_2$, 5 mM CsCl and 20 mM TEA. (A) A t-test showed that CALP1 did not significantly alter $I_A$ at +20 mV [t (4) = 1.059, 0.349. (B) A t-test showed that CALP1 did not significantly alter $R_{IN}$ at -50 mV [t (4) = -0.195, 0.855.] (C) A t-test showed that CALP1 did not significantly alter $I_A$ $V_{1/2}$ activation [t (4) = -1.805, 0.145.] (D) A t-test showed that CALP1 did not significantly alter $V_{Rest}$ [t (4) = -0.330, 0.758.] (E) A t-test showed that CALP1 did not significantly alter $I_A$ $V_{1/2}$ inactivation [t (4) = -1.368, 0.243.] Error bars are SEM.

*Currents in A21387 and caffeine were not measured due to instability*

We did not measure ionic currents in low calcium for A21387 and caffeine as it was observed that cells were unstable under these conditions. A few cells with A21387 seemed to depolarize with application but this was not surprising nor was it statistically significant (VRest before = -35.75 ± 2.23 mV, Vrest in 0.1 µM A21387 = -32.25 ± 3.35mV [paired t-test; t (4) = -2.646, p = 0.076]. $R_{IN}$ measured at Vrest, however, was unchanged, $R_{IN}$ before = 6 ± 0.5 MΩ, $R_{IN}$ in 0.1 µM A21387 = 5.875 ± 0.4 MΩ [paired t-test; t (4) = 0.200 , p = 0.429]. The finding that A21387 significantly reduced proctolin-induced $I_{MI}$ slope suggests that this agent was active.

*Cyclosporine may increase maximal $I_A$ current but did not significantly affect other measured properties.*

As shown in Figure G4.10, cyclosporine did increase $I_A$ maximal conductance in the high dose condition. This and previously mentioned literature (Ransdell et al., 2012) suggests cyclosporine was having an effect in this system.

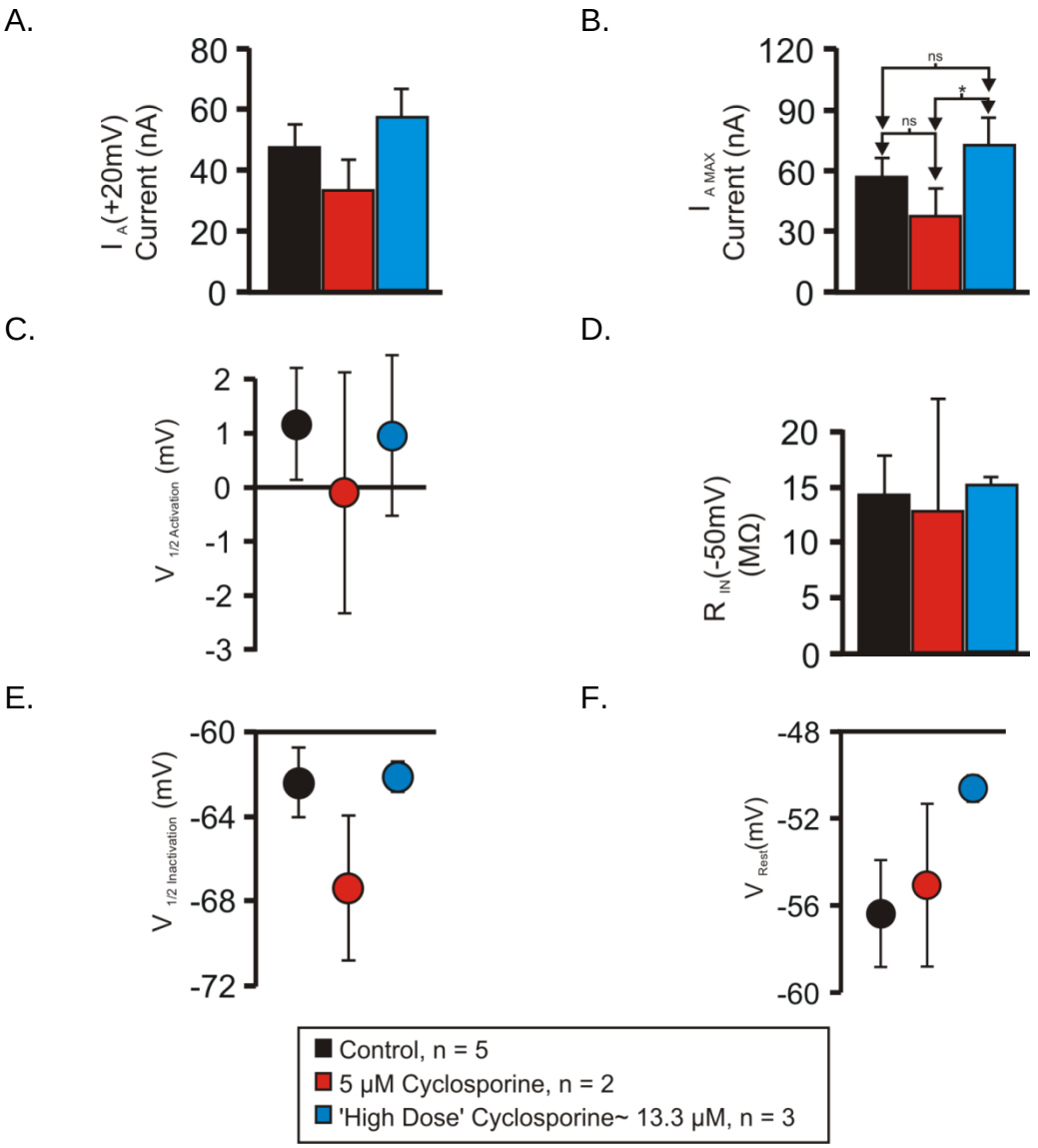


**Figure G4.10. The Calcineurin Inhibitor Cyclosporine May Increase Maximal $I_A$ Current.** Saline contained 0.1 μM TTX, 10 μM PTX, 200 μM $CdCl_2$, 5 mM CsCl and 20 mM TEA. (A) A one-way repeated measures ANOVA showed that cyclosporine did not affect $I_A$ at +20 mV [Cyclosporine; F (2, 3) = 3.24, p = 0.178] (B) A one-way repeated measures ANOVA showed that cyclosporine did affect $I_A$ maximal current [Cyclosporine; F (2, 3) = 10.309, p = 0.045] (C) A one-way repeated measures ANOVA showed that cyclosporine did not affect $I_A$ $V_{1/2}$ activation [Cyclosporine; F (2, 3) = 0.163, p = 0.857] (D) A one-way repeated measures ANOVA showed that cyclosporine did not affect $R_{IN}$ at -50 mV [Cyclosporine; F (2, 3) = 0.253, p = 0.792] (E) A one-way repeated measures ANOVA showed that cyclosporine did not affect $I_A$ $V_{1/2}$ Inactivation [Cyclosporine; F (2, 3) = 3.968, p = 0.144] (F) A one-way repeated measures ANOVA showed that cyclosporine did not affect $V_{Rest}$ [Cyclosporine; F (2, 3) = 1.703, p = 0.321] Error bars are SEM. Tukey; *, $p < 0.05$.

*NPS-2143 does not affect measured $I_A$ properties, $R_{In}$, or $V_{Rest}$.*

In contrast to its effect on proctolin-induced $I_{MI}$ voltage dependence, NPS-2143 did not show any significant effect on $I_A$ properties, $R_{IN}$ or $V_{Rest}$ (Figure G4.11). The finding that proctolin-induced $I_{MI}$ voltage dependence is modulated by NPS-2143 suggests that this agent was active in our system.

*Effects of Dynasore*

As dynasore is an inhibitor of dynamin and endocytosis, one might expect that the surface area of the membrane may grow. With increased surface area, one might expect increased capacitance. We therefore measured capacitance in current clamp according to the fitting procedures described by Golowasch et el., (2009). These authors found that current clamp measurements are most accurate for estimating capacitance in non-isopotential cells (Golowasch et al., 2009). A paired t-test showed that a 20 minute incubation in 33 µM dynasore was not sufficient to alter capacitance [ $\mu_{Before}$ = 69.5 ± 17.9 nF, $\mu_{After}$ = 67.4 ± 18.1 nF; t (17) = 0.104, p = 0.918). The modulation of W7-induced increase in slope suggests that dynasore was working in our system.

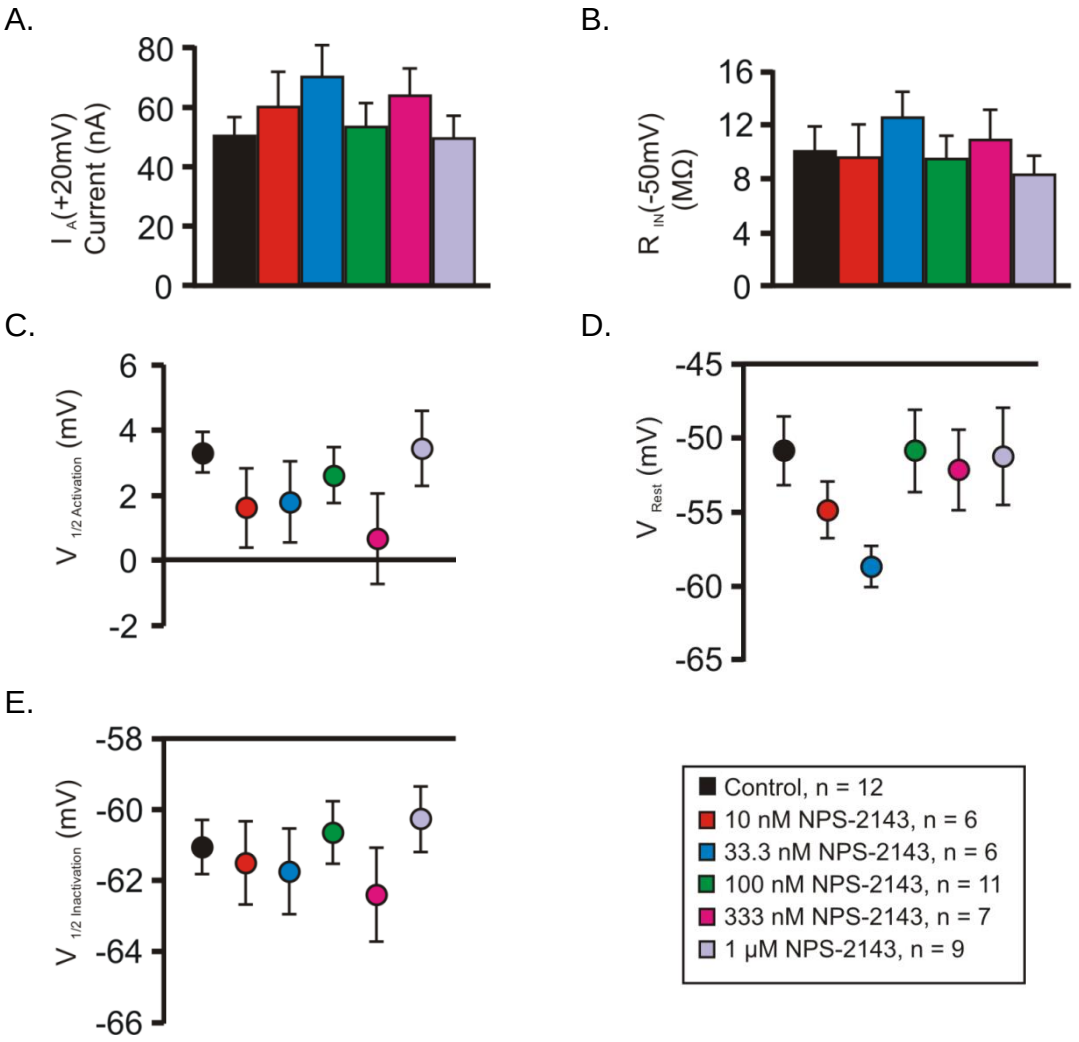


**Figure G4.11.. The CaSR Antagonist NPS-2143 does not Modulate $I_A$ Properties, VRest or $R_{IN}$.** Saline contained 0.1 µM TTX, 10 µM PTX, 200 µM CdCl2, 5 mM CsCl and 20 mM TEA. (A) A one-way repeated measures ANOVA showed that NPS-2143 did not significantly change $I_A$ at +20 mV [NPS-2143; F (5, 34) = 0.916, p = 0.482.] (B) A one-way repeated measures ANOVA showed that NPS-2143 did not significantly change $R_{IN}$ at -50 mV [NPS-2143; F (5, 34) = 0.958, p = 0.457.] (C) A one-way repeated measures ANOVA showed that NPS-2143 did not significantly change $I_A$ $V_{1/2}$ activation [NPS-2143; F (5, 34) = 0.724, p = 0.610.] (D) A one-way repeated measures ANOVA showed that NPS-2143 did not significantly change $V_{Rest}$ [NPS-2143; F (5, 34) = 1.526, p = 0.208.] (E) A one-way repeated measures ANOVA showed that NPS-2143 did not significantly change $I_A$ $V_{1/2}$ inactivation [NPS-2143; F (5, 34) = 0.628, p = 0.680.] Error bars are SEM.

# Chapter 5: Discussion

## 5.1. Activation

In this thesis, the question was posed whether the proctolin receptor was a G-protein and whether this receptor signaled to $I_{MI}$ directly or through an intermediary signaling pathway. It was hypothesized that the proctolin receptor was a G-protein coupled receptor that activated another pathway rather than being directly coupled to its effector. Our findings, as shown by our experiments with pertussis toxin, GDP-βS and GTP-γS, suggest that proctolin-induced $I_{MI}$ is coupled to a G-protein whose sensitivity to pertussis is modulated by external calcium. We found, as shown by our calmidazolium and dantrolene results, that $I_{MI}$ appears to signal through intracellular calcium, and likely through a calmodulin mediated mechanism, specifically, calmodulin-dependent kinases as supported by our calmidazolium, staurosporine, KN-93 and ML-7 results. A model is proposed for proctolin-induced $I_{MI}$ based on calmodulin signaling as illustrated in Figure 3.28 & 3.29.

*Model of proctolin-induced $I_{MI}$ signaling provides a potential mechanism to explain convergence.*

Although our hypothesis, that proctolin-induced $I_{MI}$ is activated by a G-protein activated signaling pathway sounds trivial on the surface, we believe that it is not. The demonstration of convergence of six neuromodulators onto the same current by Swensen and Marder (2000), suggested to us that these neuromodulators probably converge on a common intermediate. Therefore, the first step of testing this larger hypothesis is to outline the mechanism of at least one neuromodulator. The experimental results and model proposed here for proctolin-induced $I_{MI}$ identifies such a mechanism: calcium, calmodulin-activated kinases and G-protein signaling as potential points for the convergence of neuromodulators. This model provides the first step towards answering this larger issue. Our identification of intracellular calcium and calmodulin-activated kinases as being involved in proctolin-induced $I_{MI}$ signaling, suggests that both of these points could represent points of convergence which future studies can examine.

## Broader implications

As proctolin-induced $I_{MI}$ activates calcium and calmodulin-activated proteins, other neuromodulators might also activate these pathways. This has broader implications for the neuromodulation of neural networks in general. This is supported by the demonstration that currents with regions of negative slope conductance can produce a simple yet comprehensive mechanism by which neuromodulators transition neurons from non-oscillating to oscillating states (Zhao et al., 2010). Combined with the

differential expression of receptors in different subsets of neurons in a network, these mechanisms can create distinct patterns of activity (Swensen and Marder, 2001) without invoking a complexity of different signaling mechanisms.

*Future work*

Future work on this mechanism should follow two distinct directions. First, this research can be decomposed further by examining how these kinases activate effectors responsible for proctolin-induced $I_{MI}$. This can be done by focusing upon methods that make use of newly developed tools at the molecular level, such as the recently sequenced *Cancer borealis* transcriptome. We predict that dsRNA knockout of CamKII, MLCK, and ER-plasma membrane-binding proteins can be expected to more finely detail the nature of proctolin-induced $I_{MI}$ signaling. Specifically, we predict that an ML-7-sensive crab homolog of MLCK is expressed in pyloric network neurons. Further, we predict that when this MLCK-like enzyme is over-expressed, it may lead to increased proctolin-induced $I_{MI}$. In contrast, the injection of dsRNAs to knock out the MLCK-like enzyme function should result in the reduction or elimination of proctolin-induced $I_{MI}$. Similar results should be observed after manipulation of crab CamKII, which is known to be expressed in (lobster) pyloric neurons (Withers et al., 1998) and can also be found in the crab transcriptome (not shown here). Second, another important direction for this research is the integration of these findings into other research exploring the effect of neuromodulators on producing different patterns of network activity. By first replicating (or falsifying) these findings for other neuromodulators, the hypothesis first inspired by

Swensen and Marder (2000) that neuromodulators converge to a common current, and therefore, a common intermediary, can be examined. The answer to this question, and the intermediates identified, have important implications not only for network activity and oscillatory transitions, but also for understanding possible mechanisms of recovery of rhythmic activity (Thoby-Brisson and Simmers, 2000; Luther et al., 2003) after removal of neuromodulators as discussed in Chapter 1. This thesis was but a small step, towards answering these bigger questions.

## Consistency of findings

The finding that proctolin-induced $I_{MI}$ is mediated by a GPCR is consistent with literature reviewed in Chapter 1, however, especially in the context of proctolin-induced $I_{MI}$'s signaling via the ubiquitous elevation of intracellular calcium levels, we predict that other non-GPCR's may modulate or produce $I_{MI}$, provided that they sufficiently modulate intracellular calcium levels. The model provided, although still incomplete, is more satisfactory than the alternative mechanism of direct-GPCR coupling for two reasons: First, it provides a more coherent mechanism by which the activation of different neuromodulator receptors can converge onto the same target (i.e. $I_{MI}$). Second, it will provide a starting point to examine other processes associated with recovery of rhythmic activity in chronically decentralized preparations. It is known that these processes require transcription (Thoby-Brisson and Simmers, 2000), but it is

unknown how the deprivation of neuromodulators, such as proctolin, begins this process.

*Some limitations:*

As reported in Chapters 3 and 4, many of the pharmaceutical agents used in this study had not been employed in this system before. Nevertheless, although this seemed to be problematic for the interpretation of results, and increased the technical difficulties in performing these experiments, it makes the results all the more important. We take this position because although the pyloric rhythm in the STG is an excellent model with a well-established record for the study of neuromodulation of conditional oscillators, precious little is known of the efficacy of pharmaceutical agents that modulate signal transduction in this system versus comparable model systems in vertebrates or even other invertebrates. This, in turn, is why much effort was put into characterizing secondary effects of these substances as positive controls of their efficacy (Appendices of Chapters 3 and 4) .

**5.2: Voltage dependence:**

The second issue addressed in this thesis was the mechanism of calcium-dependence of the voltage dependence of neuromodulator-induced $I_{MI}$. Although it had been hypothesized by Golowasch and Marder (1992) that $I_{MI}$ voltage dependence may be due to an NMDA-like mechanism of extracellular calcium block of the modulator-activated channels, we found this hypothesis to be unsatisfactory to explain both their findings (dependence on calcium), and the findings of Swensen and Marder (2000) (bath application of the calmodulin inhibitor W7 altered neuromodulator-induced voltage dependence). Our original starting hypothesis to explain $I_{MI}$ voltage-dependence involved an intracellular calcium effect via activation of calmodulin or calmodulin-activated proteins. Although this activated-calmodulin hypothesis of $I_{MI}$ voltage dependence was supported by application of calmodulin and calmodulin-activated kinase inhibitors in normal calcium, calmodulin activators in the presence of low calcium, failed to rescue $I_{MI}$ voltage dependence. This suggested that although calmodulin was necessary for $I_{MI}$ voltage dependence, it was not sufficient. We therefore proposed an alternative hypothesis that LP cells actively sense extracellular calcium; this calcium activates a calcium sensing receptor (CaSR), which in turn provides a voltage-dependent signal to $I_{MI}$. This hypothesis explains the previously established

dependence on external calcium and dependence on internal calmodulin since it is known that CaSR requires in other systems requires bound calmodulin for stable surface expression (Huang et al., 2010). This could not be explained by our previous models, as the NMDA-hypothesis predicts no requirement for intracellular calcium. Similarly, the activated calmodulin hypothesis, predicts rescue of voltage dependence by calmodulin activators in low calcium. In contrast, the CaSR hypothesis explained extracellular calcium dependence as calcium is its ligand thus explaining the low calcium reduction in voltage dependence. Interestingly, it also explains why calmodulin activators do not restore voltage dependence in low calcium: while activated calmodulin stabilizes CaSR surface expression, it does nothing to change the reduction in extracellular calcium. Our results provide direct support for this hypothesis with perhaps the strongest support coming from the finding that preincubation in endocytosis inhibitors blocked W7 induced loss of voltage dependence. All these results are incorporated into our schematic description of our results and emerging shown in Figure 4.31.

## Broader implications

As mentioned previously, there is a growing literature documenting the importance of CaSR in regulating neuronal properties (Lu et al., 2009; Vyleta and Smith, 2011). This is increasingly important because although calcium is ubiquitously recognized as an important intracellular second messenger (Deleon et al., 1995; Lnenicka et al., 1998; Van Eldik and Watterson, 1998; Shiells and Falk, 1999; El Far et al.,

2001b; Hille, 2001; Gomperts et al., 2002; Alberts, 2008; Blazer et al., 2010)[41], modulator of biophysical properties (Steinbach et al., 1944; Frankenhaeuser and Hodgkin, 1957; Bezanilla and Armstrong, 1972; Armstrong, 1974; Yamamoto et al., 1984; Leibowitz et al., 1986; Nilius, 1988; Armstrong and Cota, 1991; Armstrong, 1999; Zhang et al., 2012a) and synaptic transmission (Dale, 1939; Kandel et al., 1991; Johnston and Wu, 1995; Purves, 1997; Hille, 2001; Squire, 2003)[42], there is relatively little acknowledgement of CaSR as an extracellular modulator, itself, outside of bone, parathyroid and liver (probably due to complications in studying the many confounding effects). Further, despite the literature reviewed in Chapter 1, we could find no precedent for extracellular calcium modulating voltage dependence of a neuromodulator-induced current by the mechanism proposed here. Therefore, this may represent an altogether novel mechanism for the regulation of voltage dependence. As voltage dependence is the crucial determinant of negative slope, and negative slope has been shown to be essential for burst generation and neuromodulation both in this system (Zhao et al., 2010; Bose et al., 2014b), and others (Kehoe, 1990; Bayliss et al., 1992; Talley et al., 2000; Del Negro et al., 2002; Brickley et al., 2007; Pang et al., 2009; Xu et al., 2009), this finding could have profound consequences for how neuromodulation is thought of on a more general level. For example, based upon our unexpected finding that gallein affected proctolin-induced $I_{MI}$ voltage dependence

[41] These references were truncated in favor of non-primary sources as the amount of primary papers reviewed in this thesis that have shown intracellular calcium signaling to be involved in neuromodulator signaling, calmodulin dependent pathways and PLC-dependent pathways would take many pages. See Chapter 1 review of invertebrate signaling pathways.

[42] Dale is the only primary source provided due to this being so well-established

without affecting activation, we predict that other neuromodulators may exist that act exclusively on the voltage dependence of other neuromodulators.

## Future work

Although we have shown several key pieces of evidence to answer our questions as thoroughly as possible, the effects of pharmacological agents are always open to interpretation. Therefore, it is suggested that now that CaSR signaling has been shown to be likely involved in this system, studies both confirming its existence by using molecular-genetic methods, and examining its functional consequences are recommended. To see whether there is any support for CaSR even being present in *C. borealis*, we did an amino acid BLAST of the crab transcriptome (provided by D. Schulz, unpublished work), using the amino acid sequence for human CaSR (accession P41180). This BLAST showed a match in the crab transcriptome with 50% homology to the human sequence and an e-score of $5 \times 10^{-104}$. Taking this sequence from the crab, and running an amino acid BLAST on the crustacean *Daphnia pulex*, we found six hits with e-values = 0, and 40-60% homology. All of these encode mGluRs, supporting our contention that CaSR may be present in the crab since mGluRs are in the same GPCR family (III) as CaSR (Huang et al., 2010). This not only lends support to our claim that CaSR is present, but also suggests interesting future experiments. By injecting and overexpressing capped and polyadenylated versions of mRNAs derived from these sequences or KO of these

sequences through dsRNA injections, in conjunction with simultaneous monitoring of the effect of glutamate responses and the voltage-dependence of neuromodulator-induced $I_{MI,}$ it is predicted that one of these sequences will modulate $I_{MI}$ voltage dependence. Although technically demanding, these experiments have been and will be rewarding.

# References:


Alberts B (2008) Molecular biology of the cell, 5th Edition. New York: Garland Science.

Armstrong CM (1971) Interaction of tetraethylammonium ion derivatives with the potassium channels of giant axons. J Gen Physiol 58:413-437.

Armstrong CM (1974) Ionic pores, gates, and gating currents. Q Rev Biophys 7:179-210.

Armstrong CM (1999) Distinguishing surface effects of calcium ion from pore-occupancy effects in Na+ channels. Proc Natl Acad Sci U S A 96:4158-4163.

Armstrong CM, Cota G (1991) Calcium ion as a cofactor in Na channel gating. P Natl Acad Sci USA 88:6528-6531.

Ascher P, Bregestovski P, Nowak L (1988) N-methyl-D-aspartate-activated channels of mouse central neurones in magnesium-free solutions. J Physiol 399:207-226.

Baines RA, Downer RGH (1992) Comparative-Studies on the Mode of Action of Proctolin and Phorbol-12,13-Dibutyrate in Their Ability to Contract the Locust Mandibular Closer Muscle. Archives of Insect Biochemistry and Physiology 20:215-229.

Baines RA, Walther C, Hinton JM, Osborne RH, Konopinska D (1996) Selective activity of a proctolin analogue reveals the existence of two receptor subtypes. J Neurophysiol 75:2647-2650.

Bal T, Nagy F, Moulins M (1994) Muscarinic modulation of a pattern-generating network: control of neuronal properties. J Neurosci 14:3019-3035.

Ballo AW, Keene JC, Troy PJ, Goeritz ML, Nadim F, Bucher D (2010a) Dopamine modulates Ih in a motor axon. The Journal of neuroscience : the official journal of the Society for Neuroscience 30:8425-8434.

Ballo AW, Keene JC, Troy PJ, Goeritz ML, Nadim F, Bucher D (2010b) Dopamine modulates Ih in a motor axon. J Neurosci 30:8425-8434.

Banner SE, Wood SJ, Osborne RH, Cattell KJ (1990) Tyramine antagonizes proctolin-induced contraction of the isolated foregut of the locust Schistocerca gregaria by an interaction with octopamine2 receptors. Comp Biochem Physiol C 95:233-236.

Bayliss DA, Viana F, Berger AJ (1992) Mechanisms underlying excitatory effects of thyrotropin-releasing hormone on rat hypoglossal motoneurons in vitro. Journal of neurophysiology 68:1733-1745.

Benham CD, Bolton TB, Lang RJ (1985) Acetylcholine activates an inward current in single mammalian smooth muscle cells. Nature 316:345-347.

Benson DM, Blitzer RD, Landau EM (1988) An analysis of the depolarization produced in guinea-pig hippocampus by cholinergic receptor stimulation. J Physiol 404:479-496.

Benson JA (1992) Electrophysiological Pharmacology of the Nicotinic and Muscarinic Cholinergic Responses of Isolated Neuronal Somata from Locust Thoracic Ganglia. Journal of Experimental Biology 170:203-233.

Benson JA, Levitan IB (1983) Serotonin increases an anomalously rectifying K+ current in the Aplysia neuron R15. Proc Natl Acad Sci U S A 80:3522-3525.

Berridge MJ (1989) The Albert Lasker Medical Awards. Inositol trisphosphate, calcium, lithium, and cell signaling. Jama 262:1834-1841.

Bezanilla F, Armstrong CM (1972) Negative conductance caused by entry of sodium and cesium ions into the potassium channels of squid axons. J Gen Physiol 60:588-608.

Bishop CA, Krouse ME, Wine JJ (1991a) Peptide cotransmitter potentiates calcium channel activity in crayfish skeletal muscle. J Neurosci 11:269-276.

Bishop CA, Krouse ME, Wine JJ (1991b) Peptide cotransmitter potentiates calcium channel activity in crayfish skeletal muscle. Journal of Neuroscience 11:269-276.

Blazer LL, Roman DL, Chung A, Larsen MJ, Greedy BM, Husbands SM, Neubig RR (2010) Reversible, allosteric small-molecule inhibitors of regulator of G protein signaling proteins. Mol Pharmacol 78:524-533.

Bolton TB, Zholos AV (1997) Activation of M2 muscarinic receptors in guinea-pig ileum opens cationic channels modulated by M3 muscarinic receptors. Life Sci 60:1121-1128.

Bose A, Golowasch J, Guan Y, Nadim F (2014a) The role of linear and voltage-dependent ionic currents in the generation of slow wave oscillations. Journal of computational neuroscience 37:229-242.

Bose A, Golowasch J, Guan Y, Nadim F (2014b) The role of linear and voltage-dependent ionic currents in the generation of slow wave oscillations. J Comput Neurosci 37:229-242.

Brehm P, Eckert R (1978) Calcium entry leads to inactivation of calcium channel in Paramecium. Science 202:1203-1206.

Brickley SG, Aller MI, Sandu C, Veale EL, Alder FG, Sambi H, Mathie A, Wisden W (2007) TASK-3 two-pore domain potassium channels enable sustained high-frequency firing in cerebellar granule neurons. The Journal of neuroscience : the official journal of the Society for Neuroscience 27:9329-9340.

Brown PT, Herbert P, Woodruff RI (2010) Vitellogenesis in Oncopeltus fasciatus: PLC/IP(3), DAG/PK-C pathway triggered by CaM. J Insect Physiol 56:1300-1305.

Bruice PY (2001) Organic chemistry, 3rd Edition. Upper Saddle River, N.J.: Prentice Hall.

Budde T, Meuth S, Pape HC (2002) Calcium-dependent inactivation of neuronal calcium channels. Nat Rev Neurosci 3:873-883.

Burch RM, Luini A, Axelrod J (1986) Phospholipase A2 and phospholipase C are activated by distinct GTP-binding proteins in response to alpha 1-adrenergic stimulation in FRTL5 thyroid cells. Proc Natl Acad Sci U S A 83:7201-7205.

Butera RJ, Jr., Rinzel J, Smith JC (1999) Models of respiratory rhythm generation in the pre-Botzinger complex. I. Bursting pacemaker neurons. Journal of neurophysiology 82:382-397.

Cazzamali G, Hauser F, Kobberup S, Williamson M, Grimmelikhuijzen CJ (2003) Molecular identification of a Drosophila G protein-coupled receptor specific for crustacean cardioactive peptide. Biochem Bioph Res Co 303:146-152.

Chakravarti B, Chattopadhyay N, Brown EM (2012) Signaling through the extracellular calcium-sensing receptor (CaSR). Adv Exp Med Biol 740:103-142.

Chen S, Inoue R, Ito Y (1993) Pharmacological characterization of muscarinic receptor-activated cation channels in guinea-pig ileum. Br J Pharmacol 109:793-801.

Chen Z, Lee FY, Bhalla KN, Wu J (2006) Potent inhibition of platelet-derived growth factor-induced responses in vascular smooth muscle cells by BMS-354825 (dasatinib). Mol Pharmacol 69:1527-1533.

Chen ZF, Wang H, Matsumura K, Qian PY (2012) Expression of calmodulin and myosin light chain kinase during larval settlement of the Barnacle Balanus amphitrite. PLoS One 7:e31337.

Cheng SX, Okuda M, Hall AE, Geibel JP, Hebert SC (2002) Expression of calcium-sensing receptor in rat colonic epithelium: evidence for modulation of fluid secretion. Am J Physiol Gastrointest Liver Physiol 283:G240-250.

Chung HW, Park JW, Lee EJ, Jung KH, Paik JY, Lee KH (2013) 131I-MIBG targeting of neuroblastoma cells is acutely enhanced by KCl stimulation through the calcium/calmodulin-dependent kinase pathway. Cancer biotherapy & radiopharmaceuticals 28:488-493.

Chuo CP, Liang SM, Sung HH (2005) Signal transduction of the prophenoloxidase activating system of prawn haemocytes triggered by CpG oligodeoxynucleotides. Fish Shellfish Immunol 18:149-162.

Clark MC, Dever TE, Dever JJ, Xu P, Rehder V, Sosa MA, Baro DJ (2004) Arthropod 5-HT2 receptors: a neurohormonal receptor in decapod crustaceans that displays agonist independent activity resulting from an evolutionary alteration to the DRY motif. J Neurosci 24:3421-3435.

Conigrave AD, Hampson DR (2010) Broad-spectrum amino acid-sensing class C G-protein coupled receptors: molecular mechanisms, physiological significance and options for drug development. Pharmacol Therapeut 127:252-260.

Conigrave AD, Ward DT (2013) Calcium-sensing receptor (CaSR): pharmacological properties and signaling pathways. Best Pract Res Clin Endocrinol Metab 27:315-331.

Conigrave AD, Mun HC, Brennan SC (2007) Physiological significance of L-amino acid sensing by extracellular Ca(2+)-sensing receptors. Biochem Soc T 35:1195-1198.

Connor JA, Stevens CF (1971) Prediction of repetitive firing behaviour from voltage clamp data on an isolated neurone soma. J Physiol 213:31-53.

Crunelli V, Mayer ML (1984) Mg2+ dependence of membrane resistance increases evoked by NMDA in hippocampal neurones. Brain Res 311:392-396.

Dale HH (1939) Physiology of the Nervous System. Science 90:393-394.

Darboux I, Lingueglia E, Pauron D, Barbry P, Lazdunski M (1998) A new member of the amiloride-sensitive sodium channel family in Drosophila melanogaster peripheral nervous system. Biochem Bioph Res Co 246:210-216.

Davies SP, Reddy H, Caivano M, Cohen P (2000) Specificity and mechanism of action of some commonly used protein kinase inhibitors. The Biochemical journal 351:95-105.

Del Negro CA, Koshiya N, Butera RJ, Jr., Smith JC (2002) Persistent sodium current, membrane properties and bursting behavior of pre-botzinger complex inspiratory neurons in vitro. J Neurophysiol 88:2242-2250.

Deleon M, Wang Y, Jones L, Perezreyes E, Wei XY, Soong TW, Snutch TP, Yue DT (1995) Essential Ca2+-Binding Motif for Ca2+-Sensitive Inactivation of L-Type Ca2+ Channels. Science 270:1502-1506.

Dingledine R (1983) N-methyl aspartate activates voltage-dependent calcium conductance in rat hippocampal pyramidal cells. J Physiol 343:385-405.

Doi A, Ramirez JM (2008) Neuromodulation and the orchestration of the respiratory rhythm. Respiratory physiology & neurobiology 164:96-104.

Donini A, Lange AB (2002) The effects of crustacean cardioactive peptide on locust oviducts are calcium-dependent. Peptides 23:683-691.

Dragoi G, Buzsaki G (2006) Temporal encoding of place sequences by hippocampal cell assemblies. Neuron 50:145-157.

Eckstein F, Cassel D, Levkovitz H, Lowe M, Selinger Z (1979) Guanosine 5'-O-(2-thiodiphosphate). An inhibitor of adenylate cyclase stimulation by guanine nucleotides and fluoride ions. J Biol Chem 254:9829-9834.

Edwards JS (2006) The central nervous control of insect flight. 1961. The Journal of experimental biology 209:4411-4413.

Egerod K, Reynisson E, Hauser F, Williamson M, Cazzamali G, Grimmelikhuijzen CJ (2003) Molecular identification of the first insect proctolin receptor. Biochem Bioph Res Co 306:437-442.

El Far O, Bofill-Cardona E, Airas JM, O'Connor V, Boehm S, Freissmuth M, Nanoff C, Betz H (2001a) Mapping of calmodulin and Gbetagamma binding domains within the C-terminal region of the metabotropic glutamate receptor 7A. J Biol Chem 276:30662-30669.

El Far O, Bofill-Cardona E, Airas JM, O'Connor V, Boehm S, Freissmuth M, Nanoff C, Betz H (2001b) Mapping of calmodulin and Gbetagamma binding domains within the C-terminal region of the metabotropic glutamate receptor 7A. The Journal of biological chemistry 276:30662-30669.

Elgersma Y, Fedorov NB, Ikonen S, Choi ES, Elgersma M, Carvalho OM, Giese KP, Silva AJ (2002) Inhibitory autophosphorylation of CaMKII controls PSD association, plasticity, and learning. Neuron 36:493-505.

Engberg I, Flatman JA, Lambert JD (1978) The action of N-methyl-D-aspartic and kainic acids on motoneurones with emphasis on conductance changes [proceedings]. Br J Pharmacol 64:384P-385P.

Erxleben CFJ, deSantis A, Rathmayer W (1995) Effects of proctolin on contractions, membrane resistance, and non-voltage-dependent sarcolemmal ion channels in crustacean muscle fibers. Journal of Neuroscience 15:4356-4369.

Fellner SK, Parker L (2004) Ionic strength and the polyvalent cation receptor of shark rectal gland and artery. J Exp Zool A Comp Exp Biol 301:235-239.

Fenelon VS, Casasnovas B, Simmers J, Meyrand P (1998) Development of rhythmic pattern generators. Current opinion in neurobiology 8:705-709.

Ficker E, Taglialatela M, Wible BA, Henley CM, Brown AM (1994) Spermine and spermidine as gating molecules for inward rectifier K+ channels. Science 266:1068-1072.

Fisone G, Borgkvist A, Usiello A (2004) Caffeine as a psychomotor stimulant: mechanism of action. Cellular and Molecular Life Sciences 61:857-872.

Flamm RE, Fickbohm D, Harris-Warrick RM (1987) cAMP elevation modulates physiological activity of pyloric neurons in the lobster stomatogastric ganglion. J Neurophysiol 58:1370-1386.

Forssberg H, Grillner S, Halbertsma J (1980) The locomotion of the low spinal cat. I. Coordination within a hindlimb. Acta physiologica Scandinavica 108:269-281.

Frankenhaeuser B, Hodgkin AL (1957) The Action of Calcium on the Electrical Properties of Squid Acons. J Physiol 137:218-244.

Freichel M, Tsvilovskyy V, Camacho-Londono JE (2014) TRPC4- and TRPC4-containing channels. Handb Exp Pharmacol 222:85-128.

Freschi JE (1989) Proctolin activates a slow, voltage-dependent sodium current in motoneurons of the lobster cardiac ganglion. Neurosci Lett 106:105-111.

Freschi JE (1991) The effect of subtype-selective muscarinic receptor antagonists on the cholinergic current in motoneurons of the lobster cardiac ganglion. Brain Res 552:87-92.

Freschi JE, Livengood DR (1989a) Membrane current underlying muscarinic cholinergic excitation of motoneurons in lobster cardiac ganglion. J Neurophysiol 62:984-995.

Freschi JE, Livengood DR (1989b) Membrane current underlying muscarinic cholinergic excitation of motoneurons in lobster cardiac ganglion. Journal of neurophysiology 62:984-995.

Friedrich RW, Molnar GF, Schiebe M, Mercier AJ (1998) Protein kinase C is required for long-lasting synaptic enhancement by the neuropeptide DRNFLRFamide in crayfish. J Neurophysiol 79:1127-1131.

Ganitkevich V, Isenberg G (1992) Caffeine-induced release and reuptake of Ca2+ by Ca2+ stores in myocytes from guinea-pig urinary bladder. J Physiol 458:99-117.

Garcia-Alvarez G, Lu B, Yap KA, Wong LC, Thevathasan JV, Lim L, Ji F, Tan KW, Mancuso JJ, Tang W, Poon SY, Augustine GJ, Fivaz M (2015) STIM2 regulates PKA-dependent phosphorylation and trafficking of AMPARs. Mol Biol Cell 26:1141-1159.

Garcia VJ, Daur N, Temporal S, Schulz DJ, Bucher D (2015) Neuropeptide receptor transcript expression levels and magnitude of ionic current responses show cell type-specific differences in a small motor circuit. J Neurosci 35:6786-6800.

Gierschik P (1992) ADP-ribosylation of signal-transducing guanine nucleotide-binding proteins by pertussis toxin. Curr Top Microbiol Immunol 175:69-96.

Gilman AG (1987) G proteins: transducers of receptor-generated signals. Annu Rev Biochem 56:615-649.

Golowasch J, Marder E (1992a) Ionic currents of the lateral pyloric neuron of the stomatogastric ganglion of the crab. J Neurophysiol 67:318-331.

Golowasch J, Marder E (1992b) Proctolin activates an inward current whose voltage dependence is modified by extracellular Ca2+. J Neurosci 12:810-817.

Golowasch J, Paupardin-Tritsch D (1996) A biphasic dopaminergic modulation of the high voltage-activated Ba2+ current of identified snail neurons. Invertebr Neurosci 2:199-208.

Golowasch J, Thomas G, Taylor AL, Patel A, Pineda A, Khalil C, Nadim F (2009) Membrane capacitance measurements revisited: dependence of capacitance value on measurement method in nonisopotential neurons. J Neurophysiol 102:2161-2175.

Gomperts BD, Tatham PER, Kramer IM (2002) Signal transduction. San Diego, Calif.: Academic Press.

Gossert AD, Hinniger A, Gutmann S, Jahnke W, Strauss A, Fernandez C (2011) A simple protocol for amino acid type selective isotope labeling in insect cells with improved yields and high reproducibility. Journal of Biomolecular Nmr 51:449-456.

Groome JR, Watson WH, 3rd (1989) Second-messenger systems underlying amine and peptide actions on cardiac muscle in the horseshoe crab Limulus polyphemus. J Exp Biol 145:419-437.

Hainaut K, Desmedt JE (1974) Effect of dantrolene sodium on calcium movements in single muscle fibres. Nature 252:728-730.

Haj-Dahmane S, Andrade R (1996) Muscarinic activation of a voltage-dependent cation nonselective current in rat association cortex. J Neurosci 16:3848-3861.

Han SK, Dong XZ, Hwang JI, Zylka MJ, Anderson DJ, Simon MI (2002) Orphan G protein-coupled receptors MrgA1 and MrgC11 are distinctively activated by RF-amide-related peptides through the G alpha(q/11) pathway. P Natl Acad Sci USA 99:14740-14745.

Harper JL, Daly JW (2000) Effect of calmidazolium analogs on calcium influx in HL-60 cells. Biochem Pharmacol 60:317-324.

Harris-Warrick RM (1989) Forskolin reduces a transient potassium current in lobster neurons by a cAMP-independent mechanism. Brain Res 489:59-66.

Harris-Warrick RM, Cohen AH (1985) Serotonin modulates the central pattern generator for locomotion in the isolated lamprey spinal cord. The Journal of experimental biology 116:27-46.

Harris-Warrick RM, Coniglio LM, Barazangi N, Guckenheimer J, Gueron S (1995a) Dopamine modulation of transient potassium current evokes phase shifts in a central pattern generator network. The Journal of neuroscience : the official journal of the Society for Neuroscience 15:342-358.

Harris-Warrick RM, Coniglio LM, Levini RM, Gueron S, Guckenheimer J (1995b) Dopamine modulation of two subthreshold currents produces phase shifts in activity of an identified motoneuron. Journal of neurophysiology 74:1404-1420.

Harrison C, Traynor JR (2003) The [35S]GTPgammaS binding assay: approaches and applications in pharmacology. Life Sci 74:489-508.

Heindorff K, Baumann O (2014) Calcineurin is part of a negative feedback loop in the InsP3/Ca(2)(+) signalling pathway in blowfly salivary glands. Cell Calcium 56:215-224.

Heinrich R, Wenzel B, Elsner N (2001) Pharmacological brain stimulation releases elaborate stridulatory behaviour in gomphocerine grasshoppers - conclusions for the organization of the central nervous control. Journal of Comparative Physiology a-Neuroethology Sensory Neural and Behavioral Physiology 187:155-169.

Hempel CM, Vincent P, Adams SR, Tsien RY, Selverston AI (1996) Spatio-temporal dynamics of cyclic AMP signals in an intact neural circuitm. Nature 384:166-169.

Hille B (2001) Ion channels of excitable membranes, 3rd Edition. Sunderland, Mass.: Sinauer.

Hiripi L, Rozsa KS, Miller TA (1979) The effect of proctolin on the adenylate and guanylate cyclases in the Locusta brain at various developmental stages. Experientia 35:1287-1288.

Hooper SL, Marder E (1984) Modulation of a central pattern generator by two neuropeptides, proctolin and FMRFamide. Brain research 305:186-191.

Hooper SL, Moulins M (1990) Cellular and synaptic mechanisms responsible for a long-lasting restructuring of the lobster pyloric network. Journal of neurophysiology 64:1574-1589.

Hoshi T, Zagotta WN, Aldrich RW (1990) Biophysical and molecular mechanisms of Shaker potassium channel inactivation. Science 250:533-538.

Huang Y, Cavanaugh A, Breitwieser GE (2011) Regulation of stability and trafficking of calcium-sensing receptors by pharmacologic chaperones. Adv Pharmacol 62:143-173.

Huang Y, Zhou Y, Wong HC, Castiblanco A, Chen Y, Brown EM, Yang JJ (2010) Calmodulin regulates Ca2+-sensing receptor-mediated Ca2+ signaling and its cell surface expression. The Journal of biological chemistry 285:35919-35931.

Imoto Y, Yatani A, Reeves JP, Codina J, Birnbaumer L, Brown AM (1988) Alpha-subunit of Gs directly activates cardiac calcium channels in lipid bilayers. Am J Physiol 255:H722-728.

Inagaki M, Kawamoto S, Itoh H, Saitoh M, Hagiwara M, Takahashi J, Hidaka H (1986) Naphthalenesulfonamides as calmodulin antagonists and protein kinase inhibitors. Mol Pharmacol 29:577-581.

Izhikevich EM (2007) Dynamical systems in neuroscience : the geometry of excitability and bursting. Cambridge, Mass.: MIT Press.

Johansson MW, Soderhall K (1993) Intracellular signaling in arthropod blood cells: involvement of protein kinase C and protein tyrosine phosphorylation in the response to the 76-kDa protein or the beta-1,3-glucan-binding protein in crayfish. Dev Comp Immunol 17:495-500.

Johnson BR, Harris-Warrick RM (1990) Aminergic modulation of graded synaptic transmission in the lobster stomatogastric ganglion. The Journal of neuroscience : the official journal of the Society for Neuroscience 10:2066-2076.

Johnson BR, Peck JH, Harris-Warrick RM (1993a) Dopamine induces sign reversal at mixed chemical-electrical synapses. Brain research 625:159-164.

Johnson BR, Peck JH, Harris-Warrick RM (1993b) Amine modulation of electrical coupling in the pyloric network of the lobster stomatogastric ganglion. Journal of comparative physiology A, Sensory, neural, and behavioral physiology 172:715-732.

Johnson EC, Bohn LM, Barak LS, Birse RT, Nassel DR, Caron MG, Taghert PH (2003) Identification of Drosophila neuropeptide receptors by G protein-coupled receptors-beta-arrestin2 interactions. The Journal of biological chemistry 278:52172-52178.

Johnston D, Wu SM-s (1995) Foundations of cellular neurophysiology. Cambridge, Mass.: MIT Press.

Kandel ER, Schwartz JH, Jessell TM (1991) Principles of neural science, 3rd Edition. Norwalk, Conn.: Appleton & Lange.

Kashiwagi T, Meyer-Rochow VB, Nishimura K, Eguchi E (2000) Light activation of phospholipase A2 in the photoreceptor of the crayfish (Procambarus clarkii). Acta Neurobiol Exp (Wars) 60:9-16.

Katada T (2012) The inhibitory G protein G(i) identified as pertussis toxin-catalyzed ADP-ribosylation. Biol Pharm Bull 35:2103-2111.

Kehoe J (1990) Cyclic AMP-induced slow inward current: its synaptic manifestation in Aplysia neurons. J Neurosci 10:3208-3218.

Khorkova O, Golowasch J (2007) Neuromodulators, not activity, control coordinated expression of ionic currents. J Neurosci 27:8709-8718.

Kiehn O, Harris-Warrick RM (1992) Serotonergic stretch receptors induce plateau properties in a crustacean motor neuron by a dual-conductance mechanism. Journal of neurophysiology 68:485-495.

Kilman VL, Marder E (1996) Ultrastructure of the stomatogastric ganglion neuropil of the crab, Cancer borealis. The Journal of comparative neurology 374:362-375.

Kim BJ, Chang IY, Choi S, Jun JY, Jeon JH, Xu WX, Kwon YK, Ren D, So I (2012) Involvement of Na(+)-leak channel in substance P-induced depolarization of pacemaking activity in interstitial cells of Cajal. Cell Physiol Biochem 29:501-510.

Kitazawa T, Kobayashi S, Horiuti K, Somlyo AV, Somlyo AP (1989) Receptor-coupled, permeabilized smooth muscle. Role of the phosphatidylinositol cascade, G-proteins, and modulation of the contractile response to Ca2+. J Biol Chem 264:5339-5342.

Komori S, Unno T, Nakayama T, Ohashi H (1998) M2 and M3 muscarinic receptors couple, respectively, with activation of nonselective cationic channels and potassium channels in intestinal smooth muscle cells. Jpn J Pharmacol 76:213-218.

Kong KC, Tobin AB (2011) The role of M(3)-muscarinic receptor signaling in insulin secretion. Commun Integr Biol 4:489-491.

Krueger KM, Barbieri JT (1995) The family of bacterial ADP-ribosylating exotoxins. Clin Microbiol Rev 8:34-47.

Kubiak TM, Larsen MJ, Bowman JW, Gearyt TG, Lowery DE (2008) FMRFamide-like peptides encoded on the flp-18 precursor gene activate two Isoforms of the orphan Caenorhabditis elegans G-protein-coupled receptor Y58G8A.4 heterologously expressed in mammalian cells. Biopolymers 90:339-348.

Kumamoto E (1996) Neuromodulation by Mg2+ and polyamines of excitatory amino acid currents in rodent neurones in culture. Magnes Res 9:317-327.

Kupper J, Ascher P, Neyton J (1998) Internal Mg2+ block of recombinant NMDA channels mutated within the selectivity filter and expressed in Xenopus oocytes. J Physiol 507 ( Pt 1):1-12.

Lange AB (1988) Inositol phospholipid hydrolysis may mediate the action of proctolin on insect visceral muscle. Archives of Insect Biochemistry and Physiology 9:201-209.

Lecorronc H, Hue B (1993) Electrophysiological Evidence for the Modulation of Acetylcholine-Release by Endogenous Acetylcholine in the Cockroach Central-Nervous-System. Journal of Experimental Biology 175:305-310.

Lee D, Vanden Broeck J, Lange AB (2013) Identification and expression of the CCAP receptor in the Chagas' disease vector, Rhodnius prolixus, and its involvement in cardiac control. PLoS One 8:e68897.

Lehninger AL, Nelson DL, Cox MM (2000) Lehninger principles of biochemistry, 3rd Edition. New York: Worth Publishers.

Leibowitz MD, Sutro JB, Hille B (1986) Voltage-dependent gating of veratridine-modified Na channels. J Gen Physiol 87:25-46.

Lemos JR, Levitan IB (1984) Intracellular injection of guanyl nucleotides alters the serotonin-induced increase in potassium conductance in Aplysia neuron R15. J Gen Physiol 83:269-285.

Levi R, Selverston AI (2006) Mechanisms underlying type I mGluR-induced activation of lobster gastric mill neurons. J Neurophysiol 96:3378-3388.

Levi R, Samoilova M, Selverston AI (2003) Calcium signaling components of oscillating invertebrate neurons in vitro. Neuroscience 118:283-296.

Li B, Beeman RW, Park Y (2011) Functions of duplicated genes encoding CCAP receptors in the red flour beetle, Tribolium castaneum. Journal of insect physiology 57:1190-1197.

Liscovitch M, Chalifa V, Danin M, Eli Y (1991) Inhibition of neural phospholipase D activity by aminoglycoside antibiotics. Biochem J 279 ( Pt 1):319-321.

Lnenicka GA, Arcaro KF, Calabro JM (1998) Activity-dependent development of calcium regulation in growing motor axons. The Journal of neuroscience : the official journal of the Society for Neuroscience 18:4966-4972.

Lochner A, Moolman JA (2006) The many faces of H89: a review. Cardiovasc Drug Rev 24:261-274.

Lodish HF (2008) Molecular cell biology, 6th Edition. New York: W.H. Freeman.

Lu B, Su Y, Das S, Liu J, Xia J, Ren D (2007) The neuronal channel NALCN contributes resting sodium permeability and is required for normal respiratory rhythm. Cell 129:371-383.

Lu B, Zhang Q, Wang H, Wang Y, Nakayama M, Ren D (2010) Extracellular calcium controls background current and neuronal excitability via an UNC79-UNC80-NALCN cation channel complex. Neuron 68:488-499.

Lu B, Su Y, Das S, Wang H, Wang Y, Liu J, Ren D (2009) Peptide neurotransmitters activate a cation channel complex of NALCN and UNC-80. Nature 457:741-744.

Lu TZ, Feng ZP (2012) NALCN: a regulator of pacemaker activity. Molecular neurobiology 45:415-423.

Luther JA, Robie AA, Yarotsky J, Reina C, Marder E, Golowasch J (2003) Episodic bouts of activity accompany recovery of rhythmic output by a neuromodulator- and activity-deprived adult neural network. J Neurophysiol 90:2720-2730.

Mandadi S, Numazaki M, Tominaga M, Bhat MB, Armati PJ, Roufogalis BD (2004) Activation of protein kinase C reverses capsaicin-induced calcium-dependent desensitization of TRPV1 ion channels. Cell Calcium 35:471-478.

Manion MK, Su Z, Villain M, Blalock JE (2000) A new type of Ca(2+) channel blocker that targets Ca(2+) sensors and prevents Ca(2+)-mediated apoptosis. FASEB J 14:1297-1306.

Marder E, Paupardin-Tritsch D (1978) The pharmacological properties of some crustacean neuronal acetylcholine, gamma-aminobutyric acid, and L-glutamate responses. J Physiol 280:213-236.

Marder E, Calabrese RL (1996) Principles of rhythmic motor pattern generation. Physiological reviews 76:687-717.

Mayer ML, Westbrook GL (1984) Mixed-agonist action of excitatory amino acids on mouse spinal cord neurones under voltage clamp. J Physiol 354:29-53.

Mayer ML, Westbrook GL (1985a) The action of N-methyl-D-aspartic acid on mouse spinal neurones in culture. J Physiol 361:65-90.

Mayer ML, Westbrook GL (1985b) The action of N-methyl-D-aspartic acid on mouse spinal neurones in culture. The Journal of physiology 361:65-90.

Mayer ML, Westbrook GL (1987) Permeation and block of N-methyl-D-aspartic acid receptor channels by divalent cations in mouse cultured central neurones. J Physiol 394:501-527.

Mayer ML, Westbrook GL, Guthrie PB (1984) Voltage-dependent block by Mg2+ of NMDA responses in spinal cord neurones. Nature 309:261-263.

Maynard DM, Dando MR (1974) The structure of the stomatogastric neuromuscular system in Callinectes sapidus, Homarus americanus and Panulirus argus (Decapoda Crustacea). Philosophical transactions of the Royal Society of London Series B, Biological sciences 268:161-220.

Mazzocco-Manneval C, Kuczer M, Konopinska D, Fournier B, Loughton BG, Puiroux J (1998) Pharmacological studies of proctolin receptors on foregut and hindgut of Blaberus craniifer. Peptides 19:1641-1651.

McGehee DS, Aldersberg M, Liu KP, Hsuing S, Heath MJ, Tamir H (1997) Mechanism of extracellular Ca2+ receptor-stimulated hormone release from sheep thyroid parafollicular cells. J Physiol 502 ( Pt 1):31-44.

Meeusen T, Mertens I, Clynen E, Baggerman G, Nichols R, Nachman RJ, Huybrechts R, De Loof A, Schoofs L (2002) Identification in Drosophila melanogaster of the invertebrate G protein-coupled FMRFamide receptor. P Natl Acad Sci USA 99:15363-15368.

Meggio F, Donella Deana A, Ruzzene M, Brunati AM, Cesaro L, Guerra B, Meyer T, Mett H, Fabbro D, Furet P, et al. (1995) Different susceptibility of protein kinases to staurosporine inhibition. Kinetic studies and molecular bases for the resistance of protein kinase CK2. Eur J Biochem 234:317-322.

Morton DB, Simpson PJ (2002) Cellular signaling in eclosion hormone action. J Insect Physiol 48:1-13.

Mykles DL, Adams ME, Gaede G, Lange AB, Marco HG, Orchard I (2010a) Neuropeptide Action in Insects and Crustaceans. Physiological and Biochemical Zoology 83:836-846.

Mykles DL, Adams ME, Gade G, Lange AB, Marco HG, Orchard I (2010b) Neuropeptide action in insects and crustaceans. Physiol Biochem Zool 83:836-846.

Nawy S (2000) Regulation of the on bipolar cell mGluR6 pathway by Ca2+. J Neurosci 20:4471-4479.

Nemeth EF, Delmar EG, Heaton WL, Miller MA, Lambert LD, Conklin RL, Gowen M, Gleason JG, Bhatnagar PK, Fox J (2001) Calcilytic compounds: potent and selective Ca2+ receptor antagonists that stimulate secretion of parathyroid hormone. J Pharmacol Exp Ther 299:323-331.

Nilius B (1988) Calcium block of guinea-pig heart sodium channels with and without modification by the piperazinylindole DPI 201-106. J Physiol 399:537-558.

Nowak L, Bregestovski P, Ascher P, Herbet A, Prochiantz A (1984) Magnesium gates glutamate-activated channels in mouse central neurones. Nature 307:462-465.

Nowak LM, Macdonald RL (1983) Muscarine-sensitive voltage-dependent potassium current in cultured murine spinal cord neurons. Neurosci Lett 35:85-91.

Nwoga J, Bittar EE (1985) Stimulation by proctolin of the ouabain-insensitive sodium efflux in single barnacle muscle fibers. Comp Biochem Physiol C 81:345-350.

Nykamp DA, Lange AB (2000) Interaction between octopamine and proctolin on the oviducts of Locusta migratoria. Journal of Insect Physiology 46:809-816.

Oancea E, Meyer T (1996) Reversible desensitization of inositol trisphosphate-induced calcium release provides a mechanism for repetitive calcium spikes. The Journal of biological chemistry 271:17253-17260.

Orchard I, Lange AB (1987) The Release of Octopamine and Proctolin from an Insect Visceral Muscle - Effects of High-Potassium Saline and Neural Stimulation. Brain Research 413:251-258.

Orchard I, Belanger JH, Lange AB (1989) Proctolin: a review with emphasis on insects. J Neurobiol 20:470-496.

Ott L, Longnecker M (2001) An introduction to statistical methods and data analysis, 5th Edition. Australia ; Pacific Grove, CA: Duxbury.

Ouyang Q, Goeritz M, Harris-Warrick RM (2007) Panulirus interruptus Ih-channel gene PIIH: modification of channel properties by alternative splicing and role in rhythmic activity. J Neurophysiol 97:3880-3892.

Panama BK, Lopatin AN (2006) Differential polyamine sensitivity in inwardly rectifying Kir2 potassium channels. J Physiol 571:287-302.

Pang DS, Robledo CJ, Carr DR, Gent TC, Vyssotski AL, Caley A, Zecharia AY, Wisden W, Brickley SG, Franks NP (2009) An unexpected role for TASK-3 potassium channels in network oscillations with implications for sleep mechanisms and anesthetic action. P Natl Acad Sci USA 106:17546-17551.

Park Y, Kim YJ, Adams ME (2002) Identification of G protein-coupled receptors for Drosophila PRXamide peptides, CCAP, corazonin, and AKH supports a theory of ligand-receptor coevolution. P Natl Acad Sci USA 99:11423-11428.

Partington CR, Edwards MW, Daly JW (1980) Calcium-dependent desensitization of adenylate cyclase in rat cerebral cortical slices. Journal of neurochemistry 34:76-82.

Pawlak V, Wickens JR, Kirkwood A, Kerr JN (2010) Timing is not Everything: Neuromodulation Opens the STDP Gate. Front Synaptic Neurosci 2:146.

Payne JL, Dyer JA (1975) Betting After the Race is Over: The Perils of Post Hoc Hypothesizing. American Journal of Political Science 19:559-564.

Peterson BZ, DeMaria CD, Adelman JP, Yue DT (1999) Calmodulin is the Ca2+ sensor for Ca2+ -dependent inactivation of L-type calcium channels. Neuron 22:549-558.

Pfaffinger PJ, Martin JM, Hunter DD, Nathanson NM, Hille B (1985) GTP-binding proteins couple cardiac muscarinic receptors to a K channel. Nature 317:536-538.

Pfaffinger PJ, Leibowitz MD, Subers EM, Nathanson NM, Almers W, Hille B (1988) Agonists that suppress M-current elicit phosphoinositide turnover and Ca2+ transients, but these events do not explain M-current suppression. Neuron 1:477-484.

Philipp B, Rogalla N, Kreissl S (2006) The neuropeptide proctolin potentiates contractions and reduces cGMP concentration via a PKC-dependent pathway. The Journal of experimental biology 209:531-540.

Pitcher J, Lohse MJ, Codina J, Caron MG, Lefkowitz RJ (1992) Desensitization of the isolated beta 2-adrenergic receptor by beta-adrenergic receptor kinase, cAMP-dependent protein kinase, and protein kinase C occurs via distinct molecular mechanisms. Biochemistry 31:3193-3197.

Powis G, Seewald MJ, Gratas C, Melder D, Riebow J, Modest EJ (1992) Selective inhibition of phosphatidylinositol phospholipase C by cytotoxic ether lipid analogues. Cancer Res 52:2835-2840.

Puiroux J, Pedelaborde A, Loughton BG (1998) Partial purification of a putative proctolin receptor from the African migratory locust. Insect Biochem Molec 28:887-893.

Purves D (1997) Neuroscience. Sunderland, Mass.: Sinauer Associates.

Putney JW (2009) Capacitative calcium entry: from concept to molecules. Immunol Rev 231:10-22.

Putney JW, Jr. (2005) Capacitative calcium entry: sensing the calcium stores. J Cell Biol 169:381-382.

Qazi S, Trimmer BA (1999a) The role of nitric oxide in motoneuron spike activity and muscarinic-evoked changes in cGMP in the CNS of larval Manduca sexta. J Comp Physiol A 185:539-550.

Qazi S, Trimmer BA (1999b) The role of inositol 1,4,5-trisphosphate 5-phosphatase in inositol signaling in the CNS of larval Manduca sexta. Insect Biochem Mol Biol 29:161-175.

Ransdell JL, Nair SS, Schulz DJ (2012) Rapid homeostatic plasticity of intrinsic excitability in a central pattern generator network stabilizes functional neural network output. The Journal of neuroscience : the official journal of the Society for Neuroscience 32:9649-9658.

Rathmayer W, Djokaj S, Gaydukov A, Kreissl S (2002) The neuromuscular junctions of the slow and the fast excitatory axon in the closer of the crab Eriphia spinifrons are endowed with different Ca2+ channel types and allow neuron-specific modulation of transmitter release by two neuropeptides. Journal of Neuroscience 22:708-717.

Rezazadeh S, Claydon TW, Fedida D (2006) KN-93 (2-[N-(2-hydroxyethyl)]-N-(4-methoxybenzenesulfonyl)]amino-N-(4-chlorocinnamyl)-N -methylbenzylamine), a calcium/calmodulin-dependent protein kinase II inhibitor, is a direct extracellular blocker of voltage-gated potassium channels. J Pharmacol Exp Ther 317:292-299.

Ribeiro JA, Sebastiao AM (2010) Caffeine and adenosine. J Alzheimers Dis 20 Suppl 1:S3-15.

Rivers DB, Rocco MM, Frayha AR (2002) Venom from the ectoparasitic wasp Nasonia vitripennis increases Na+ influx and activates phospholipase C and phospholipase A2 dependent signal transduction pathways in cultured insect cells. Toxicon 40:9-21.

Rosenmund C, Feltz A, Westbrook GL (1995) Calcium-dependent inactivation of synaptic NMDA receptors in hippocampal neurons. Journal of neurophysiology 73:427-430.

Saidak Z, Brazier M, Kamel S, Mentaverri R (2009) Agonists and allosteric modulators of the calcium-sensing receptor and their therapeutic applications. Molecular pharmacology 76:1131-1144.

Saitoh M, Ishikawa T, Matsushima S, Naka M, Hidaka H (1987) Selective inhibition of catalytic activity of smooth muscle myosin light chain kinase. J Biol Chem 262:7796-7801.

Schacht J (1976) Inhibition by neomycin of polyphosphoinositide turnover in subcellular fractions of guinea-pig cerebral cortex in vitro. J Neurochem 27:1119-1124.

Schreibmayer W, Dessauer CW, Vorobiov D, Gilman AG, Lester HA, Davidson N, Dascal N (1996) Inhibition of an inwardly rectifying K+ channel by G-protein alpha-subunits. Nature 380:624-627.

Schwertz DW, Kreisberg JI, Venkatachalam MA (1984) Effects of aminoglycosides on proximal tubule brush border membrane phosphatidylinositol-specific phospholipase C. J Pharmacol Exp Ther 231:48-55.

Sedlmeier D, Dieberg G (1983) Crayfish abdominal muscle adenylate cyclase. Studies on the stimulation by a Ca2+-binding protein. Biochem J 211:319-322.

Selverston AI, Russell DF, Miller JP (1976) The stomatogastric nervous system: structure and function of a small neural network. Progress in neurobiology 7:215-290.

Shiells RA (1999) Ca(2+)-induced light adaptation in retinal ON-bipolar cells. Keio J Med 48:140-146.

Shiells RA, Falk G (1992) The glutamate-receptor linked cGMP cascade of retinal on-bipolar cells is pertussis and cholera toxin-sensitive. Proceedings Biological sciences / The Royal Society 247:17-20.

Shiells RA, Falk G (1999) A rise in intracellular Ca2+ underlies light adaptation in dogfish retinal 'on' bipolar cells. The Journal of physiology 514 ( Pt 2):343-350.

Shiells RA, Falk G (2000) Activation of Ca2+--calmodulin kinase II induces desensitization by background light in dogfish retinal 'on' bipolar cells. J Physiol 528 Pt 2:327-338.

Shiells RA, Falk G (2001) Rectification of cGMP-activated channels induced by phosphorylation in dogfish retinal 'on' bipolar cells. J Physiol 535:697-702.

Shiells RA, Falk G (2002) Potentiation of 'on' bipolar cell flash responses by dim background light and cGMP in dogfish retinal slices. The Journal of physiology 542:211-220.

Spruston N, Nusbaum MP (1991 ) Cyclic Nucleotide-Mediated Modulation of the Pyloric Motor Pattern in the Stomatogastric Ganglion of the Crab Cancer borealis Biol Bull 329-330.

Squire LR (2003) Fundamental neuroscience, 2nd Edition. Amsterdam ; Boston: Academic Press.

Steinbach HB, Spiegelman s, kowata n (1944) The effects of potassium and calcium on the electrical properties of squid axons†. j Cell and comparative Physiol 24:147-154.

Steriade M, McCormick DA, Sejnowski TJ (1993) Thalamocortical oscillations in the sleeping and aroused brain. Science 262:679-685.

Swayne LA, Mezghrani A, Lory P, Nargeot J, Monteil A (2010) The NALCN ion channel is a new actor in pancreatic beta-cell physiology. Islets 2:54-56.

Swayne LA, Mezghrani A, Varrault A, Chemin J, Bertrand G, Dalle S, Bourinet E, Lory P, Miller RJ, Nargeot J, Monteil A (2009) The NALCN ion channel is activated by M3 muscarinic receptors in a pancreatic beta-cell line. EMBO Rep 10:873-880.

Swensen AM (2000) Network consequences of convergent modulation in the stomatogastric nervous system of the crab, cancer borealis. In: Neuroscience, p 143. Waltham: Brandeis.

Swensen AM, Marder E (2000) Multiple peptides converge to activate the same voltage-dependent current in a central pattern-generating circuit. J Neurosci 20:6752-6759.

Swensen AM, Marder E (2001) Modulators with convergent cellular actions elicit distinct circuit outputs. J Neurosci 21:4050-4058.

Taengchaiyaphum S, Havanapan PO, Roytrakul S, Lo CF, Sritunyalucksana K, Krittanai C (2013) Phosphorylation is required for myosin regulatory light chain (PmMRLC) to control yellow head virus infection in shrimp hemocytes. Fish Shellfish Immunol 34:1042-1049.

Talley EM, Lei Q, Sirois JE, Bayliss DA (2000) TASK-1, a two-pore domain K+ channel, is modulated by multiple neurotransmitters in motoneurons. Neuron 25:399-410.

Tam AK, Gardam KE, Lamb S, Kachoei BA, Magoski NS (2011) Role for protein kinase C in controlling Aplysia bag cell neuron excitability. Neuroscience 179:41-55.

Tamaoki T, Nomoto H, Takahashi I, Kato Y, Morimoto M, Tomita F (1986) Staurosporine, a potent inhibitor of phospholipid/Ca++dependent protein kinase. Biochem Biophys Res Commun 135:397-402.

Tang WJ, Gilman AG (1991) Type-specific regulation of adenylyl cyclase by G protein beta gamma subunits. Science 254:1500-1503.

Thoby-Brisson M, Simmers J (1998) Neuromodulatory inputs maintain expression of a lobster motor pattern-generating network in a modulation-dependent state: evidence from long-term decentralization in vitro. J Neurosci 18:2212-2225.

Thoby-Brisson M, Simmers J (2000) Transition to endogenous bursting after long-term decentralization requires De novo transcription in a critical time window. J Neurophysiol 84:596-599.

Tillotson D (1979) Inactivation of Ca conductance dependent on entry of Ca ions in molluscan neurons. Proc Natl Acad Sci U S A 76:1497-1500.

Tornquist K, Ekokoski E (1996) Inhibition of agonist-mediated calcium entry by calmodulin antagonists and by the Ca2+/calmodulin kinase II inhibitor KN-62. Studies with thyroid FRTL-5 cells. J Endocrinol 148:131-138.

Toullec D, Pianetti P, Coste H, Bellevergue P, Grand-Perret T, Ajakane M, Baudet V, Boissin P, Boursier E, Loriolle F, et al. (1991) The bisindolylmaleimide GF 109203X is a potent and selective inhibitor of protein kinase C. J Biol Chem 266:15771-15781.

Tran TM, Friedman J, Qunaibi E, Baameur F, Moore RH, Clark RB (2004) Characterization of agonist stimulation of cAMP-dependent protein kinase and G protein-coupled receptor kinase phosphorylation of the beta2-adrenergic receptor using phosphoserine-specific antibodies. Mol Pharmacol 65:196-206.

Trimmer BA (1994) Characterization of a Muscarinic Current That Regulates Excitability of an Identified Insect Motoneuron. Journal of Neurophysiology 72:1862-1873.

Trimmer BA (1995) Current excitement from insect muscarinic receptors. Trends Neurosci 18:104-111.

Uzdensky A, Kolosov M, Bragin D, Dergacheva O, Vanzha O, Oparina L (2005) Involvement of adenylate cyclase and tyrosine kinase signaling pathways in response of crayfish stretch receptor neuron and satellite glia cell to photodynamic treatment. Glia 49:339-348.

Van Eldik LJ, Watterson DM (1998) Calmodulin and signal transduction. San Diego: Academic Press.

Van Soest PF, Lodder JC, Kits KS (2000) Activation of protein kinase C by oxytocin-related conopressin underlies pacemaker current in Lymnaea central neurons. J Neurophysiol 84:2541-2551.

van Tol-Steye H, Lodder JC, Planta RJ, van Heerikhuizen H, Kits KS (1997) Convergence of multiple G-protein-coupled receptors onto a single type of potassium channel. Brain Res 777:119-130.

Vemana S, Pandey S, Larsson HP (2008) Intracellular Mg2+ is a voltage-dependent pore blocker of HCN channels. Am J Physiol Cell Physiol 295:C557-565.

Vezenkov SR, Danalev DL (2009) From molecule to sexual behavior: the role of the neuropentapeptide proctolin in acoustic communication in the male grasshopper Chorthippus biguttulus. Eur J Pharmacol 619:57-60.

Vyleta NP, Smith SM (2011) Spontaneous glutamate release is independent of calcium influx and tonically activated by the calcium-sensing receptor. J Neurosci 31:4593-4606.

Wagenmakers E-J, Wetzels R, Borsboom D, van der Maas HL, Kievit RA (2012) An agenda for purely confirmatory research. Perspectives on Psychological Science 7:632-638.

Walther C, Zittlau KE, Murck H, Voigt K (1998) Resting membrane properties of locust muscle and their modulation I. Actions of the neuropeptides YGGFMRFamide and proctolin. J Neurophysiol 80:771-784.

Wegener C, Nassel DR (2000) Peptide-induced Ca(2+) movements in a tonic insect muscle: effects of proctolin and periviscerokinin-2. Journal of neurophysiology 84:3056-3066.

Weiser DC, Shenolikar S (2003) Use of protein phosphatase inhibitors. Current protocols in protein science / editorial board, John E Coligan [et al] Chapter 13:Unit 13 10.

Wenzel B, Elsner N, Heinrich R (2002) mAChRs in the grasshopper brain mediate excitation by activation of the AC/PKA and the PLC second-messenger pathways. Journal of Neurophysiology 87:876-888.

Willoughby D, Yeoman MS, Benjamin PR (1999) Inositol-1,4,5-trisphosphate and inositol-1,3,4,5-tetrakisphosphate are second messenger targets for cardioactive neuropeptides encoded on the FMRFamide gene. J Exp Biol 202:2581-2593.

WILSON DM (1961) The Central Nervous Control of Flight in a Locust. Journal of Experimental Biology 38:471-490.

Withers MD, Kennedy MB, Marder E, Griffith LC (1998) Characterization of calcium/calmodulin-dependent protein kinase II activity in the nervous system of the lobster, Panulirus interruptus. Invert Neurosci 3:335-345.

Wong R, Fabian L, Forer A, Brill JA (2007) Phospholipase C and myosin light chain kinase inhibition define a common step in actin regulation during cytokinesis. BMC Cell Biol 8:15.

Xu XF, Tsai HJ, Li L, Chen YF, Zhang C, Wang GF (2009) Modulation of leak K(+) channel in hypoglossal motoneurons of rats by serotonin and/or variation of pH value. Sheng Li Xue Bao 61:305-316.

Yamamoto D, Yeh JZ, Narahashi T (1984) Voltage-dependent calcium block of normal and tetramethrin-modified single sodium channels. Biophys J 45:337-344.

Yamamoto H, Tachibana A, Saikawa W, Nagano M, Matsumura K, Fusetani N (1998) Effects of calmodulin inhibitors on cyprid larvae of the barnacle, Balanus amphitrite. J Exp Zool 280:8-17.

Yamanaka G, Eckstein F, Stryer L (1986) Interaction of retinal transducin with guanosine triphosphate analogues: specificity of the gamma-phosphate binding region. Biochemistry 25:6149-6153.

Zarubin TP, Chang ES, Mykles DL (2009) Expression of recombinant eyestalk crustacean hyperglycemic hormone from the tropical land crab, Gecarcinus lateralis, that inhibits Y-organ ecdysteroidogenesis in vitro. Mol Biol Rep 36:1231-1237.

Zhang H, Rodgers EW, Krenz WD, Clark MC, Baro DJ (2010) Cell specific dopamine modulation of the transient potassium current in the pyloric network by the canonical D1 receptor signal transduction cascade. J Neurophysiol 104:873-884.

Zhang JC, Lau PM, Bi GQ (2009) Gain in sensitivity and loss in temporal contrast of STDP by dopaminergic modulation at hippocampal synapses. P Natl Acad Sci USA 106:13028-13033.

Zhang JZ, Yarov-Yarovoy V, Scheuer T, Karbat I, Cohen L, Gordon D, Gurevitz M, Catterall WA (2012a) Mapping the interaction site for a beta-scorpion toxin in the pore module of domain III of voltage-gated Na(+) channels. J Biol Chem 287:30719-30728.

Zhang Y, Niu X, Brelidze TI, Magleby KL (2006) Ring of negative charge in BK channels facilitates block by intracellular Mg2+ and polyamines through electrostatics. J Gen Physiol 128:185-202.

Zhang YH, Wu W, Sun HY, Deng XL, Cheng LC, Li X, Tse HF, Lau CP, Li GR (2012b) Modulation of human cardiac transient outward potassium current by EGFR tyrosine kinase and Src-family kinases. Cardiovasc Res 93:424-433.

Zhao F, Li P, Chen SR, Louis CF, Fruen BR (2001) Dantrolene inhibition of ryanodine receptor Ca2+ release channels. Molecular mechanism and isoform selectivity. J Biol Chem 276:13810-13816.

Zhao S, Golowasch J, Nadim F (2010) Pacemaker neuron and network oscillations depend on a neuromodulator-regulated linear current. Front Behav Neurosci 4:21.

Zhao S, Sheibanie AF, Oh M, Rabbah P, Nadim F (2011) Peptide neuromodulation of synaptic dynamics in an oscillatory network. The Journal of neuroscience : the official journal of the Society for Neuroscience 31:13991-14004.

Zholos AV (2014) Trpc5. Handb Exp Pharmacol 222:129-156.

Zholos AV, Bolton TB (1995) Effects of divalent cations on muscarinic receptor cationic current in smooth muscle from guinea-pig small intestine. J Physiol 486 ( Pt 1):67-82.

Zholos AV, Bolton TB (1996) A novel GTP-dependent mechanism of ileal muscarinic metabotropic channel desensitization. Br J Pharmacol 119:997-1005.

Zhou L, Zhao S, Nadim F (2007) Neuromodulation of short-term synaptic dynamics examined in a mechanistic model based on kinetics of calcium currents. Neurocomputing 70:2050-2054.

Zwiernik MJ, Kay DP, Moore J, Beckett KJ, Khim JS, Newsted JL, Roark SA, Giesy JP (2008) Exposure and effects assessment of resident mink (Mustela vison) exposed to polychlorinated dibenzofurans and other dioxin-like compounds in the Tittabawassee River basin, Midland, Michigan, USA. Environ Toxicol Chem 27:2076-2087.